4-27-2016

Functionalizing Intact Allografts through Polymer Coating and Growth Factor Delivery

Farzana Sharmin
fssharmi2003@gmail.com

Functionalizing Intact Allografts through Polymer Coating and Growth Factor Delivery

Farzana Sharmin, PhD

University of Connecticut, [2016]

Each year approximately 600,000 and 2.2 million bone graft procedures are performed worldwide with 600,000 of them performed only in the United States. With a high success rate of osteo-integration and limited activation of the immune response, autografts are currently considered the gold standard for bone grafting. However, autografts are limited by the volume of bone tissue that can be harvested and by the threat of donor site morbidity. Allografts are alternatives to autografts since they are available in nearly unlimited supply and avoid donor-site morbidity and pain. However, allografts have been shown to be less frequently osteoinductive than autografts due to lack of biological factors, i.e., cells, growth factors. Limited vascularization, new bone formation and remodeling associated with large allograft healing are directly associated with clinical failure due to non-unions, late graft fractures and infections.

The objective of this thesis is to increase the functionality and subsequent incorporation of allograft into host bone by applying a thin polymeric coating to allografts that would be capable of carrying and delivering growth factors with quantitative precision in hopes of increasing the ability of allografts to heal large scale bone defects. It is hypothesized that loading the dual growth factors, bone morphogenetic protein-2 (BMP-2) and vascular endothelial growth factor (VEGF), onto a polymeric coating with two different techniques will result in short term and long term delivery kinetics. We also hypothesized that dual sequential delivery of BMP-2 and VEGF will show enhanced bone repair over BMP-2 delivered alone. We introduced a thin coating of **poly(lactide-co-glycolide) (PLGA),** that has been used for orthopaedic and

musculoskeletal applications, to functionalize rat femoral allografts. Allografts was coated and loaded with **BMP-2 and VEGF** independently and simultaneously using two different loading techniques, surface adsorption and encapsulation, each with distinct delivery kinetics. The rapid release of VEGF stimulated **osteoclastogenesis** and the sustained release of BMP-2 encouraged **osteogenesis**. The bioactivity of the growth factors, BMP-2 and VEGF was evaluated through different bioassays using Human Mesenchymal Stem Cells (hMSCs) and Bone Marrow Macrophages (BMMs), respectively. Healing of rat femoral segmental defect was assessed after 4 and 8 weeks to determine the effect of controlled release of VEGF and BMP-2.

Functionalizing Intact Allografts through Polymer Coating and Growth Factor Delivery

Farzana Sharmin
B.S., Rutgers University, [2008]

A Dissertation

Submitted in Partial Fulfillment of the

Requirements for the Degree of

Doctor of Philosophy

at the

University of Connecticut

[2016]

APPROVAL PAGE

Doctor of Philosophy Dissertation

Functionalizing Intact Allografts through Polymer Coating and Growth Factor Delivery

Presented by
Farzana Sharmin

Major Advisor_____

Yusuf Khan, Ph.D.

Associate Advisor_____

Mei Wei, Ph.D.

Associate Advisor_____

Lakshmi Nair, Ph.D.

Associate Advisor_____

Jon Goldberg, Ph.D.

Associate Advisor_____

Archana Sanjay, Ph.D.

University of Connecticut

2016

Dedicated to my two loving and patient parents

Fatema and Ansarul for their unconditional love and endless support

And to the brightest sunshine of my life, my daughter Aaleena

ACKNOWLEDGMENTS

I would like to take this opportunity to express my gratitude to those people without whom this work would have not been possible. First and foremost, I would like to thank my advisor and mentor, Dr. Yusuf Khan for his constant guidance and support. I am truly grateful for not only the past five years of his advisement, but also for the many more to come. His wisdom and friendship have given me the confidence to recognize my goals, and the courage to pursue them. Dr. Khan's commitment and enthusiasm for research, and never-ending encouragement has made my daily lab atmosphere truly enjoyable. He is the most patient person I have ever met and his way of treating students with respect is incredible. From Dr. Khan, I have learned the true value of patience and dignity. I will try to emulate these two qualities for the rest of my life, and hopefully I can practice them to be a better professional. I am truly indebted to my advisor for giving the opportunity to complete my PhD work under his advisement.

I would like to thank my advisory committee members: Dr. Lakshmi Nair, Dr. Mei Wei, Dr. Sanjay Archana and Dr. Jon Goldberg for their support and expertise. To Dr. Nair, many thanks for sharing your interdisciplinary expertise in chemistry, *in vitro* and *in vivo* work. Your passion toward research makes me enthusiastic going forward in my research career. To Dr. Wei, I owe a debt of gratitude for taking a chance on admitting me into the MSE PhD program here at the University of Connecticut. I have tried my best to make sure that you feel the chance was worth taking. I would like to extend my sincere gratitude to Dr. Sanjay for taking the time to teach me osteoclast cell culture. To Dr. Sanjay, you are truly a great educator and mentor. To Dr. Goldberg, thank you for challenging me during my thesis proposal defense. Your questions and comments made me think thoroughly on the topic and I have tried my best to address all your concerns into my dissertation. I would like to thank Musculoskeletal Transplant Foundation (MTF) and Armed Forces Institute of Regenerative Medicine (AFIRM) for funding my research.

I am especially grateful to all members of the Institute for Regenerative Engineering. Their support and friendship have made my doctoral experience an enjoyable and a memorable period of my life. Heartfelt thanks to Keshia Ashe for our conversations about our research, careers and STEM education. For the rest of my life, I will cherish those memories, and please know, I never want

those conversations to be over. I am forever grateful to Eva Kan for helping me with troubleshooting various assay kits and placing purchase orders. In addition, I would like to thank my mentee and Master's student, Seth Malinowski for his constant help and encouragement with the *in vivo* work.

I owe a tremendous amount of gratitude to Dr. Michael O'Sullivan for his endless support and guidance with animal surgery. I would like to thank Dr. Doug Adams and Ms. Vilmaris Diaz-Doran and Ms. Renata Rydzik for their help with MicroCT. In addition, I would like to thank Ms. Nancy Troiano from histology group at Yale University for her help with histology and imaging, Ms. Maya Yancova for SEM imaging and Ms. Judy Kalinowski for osteoclast cell studies.

Finally, I would like to dedicate my thesis to my family. My family is the source of motivation and support system in my life. I thank my parents for giving me everything that I have ever wanted, and most importantly, unconditional love and endless sacrifices that they made to support my dreams. I thank my loving husband, Dr. Anas Mazady, for proofreading my thesis and always encouraging me and believing in me. I would like to thank my brother, Ovi, for always being there for me and supporting me through everything. I would like to dedicate this thesis to the greatest love of my life, my daughter, Aaleena. You are each a blessing and I am eternally grateful for having you as the invariable constant in my life. This thesis would not have been possible without the support of my family, especially my parents. Lastly and above all else, I would like to thank the Almighty, as it is truly through Him that all things are possible.

Table of Contents

LIST OF FIGURES

LIST OF TABLES

1. INTRODUCTION

1.1. Biology of Bone

Bone is a metabolically active and highly organized connective tissue which constitutes an internal support for all higher vertebrates. The main functions of bone are: a) it is a major organ for calcium homeostasis and a significant store of phosphate, magnesium, potassium, and bicarbonate; b) bones provide mechanical support for the soft tissues; c) it provides protection of internal vital organs; and d) bone is the major site of hematopoiesis in the human adult. By mass, bone is 8% water, 22% protein, and 70% mineral [1]. The organic portion of bone is primarily type I collagen while the inorganic portion is mainly calcium phosphate. Like other connective tissues, the structural organization of bone is a robust ECM coupled with a relatively sparse distribution of cells. Bone cells have the ability to form and deposit calcium phosphate within their extracellular matrixes.

1.1.1. Overview and Structure of Bone

The adult human skeleton has about 213 bones, excluding the sesamoid bones. The appendicular skeleton has 126 bones, axial skeleton 74 bones, and auditory ossicles six bones [2]. Each bone constantly undergoes remodeling during life to help it adapt to changing biomechanical forces, as well as remodeling to remove old, micro-damaged bone and replace it with new, mechanically stronger bone to help preserve bone strength. Cells penetrate throughout the mineralized tissue constantly facilitate new bone formation through the process of *apposition*, in which cells deposit new matrix on existing bone surfaces that eventually becomes

mineralized. At the same time, a distinctly different class of cell resorbs the old bone matrix to make the way for the fresh bone.

The four general categories of bones are long bones, short bones, flat bones, and irregular bones. Long bones include the clavicles, humeri, radii, ulnae, metacarpals, femurs, tibiae, fibulae, metatarsals, and phalanges. Short bones include the carpal and tarsal bones, patellae, and sesamoid bones. Flat bones include the skull, mandible, scapulae, sternum, and ribs. Irregular bones include the vertebrae, sacrum, coccyx, and hyoid bone. The adult human skeleton is composed of 80% cortical bone and 20% trabecular bone overall. Cortical bone, the outer, denser envelope of most bones, plays a major role in the support function and trabecular or cancellous bone, which is metabolically more active and is highly vascular and is responsible for blood cell production.

The long bones are composed of a hollow shaft, or diaphysis; flared, cone-shaped metaphyses below the growth plates; and rounded epiphyses above the growth plates (figure 1.1.1.1). The diaphysis is composed primarily of dense cortical bone, whereas the metaphysis and epiphysis are composed of trabecular meshwork bone surrounded by a relatively thin shell of dense cortical bone. The diaphysis contains the medullary cavity filled with bone marrow. Cortical bone is a very dense material with 5% to 10% porosity. Trabecular bone, commonly found in the end of long bones is highly porous with 50-90% porosity. The periosteum is a fibrous connective tissue sheath that surrounds the outer cortical surface of bone, contains blood vessels, nerve fibers, and osteoblasts and osteoclasts. Periosteum bone formation remains active during our lifespan. In case of bone fracture, periosteum promotes formation of cartilaginous callus, followed by ossification. It also provides vascular and nerve supply to bones and serves as attachment sites for surrounding tendons and muscles. The endosteum is a membranous structure

covering the inner surface of cortical bone, trabecular bone, and the blood vessel canals (Volkman's canals) present in bone. The endosteum is in contact with the bone marrow space, trabecular bone, and blood vessel canals and contains blood vessels, osteoblasts, and osteoclasts. Both cortical and trabecular bones are composed of osteons [3].

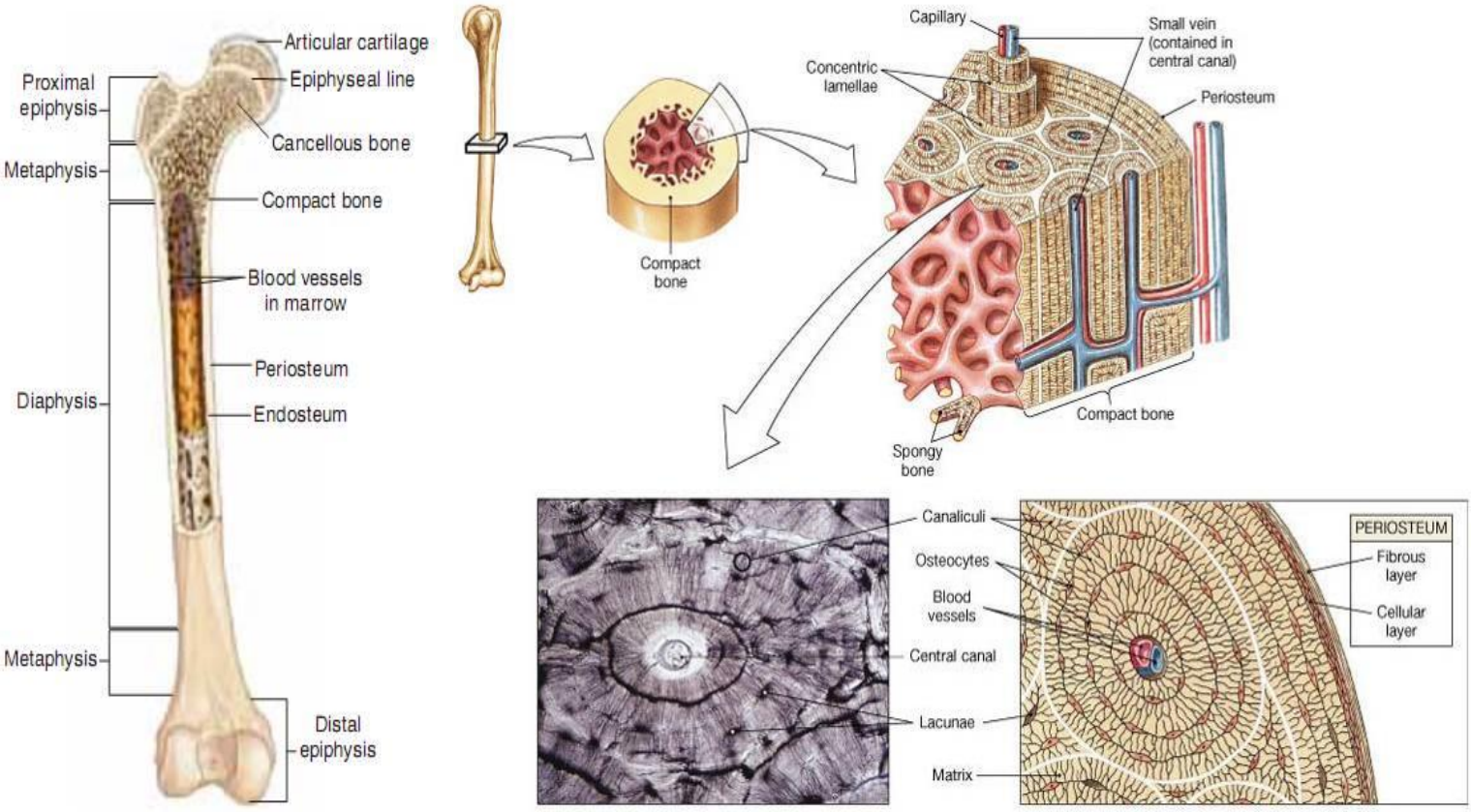

Figure 1.1.1.1 : Diagrams of cortical and trabecular bones in long bone and bone matrix arranged in the form of concentric rings, lamellae, centered around Harversian canals to form osteons [3].

In cortical bone the osteons are known as Haversian systems. In cortical bone, 3-8 lamellae of continuous collagen fibril (50-500 nm) arrange in a concentric manner around a central harversian canal to form osteon or harversian systems. These canals are occupied by blood vessels to supply nutrients.

1.1.2. Bone cells and their functions

Mature bone tissue consists of three primary cell types: osteoblasts, osteocytes, and osteoclasts (figure 1.1.2.1).

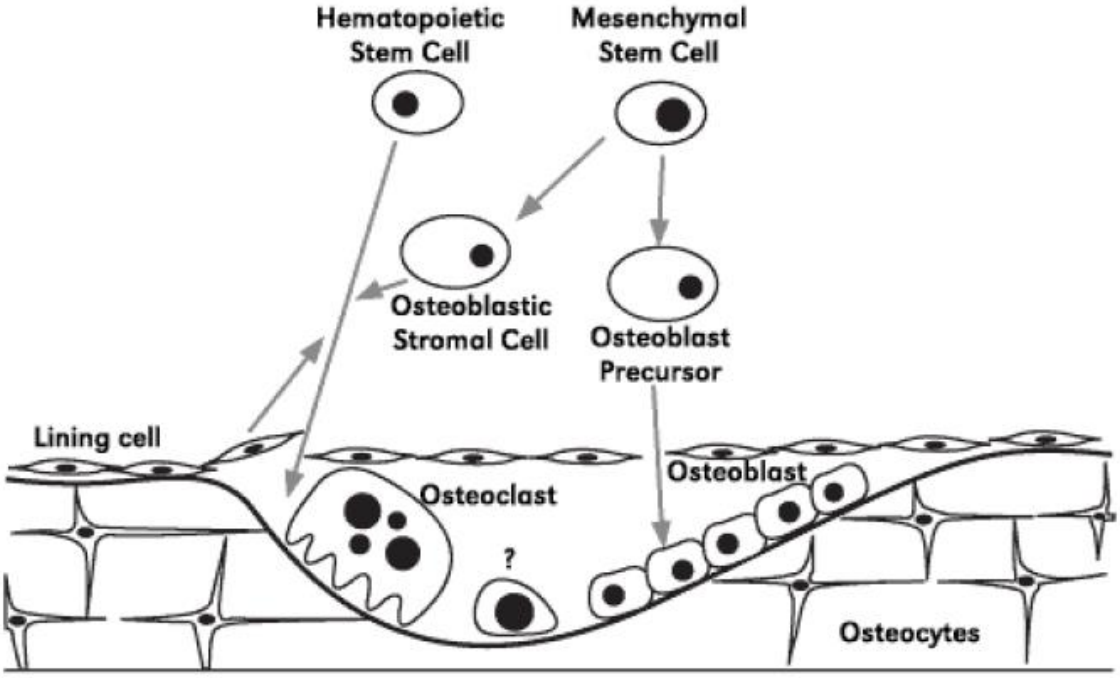

Figure 1.1.2.1: Bone cell types and organizations. Osteoblasts, osteoclasts and bone lining cells reside on the surface of the bone whereas osteocytes are in the interior matrix of the bone. Mesenchymal stem cells differentiate into osteoblasts whereas osteoclast stem from hematopoietic cells [4].

Osteoblasts and osteoclasts are present on the surfaces of bone, while osteocytes permeate the mineralized interior. Osteoblasts are fully differentiated bone cells, present on bone forming surfaces and are responsible for synthesis and regulation of matrix mineralization. Osteocytes are terminally differentiated osteoblasts that are incased by the mineralized matrix and support

overall bone structure. Osteoclasts are large, multinucleated cells that are derived from different cellular precursors (hematopoietic stem cells), and are responsible for bone resorption. Mature bone cells, lacking the ability to divide and proliferate, are formed from proliferative mesenchymal stem cells. During embryonic development, three germ layers are formed; the ectoderm, the mesoderm, and the endoderm. The mesoderm is the middle germ layer consisting of multipotent mesenchymal stem cells that eventually give rise to (among other things) the entire vascular and lymphatic systems and all connective tissue. Several classes of mesoderm-derived stem cells exist and are distinguished according to the types of cells they may become. Mesenchymal stem cells found in the bone marrow or periosteum are capable of being induced to differentiate into osteoprogenitors that can then become osteoblasts, osteocytes, and bone lining cells, whereas osteoclasts originate from the hematopoietic stem cells in blood [5].

1.1.2.1. Osteoblast

Osteoblasts are cuboidal cells that are located along the bone surface comprising 4–6% of the total resident bone cells and are largely known for their bone forming function. Osteoblasts are derived from mesenchymal stem cells (MSC). The commitment of MSC towards the osteoprogenitor lineage requires the expression of specific genes, following timely programmed steps, including the synthesis of bone morphogenetic proteins (BMPs) and members of the Wingless (Wnt) pathways. The expressions of Runt related transcription factors 2 (RUNX2), Distal-less homeobox 5 (Dlx5), and osterix (Osx) are crucial for osteoblast differentiation. Additionally, Runx2 is a master gene of osteoblast differentiation, as demonstrated by the fact that Runx2-null mice are devoid of osteoblasts. Runx2 has demonstrated to upregulate osteoblast-related genes such as ColIA1, ALP, BSP, BGLAP, and OCN. Once a pool of

osteoblast progenitors expressing Runx2 and ColIA1 has been established during osteoblast differentiation, there is a proliferation phase. In this phase, osteoblast progenitors show alkaline phosphatase (ALP) activity, and are considered preosteoblasts. The transition of preosteoblasts to mature osteoblasts is characterized by an increase in the expression of Osx and in the secretion of bone matrix proteins such as osteocalcin (OCN), bone sialoprotein (BSP) I/II, and collagen type I. Moreover, the osteoblasts undergo morphological changes, becoming large and cuboidal cells. The synthesis of bone matrix by osteoblasts occurs in two main steps: deposition of organic matrix and its subsequent mineralization. Osteoblasts are very rich in ALP, which participates in the mineralization process. Osteoblasts deposit about ~0.5 μm of matrix per day and their forming period lasts about 100 days [6-8]. Some of the osteoblasts are then entrapped within the matrix which they formed and are called osteocytes; others become flattened cells on the surface of the bone, and are called lining cells.

1.1.2.2. Osteoclast

Osteoclasts are terminally differentiated multinucleated cells, which originate from mononuclear cells of the hematopoietic stem cell lineage, under the influence of several factors. Among these factors the macrophage colony-stimulating factor (M-CSF), secreted by osteoprogenitor mesenchymal cells and osteoblasts, and RANK ligand, secreted by osteoblasts, osteocytes, and stromal cells, are included. Together, these factors promote the activation of transcription factors and gene expression in osteoclasts. M-CSF binds to its receptor (cFMS) present in osteoclast precursors, which stimulates their proliferation and inhibits their apoptosis. RANKL is a crucial factor for osteoclastogenesis and is expressed by osteoblasts, osteocytes, and stromal cells. When it binds to its receptor RANK in osteoclast precursors, osteoclast formation

is induced. On the other hand, another factor called osteoprotegerin (OPG), which is produced by a wide range of cells including osteoblasts, stromal cells, and gingival and periodontal fibroblasts, binds to RANKL, preventing the RANK/RANKL interaction and, consequently, inhibiting the osteoclastogenesis. Thus, the RANKL/RANK/OPG system is a key mediator of osteoclastogenesis. Parathyroid hormone (PTH) inhibits OPG and thus helps in enhancing RANKL expression (Figure 1.1.2.2.1).

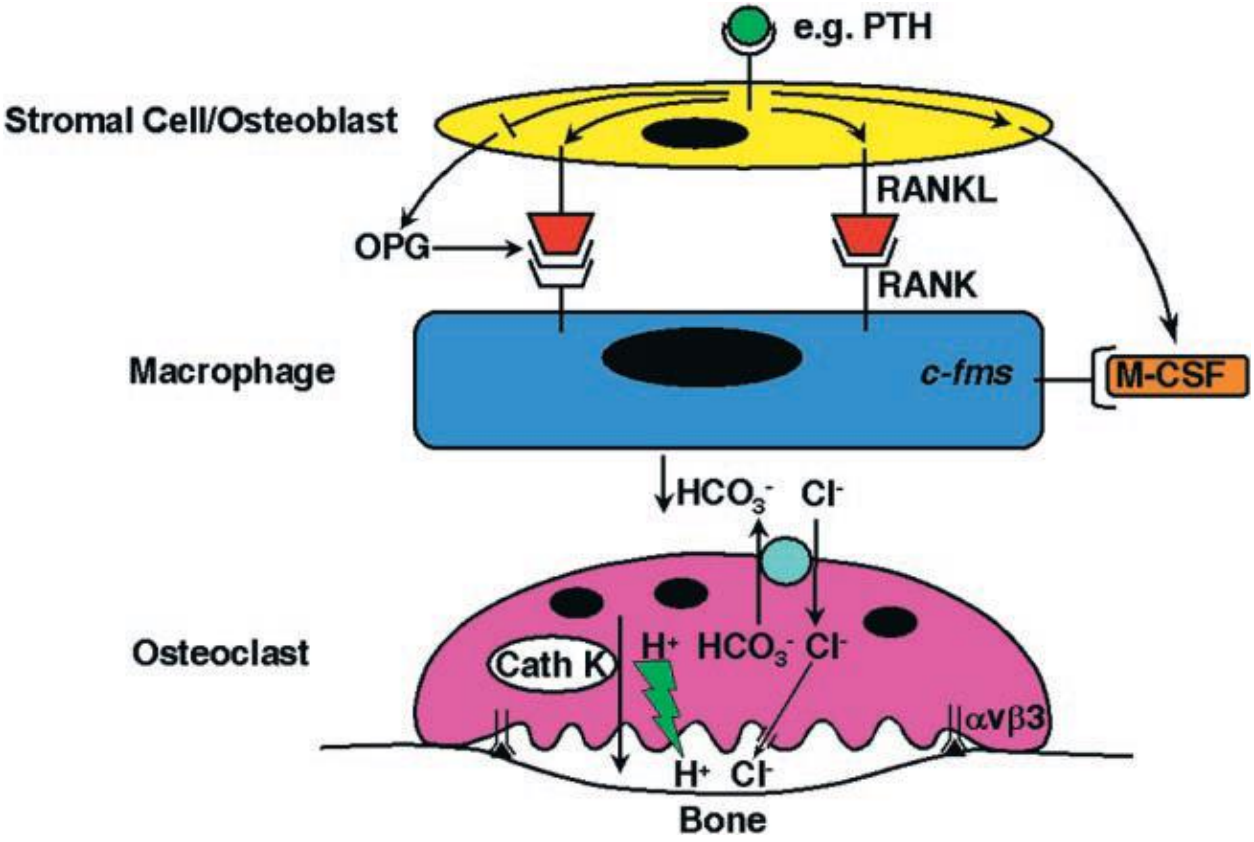

Figure 1.1.2.2.1: Mechanisms of osteoclast formation and bone resorption. Stromal cells and osteoblasts express RANKL and M-CSF, which are up-regulated by osteoclastogenic molecules such as PTH. RANKL and M-CSF, interacting with their receptors on monocyte/macrophage cells, induce osteoclast formation. As these osteoclasts mature and form ruffled membrane, they

acidifies an extracellular microenvironment. Cathepsin K, a lysosome protease cause the degradation of demineralized organic matrix [9].

Osteoclasts are bone dissolving cells that carry out the resorption of mineralized tissue. During bone resorption, osteoclasts attach to the active site of bone surface. They have two distinct plasma membrane regions: a ruffled border where the active resorption occurs and a clear or sealing zone that attaches the osteoclasts to the underlying matrix. Binding of osteoclasts to bone matrix causes them to become polarized, with the bone resorbing surface developing a ruffled border that forms when acidified vesicles that contain matrix metalloproteinases and cathepsin K are transported *via* microtubules to fuse with the membrane. The ruffled border secretes H^+ ions *via* H^+ -ATPase and chloride channels and causes exocytosis of cathepsin K and other enzymes in the acidified vesicles. The sealing zone surrounds the ruffled border and forms the resorption lacuna. In the sealing zone, the osteoclasts secrete hydrochloric acid to acidify and dissolve the hydroxyapatite crystals which constitute the mineral portion of extracellular matrix. The matrix degradation products ae removed from the resorption lacuna and transported into the extracellular space through the basolateral membrane of the osteoclasts. It has recently been demonstrated that the osteoclastogenic potential may differ depending on the bone site considered. It has been reported that osteoclasts from long bone marrow are formed faster than in the jaw. This different dynamic of osteoclastogenesis possibly could be, due to the cellular composition of the bone-site specific marrow [10, 11].

1.1.2.3. Osteocytes

Osteocytes, which comprise 90–95% of the total bone cells, are the most abundant and long-lived cells, with a lifespan of up to 25 years [12, 13]. The morphology of embedded

osteocytes differs depending on the bone type. For instance, osteocytes from trabecular bone are more rounded than osteocytes from cortical bone, which display an elongated morphology. Osteocytes are derived from MSCs lineage through osteoblast differentiation. In this process, four recognizable stages have been proposed: osteoid-osteocyte, preosteocyte, young osteocyte, and mature osteocyte. At the end of a bone formation cycle, a subpopulation of osteoblasts becomes osteocytes incorporated into the bone matrix. Once the stage of mature osteocyte totally entrapped within mineralized bone matrix is accomplished, several of the previously expressed osteoblast markers such as OCN, BSPII, collagen type I, and ALP are downregulated. On the other hand, osteocyte markers including dentine matrix protein 1 (DMP1) and sclerostin are highly expressed. Within the matrix, osteocytes residing in lacunae provide the communication network between adjacent osteocytes, osteoblasts and bone lining cells on the external surfaces of bone by extending out processes within the canaliculi and establishing contact to adjacent cells via gap junctions. Such an extensive network of canaliculi also allows the diffusion of nutrients and metabolites through the mineralized matrix and blood vessels. Moreover, osteocyte apoptosis has been recognized as a chemotactic signal to osteoclastic bone resorption. In agreement, it has been shown that during bone resorption, apoptotic osteocytes are engulfed by osteoclasts. In addition, osteocytes act as mechanosensors in bone. Osteocytes can sense and signal transport functions and promote the translation of mechanical stimuli into biochemical signals to initiate formation or resorption responses [14].

1.1.2.4. Bone lining cells

Bone lining cells are thin, flat and elongated inactive cells that line with bone surfaces. They are originated from osteoblasts but have fewer cytoplasm and organelles. Recent studies

have shown that bone lining cells are able to communicate with the entrapped osteocytes and contribute to the anchorage of hematopoietic stem cells and their subsequent differentiation into osteoclasts. These lining cells secrete matrix metalloproteinase to remove the thin layer of osteoid covering the bone matrix and aid in the attachment of osteoclasts to specific bind sites and initiate bone resorption. After remodeling, a collagen layer is secreted by the bone lining cells to cover the bone surfaces [12].

1.1.3. Bone Matrix and Markers

Bone matrix is composed of both organic (35%) and inorganic components (65%). The inorganic material of bone consists predominantly of phosphate and calcium ions; however, significant amounts of bicarbonate, sodium, potassium, citrate, magnesium, carbonate, fluorite, zinc, barium, and strontium are also present. Calcium and phosphate ions nucleate to form the hydroxyapatite crystals, which are represented by the chemical formula $Ca_{10}(PO4)_6(OH)_2$. Together with collagen, the non-collagenous matrix proteins form a scaffold for hydroxyapatite deposition and such association is responsible for the typical stiffness and resistance of bone tissue. The inorganic phase is comprised of 65% of the bone matrix and play important roles in conferring compression resistance. The non-collagenous proteins contribute to the regulation of hydroxyapatite crystal size, orientation and mineral deposition by binding to calcium or releasing phosphate ion [16, 17,18].

The organic phase is primarily consisted of type I collagen (90% of organic phase). The non-collagenous proteins (10% of organic phase) include: glycoproteins (osteonectin, osteopontin, bone morphogenetic proteins and bone sialoprotein), proteoglycans (hyaluronan, decorin, biglycan and chondroitin sulfate) and a few protein with γ-carboxyglutamic acid (Gla)

(osteocalcin). These proteins regulate the cell differentiation and matrix mineralization via temporal and spatial expression. Figure 1.1.3.1 shows the cellular production of various osteoblastic markers including calcium, osteocalcin (OCN), osteopontin (OPN), alkaline phosphatase (ALP), and collagen type I (collagen I) relative to culture time and their effect on osteoblastic differentiation, proliferation and matrix mineralization.

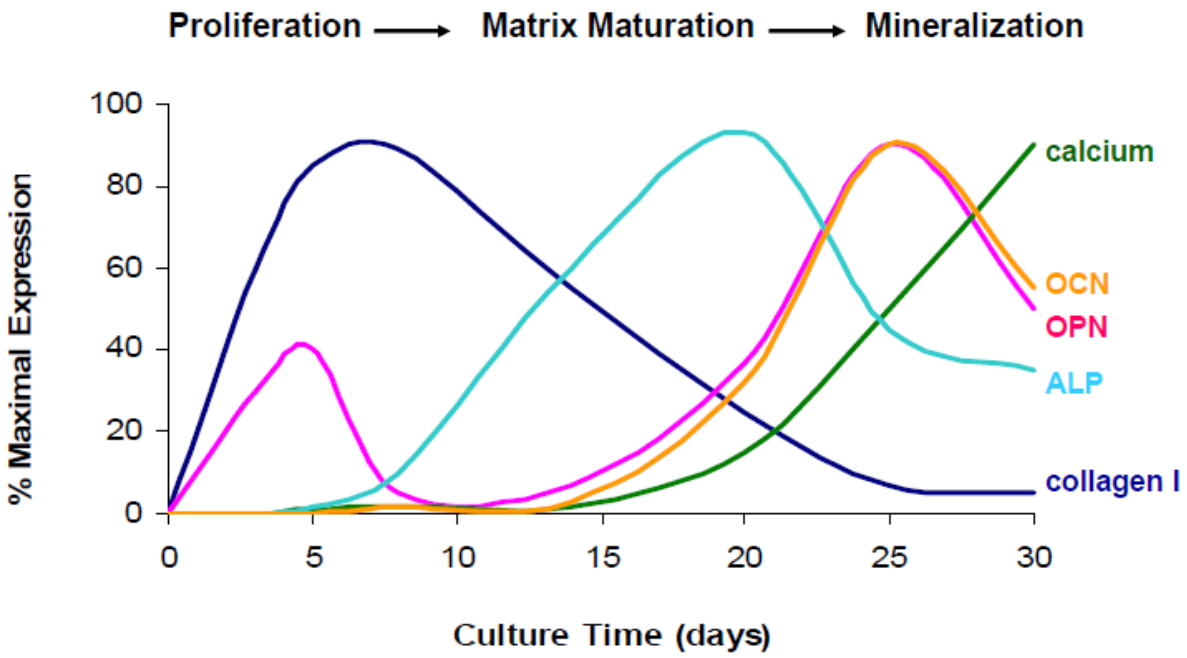

Figure 1.1.3.1: Expression of osteoblast markers shown relative to culture time and their contribution in different phases of f bone matrix formation [15].

Osteopontin (OPN) is a secreted glycoprotein that was originally found in osteoblasts. It is produced by a variety of cells, including preosteoblasts, osteoblasts, osteocytes, endothelial cells, and macrophages, and its synthesis is stimulated by vitamin D3. The role of OPN in mineralization process attributes to 1) inhibition on apatite formation and growth; 2) regulation on the shape of hydroxyapatite crystal. It is also believed that OPN is important in recruiting osteoclast precursors and binding them to the mineralized bone matrix.

Osteocalcin (OCN) is a calcium-binding protein that is the most abundant non-collagenous protein in bone tissue. It is known to have a role in the process of bone mineralization, during which it binds to calcium phosphate in the ECM of osteoblasts. It is primarily synthesized during the matrix mineralization stage of osteoblastic development, but may be marginally produced at earlier stages of matrix maturation. It has been suggested that OCN acts as a chemoattractant for osteoblasts, osteoclasts, and blood monocytes. Most of an organism's OCN is localized within the bone cell matrices, however, when osteoblasts are producing large amounts of OCN during the mineralization phase of osteoblastic development, some OCN is also emitted into the blood. It is for this reason that serum levels of OCN are considered to be indicative of new bone formation.

Alkaline phosphatase (ALP) is an enzyme that is associated with cell plasma membrane. ALP is found in several other non-mineralized tissues including liver, kidney, intestine and placenta. ALP gene expression generally begins when a cell transitions from the proliferative to the matrix maturation stage, peaks during matrix maturation, and then decreases upon entrance of the osteoblastic mineralization stage. The role of ALP in mineralization can be summarized: 1) ALP hydrolyzes phosphate ester and results in the increase of local phosphate concentrate ultimately promoting bone mineral formation; 2)ALP hydrolyzes pyrophosphate, a calcification inhibitor, into phosphate molecules; 3) ALP transfers phosphate groups from the extracellular fluid and binds calcium to facilitate calcium phosphate precipitation [16,17].

Bone resorption markers include an enzyme, tartrate resistant acid phosphatase (TRAP), and products of bone breakdown, which include calcium and bone matrix degradation products such as hydroxyproline, pyridinium cross-links, and telopeptides [16].

1.1.4. Bone Fracture and Repair

There are two different mechanisms of ossification in normal bone healing: intramembranous and endochondral ossification. In either case, mesenchymal cellular condensation first occurs and serves as a template for the subsequent bone formation. Intramembranous bone formation involves mesenchymal progenitor cells differentiating directly into osteoblasts, and the subsequent development of parts of the mandible and clavicle, and many cranial bones. Most bones in the body (i.e., all long bones and vertebrae), however, are formed through endochondral bone formation. This process involves mesenchymal progenitor cells first differentiating into chondrocytes, which are responsible for depositing a cartilaginous template that is later, mineralized and replaced by bone.

Fractured cortical bone is repaired by a callus formation mechanism, in which new bone (callus) composed of fibrous tissue, blood vessels, cartilage, and bone forms in order to bridge the gap between the two fractured bone fragments. This fracture healing process involves four sequential stages: hematoma formation (inflammation), soft callus formation, hard callus formation and bone remodeling (figure 1.1.4.1). These stages often overlap with each other temporally [18,19].

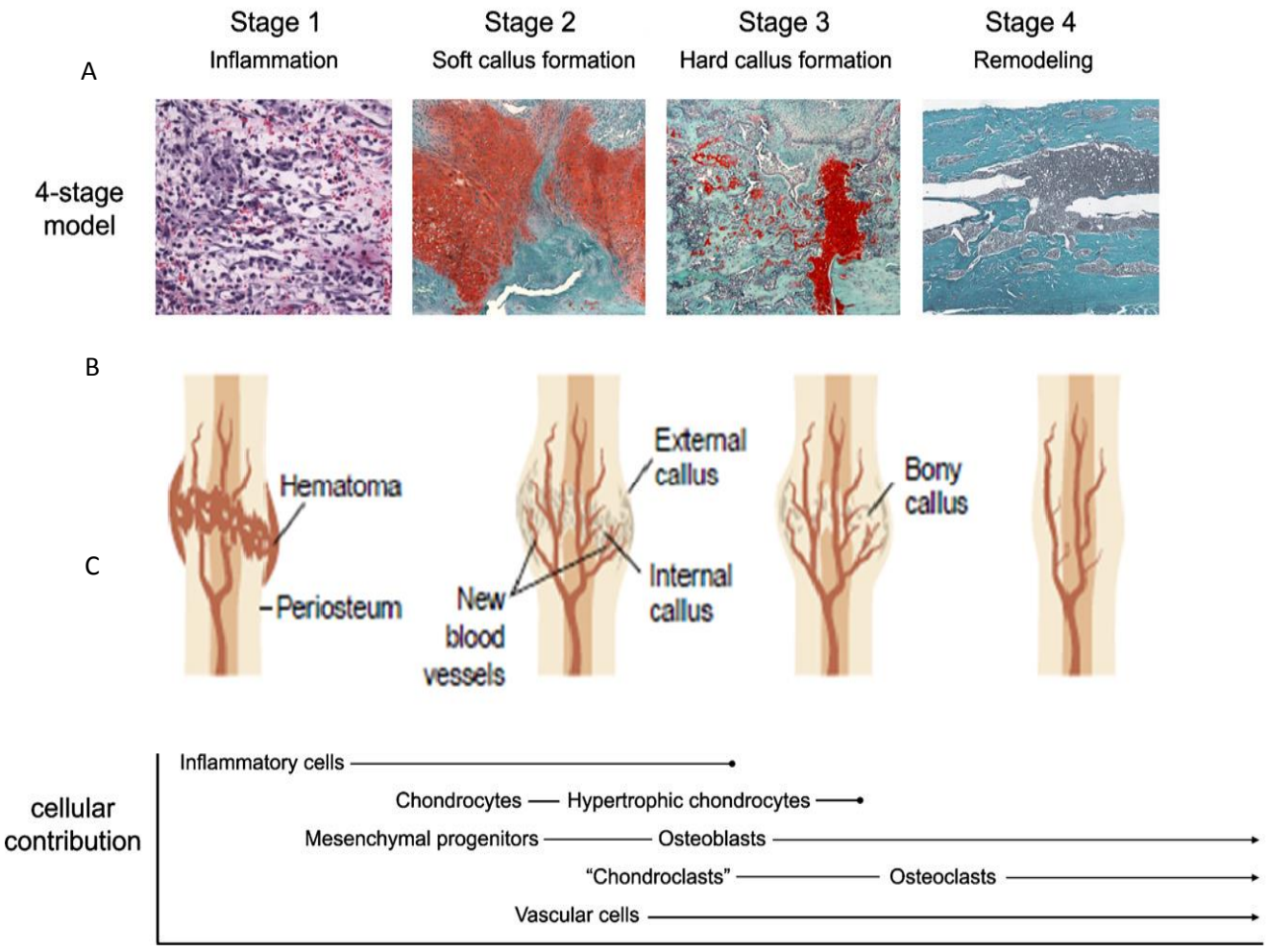

Figure 1.1.4.1: A four-stage model of fracture repair. (A) Histological images of fracture healing showing soft callus is systematically remodeled; (B) Repair of fractures by callus production occurs in four overlapping phases; (C) Cellular contribution to the fracture healing process [18,19].

1.1.4.1. Inflammation

The first stage of cortical bone healing is inflammation. Following the fracture, disruption of blood vessels and normal vascular function causes the activation of non-specific wound

healing pathways. The bleeding results in formation of hematoma between fractured fragments. Degranulated platelets, macrophages, and other inflammatory cells (granulocytes, lymphocytes, and monocytes) infiltrate the hematoma between the fractured fragments and combat infection, secrete cytokines and growth factors, and advance clotting into a fibrinous thrombus. Over time, capillaries grow into the clot, which is reorganized into granulation tissue. Macrophages, giant cells and other phagocytic cells clear degenerated cells and other debris. Eventually, hemostasis is achieved within the hematoma as platelets bind to the fibrillar collagen that forms throughout the site. These platelets release various vasoactive mediators and growth factors in order to influence cell migration, proliferation, and differentiation. New blood vessels are formed from preexisting ones through the process of angiogenesis within the hematoma as inflammatory cells, fibroblasts, and preosteoblasts are recruited by growth factors and cytokines that are released by the inflammatory response. The increased cellular proliferation throughout the injury site is seen within the first 8 hours of post injury and reaches its maximum around 24 hours. In the next few days, the cellular activity subsides and confines to the fracture area. This stage can last up to a month.

1.1.4.2. Soft Callus Formation

The second stage of cortical bone healing is soft (or primary) callus formation, in which a fibrocartilagous callus forms. In this stage, chondrocytes and fibroblasts produce a semi-rigid soft callus that is able to provide mechanical support to the fracture, as well as act as a template for the bony callus that will later supersede it. The growth of the separated cartilaginous regions continues until they unite to generate a big fibrocartilaginous callus bridging the fracture. Finally, chondrocytes become hypertrophic and mineralize the cartilaginous matrix. At the same

time, intramembranous ossification occurs at the periosteum and an external callus is created along the periphery of the fracture.

1.1.4.3. Hard Callus Formation

This stage of bone healing is also known as primary bone formation stage, which is the most active osteogenesis period. It is characterized by high levels of osteoblast activity and the formation of mineralized bone matrix, which arises directly in the peripheral callus. In order for bridging new hard callus to form, the insecure soft callus is gradually removed, followed by revascularization. The new bone is known as the *hard callus* and it is typically irregular and under-remodeled. However, it has an increased diameter compared to the original cortex and thus provides sufficient stability to the defect site. In summary, the primary bone formation phase displays the most rapid osteogenesis, involving (1) bone cell recruitment and woven bone formation; (2) chondrocyte apoptosis, osteoclast recruitment, and mineralized cartilage resorption; and (3) continued neo-angiogenesis.

1.1.4.4. Bone Remodeling

In the final stage of bone remodeling (over 12 weeks), the woven bone hard callus is gradually remodeled to lamellar bone and the size of the callus is decreased to that of pre-existing bone. During this renewal process small pockets of old bone are replaced by new bone. It has been estimated that in humans, as much as 25% of trabecular bone and 3% of cortical bone is resorbed and replaced each year [20]. A remodeling site is initiated by the appearance of osteoclasts (and precursors) following any of several humoral or local stimuli to resorption. The osteoclasts proceed to resorb an amount of bone which produces a small resorption pit

(Howship's lacuna), following which, they move to another site. This resorptive phase is followed by an active reversal phase when the cement line is deposited. During the subsequent formative phase, actively synthesizing cuboidal osteoblasts appear and begin to deposit uncalcified matrix (osteoid) which is later mineralized. Resorption and formation always occur successively in the same location and always in the same order [21]. This sequence of resorption and formation has been referred to as a basic multicellular unit of bone turnover (BMU) as illustrated in figure 1.1.4.4.1. The process of bone resorption followed by an equal amount of formation has been termed coupling. This remodeling phase may take 3 months to several years to complete [20].

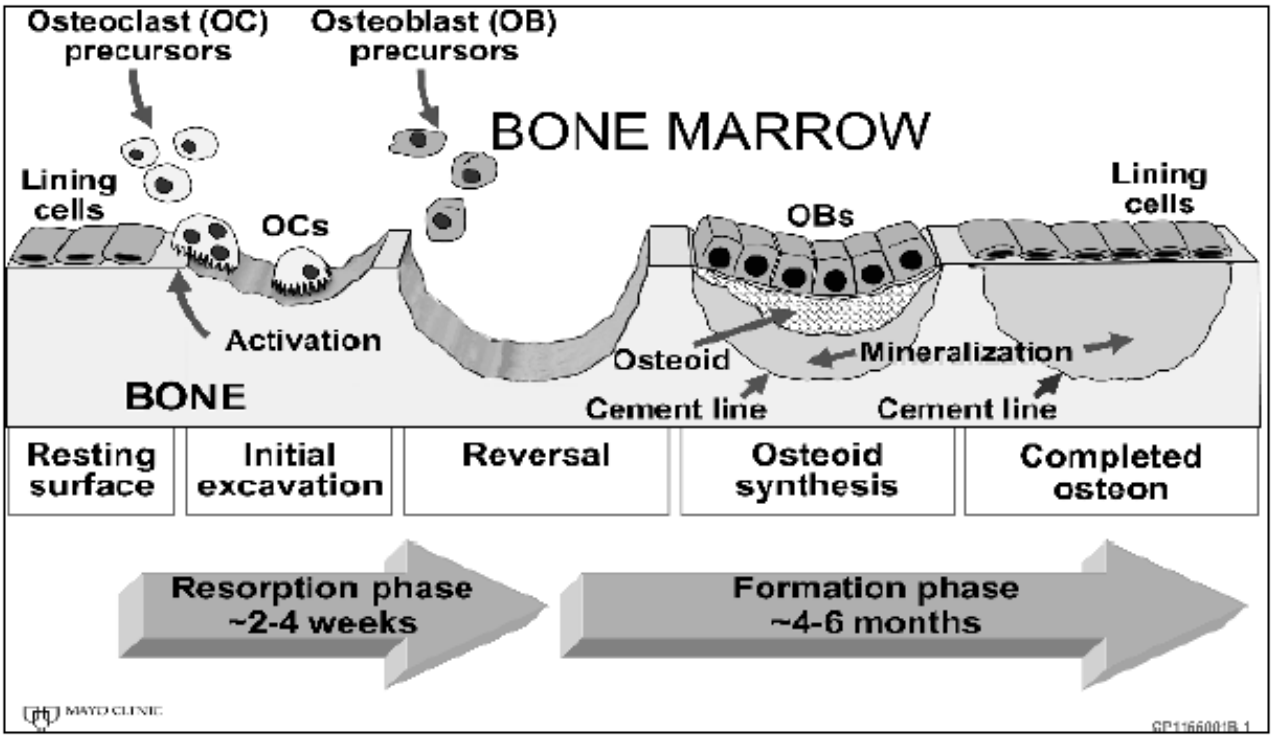

Figure 1.1.4.4.1: The remodeling cycle in bone. Representation of Bone Multicellular Units (BMUs) showing the various stages of cellular activity including resorption of old bone by osteoclasts and the subsequent formation of new bone by osteoblasts. For simplicity of illustration, the cartoon shows remodeling in only two dimensions, whereas *in vivo* it occurs in three dimensions, with osteoclasts continuing to enlarge the cavity at one end and osteoblasts beginning to fill it in at the other end [22].

1.2. Growth Factors Associated with Healing Process

A cell receives information from a growth factor through the binding of the factor to its receptor, which is integrated in the cell's plasma membrane. Each factor is associated with a specific receptor to which it binds with a high affinity in order to stimulate an intercellular response. The signal from the factor-binding may be transmitted to the cell in several different ways, depending on the specific factor-receptor pair. Many growth factors have been purified and their amino acids sequenced, enabling researchers to isolate the corresponding human cDNA. With the cDNA sequences, it is possible to achieve recombinant growth factor expression in pharmaceutical amounts.

As discussed in the previous section bone healing is a very intricate phenomenon that involves many different steps and components throughout its process. Following a fracture, a blood clot is formed at the injury site, causing platelets to release granules to transform the clot into a hematoma. The ECM created allows for inflammatory cells such as neutrophils, monocytes, and lymphocytes to access the hematoma. Along with these inflammatory cells, mesenchymal stem cells (MSC's) are recruited within a couple hours of the fracture. This cellular response is coordinated by and involves the secretion of a range of cytokines and growth factors including transforming growth factor-β(TGF-β), platelet-derived growth factor (PDGF), fibroblast growth factor-2 (FGF-2), vascular endothelial growth factor (VEGF), macrophage colony stimulating factor (MCSF), interleukins-1 and -6 (IL-1 and -6), bone morphogenetic proteins (BMPs), and tumor necrosis factor-α(TNF-α). These factors facilitate the recruitment of additional inflammatory cells in a positive feedback loop, and also the migration and invasion of multipotent mesenchymal stem cells. In the second stage of healing, the differentiation of these MSC's into chondrocytes causes the formation of cartilage. Fibroblast proliferation and

chondrocyte proliferation/ differentiation are stimulated by the coordinated expression of growth factors including TGF-β2 and -β3, PDGF, fibroblast growth factor-1 (FGF-1), and insulin-like growth factor (IGF). Additionally, members of the BMP family assist in promoting cell proliferation and chondrogenesis. Invasion of the soft callus by vascular endothelial cells, angiogenesis, and capillary in-growth is stimulated by pro-angiogenic factors including VEGF, BMPs, FGF-1 and TGF-β. In addition, angiopoietin I and II regulate vascular morphogenesis of larger vessels and development of collateral branches from existent vessels. In the primary bone phase formation, there's an increase in TNF-α, receptor activator of nuclear factor kappa B ligand (RANKL) and macrophage colony-stimulating factor (MCSF), associated with mineralized cartilage resorption, the recruitment of mesenchymal stem cells and induces apoptosis of hypertrophic chondrocytes. Activity of BMP-3, BMP-4, BMP-7, and BMP-8 increase in association with the resorption of calcified cartilage and promote recruitment of cells in the osteoblastic lineage. VEGFs are upregulated to stimulate neo-angiogenesis. In the remodeling phase, osteoblasts and osteoclasts work in combination to create secondary bone and through the process of remodeling restore the bone to its original size, shape, and structure. During this stage the activity of IL-1 and IL-6 increase, whereas RANKL, MCSF, and TGF-β activity slowly diminish. This cascade of events is caused by the presence and activation of different growth factors and cytokines at specific time points. A list of the major growth factors during the different stages of bone healing is shown in table 1.2.1 [23, 24]:

Table 1.2.1: Growth factors associated with fracture healing [23, 24]

Cytokines/Growth Factors	Bone healing stages		Overall action
• IL-1, 6	1.Inflammation	•	• Hematoma

• TNFα • PDGFs • GDF-8 • RANKL, M-CSF • OPG			• Inflammation • MSCs recruitment
• VEGFs • BMPs • TGFβs • Angiopoietin • FGF-I • IGF	2.Soft callus (fibrocartilagous callus) Formation	•	• Chondrogenesis • Endochondral ossification • Osteoblast/Osteoclast precursors recruitment • Vascular ingrowth • New angiogenesis
• VEGFs • BMP-2, 7 • RANKL and M-CSF • Angiopoietin	3.Cartilage resorption and primary bone formation	•	• Chondrocyte apoptosis • Cartilage resorption • Osteoblast/Osteoclast precursors differentiation • Woven bone formation

• IL-1, IL-6 • RANKL and M-CSF	4.Secondary bone formation and remodeling	•	• Bone remodeling • Osteoblast activity • Marrow establishment

1.2.1. Bone Morphogenetic Protein-2 (BMP-2)

Bone morphogenetic proteins (BMPs) are members of the transforming growth factor β (TGFβ) family. They are involved in numerous mechanisms of organogenesis, notably in skeletogenesis. Thus far, around 20 different proteins have been named BMP in humans, but not all members are truly osteogenic. The bone-inducing BMPs can be divided into several subgroups, according to homology of their amino acid sequences. BMP-2 and BMP-4 comprise one subgroup; the second group consists of BMP-5, BMP-6, BMP-7 and BMP-8, while BMP-9 and BMP-10 form the third osteogenic group. The other members of the BMP family do not possess osteogenic properties. BMP-1 is actually a metalloprotease and not a member of the superfamily, whereas BMP-3 and BMP-13 function as BMP antagonists/inhibitors rather than as BMPs [25]. In bone, BMPs are produced by osteoprogenitor cells, osteoblasts, chondrocytes and platelets. After their release, the extracellular matrix functions as a temporary storage for BMPs. The regulatory effects of BMPs depend upon the target cell type, its differentiation stage, the local concentration of BMPs, as well as the interactions with other secreted proteins. BMPs induce a sequential cascade of events leading to chondrogenesis, osteogenesis, angiogenesis and controlled synthesis of extracellular matrix. Of all BMPs, BMP-2 is essential for fracture healing. The BMP-2 signal transduction pathway is complex, but in brief, once BMP-2 has bound to its

receptor complex, a signaling cascade is activated in which the Type II receptor kinase phosphorylates the Type I receptor, which then phosphorylates the intracytoplasmic signaling molecules, Smads 1, 5, and 8. Smads 1, 5, and 8 bind to Smad 4 and then translocate into the nucleus of the cell to activate transcriptional factors for certain osteoblastic genes [26]. Activated transcription factors enhance the expression of the osteoblastic mRNA and ultimately lead to increased production of proteins such as osteocalcin and alkaline phosphatase required for osteoblastic phenotype development, bone remodeling and mineralization. BMP-2 has shown strong osteoinductive activity both *in vitro* and *in vivo*. *In vitro* effects of BMPs are observed at very low dosages (5-20 ng/mL). Normal bone has been estimated to contain about 0.002 mg of BMP per kilogram of pulverized bone. However, current commercially available rhBMPs are used in large dosages (up to 40 mg of some products), probably because of their intense proteolytic consumption during the early stages of post-surgical repair, especially for orthopedic spinal fusion procedures [27]. Animal studies have shown a half-life of 7-16 min systemically, and up to 8 days locally when implanted on a collagen sponge [28]. The possible negative side effects for patients due these high doses of BMP-2 may result in vertebral osteolysis, ectopic bone formation, radiculitis and cervical soft tissue swelling [30].

1.2.2. Vascular Endothelial Growth Factor (VEGF)

Vascular endothelial growth factor (VEGF) is a potent mitogen, which increases the number of capillaries in a given network and is essential for angiogenesis, the mechanism to remodel initial vascular network. VEGF acts as a chemotactic factor for the proliferation of endothelial cells. Under hypoxic conditions, VEGF is upregulated by HIF-1, which stimulates vessel permeability, proliferation/survival, migration and differentiation into mature blood

vessels [30, 31]. It is well known that VEGF is required for effective coupling of angiogenesis to endochondral and membranous bone formation during skeletal development. VEGF plays significant role in osteoblast functionality. Studies have shown that VEGF has dose-dependent chemoattractive effect on primary human osteoblasts and human mesenchymal progenitor cells. Human-derived mesenchymal cells express VEGF and VEGFR-1, a VEGF receptor, during their differentiation and VEGF increases ALP activity in primary human osteoblastic cells [32, 33]. In endochondral ossification, an essential process for formation and growth of long bones, VEGF is responsible for regulating blood vessel invasion (neovascularization) into hypertrophic cartilage. The entering blood vessels bring undifferentiated mesenchymal cells into the mineralization front and later differentiate into osteoblasts and engage in osteogenesis. VEGF also plays a vital role in osteoclast differentiation and bone resorption. Studies showed that VEGF can directly enhance osteoclastic bone resorption. Nakagawa et al., demonstrated VEGF caused a dose- and time-dependent increase in the area of bone resorption pits excavated by the purified rabbit mature osteoclast. They detected two distinct VEGF receptors, KDR/Flk- 1 and Flt-1, in osteoclasts at the gene and protein levels, and VEGF induced tyrosine phosphorylation of proteins in osteoclasts. Thus, osteoclastic function and angiogenesis are upregulated by a common mediator, VEGF [34]. Yang et al. also reported that VEGF regulates survival of mature osteoclasts via VEGFR-2 signaling [35]. Liu et al. showed in a recent *in vivo* study with mutant mice that VEGF can stimulate osteoclast differentiation [36]. They suggested VEGF stimulates osteoclast formation in a paracrine mechanism. Helmrich et al. investigated a cell-based gene therapy approach to generate osteogenic grafts with an increased vascularization potential in an ectopic nude rat model *in vivo*. The study showed that the expression VEGF in the defect site not only improved vascularization but also increased the recruitment of the TRAP and Cathepsin K-

positive osteoclasts [37]. Henriksen et al. conducted a combination of ex vivo bone culture and *in vitro* cell migration assays to study the role of Receptor activator of nuclear factor kappa-B ligand (RANKL) and VEGF in osteoclast recruitment through chemotactic properties during bone regeneration. Results demonstrated that RANKL and VEGF stimulate osteoclast recruitment and induce bone resorption through a signaling pathway different from M-CSF, a well characterized chemoattractant for osteoclasts. Addition of the antagonists of RANKL and VEGF led to reduced recruitment of osteoclasts in ex vivo cultures of embryonic bones [38]. When introduced intravenously, VEGF has a half-life of less than 30 minutes, requiring many doses or massive amounts of growth factor, which can lead to detrimental vessel formation in non-target areas [39]. It is essential to deliver the proper dosage of the growth factor to grow quality neo-vasculature.

1.3. Bone Grafts and bone graft substitutes

A bone graft is surgery to place new bone or bone substitutes into spaces around a broken bone or bone defects. Currently, the United States, as well as other countries worldwide, are experiencing an exceedingly high demand for functional bone grafts, as the statistics have risen above half a million recipient patients and costing over $2.5 billion annually in the United States. This figure not only doubles on a global basis, but is also expected to double by 2020 due to a variety of factors, including the growing baby boomer population and increased life expectancy [40]. Bone grafts are utilized in a wide array of clinical settings to augment bone repair and regeneration. There are four broad clinical situations in which bone grafting is performed: (1) to stimulate healing of fractures, either fresh fractures or fractures that have failed to heal after an initial treatment attempt; (2) to stimulate healing between two bones across a diseased joint. This

situation is called “arthrodesis” or “fusion”; (3) to regenerate bone which is lost or missing as a result of trauma, infection, or disease. Settings requiring reconstruction or repair of missing bone can vary from filling small cavities to replacing large segments of bone up to 12 inches in length; (4) to improve the bone healing response and regeneration of bone tissue around surgically implanted devices, such as artificial joints replacements (e.g. total hip replacement or total knee replacement) or plates and screws used to hold bone alignment [41]. Autografts are considered as the gold standard for bone graft procedure as they contain osteogenic bone cells, marrow cells, and an osteoconductive collagen matrix suitable for new and existing bone cell attachment and migration, as well as osteoinductive proteins and factors endogenous to bone. However, the autograft requires a second surgery at the tissue harvest site, which increases post-operative pain and the possibility of surgical complications at the site. The best alternative to autograft is allograft, tissue taken from a donor or cadaver. Although secondary surgery or donor site morbidity is less of a problem, there is a minimal but real risk of disease transmission from donor to recipient with allografts [42, 43], and there have been reports of additional allograft-associated complications in which as many as 30%-60% of allograft implants encounter some complication when evaluated at the 10-year mark. Bone graft substitutes have been proposed as alternatives to allografts but they have also shown limited tissue ingrowth. Traditional scaffold design supports bone formation through intramembranous ossification with limited to no vascularization leading to graft core necrosis and, thus, poor bone formation. Therefore there is a need to develop a biocompatible scaffold that (i) closely mimics the natural bone extracellular matrix niche, (ii) recruit osteogenic cells to lay down the bone tissue matrix, (iii) contain morphogenic signals to help direct the cells to the phenotypically desirable type, and (iv) allow sufficient vascularization

to meet the growing tissue nutrient supply and clearance needs. Table 1.3.1 demonstrates various bone grafts and graft substitutes and their advantages and limitations [44].

Table 1.3.1: List of graft options for bone repair [44]

Bone Graft	Structural Strength	Osteo-conduction	Osteo-induction	Osteo-genesis
Autograft				
Cancellous	No	+++	+++	+++
Cortical	+++	++	++	++
Allograft				
Cancellous	No	++	+	No
Cortical	+++	+	+	No
De-mineralized Bone Matrix (DBM)	No	+	+	No
Bone graft substitutes				
Coralline HA	+	++	No	No
Collagen-based matrices	No	+	No	No
Calcium phosphate	+++	++	No	No
Calcium sulfate	No	+	+	+
Bioactive silicate	+	++	++	++
Biodegradable Polymers (e.g., PLGA)	+	++	No	+

1.3.1. Autograft

Autografts are currently the gold standard method of bone grafting in which the donor tissue is harvested from the recipient's own body. As autografts intrinsically possess optimal biocompatibility, three-dimensional pore structure, and biological components, they represent the most ideal bone grafting option and boast an 80-90% success rate. In short, the autograft possesses all the requirements for an ideal bone substitute; osteoconductivity, osteogenicity, and

osteoinductivity. However, although the grafted tissue may be optimal at the defect site, the threat of donor-site morbidity and the limited supply of donor tissue impose restrictions on autograft procedures. In fact, there are relatively few bones in the human body that can be harvested without incurring significant morbidity, for example the iliac crest, rib, and fibula. A retrospective study by Silber et al followed the healing of 187 patients who had undergone autologous anterior iliac crest bone graft harvest for anterior cervical discectomy and fusion procedures, all of which were performed by the same surgeon. Patients were interviewed an average of 48 months post-surgery, and reported that although there was a 92.5% degree of satisfaction with the cosmetic result, 26.1% of the patients reported pain at the donor site [45]. Recovery time depends on the injury or defect being treated and the size of the bone graft. Patient recovery may take 2 weeks to 3 months. The bone graft itself will take up to 3 months or longer to heal.

1.3.2. Allograft

Allograft procedures, in which the grafting tissue is harvested from a cadaver, are common alternatives to autografts. The advantages of using structural allografts are: (1) the patient does not have to donate the bone graft, so the surgery is shorter, and there may be less postoperative pain (2) biologic constructs (3) mechanically strong (e.g., cortical allograft) (3) simple to use; grafts can be customized in operating room (4) easily available and inexpensive (vs. synthetic spinal devices) (5) easy radiographic fusion assessment (vs. radiopaque devices). Allograft, removed from organ donor is usually kept in bone banks. The bone bank follows procedures intended to sterilize the bone graft and perform tests on the bone for diseases such as hepatitis and AIDS. The earliest collections of allograft tissue, or bone banks, were established in

the beginning of the 20th century when Bauer refrigerated bone samples for 3 weeks and then implanted them in dogs [44]. Allografts were prepared for storage at this point by chilling or heating, but it was soon determined that boiling the bone samples rendered them inferior in healing to autografts because the endogenous proteins and factors were undoubtedly destroyed during heating. The big leap forward in bone banking came during World War II when new methods of bone storage preparation were studied, including freezing, freeze-drying, deproteinating, irradiating, autoclaving, demineralizing, and chemically treating the harvested bone [46]. The challenge that exists with allografts is to ensure their sterility while imparting appropriate biologic and biomechanical properties to the defect. In order to provide disease-free bone grafts that will not elicit an immune response in the host, the donor tissue must be processed with treatment solutions and/or radiation methods in order to remove cellular and viral components. As a result of sterilization process allograft, void of osteoinductive components show decreased revascularization and graft incorporation. Therefore, an allograft does not always heal as well or as quickly as an autograft. In addition to the loss of osteoinductivity, processing techniques may also alter the mechanical properties of the allograft. Studies have shown the compressive modulus of allographic bone to decrease by 30% after undergoing lyophilization and 10-20% after exposure to gamma radiation [47]. The allograft also carries a risk of transferring infectious diseases, although it is rigidly tested.

Demineralized bone matrix (DBM) is a commonly used allographic form in which donated tissue is morcellized and exposed to a demineralizing agent such as hydrochloric acid in order to remove the mineral content of the bone. This process makes DBM much safer than mineralized allographic tissue, which is more likely to retain viral components in the intact blood spaces such as the marrow and blood vessels. After the decalcification step, all blood elements

are removed from the DBM with subsequent treatment solutions. Depending on the type of demineralizing agent used, DBM has the potential to retain osteoinductive properties from native extracellular matrix that induce cellular differentiation. Morcellized allograft tissue and demineralized allograft tissue (demineralized bone matrix or DBM) have demonstrated better or faster incorporation than intact large allograft bone but neither of these tissue types is load-bearing, considerably reducing their indications and applications [48].

1.3.3. Bone Graft Substitutes

Synthetic bone graft substitutes offer alternative grafting methods that avoid the difficulties associated with conventional autografts and allografts. A variety of commercial implants approved by the U.S. Food and Drug Administration are currently available for clinical use. Materials used to construct synthetic bone grafts range from natural (collagen) and synthetic (poly(lactide-*co*-glycolide)) polymers to ceramics such as calcium phosphates and sulfates and may be used alone or in combination. Although synthetic bone graft options offer virtually unlimited supply and minimal disease transmission possibilities, they do not incorporate every component of the ideal autologous bone graft. A list of commercially available bone grafts is shown in table 1.3.3.1 [49].

Table 1.3.3.1: List of bone graft substitutes that are commercially available [49]

Company	Commercially available product	Composition	Commercially available form	Claimed mechanisms of action
DePuy Spine	HEALOS®	Mineralized collagen matrix	Variety of strip sizes	• Osteoconduction • Creeping substitution • Osteoinduction

				• Osteogenesis when mixed with bone marrow aspirate
	Optecure®	DBM suspended in a hydrogel carrier	Dry mix kit delivered with buffered saline	• Osteoconduction • Bioresorbable • Osteoinduction • Osteogenesis when mixed with autogenous bone graft
Integra Orthobiologics	Integra Mozaik™	80% highly purified b-TCP/ 20% highly purified Type-1 collagen	Strip and putty	• Osteoconduction • Bioresorbable
Medtronic Spinal & Biologics	INFUSE® Bone Graft	rhBMP-2 protein on an absorbable collagen sponge	Multiple kit sizes	• Bioresorbable carrier • Osteoinduction • Chemotaxis of stem cells; indirect Osteogenesis
NovaBone	NovaBone®	Bioactive silicate	Particulate, putty and Morsels	• Osteoconduction • Bioresorbable • Osteostimulation
Biomet Osteobiologics	ProOsteon® 500R	Coralline-derived HA/CC composite	Granular or block	• Osteoconduction • Bioresorbable
Synthes	Calceon® 6	Calcium sulfate	Pellets	• Osteoconduction • Bioresorbable
Stryker Biotech	OP-1® Implant	rhBMP-7 with Type-1 bone collagen	Lyophilized powder reconstituted with saline to form wet sand-like consistency	• Bioresorbable scaffold • Osteoinduction

1.3.4. Challenges Associated with Allograft Healing

Massive bone allografts have been used primarily for limb salvage in orthopaedic oncology and remain an option for reconstructing large bony defects. The primary function of the structural allograft is to provide immediate structural support. Implanted bone allograft can transmit disease, therefore, safety is a prime consideration in the use of allograft transplant. It is reported that fresh allograft can be immunogenic. From least to most immunogenic, rank order is, freeze-dried allograft, fresh- frozen allografts, fresh non vascularized allograft and fresh vascularized allograft. It is necessary to inactivate and remove any harmful agents from the bone to reduce the risk of disease transmission, since only unprocessed, fresh-frozen allografts have been documented as sources of viral infection in recipients of bone grafts. Procedures designed to ensure the supply of safe bone include guidelines on donor selection, tissue quarantine and tissue processing. Long bones are procured under sterile conditions in the operating theatre after organ ex-plantation. The mechanical properties of the bone are excellent as the donors are young. Bone allograft tissue can be processed under strict aseptic conditions or be sterilized at the final stage, usually with irradiation. Some of the processing techniques include demineralization, freeze- drying, fresh- freezing, cryopreservation, and sterilization. Ethanol, acetone and ether are often used, as they have been shown to inactivate coated viruses such as HIV and the hepatitis viruses [50]. Large intact allograft are usually procured sterile from organ donors and stored at -80˚C. All these tissue processing steps eliminates cellular and viral components, growth factors and proteins that were present in the native allograft tissue. As a result, the graft become very desirable for immunity but undesirable for bone repair. The graft completely loses its ability to make bone because of the absence of viable osteogenic cells.

An allograft serve primarily as a spacer that allows osteoconduction of the host cells into its mass, resulting in progressive incorporation of the graft into the host bone. Five-year follow-up studies have demonstrated substantial concerns with allograft incorporation into host bone particularly with intact allograft tissue [51, 52]. Incorporation is a series of events leading to gradual replacement of the old necrotic bone by living new bone as a result of creeping substitution, a mechanism of osteoclastic resorption followed by deposition of new bone. A bone graft is considered to be incorporated when there is no abrupt histological change between the host bone and the graft. Stevenson et al defined successful incorporation as the graft uniting with the host, with the graft-host bone construct able to tolerate physiological loads without fracture or pain. From the perspective of basic science, the complete incorporation is defined as rapid vascularization and substitution of original graft bone with new host bone without substantial loss of strength. The process of bone graft incorporation involves an initial hemorrhage and hematoma within and around the graft that serves to nourish the graft until distinct capillaries and vasculature develops. With the initial injury from surgery, there is an inflammatory response, resulting in granulation tissue ingrowth into the graft. This process of tissue ingrowth will serve to revascularize the tissue and bring osteoprogenitor cells into the graft. Once revascularization is complete, viable cells within the graft and the recipient osteoprogenitor cells will begin to resorb the old bone and form new bone via *creeping substitution* [53]. After new bone is formed, it is mineralized and remodeled. In cortical bone, or cortical-cancellous grafts for that matter, the revascularization and resorption process follows along peripheral haversian canals. Unlike cancellous grafts that incorporate by creeping substitution initiated by osteoblasts, cortical graft incorporation is initiated by osteoclast resorption in a process often called *reverse creeping substitution*. Extensive resorption occurs as early as 2 weeks and increases up to 6 weeks,

resulting in relative weakness that can persist for 6 to 12 months [54]. Incorporation of the cortical bone begins at the graft/recipient junction and proceeds to the center of the graft. However, this intricate process of incorporation is very limited in large segmental allograft and there remains a final bulk of dead bone that has been poorly substituted by new bone. Efforts have been made to overcome this limited substitution by improving the revascularisation of the bone via perforation and the introduction of stem cells and growth factors. Despite this, no major progress in clinical series using massive allografts has been accomplished so far. This reduced incorporation has secondary manifestations that influence the overall healing capacity of the defect site such as poor mechanical integrity at the interface, poor mechanical properties of the allograft. Intact allografts exhibit limited creeping substitution, delayed non-union of the host allograft/implant interface, bone callus bridging of the allograft/implant segment, and limited bone remodeling with increased frequency of fatigue fracture. Each secondary manifestation may lead to failure of the structural allograft and does so as often as 60% of the time according to ten year follow-up studies [55]. Cortical allografts remain significantly weaker than cortical autografts for considerable time after surgery. Given enough time and a weight bearing, stable construct, most segmental cortical allografts eventually resemble autografts biomechanically and structurally, although significantly more un-remodeled necrotic bone remain present in allografts. In autograft healing, both graft and host bones contribute toward healing whereas, large allografts do not contain living cells, therefore, graft incorporation relies only on host cells and tissues. In summary the complications associated with intact allograft healing are: (1) inadequate vascularization; (2) micro-fractures occur in graft areas in which no bony apposition is found and in areas of bone without subchondral resorption; (3) lack of creeping substitution,

osteoclastic resorption of dead bone from the allograft and its replacement by new living bone made by osteoblasts from the host.

1.4. Bone Tissue Engineering

Tissue engineering (TE) aims to replace or facilitate the regrowth of damaged or diseased tissue by utilizing biomaterials, cells, and bioactive molecules alone or in combination with one another. The need for TE stems from the limited availability of autologous tissue and the potential for immunorejection of allogeneic sources and is bolstered by the numerous and growing availability of advanced material fabrication methods of novel biocompatible biomaterials. The strategies involved in designing and building engineered scaffolds are diverse but often focus on the biomaterial as a synthetic extracellular environment to organize cells into a three-dimensional architecture and to present stimuli that can direct the growth and formation of a desired tissue. The promise of TE would empower scientists to grow tissues and organs in the laboratory and safely implant them when the host body is incapable of self-healing. This possibly offers an alternative to organ transplantation, which, although an important clinical tool, has its limitations. The goals of TE integrate so well with the goals of regenerative medicine that as each field progresses, the distinction between them becomes ever less clear.

Recently, a new field has evolved that seeks to unite TE and regenerative medicine with an additional focus on the integration of stem cells, developmental biology, and advanced materials science. This field, termed ‘regenerative engineering’, seeks to integrate these fields in pursuit of the current clinical challenge of complex tissue regeneration where more than one tissue type, often in direct proximity to another distinct tissue type, is regenerated [56]. The complexity of regenerating neighboring tissues with distinct structural and chemical requirements cannot be

underestimated, and mandates a renewed focus on these specific challenges. Regenerative engineering seeks to build on what has been accomplished thus far in TE and regenerative medicine, and move the field forward towards true clinical implementation.

A key moment in organ transplant history was in 1954 with the first successful kidney transplant. Development in the field continued into the 1960s with successful pancreas–kidney, liver, and later in the 1980s with heart–lung, single lung, double lung, and living-donor liver transplants [57]. Despite the utility of organ transplantation there is a real mismatch in supply and demand in respect of organs and tissues available for transplantation. Data published by United Network for Organ Sharing (UNOS) listed only 11,579 people receiving transplants from January 2013 to May 2013, while 76,223 people were recorded as waiting-list candidates (Figure 1.4.1) [126]. While the simple hope of TE is that discrepancies like this would be obviated, its potential full impact is far broader than this: in addition to reducing the need for organ replacement TE, and now with advanced biomaterials science, developmental biology, and a focus on stem cell integration, regenerative engineering could, for instance, greatly accelerate the development of new drug delivery systems that may reduce the need for transplantation through novel drug delivery applications and other novel treatments.

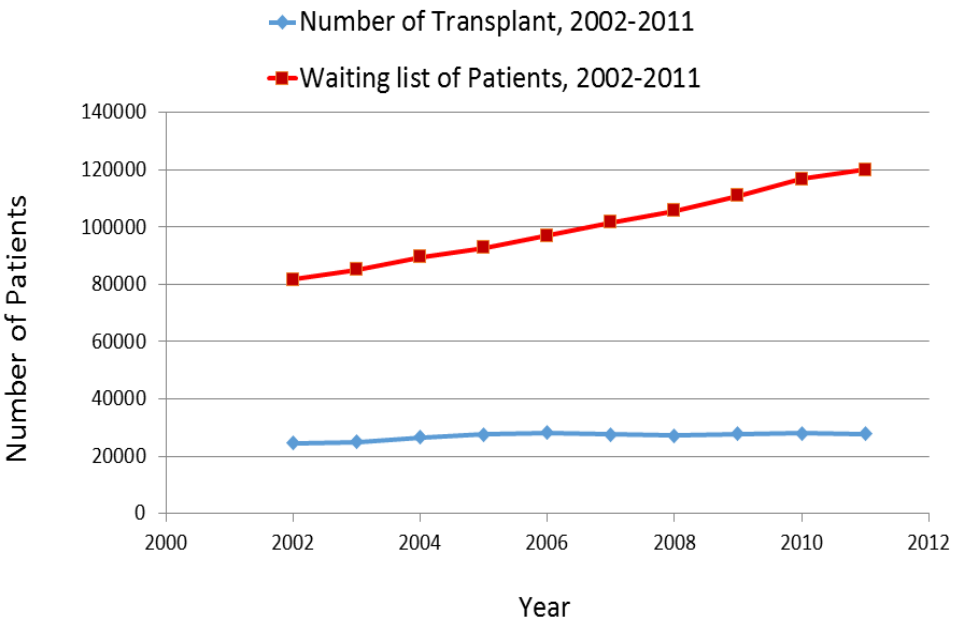

Figure 1.4.1: UNOS organ transplant statistics for 2002 to 2012 [126].

TE approach involves three main components: biomaterials to form a substrate onto which cells and biological molecules can reside; proteins and/or peptides that function to influence cell behavior; and, the cells to build the tissue (Figure 1.4.2). Designing the substrate or scaffold (the first of the three components) onto which new tissue may grow has become a critical part of the development process. Although some scaffolds simply involve the injection of a material into the defect site, those that are designed to provide structural support with a specific architecture require additional preparation prior to implantation. For instance, often the tissue engineer chooses to incorporate biological molecules (the second of the three components) like growth factors or peptides into the scaffold to control proliferation and/or differentiation of progenitor cells to increase the rate of tissue healing. The choice of cells (the third component) that are seeded onto the scaffold to supplement the process of cell migration from the host and therefore accelerate the overall tissue formation can greatly influence the success of the overall repair. These three

components – the design of the scaffolds, the use of growth factors and other biological molecules, and the cells chosen to seed onto the scaffold – are reviewed in depth below. This is not meant as an exhaustive survey of the field as that is beyond the scope of this chapter, but an update on select approaches to tissue regeneration. It will be noted that these three components exist neither alone nor always in combination toward whole tissue regeneration, but rather as a combination of one, two, or three elements.

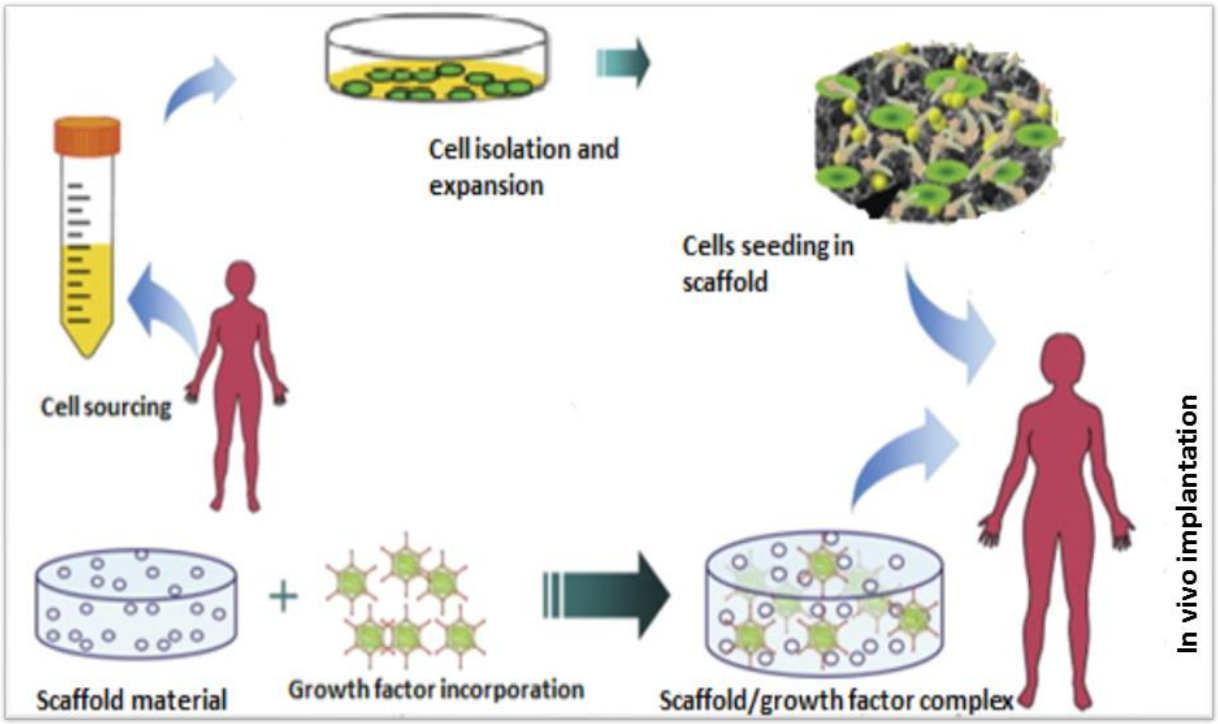

Figure 1.4.2: Tissue engineering paradigm. Cells isolated from donor/source.; seed cells in combination with appropriate growth factors onto scaffold; implant the engineered scaffold in the defect site [126].

Natural biomaterials are widely available in nature and derived from natural sources, mostly from plants, animals, and microorganisms. Recent research has been focused on polysaccharide-derived polymers such as chitin and chitosan, hyaluronic acid (HA), alginate,

starch, and cellulose-based polymers for the development of scaffolds for bone, cartilage, and skin regeneration [58]. Native collagens form the main structural components of the ECM of many tissues, such as bone, skin, teeth, tendons, cartilage, and ligaments. Twenty-seven types of collagens have been identified to date, but collagen type I is the most abundant and widely investigated. A broad range of collagen-based scaffolds have been developed and commercialized in recent times. For example, bi-layered collagen gels seeded with human fibroblasts in the upper layer and keratinocytes in the upper layer have been used as the dermal matrix, an artificial skin product commercialized by Organogenesis in the USA under the name of Apligraf in 1998 [59]. Collagen sponges have been used as an osteoconductive carrier of bone morphogenetic protein (BMP-2) for spinal fusion marketed by Medtronic in the USA [60] Collagraft, commercialized by Angiotech Pharmaceuticals, Inc., Canada, is a mixture of porous hydroxyapatite and tricalcium phosphate and animal derived collagen I, and has been used clinically for the treatment of long bone fractures for more than a decade. Healos Bone Graft Replacement by DePuy Orthopedics, USA, is an osteoconductive matrix constructed of crosslinked collagen fibers that are fully coated with hydroxyapatite. It has been approved recently for clinical use as a bone graft substitute in spinal fusions [62].

The application and use of synthetic polymers in tissue regeneration is relatively recent compared to natural polymers. In the past 50 years with the synthesis of novel synthetic biomaterials, scientists have been able to simulate many key aspects of the extracellular microenvironment [63]. Scaffolds can be produced from a variety of materials, including metals, ceramics, and polymers. Metallic alloys are popular for both dental and bone implants [64] while ceramics with good osteoconductivity have been used for bone tissue engineering [65]. However, both metals and ceramics have significant drawbacks. Metals are not biodegradable and do not

provide a biomimetic matrix for cell growth and tissue formation. Ceramics, meanwhile, also have limited biodegradability and are difficult to process into highly porous structures due to their brittleness. In contrast, polymers have great processing flexibility and their biodegradability can be imparted through molecular design. Therefore, polymers are the dominant scaffolding materials used in TE. In the process of developing scaffolds, synthetic polymers hold numerous advantages over natural materials. Key among those advantages is the ability to tailor mechanical properties and degradation kinetics for various applications. Synthetic polymers can be engineered into various shapes with optimum pore sizes and surface textures, conducive to tissue formation. Furthermore, polymers can be designed with chemical functional groups that can induce tissue ingrowth. Aliphatic polyesters, including poly(glycolic acid) (PGA), poly(lactic acid) (PLA), and their copolymer poly[(lactic acid)-co-(glycolic acid)] (PLGA) are the most widely used synthetic polymeric materials in TE. These polymers are well characterized and have gained FDA approval for certain clinical application (e.g., sutures). PGA is a rigid thermoplastic material with high crystallinity making it less soluble in most organic solvents; a troublesome property if trying to form scaffolds. PGA is widely used in medical application as resorbable sutures (dexon, American Cyanamide Co). The degradation process of the material occurs in two stages: the first stage involves the diffusion of water into the amorphous (non-crystalline solid) regions of the matrix followed by the degradation of the crystalline structure of the polymer. The rapid degradation rate of PGA causes the weak mechanical integrity of the scaffolds [66]. Poly(lactic acid) (PLA) is more hydrophobic and stable against hydrolysis than PGA. PLA degrades to form lactic acid, naturally present in the body. No significant amounts of accumulation of harmful degradation products of PLA have been reported. Both *in vitro* and *in vivo* studies have been carried out to determine the biocompatibility of PLA and PGA. Many studies suggest that these polymers are sufficiently

biocompatible [67, 68]. Poly(lactide-co-glycolide) (PLGA), copolymer of PLA and PGA, has been used in many biomedical applications, for example, sutures, drug delivery devices, and TE scaffolds. Due to its good biodegradability, biocompatibility, and process ability, PLGA has been considered for many TE applications, such as the skeletal muscle [69], bone [70], cartilage [71], ligament/tendon [72], and nerve [73]. Synthetic polymers, such as Polycaprolactone (PCL) a semicrystalline polyester shows very low *in vivo* degradation rate up to 3–4 years. Therefore, it is used in long-term implant delivery devices. PCL films modified with arginine-glycine-aspartate (RGD) peptide (which promotes cell adhesion by acting as a binding site for integrins) served to promote the attachment and spreading of mesenchymal stem cells (MSCs) [74]. Other synthetic biodegradable polymers, including poly(3-hydroxybutyrate) (PHB) [75], polyurethanes (PU) [76], polycarbonate (PC) [77], poly(ortho ester) (POE) [78], poly(propylene fumarate) (PPF) [79], and polyphosphazenes (PP) [80] have also been used as scaffolding biomaterials. Biodegradable bioceramics are designed to aid in the self-repair processes of the living organism, and are subsequently resorbed. Tricalcium phosphates, calcium sulfates, HA, and certain compositions of glasses and glass-ceramics have been recently investigated as biodegradable bioceramics.

Hydrogels can be used as space-filling scaffolds, for cell delivery, and for bioactive molecule delivery [81]. Gilbert *et al.* demonstrated how adult muscle stem cells on engineered hydrogel substrates can be proliferated *in vitro* with higher efficiency, leading to better host tissue integration. These stem cells would normally lose their pluripotency and undergo massive cell death within the first weeks of culture on rigid plastic culture dishes. However, when cultured on chemically crosslinked bioactive poly(ethylene glycol) (PEG) hydrogels, the cells showed signs of self-renewal and were engrafted with substantially better integration in a muscle implant model [82]. Hydrogel-based products have been made available for patient care in the recent years. For

example, soft contact lenses are typically made from poly(hydroxyethylmethacrylic) acid [poly(HEMA)] while biological adhesives routinely used in surgical procedures have been made from reconstituted fibrin or albumin. Hydrogels are currently extensively investigated for bone, cartilage, intervertebral, and cardiac regeneration. Moreover, 'smart' hydrogels are raising significant interest due to their ability to change shapes. They can dynamically shrink, swell, or degrade based on exposure to changing stimuli such as pH, temperature, and other activators. They are often used for vascular applications, since their smart capabilities allow them to be maneuvered through small, tight pathways [83].

One of the most important aspects of regenerative engineering is to have cells that are able to differentiate and proliferate based not only on the cell type, but also the environment that surrounds them. The scaffold acts similarly to an ECM, creating an environment that is conducive to integration, differentiation, and cell growth. With that in mind, it is extremely important to select a cell source that not only matches the overall goal of the implantation, but that also integrates well with compatible scaffolding. Obtaining cells that are able to differentiate and proliferate to the correct degree is imperative in successful tissue regeneration, as many damaged tissues are not able to regenerate the native tissue to an acceptable extent. The most common types of stem cell used are progenitor stem cells. These cells, while having undergone some degree of differentiation, are still able to differentiate into multiple lineages. They can also be isolated, cultured and differentiated into the appropriate lineage before being transplanted into the patient. Human mesenchymal stem cells (MSCs) are of particular interest due to their multilineage potential, being able to differentiate into many different cell types like osteogenic, adipogenic, and chondrogenic [84]. They are used for vastly different functionalities, treating hundreds of symptoms from a wide spectrum of ailments [85]. Neural stem cells (NSCs) are used for differentiation into almost all

types of neural lineages, but there a large amount of difficulty has been encountered in creating the desired type and number of cells when expanding the NSCs. Epithelial stem cells have been used for skin grafts, as well as things such as ocular regeneration. Considerable research efforts have been directed toward human induced pluripotent stem cells (hiPSCs) that are able to differentiate into many lineages, acting very similarly to ESCs [86]. These hiPSCs are capable of different functionalities and are also procured much more easily than most other stem cell types. They are created by inducing a forced expression of specific genes in order to cause a specific expression. Cells are often taken from bone marrow, hair keratinocytes, or skin fibroblasts to create an array of functions, as noted by Streckfuss-Bomeke *et al* [87]. Somewhat similar to MSCs, it has also been found that it is possible to extract stem cells from the amnion and amniotic fluid that have similar capabilities. Corradetti *et al*. showed that MSCs from the amniotic fluid are capable of many different functions from their original lineages [88]. With so many different types of stem cells to choose from for tissue regeneration procedures, steps must be taken to ensure the correct cell type is selected. Grompe *et al*. created a tracing system in order to show the differentiation process of stem cell systems [89]. This allowed for better selection of different cells for different functions. In order to harvest the stem cells for implantation, they must first be isolated and expanded in culture. Because it is difficult to harvest a large number of stem cells, expansion is important in order to have a viable level of cells for transplantation. The environment and methods to culture the stem cells is of particular importance, as it can result in changes to the growth rate and extent of the expansion.

Growth factors are therapeutic agents for tissue regeneration. Different growth factors are used in order to create differentiation of cells towards a specific phenotype. The following are some of the more commonly used growth factors given their efficacy and the tissue types they

have been found to repair and regenerate effectively: nerve growth factor (NGF), epidermal growth factor (EGF), vascular endothelial growth factor (VEGF), and bone morphogenetic proteins (BMPs). Nerve growth factor is normally used to help with nerve damage and neurodegenerative disorders. NGF is used to maintain neuronal survival and promote axonal elongation. It has also been used to treat disorders such as Alzheimer's disease or Huntington's disease [90]**.** By promoting neuronal growth, NGF can be used for brain and spinal cord injuries. Bone morphogenetic proteins are used extensively and have been called the gold standard for enhancing bone formation and cell proliferation [91]. Due to their extensive osteoinductive properties and ability to stimulate osteoblast proliferation, BMPs are able to help form new bone, as well as help it continue to grow. They are applicable for bone defects almost anywhere within the body. Vascular endothelial growth factor is a growth factor that is used to form blood vessels. Its job is to not only induce endothelialization of existing vessels, but also to promote angiogenesis (the process of forming new blood vessels from pre-existing tissue). VEGF can also recruit endothelial cells to migrate to where they are needed. Epidermal growth factor is a growth factor used for skin injuries such as incisions and burns. It supports epidermal cell growth, proliferation, and migration. It is also able to catalyze the creation of collagen to help with wound healing. It is used to engineer new skin, as well as heal existing skin [92]. Using these (or similar) growth factors, many different cell types can be proliferated and differentiated. Tissue engineered scaffolds incorporate these growth factors to ensure that the correct type of cells are created to treat the defect. In order to do this, it is important to know how the growth factor will react with the extracellular matrix of the scaffold, as well as to the material of the scaffold itself.

1.5. Poly(lactide-co-glycolide) (PLGA) and its Application in Tissue Engineering

Poly (lactide-co-glycolide) (PLGA) is the copolymer of poly-(lactic acid)/polylactide (PLA) and poly-(glycolic acid)/polyglycolide (PGA). Poly lactic acid contains an asymmetric α-carbon which is typically described as the D or L form in classical stereochemical terms and sometimes as R and S form, respectively. The enantiomeric forms of the polymer PLA are poly D-lactic acid (PDLA) and poly L-lactic acid (PLLA). PLGA is generally an acronym for poly D,L-lactic-co-glycolic acid where D- and L- lactic acid forms are in equal ratio (figure 1.5.1) [93]

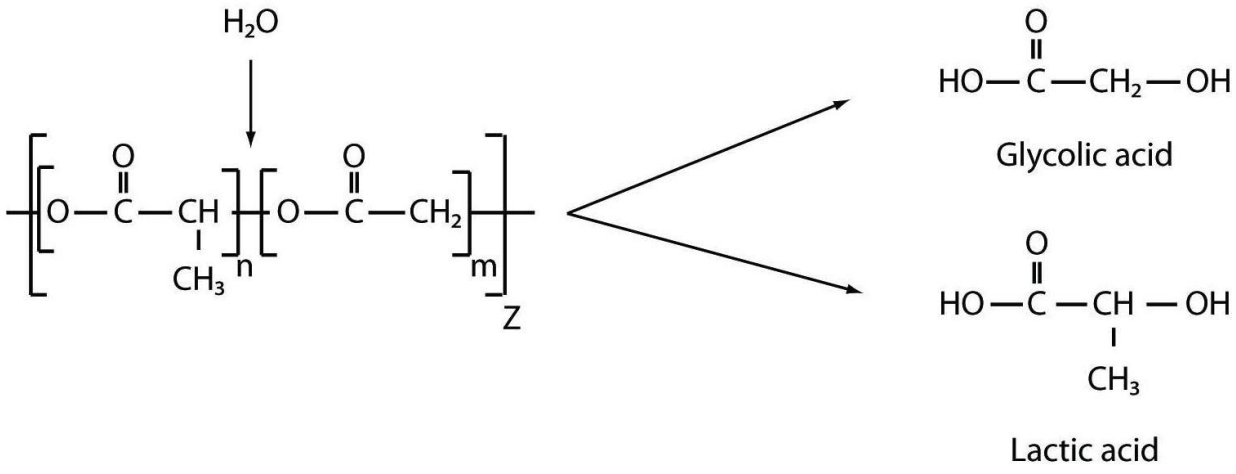

Figure 1.5.1: Chemical formula of poly(lactide-co-glycolide) (PLGA) [93]

PGA has highly crystalline structure and higher hydrophilicity and faster degradation rate, whereas PLA has less crystalline structure and shows poor hydrophilicity and slow degradation rate. Crystalline PGA, when co-polymerized with PLA, reduces the degree of crystallinity of PLGA and as a result increase the rate of hydration and hydrolysis. PLGA copolymers are amorphous in nature with glass transition temperature between 45 and 55°C. Higher content of PGA leads to quicker rates of degradation with an exception of 50:50 ratio of PLA/PGA, which exhibits the fastest degradation, with higher PGA content leading to increased degradation

interval below 50%. For instance, PLGA 50:50 degrades at a faster rate as compared with PLGA 85:15 due to the higher hydrophobic lactide content of the latter. PLGA undergoes hydrolytic degradation in aqueous environment where ester linkages present along the polymer backbone are randomly hydrolyzed to lactic and glycolic acids that are finally broken down to form energy, carbon dioxide and water by the normal metabolic pathways of the body. The degradation of PLGA copolymer is the collective process of bulk diffusion, surface diffusion, bulk erosion and surface erosion. The degradation time of the frequently used PLGA family of polymers ranges from 1 to 2 months for completely amorphous PLGA 50:50 and up to 1–2 years for the semi-crystalline poly L-lactide (PLLA). As a drug delivery vehicle PLGA shows biphasic release pattern. The initial burst release of drug occurs as water penetrates into polymer matrix, causes random scission of PLGA and drug on surface of the polymer release through desorption. The sustain release of drug occur when the polymer breaks down by hydrolysis into soluble oligomeric and monomeric products and creates a passage for drug to be released by diffusion and erosion until complete polymer dissolved [94]. PLGA polymers are easy to process as they are soluble in wide range of solvents such as dichloromethane, tetrahydrofuran, ethyl acetate, chloroform, hexafluoroisopropanol, acetone and benzyl alcohol. Table 1.5.1 shows physical and chemical properties of PLGA, PLA and PGA [95].

Table 1.5.1: Physical and Chemical properties of PLGA compositions [95]

Polymer	Inherent viscosity (dl/g)	Density (g/ml)	Crystalline melt transition (°C)	Glass transition temp (°C)	Solubility (at 5% w/w)	Approx. degradation (months)
50:50 DL-PLG	0.55–0.75	1.34	Amorphous	45–50	1 2 3 4 5 6	1–2
65:35 DL-PLG	0.55–0.75	1.30	Amorphous	45–50	1 2 3 4 5 6	3–4
75:25 DL-PLG	0.55–0.75	1.30	Amorphous	50–55	1 2 3 4 5 6	4–5

85:15 DL-PLG	0.55–0.75	1.27	Amorphous	50–55	1 2 3 4 5 6	5–6
DL-PLA	0.55–0.75	1.25	Amorphous	50-60	1 2 3 4 5 6	12–16
L-PLA	0.90-1.20	1.24	173–178	60-65	1 4 5	>24
PGA	1.40-1.80	1.53	225–230	35-40	5	6–12

Solvents: 1 = dichloromethane; 2 = tetrahydrofuran; 3 = ethyl acetate; 4 = chloroform; 5 = hexafluoroisopropanol; 6 = acetone.

1.6. Growth-Factor Loading Techniques

Incorporating growth factors to bone grafts/ substitutes can encourage osteoinductivity in the defect site. The growth factors are expected to be delivered to cells seeded on the scaffold or localized at the defect site and stimulate the differentiation of osteoprogenitors down the osteoblastic lineage. The choice of which growth factor to load depends on the inductive effects that one hopes to impart on the targeted cells. For example, growth factors such as insulin-like growth factor-1 (IGF-1), bone morphogenetic protein-2 (BMP-2), and vascular endothelial growth factor (VEGF) induce cellular differentiation towards adipose, osteoblast, and endothelial lineages, respectively. With the appropriate growth factor selected, the loading method is next to be considered. As proteins, the activity of growth factors depends on their conformation and ability to interact with their cellular receptors. Growth factors may be denatured if exposed to extremes in temperature or pH and must therefore be loaded under appropriate conditions. Therefore, while loading the protein it is imperative to consider that the loading method doesn't denature the protein conformation and also maintains a sufficient concentration of the growth factors that mimics the physiological range for bone regeneration. In order to do this, the growth factor must be bound to the system in such a way that causes the desired release kinetics. The timing and duration of release, as well as how it is administered, are very important to optimize healing. Growth factors *in vivo* degrade due to denaturation, oxidation, or proteolysis. These

challenges must be controlled if the factors are to be delivered from an implanted construct to achieve a release profile that can mimic that of the natural healing process.

1.6.1. Non-Covalent Growth Factor Immobilization

Strategies for non-covalent binding of growth factors into carrier matrix include physical encapsulation and surface adsorption. Growth factors can be physically entrapped into scaffolds by dispersing the proteins into the scaffold material prior to scaffold construction. Scaffolds used for physical encapsulation can be designed to have specific mechanical properties, degradation rates, and porosity to elicit desired cellular responses. These types of growth factor delivery systems can be created using techniques such as phase separation, solvent casting and particulate leaching, melt molding, freeze drying, phase emulsion, and gas foaming. There are many different fabrication methods for physical encapsulation, all with different benefits and drawbacks that make them effective in certain applications. The table below outlines the most common techniques, along with their advantages and disadvantages.

Table 1.6.1.1: Growth Factor Encapsulation Techniques [39]

Technique	Advantages	potential disadvantages
solvent casting/particulate leaching	control over porosity, pore sizes and crystallinity; high porosity	residual solvents and porogen materials; limited mechanical properties
freeze drying	high porosity and interconnectivity	limited pore sizes range (15–35 μm)
phase separation	high porosity	limited pore sizes, residual solvents (1–10 μm)

Technique	Advantages	potential disadvantages
melt moulding	control over macrogeometry, porosity and pore size; free of harsh organic solvents	high temperatures
high internal-phase emulsion	control over porosity, pore size and interconnectivity	limited polymer types and mechanical properties
in situ polymerization	injectable; control over mechanical properties	residual monomers and cross-linking agents, limited porosity
gas foaming	free of organic solvents; control over porosity	pore interconnectivity

Both natural and synthetic biomaterials can be to design three- dimensional scaffolds to load and deliver growth factors for bone regeneration. Synthetic polymers such as aliphatic polyesters, including poly (glycolic acid) (PGA), poly(lactic acid) (PLA), and their copolymer poly[(lactic acid)-co-(glycolic acid)] (PLGA), poly(ε-caprolactone) (PCL) and its copolymer are the most widely used for encapsulating growth factors into polymeric delivery systems. These scaffolds can be engineered into different shapes such as sphere, cylinder, thin-films etc. depending on the parameters necessary for the specific experiment. Gelatin, silk fibroin, cellulose, chitin and chitosan, hyaluronic acid (HA), alginate, and collagen are natural carrier materials that have been used for delivering bone growth factors due to their protein affinity, biocompatible byproducts, and mild processing conditions. Being fully encapsulated, the loading and release kinetics of the growth factors are controlled largely by the physical, chemical and biological properties of the polymers. In PLGA, polymer composition is the most important factor in hydrophilicity and degradation of the polymer and hence in controlling release rate of

the protein. PLGA 65:35 shows higher degradation than PLGA 75:25. Presence of higher ratio of highly crystalline PGA makes PLGA polymer more hydrophilic and thus exhibits faster degradation and drug release rate [94].

The approach of loading proteins on pre-made scaffolds presents an attractive option for tissue engineered growth factor delivery. Furthermore, the surface area that the growth factor contacts is the same as that which cells eventually approach, making the proteins more accessible to the cells than if they were hidden within the material. Depending on the protein's hydrophilicity, they tend to desorb from the scaffold too quickly upon implantation in a "burst" effect. Deluca et al. have reported a series of experiments in which they loaded BMP-2 on porous PLGA microspheres by soaking the spheres in the BMP-2 concentrated solution. Deluca et al. defined "bound" (adsorbed to the surface of the PLGA microsphere) and "free" (physically entrapped within the pores of the microsphere) proteins [96,97]. They reported that increasing NaCl and buffer concentrations decreased the amount of protein adsorbed to PLGA. It was suggested that relative to the pI of the BMP-2 (~9) and the pKa of the PLGA (~3), there exists an intermediate pH range in which the positively charged protein and the negatively charged carboxylic acid end groups on the polymer interact via isoelectric bonding. Increased number of ionic species in the buffer was determined to have caused charge shielding, which resulted in the decrease of attractive forces between the polymer and protein. A subsequent study by the Deluca group investigated the effect of different properties of the polymer on protein-loading [98]. Microspheres made from a range of hydrophilic and hydrophobic PLGA were constructed by varying the molecular weight (MW), polydispersity, and acid number of the polymer and BMP-2 was incorporated. PLGA with various degrees of end-capping were used in order to adjust the polymer acid number of the microspheres, which was directly related to the number of free

carboxylic acid functionalities. Higher acid values showed an increase in BMP-2 binding. Also, hydrophilic PLGA, which had greater acid numbers and therefore greater ionic reactivity than the hydrophobic form, exhibited the greatest protein adsorption capacity. By increasing the polymer acid number, the group effectively provided more negative moieties per unit of scaffold surface area on which the positively charged protein could adsorb. The MW of the polymer is also linearly correlated with the protein binding.

1.6.2. Covalent Growth Factor Immobilization

Covalent tethering of growth factors is another way of incorporating growth factor to scaffolds. This method allows prolong availability of growth factors, spatial control of growth factors and reduce the required doses of growth factors, subsequently reduce the cost and the efficacy of growth factor based devices. In order to load growth factor using the tethering method reactive groups need to be available both in the growth factors and substrates. Utilizing crosslinkers such as water-soluble carbodiimide (e.g., EDC), monoacrylated PEG-succinimidyl ester, and photo-immobilization to functionalize growth factors and then bind to polymers are commonly used methods for covalent immobilization of growth factors. Sulfosuccinimidyl- 4-(N-maleimidomethyl)cyclohexane-1-carboxylate (sulfo-SMCC) is a heterobifunctional crosslinker that has been used to tether VEGF to agarose, collagen, PEG-dA hydrogel [99, 100] as well as PDGF-BB to demineralized bone [101] and BMP-2 to PCL, chitosan and collagen [102,103]. Scaffolds modified with immobilized VEGF and BMP-2 showed improved neovascularization and mature bone formation, respectively, *in vivo* [104].

1.6.3. Growth Factor Loading and Delivery Systems

Bone healing is a complex process where multiple growth factors play important role in concert. Therefore, it is imperative to obtain a delivery system that can maintain inherent ECM structure of bone as well as load and deliver multiple growth factors mimicking natural bone healing. To this end, Kolambkar et al. designed a growth factor delivery system consists of an electrospun nanofiber mesh tube for guiding bone regeneration combined with peptide-modified alginate hydrogel injected inside the tube for sustained rhBMP-2 release [105]. Kempen et al. fabricated a composite scaffold consisting of PLGA microsphere loaded with BMP-2 embedded in a poly(propylene) scaffold surrounded by a gelatin hydrogel loaded with VEGF to obtain sequential delivery of growth factors[106]. Following the same trend, dual release of TGF-b1 and IGF-1 through gelatin-loaded microspheres incorporated in oligo(poly (ethylene glycol)fumarate) (OPF) hydrogels was evaluated for cartilage repair [107]. Richardson et al. engineered a PLG microsphere based system where PDGF were encapsulated into the polymer with lyophilized VEGF to promote angiogenesis in bone healing [108].

Release kinetics of growth factors depend on the way protein is loaded on the scaffold, as well as on the environmental factors of the release medium. If a factor is released too quickly, it may diffuse away from the target site and not have enough time to interact with local cells. A burst release might even induce a toxic result if the protein is immediately presented to cells in too high of a concentration. Contrariwise, an overly slow release of growth factors may cause denaturation of the proteins. Since healing of bone is a complex multidimensional process, researchers are investigating scaffold systems that are capable of delivering multiple growth factors in a temporal and spatial manner. However, controlling the rate and dosage of growth factors is not a standardized procedure. In general, factor delivery is most important during the first few weeks following graft implantation. Reconstituted recombinant growth factors are most

active during this time, as their stabilities tend to decrease when exposed to temperatures above -70°C. Furthermore, the first few weeks of healing are also the critical time for seeded precursor cells to differentiate towards the osteoblastic lineage. Drug release from 3D matrices is mostly driven by a pure diffusion mechanism, where free solutes very rapidly escape to the surrounding solution. Protein release can be also activated by external stimuli, including temperature changes, magnetism, ultrasound, electrical effect and irradiation. The size of the protein molecules also affects the release kinetics. Larger molecules may release more slowly from being bound to the surface by virtue of its larger physical size [109].

1.6.4. Design Criteria for Growth Factors Delivery Systems

A growth factor delivery system engineered for bone healing should be a combination of osteoinductive and osteoconductive properties, that way in the presence of an adequately porous shape 3D- matrix and biological stimulus cells can migrate, proliferate and differentiate and lead to the generation of ECM and vascular network osteo-integration. The materials for growth factor based delivery devices should be biocompatible, non-cytotoxic to the body. The device should degrade at a rate of few weeks to months according to the rate of tissue regeneration while maintaining appropriate release dose and profile of the incorporated growth factors. The delivery system should also be able to retain the bioactivity of the proteins during incorporation of the growth factors into the delivery systems and also over extended period of delivery time. The delivery system should have mechanical properties that are similar to those of the native bone. A weak scaffold may not have sufficient load-bearing capabilities, while an overly strong one may result in stress shielding that could lead to the resorption of the newly forming bone. Additionally, the delivery device should hold high loading protein efficiency and several growth

factors may be released sequentially in a manner that mimics the temporal profile of the healing process *in vivo* [110,111,112].

1.6.5. Release Kinetics of Growth Factors: *In Vitro* and *In Vivo*

Release kinetic is a function of the ability of the growth factors to diffuse out of the scaffold. In a purely diffusion-based system, release profile is often characterized by an initial burst; growth factors attached to the scaffold diffuse out to the defect site following concentration gradient. If the release of the growth factors is governed by the degradation of the scaffold, release profile depends on the molecular weight, concentration and hydrophobicity of the base polymer, degree of crosslinking and swelling, and the mode of degradation.

The healing cascade of bone is administrated by temporally and spatially available growth factors which are produced by the cells and ECM at the defect site. However, in a non-union defect site the spatiotemporal action of the biological and mechanical cues is perturbed. Hence, it is imperative to achieve spatiotemporal release profile of growth factors to heal bone efficiently. Literatures indicate that simultaneous delivery of low doses of two growth factors, BMP-2 and TGF-β3 can induce more bone formation over single factor delivery [113,114]. It is important to consider the synergistic effect of the growth factors while designing a multiple delivery system. The growth factors should be able to maintain their respective bioactivity and work in concert. Selection of growth factors is also crucial. If not appropriately chose, the combination of growth factors can inhibit/stimulate the activity of each growth factor and affect overall healing. For instance, in a rabbit tibia model simultaneous delivery of osteogenic BMP-2 and angiogenic basic fibroblast growth factor

(bFGF) resulted in decreased bone formation [115]. However, sequential of BMP-2 and angiogenic VEGF is widely studied and have shown increased bone formation and regeneration [116,117]. Lee et al. evaluated knee meniscus repair upon spatially released human connective tissue growth factor (CTGF) and transforming growth factor–β3 (TGFβ3) from a three-dimensional (3D)–printed biomaterial. The group treated with CTGF followed by TGFβ3 delivered to the cell culture media showed fibrochondrogenic differentiation of human MSCs whereas the cells treated with combination/simultaneous delivery of CTGF and TGFβ3 failed to yield a substantial number of fibrochondrocyte-like cells [118]. Temporal control over the release kinetics can be obtained in different ways: designing hybrid scaffolds with polymers degrade at different rate, utilizing hydrogels as a layer in a polymeric scaffold, embedding multiple growth factors in charged mesh/film on scaffolds using layer-by-layer technology are explored by researchers. Delivering growth factors in a temporally controlled environment is beneficial as this allows to achieve desired cellular activity over the course of healing time without the need for repeated dosing of the proteins.

Spatial control over growth factor release is an important issue in bone interfaces. Interfaces between bone and other tissues such as cartilage, ligament and tendon express various gene expressions which are tightly controlled in space. Mechanical and biochemical gradients are present at these interfaces. Releasing growth factors in a spatially controlled manner may influence cell phenotype, differentiation state and ECM production and organization which may have effect in tissue mechanical properties, mimicking those seen *in vivo.* A wide variety of technologies have been engineered to regulate the spatial organization of bioactive factors, and many of these have been applied for bone regeneration. Microcontact printing, non-contact technique, 2-D irradiation-based patterning, 3-D scaffolds

with microchannel, UV laser light treatment are widely studies techniques to create pattern on the scaffold to obtain spatially controlled growth factor release [119-121].

1.6.6. Dose Response of Growth Factors: *In Vitro and In Vivo*

Selecting the appropriate growth factors to regenerate the target tissue is only part of the solution of regenerative engineering. Optimal growth factor dose, carrier vehicle, and release kinetics all have to be assessed prior to the tissue scaffold implantation. Growth factors such as BMP-2 are considered to be dose dependent *in vitro*; that is the larger the dose of growth factor, the more bone tissue regeneration is observed. *In vitro* doses of BMP-2 at 1μg and larger were able to successfully bridge the defect site gap, with increasing doses resulting in an increase of bone formation, while doses at 0.5μg or lower were unable to sufficiently fill in the defect site [122]. The release of these doses *in vitro* often follows the pattern of a short burst release for the first week, followed by a more gradual increase, eventually leveling off after approximately 42 days [106]. However, the dose-dependence of growth factors changes once evaluated *in vivo*. While the *in vitro* studies concluded that doses of 1μg and larger were able to bridge the defect site and regenerate bone, *in vivo* dose-dependence increased with the dose, but started to decrease after quantities of 1μg [122]. This had been hypothesized to be due to the saturation of BMP-2 receptors, or the fact that at higher doses, new bone formation has already filled the defect site. *In vivo* implantation must also take more careful consideration of the doses present, due to the physiological side effects of high doses. While it is important to maintain a dose significant enough to bridge the defect gap and regenerate new tissue, it is also important to ensure that the dose is not large enough to cause cell toxicity, an immune response, or excess bone or tissue formation.

1.7. Dual and Sequential Delivery of VEGF and BMP-2 in Fracture Healing

It has been observed that a combination of growth factors can result in a synergistic effect on the wound healing process, and lead to more advanced tissue regeneration. One of the more prevalent and understood growth factor combinations involves the delivery of both angiogenetic and osteogenic agents, which work together to establish vascularization and new bone formation respectively. Perhaps the most commonly used combination involves vascular endothelial growth factor (VEGF) and bone morphogenetic protein 2 (BMP-2). The synergy of these two growth factors is notable, as VEGF plays multiple roles in bone formation when combined with BMP-2. VEGF is known for ability to induce new blood vessel formation. Blood vessel formation is a key component in bone formation, as the blood vessels will transport blood, oxygen, cytokines, and other healing agents to the wound site, enhancing and sustaining the new bone formation. Additionally, VEGF also plays a role in ossification, further improving its synergistic effects with BMP-2. Peng et al., for instance, have shown that VEGF antagonists reduce the induction capacity BMP-2 to form bone, while BMP-2 in the presence of VEGF showed enhanced bone formation [117]. Further, the degree of bone formation after exposure to both factors was partially dependent on the ratio of one to the other, with higher amounts of BMP-2 compared to VEGF eliciting more bone formation than the reverse. In another study of co-release of VEGF and BMP-2 examining the chemotactic role of each molecule, Ramazanoglu et al. examined expressions of collagen type I, Osteocalcin, and Osteopontin. Increased collagen I from VEGF+BMP-2 groups confirmed the chemotactic migration behavior elicited by VEGF on osteoblasts. At week 4, the VEGF+BMP-2 group showed higher osteopontin expression. Since osteopontin regulates bone remodeling by helping osteoclasts bind to bone, an increase in its expression was interpreted as an indication of bone remodeling [123]. Studies have been

reported where VEGF and VEGF receptor, VEGFR-1 have been expressed by human mesenchymal stem cells during their differentiation and that VEGF has increased the ALP activity in primary human osteoblastic cells. In intramembranous ossification during angiogenesis VEGF direct the surrounding blood vessels to invade the mesenchymal condensation and in endochondral ossification it helps to recruit the endothelial cells associated vasculature to invade the ischemic cartilaginous region. Invading vasculature allows the recruitment of osteoclasts, which subsequently remove the cartilaginous matrix and allow for osteoprogenitor cells to migrate and synthesize bone matrix. Furthermore, in addition to osteoblast formation, VEGF has been shown to stimulate osteoclast formation as well, due to its increase of RANKL expression in osteoclast precursor cells. By upregulating RANKL expression in these cells, VEGF aids in the differentiation of these precursor cells in to osteoclasts [34, 35].These additional benefits have made the VEGF and BMP synergy a favorable combination of growth factors to use in bone healing, because they address new bone formation from multiple different pathways in the healing process.

The BMP family and VEGF is widely and commonly used, but other growth factors can also affect bone healing from multiple pathways. One example of such a growth factor is the fibroblast growth factor (FGF). FGF effects the bone regeneration process in a related way to VEGF, by increasing the differentiation and proliferation of precursor cells into osteoblasts, and it has also been observed to express type 1 collagen and osteoclast differentiation. Additionally, *in vitro* studies have shown that FGF directs endothelial cell migration as well as promotes VEGF expression, meaning FGF also has the potential to express both angiogenetic and osteogenic properties [125]. Platelet derived growth factor (PDFG) is another growth factor that is thought to effect both the angiogenetic and osteogenic pathways in wound healing. PDFG

plays a role in osteogenesis by inducing the formation of cartilage and other connective tissue by stimulating fibroblasts and chondrocytes. Similar to FGF, PDGF can increase VEGF expression, therefore making it an angiogenetic factor as well [125]. In fact, a small number of other growth factors have been shown to play a role in both osteogenesis and angiogenesis, including TGF-β, IGF and HGF, and perhaps the right combination of these growth factors with each other or other growth factors can prove to be as effective as the BMP-2 and VEGF synergy.

1.8. REFERENCES

1. Bilezikian JP, Raisz LG, Rodan GA. Principal of bone biology. San Diego, CA: Academic Press; 1996.
2. Bart Clarke. Normal bone anatomy and physiology. Clin J Am Soc Nephrol. 2008 Nov; 3(Suppl 3): S131–S139.
3. Buckwalter, J. A., and R. R. Cooper. "Bone Structure and Function." Instructional Course Lectures 36 (1987): 27-48. Web.
4. United States Department of Health and Human Services “Bone Health and Osteoporosis: A Report of the Surgeon General”. 2007. http://www.surgeongeneral.gov/library/bonehealth/images/Figure2-3.gif
5. Gideon A. Rodan. Introduction to Bone Biology. Bone. 1992;13:3-6.
6. Ducy P, Schinke T, Karsenty G. The osteoblast: a sophisticated fibroblast under central surveillance. Science. 2000; 289:1501-1504.
7. Zaidi M. Skeletal remodeling in health and disease. Nat Med. 2007;13:791-801.

8. Marks SC Jr, Odgren PR. “Structure and Development of the Skeleton” Chapter 1 in: Principals of Bone Biology 2nd edition, Vol. 1, ed. Bilexikian JP, Raisz LG, Rodan GA. Academic Press: San Diego, CA. 2002.
9. Steven L. Teitelbaum. Bone Resorption by Osteoclasts. Science. 2000 Sep 1; 289 (5484):1504-8.
10. Brian R Macdonald, Maxine Gowen. The cell biology of bone. Baillire's Clinical Rheumatology. October 1993.
11. Sundeep Khosla, Jennifer J. Westendorf, and Merry Jo Oursler. Building bone to reverse osteoporosis and repair fractures. J Clin Invest. 2008;118(2):421-428
12. Lian J, Stein G. Dynamics of Bone and Cartilage Metabolism, Academic Press, 165-185, 1999.
13. Ott S. “Bone Remodeling”. Chapter 19 in: Principals of Bone Biology. Bilezikian JP, Raisz LG, Rodan GA, ed. Academic Press: San Diego. 1996.
14. Franz-Odendaal TA, Hall BK, Witten PE. Buried alive: how osteoblasts become osteocytes. Dev Dyn. 2006 Jan; 235(1):176-90.
15. Stein et al. Principals of Bone Biology. Bilezikian JP, Raisz LG, Rodan GA, ed. Academic Press: San Diego. 1996.
16. Nelson B. Watts. Clinical Utility of Biochemical Markers of Bone Remodeling. Clinical Chemistry. (1999) 45:8(B) 1359–1368.
17. Dick Heinegard and Eke Oldberg. Structure and biology of cartilage and bone matrix noncollagenous macromolecules. FASEB J. 1989 Jul;3(9):2042-51.
18. Carano RA, Filvaroff EH. Angiogenesis and bone repair. Drug Discov Today. 2003 Nov 1;8(21):980-9.

19. Aaron Schindelera, Michelle M. McDonalda, Paul Bokkoa, David G. Little. Bone remodeling during fracture repair: The cellular picture. Seminars in Cell & Developmental Biology 19 (2008) 459–466.
20. Parfitt AM. Osteonal and hemi-osteonal remodeling: the spatial and temporal framework for signal traffic in adult human bone. J Cell Biochem. 1994 Jul; 55(3):273-86.
21. Parfitt AM. Bone age, mineral density, and fatigue damage. Calcif Tissue Int. 1993;53 Suppl 1:S82-5; discussion S85-6.
22. Riggs BL, Parfitt AM. Drugs used to treat osteoporosis: The critical need for a uniform nomenclature based on their action on bone remodeling. Journal of Bone and Mineral Research 2005; 20 (2):177-84.
23. Makadia, Hirenkumar, and Steven Siegel. "Poly Lactic-co-Glycolic Acid (PLGA) as Biodegradable Controlled Drug Delivery Carrier." NCBI. U.S. National Library of Medicine, 26 Aug. 2011. Web. 23 June 2015.
24. Vo, Tiffany N., F. Kurtis Kasper, and Antonios G. Mikos. "Strategies for Controlled Delivery of Growth Factors and Cells for Bone Regeneration. "Advanced Drug Delivery Reviews (2012).
25. Suzanne N. Lissenberg-Thunnissen, David J. J. de Gorter, Cornelis F. M. Sier & Inger B. Schipper. Use and efficacy of bone morphogenetic proteins in fracture healing. International Orthopaedics (SICOT) (2011) 35:1271–1280
26. Vicki Rosen. BMP2 signaling in bone development and repair. Cytokine & Growth Factor Reviews 20 (2009) 475–480.
27. Rengachary SS. “Bone Morphogenetic Proteins: basic concepts”. Neurosurgery Focus. 13(6):1-6, 2002.

28. Poynton AR, Lane JM. Safety profile for the clinical use of bone morphogenetic proteins in the spine. Spine (Phila Pa 1976). 2002 Aug 15; 27(16 Suppl 1):S40-8.

29. Shimer AL[1], Oner FC, Vaccaro AR. Spinal reconstruction and bone morphogenetic proteins: open questions. Injury. 2009 Dec; 40 Suppl 3:S32-8.

30. Napoleone Ferrara, Hans-Peter Gerber & Jennifer LeCouter. The biology of VEGF and its receptors. Nature Medicine 9, 669 - 676 (2003).

31. Peter H. Burri , Ruslan Hlushchuk and Valentin Djonov. Intussusceptive angiogenesis: Its emergence, its characteristics, and its significance. Developmental Dynamics. Volume 231, Issue 3, pages 474–488, November 2004.

32. Fiedler J, Leucht F, Waltenberger J, Dehio C, Brenner RE. VEGF-A and PlGF-1 stimulate chemotactic migration of human mesenchymal progenitor cells. Biochem Biophys Res Commun 2005;334(2):561-8.

33. Mayr-Wohlfart U, Waltenberger J, Hausser H, Kessler S, Günther K, Dehio C, Puhl W, Brenner R. Vascular endothelial growth factor stimulates chemotactic migration of primary human osteoblasts. Bone 2002;30(3):472-7.

34. Nakagawa M, Kaneda T, Arakawa T, Morita S, Sato T, Yomada T, Hanada K, Kumegawa M, Hakeda Y. Vascular endothelial growth factor (VEGF) directly enhances osteoclastic bone resorption and survival of mature osteoclasts. FEBS Lett 2000;473(2):161-4.

35. Yang Q, McHugh KP, Patntirapong S, Gu X, Wunderlich L, Hauschka PV. VEGF enhancement of osteoclast survival and bone resorption involves VEGF receptor-2 signaling and β< sub> 3-integrin. Matrix Biology 2008;27(7):589-99.

36. Liu Y, Berendsen AD, Jia S, Lotinun S, Baron R, Ferrara N, Olsen BR. Intracellular VEGF regulates the balance between osteoblast and adipocyte differentiation. J Clin Invest 2012 Sep 4;122(9):3101-13.

37. Helmrich U, Di Maggio N, Gueven S, Groppa E, Melly L, Largo RD, Heberer M, Martin I, Scherberich A, Banfi A. Osteogenic graft vascularization and bone resorption by VEGF-expressing human mesenchymal progenitors. Biomaterials 2013;34(21):5025-35.

38. Henriksen K, Karsdal M, Delaisse JM, Engsig MT. RANKL and vascular endothelial growth factor (VEGF) induce osteoclast chemotaxis through an ERK1/2-dependent mechanism. J Biol Chem 2003 Dec 5;278(49):48745-53.

39. Lee, K., E. A. Silva, and D. J. Mooney. "Growth Factor Delivery-based Tissue Engineering: General Approaches and a Review of Recent Developments." Journal of The Royal Society Interface 8.55 (2010): 153-70. Web.

40. Lord C, Gebhardt M, Tomford W, Mankin H. Infection in bone allografts. incidence, nature, and treatment. The Journal of Bone & Joint Surgery 1988;70(3):369-76.

41. Nguyen Ngoc Hung. Basic Knowledge of Bone Grafting. www.intechopen.com

42. Laurencin CT, Ambrosio A, Borden M, Cooper Jr J. Tissue engineering: Orthopedic applications. Annu Rev Biomed Eng 1999;1(1):19-46.

43. Calori G, Mazza E, Colombo M, Ripamonti C. The use of bone-graft substitutes in large bone defects: Any specific needs? Injury 2011;42:S56-63.

44. André R. Gazdag, MD, Joseph M. Lane, MD, David Glaser, MD, and Robert A. Forster, MD. Alternatives to Autogenous Bone Graft: Efficacy and Indications. J Am Acad Orthop Surg 1995;3:1-8.

45. Silber JS[1], Anderson DG, Daffner SD, Brislin BT, Leland JM, Hilibrand AS, Vaccaro AR, Albert TJ. Donor site morbidity after anterior iliac crest bone harvest for single-level anterior cervical discectomy and fusion. Spine (Phila Pa 1976). 2003 Jan 15;28(2):134-9.

46. Berrey B, Lord CF, Gebhardt M, Mankin HJ. Fractures of allografts. frequency, treatment, and end-results. The Journal of Bone & Joint Surgery 1990;72(6):825-33.

47. Thompson RC, Pickvance E, Garry D. Fractures in large-segment allografts. The Journal of Bone & Joint Surgery 1993;75(11):1663-73.

48. Boyce T, Edwards J, Scarborough N. "Allograft bone, the influence of processing on safety and performance". Othopedic Clinics of North America. 30(4):571-581, 1999.

49. http://www.aatb.org/aatb/files/ccLibraryFiles/Filename/000000000323/BoneGraftSubstituteTable2010.pdf

50. Delloye C[1], Cornu O, Druez V, Barbier O. Bone allografts: What they can offer and what they cannot. J Bone Joint Surg Br. 2007 May;89(5):574-9.

51. Khan SN[1], Cammisa FP Jr, Sandhu HS, Diwan AD, Girardi FP, Lane JM.The biology of bone grafting. J Am Acad Orthop Surg. 2005 Jan-Feb;13(1):77-86.

52. Goldberg VM[1], Stevenson S Natural history of autografts and allografts. . Clin Orthop Relat Res. 1987 Dec;(225):7-16.

53. http://cal.vet.upenn.edu/projects/saortho/chapter_39/39mast.htm

54. Burchardt, Hans Ph.D. The Biology of Bone Graft Repair. Clinical Orthopaedics & Related Research: April 1983.

55. Wheeler DL, Enneking WF. Allograft Bone Decreases in Strength *In Vivo* Over Time. Clin Orthop Rel Res 435 36-42, 2005.

56. Amini AR, Laurencin CT, Nukavarapu SP. Bone tissue engineering: recent advances and challenges. Critical ReviewsTM 7 in Biomedical Engineering 8 2012;40(5).

57. Fact Sheet—Regenerative Medicine, National Institutes of Health, Updated 10 October 2010.

58. Khan F, Ahmad SR. Polysaccharides and Their Derivatives for Versa tile Tissue Engineering Application. Macromolecular Bioscience 2013;13(4): 395–421.

59. Awad HA, Butler DL, Boivin GP, Smith FN, Malaviya P, Huibregtse B *et al.* Autologous mesenchymal stem cell-mediated repair of tendon. Tissue Eng 1999;5(3):267–277.

60. Landsman A, Taft D, Riemer K. The role of collagen bioscaffolds, foamed collagen, and living skin equivalents in wound healing. Clin Podiatr Med Surg 2009;26(4):525–533.

61. Gautschi OP, Frey SP, Zellweger R. Bone morphogenetic proteins in clinical applications. ANZ J Surg 2007;77(8):626–631.

62. Laurencin CT, El-Amin SF. Xenotransplantation in orthopaedic surgery.J Am Acad Orthop Surg 2008 Jan;16(1):4–8.

63. Ulery BD, Nair LS, Laurencin CT. Biomedical applications of biodegradeable polymers. Journal of Polymer Science Part B: Polymer Physics 2011;49(12):832–864.

64. Niinomi M. Mechanical biocompatibilities of titanium alloys for biomedical applications. Journal of the Mechanical Behavior of Biomedical Materials 13 2008;1(1):30–42.

65. Ohtsuki C, Kamitakahara M, Miyazaki T. Bioactive ceramic-based materials with designed reactivity for bone tissue regeneration. J R Soc Interface 2009 Jun 6;6 Suppl 3:S349–60.

66. Gunatillake P, Mayadunne R, Adhikari R. Recent developments in biodegradable synthetic polymers. Biotechnol Annu Rev 2006;12:301–347.

67. Carletti E, Motta A, Migliaresi C. Scaffolds for tissue engineering and 3D cell culture. 3D cell culture: Springer; 2011. pp. 17–39.

68. Pihlajam¨aki HK, Salminen ST, Tynninen O, B¨ostman OM, Laitinen O. Tissue restoration after implantation of polyglycolide, polydioxanone, polylevolactide, and metallic pins in cortical bone: an experimental study in rabbits. Calcif Tissue Int 2010;87(1):90–98.

69. Wang P, Wu T, Tsai W, Kuo W, Wang M. Grooved PLGA films incorporated with RGD/YIGSR peptides for potential application on skeletal muscle tissue engineering. Colloids and Surfaces B: Biointerfaces 2013;110:88–95.

70. Barbanti SH, Santos Jr AR, Zavaglia CA, Duek EA. Poly (ε-caprolactone) and poly (d, l-lactic acid-co-glycolic acid) scaffolds used in bone tissue engineering prepared by melt compression–particulate leaching method. J Mater Sci Mater Med 2011;22(10):2377–2385.

71. Andreas K, Zehbe R, Kazubek M, Grzeschik K, Sternberg N, B¨aumler H, *et al.* biodegradable insulin-loaded PLGA microspheres fabricated by three different emulsification techniques: Investigation for cartilage tissue engineering. Acta biomaterialia 2011;7(4):1485–1495.

72. Sahoo S, Toh SL, Goh JC. A bFGF-releasing silk/PLGA-based biohybrid scaffold for ligament/tendon tissue engineering using mesenchymal progenitor cells. Biomaterials 2010;31(11):2990–2998.

73. Hidayah N, Fadzli A, Ng M, Ruszymah B, Naicker A, Shalimar A, *et al.* Porous PLGA sheet and acellularized muscle stuffed vein seeded with neural differentiated MSCs are potential scaffolds for nerve regeneration. Regen Res 2012;1:1–7.

74. Hersel U, Dahmen C, Kessler H. RGD modified polymers: biomaterials for stimulated cell adhesion and beyond. Biomaterials 2003;24(24):4385–4415.

75. Chen G, Wu Q. The application of polyhydroxyalkanoates as tissue engineering materials. Biomaterials 2005;26(33):6565–6578.

76. Santerre J, Woodhouse K, Laroche G, Labow R. Understanding the biodegradation of polyurethanes: from classical implants to tissue engineering materials. Biomaterials 2005;26(35):7457–7470.

77. Lee SJ, Choi JS, Park KS, Khang G, Lee YM, Lee HB. Response of MG osteoblast-like cells onto polycarbonate membrane surfaces with different micropore sizes. Biomaterials 2004;25(19):4699–4707.

78. Wang C, Ge Q, Ting D, Nguyen D, Shen H, Chen J, *et al.* Molecularly engineered poly (ortho ester) microspheres for enhanced delivery of DNA vaccines. Nature Materials 2004;3(3):190–196.

79. Fisher JP, Vehof JW, Dean D, van der Waerden, Jan Paul, Holland TA, Mikos AG, *et al.* Soft and hard tissue response to photocrosslinked poly(propylene fumarate) scaffolds in a rabbit model. J Biomed Mater Res 2002;59(3):547–556.

80. Carampin P, Conconi MT, Lora S, Menti AM, Baiguera S, Bellini S, *et al.* Electrospun polyphosphazene nanofibers for *in vitro* rat endothelial cells proliferation. Journal of Biomedical Materials Research Part A 2007;80(3):24 661–668.

81. Drury JL, Mooney DJ. Hydrogels for tissue engineering: scaffold design variables and applications. Biomaterials 2003;24(24):4337–4351.

82. Gilbert PM, Havenstrite KL, Magnusson KE, Sacco A, Leonardi NA, Kraft P, *et al.* Substrate elasticity regulates skeletal muscle stem cell self-renewal in culture. Science 2010 Aug 27;329(5995):1078–1081.

83. Lutolf MP. Biomaterials: Spotlight on hydrogels. Nature Materials 2009;8(6):451-453.

84. Chen Y, Shao J, Xiang L, Dong X, Zhang G. Mesenchymal stem cells: a promising candidate in regenerative medicine. Int J Biochem Cell Biol 2008;40(5):815–820.

85. Caplan AI. Adult mesenchymal stem cells and the NO pathways. Proc Natl Acad Sci U S A 2013 Feb 19;110(8):2695–2696.

86. Lin HT, Otsu M, Nakauchi H. Stem cell therapy: an exercise in patience and prudence. Philos Trans R Soc Lond B Biol Sci 2013 Jan 5;368(1609):rstb.2011.0334.

87. Streckfuss-Bomeke K, Wolf F, Azizian A, Stauske M, Tiburcy M, Wagner S, *et al.* Comparative study of human-induced pluripotent stem cells derived from bone marrow cells, hair keratinocytes, and skin fibroblasts. Eur Heart J 2013 Sep;34(33):2618–2629.

88. Corradetti B, Meucci A, Bizzaro D, Cremonesi F, Lange Consiglio A. Mesenchymal stem cells from amnion and amniotic fluid in the bovine. Reproduction 2013 Apr 15;145(4):391–400.

89. Grompe M. Tissue stem cells: new tools and functional diversity. Cell Stem Cell 2012;10(6):685–689.

90. Sokolsky-Papkov M, Agashi K, Olaye A, Shakesheff K, Domb AJ. Polymer carriers for drug delivery in tissue engineering. Adv Drug Deliv Rev 2007;59(4):187–206.

91. Houeland G, Romani A, Marchetti C, Amato G, Capsoni S, Cattaneo A, *et al.* Transgenic mice with chronic NGF deprivation and Alzheimer's disease-like pathology display hippocampal region-specific impairments in short- and long-term plasticities. J Neurosci 2010 Sep 29;30(39):13089–13094.

92. Johnson EE, Urist MR. One-stage lengthening of femoral nonunion augmented with human bone morphogenetic protein. Clin Orthop 1998;347:105–116.

93. http://www.controlledreleasesociety.org/publications/intrack/PublishingImages/12-2_HydrolysisofPLGA.jpg

94. Hirenkumar K. Makadia1 and Steven J. Siegel2, Poly Lactic-*co*-Glycolic Acid (PLGA) as Biodegradable Controlled Drug Delivery CarrierPolymers (Basel). Author manuscript; available in PMC 2012 May 08.

95. Durect. Lactel Absorbable Polymers: poly(D,L-lactide-coglycolide) www.absorbables.com.

96. Duggirala SS, Mehta RC, Deluca PP. Interaction of recombinant human bone morphogenetic protein-2 with poly (d, l lactide-co-glycolide) microspheres. Pharm Dev Technol 1996;1(1):11-9.

97. Schrier JA, DeLuca PP. Recombinant human bone morphogenetic protein-2 binding and incorporation in PLGA microsphere delivery systems. Pharm Dev Technol 1999;4(4):611-21.

98. C. K. Chiang, M. F. Chowdhury, R. K. Iyer, W. L. Stanford, M. Radisic. Engineering surfaces for site-specific vascular differentiation of mouse embryonic stem cells. Acta Biomater. 2010, 6, 1904.

99. L. L. Chiu, R. D. Weisel, R. Li, M. Radisic. Defining conditions for covalent immobilization of angiogenic growth factors onto scaffolds for tissue engineering. J. Tissue Eng. Regen. Med. 2011, 5, 69.

100. Chen L, He Z, Chen B, Zhao Y, Sun W, Xiao Z, Zhang J, Yang M, Gao Z, Dai J. Direct chemical cross-linking of platelet-derived growth factor-BB to the demineralized bone matrix improves cellularization and vascularization. Biomacromolecules. 2009 Dec 14;10(12):3193-8. doi: 10.1021/bm900850q.

101. E. Yamachika, H. Tsujigiwa, N. Shirasu, T. Ueno, Y. Sakata, J. Fukunaga, N. Mizukawa, M. Yamada, T. Sugahara, Immobilized recombinant human bone morphogenetic protein-2 enhances the phosphorylation of receptor-activated Smads. J. Biomed. Mater. Res.,A 2009, 88A, 599.

102. O. F. Zouani, C. Chollet, B. Guillotin, M. Durrieu. Differentiation of pre-osteoblast cells on poly(ethylene terephthalate) grafted with RGD and/or BMPs mimetic peptides. Biomaterials 2010, 31, 8245.

103. Lingyan Cao, Jing Wang, Juan Hou, Wanli Xing, Changsheng Liu. Vascularization and bone regeneration in a critical sized defect using 2-*N*,6-*O*-sulfated chitosan nanoparticles incorporating BMP-2.Biomaterials, Volume 35, Issue 2, January 2014, Pages 684–698.

104. Sharmin F, Adams D, Pensak M, Dukas A, Lieberman J, Khan Y. 2015. Biofunctionalizing devitalized bone allografts through polymer-mediated short and long term growth factor delivery. Journal of Biomedical Materials Research Part A DOI: 10.1002/jbm.a.35435.

105. Kolambkar YM, Dupont KM, Boerckel JD, Huebsch N, Mooney DJ, Hutmacher DW, Guldberg RE. An alginate-based hybrid system for growth factor delivery in the functional repair of large bone defects. Biomaterials. 2011 Jan;32(1):65-74.

106. Kempen, Diederik H.r., Lichun Lu, Teresa E. Hefferan, Laura B. Creemers, Avudaiappan Maran, Kelly L. Classic, Wouter J.a. Dhert, and Michael J. Yaszemski. "Retention of *in Vitro* and *in Vivo* BMP-2 Bioactivities in Sustained Delivery Vehicles for Bone Tissue. Biomaterials. 2008 Aug;29(22):3245-52. doi: .1016/j.biomaterials.2008.04.031. Epub 2008 May 9.

107. Kyobum Kim, Johnny Lam, Steven Lu, Patrick P. Spicer, Aline Lueckgen, Yasuhiko Tabata, Mark E. Wong, John A. Jansen, Antonios G. Mikos, and F. Kurtis Kasper. Osteochondral Tissue Regeneration using a Bilayered Composite Hydrogel with Modulating Dual Growth Factor Release Kinetics in a Rabbit Model. J Control Release. 2013 Jun 10; 168(2): 166–178.

108. T.P. Richardson, M.C. Peters, A.B. Ennett, D.J. Mooney, Polymeric system for dual growth factor delivery, Nat. Biotechnol. 19 (2001) 1029–1034.

109. Duggirala SS, Mehta RC, DeLuca PP. Interaction of recombinant human bone morphogenetic protein-2 with poly(D,L lactide-coglycolide) microspheres. Pharm Dev Technol 1996;1:11 19.

110. Tayalia P, Mooney DJ. Controlled growth factor delivery for tissue engineering. Adv Mater 2009;21:3269e85.

111. Biondi M, Ungaro F, Quaglia F, Netti PA. Controlled drug delivery in tissue engineering. Adv Drug Deliv Rev 2008;60:229e42

112. Uebersax L, Merkle HP, Meinel L. Biopolymer-based growth factor delivery for tissue repair: from natural.

113. M.E. Oest, K.M. Dupont, H.J. Kong, D.J. Mooney, R.E. Guldberg, Quantitative assessment of scaffold and growth factor-mediated repair of critically sized bone defects, J. Orthop. Res. 25 (2007) 941–950.

114. C.A. Simmons, E. Alsberg, S. Hsiong, W.J. Kim, D.J. Mooney, Dual growth factor delivery and controlled scaffold degradation enhance in vivo bone formation by transplanted bone marrow stromal cells, Bone 35 (2004) 562–569.

115. R.L. Vonau, M.P. Bostrom, P. Aspenberg, A.E. Sams, Combination of growth factors inhibits bone ingrowth in the bone harvest chamber, Clin. Orthop. Relat. Res. (2001) 243–251.

116. Mustafa Ramazanoglu, Rainer Lutz, Philipp Rusche ,Levent Trabzon, Gamze Torun Kose, Christopher Prechtl, Karl Andreas Schlegel. Bone response to biomimetic implants delivering BMP-2 and VEGF: An immunohistochemical study. Journal of Cranio-Maxillo-Facial Surgery 41 (2013) 826-835.

117. Peng H, Usas A, Olshanski A, Ho AM, Gearhart B, Cooper GM, Huard J. VEGF improves, whereas sFlt1 inhibits, BMP2-induced bone formation and bone healing through modulation of angiogenesis. J Bone Miner Res 2005;20:2017–2027.

118. Chang H. Lee, Scott A. Rodeo, Lisa Ann Fortier, Chuanyong Lu, Cevat Erisken, Jeremy J. Mao. Protein-releasing polymeric scaffolds induce fibrochondrocytic differentiation of endogenous cells for knee meniscus regeneration in sheep. Science Translational Medicine December 2014 Vol 6 Issue 266.

119. C.S. Chen, M. Mrksich, S. Huang, G.M. Whitesides, D.E. Ingber, Micropatterned surfaces for control of cell shape, position, and function, Biotechnol. Prog. 14 (1998) 356–363.

120. C. Williams, Y. Tsuda, B.C. Isenberg, M. Yamato, T. Shimizu, T. Okano, J.Y. Wong, Aligned cell sheets grown on thermo-responsive substrates with microcontact printed protein patterns, Adv. Mater. 21 (2009) 2161–2164.

121. E.D. Miller, G.W. Fisher, L.E. Weiss, L.M. Walker, P.G. Campbell, Dose-dependent cell growth in response to concentration modulated patterns of FGF-2 printed on fibrin, Biomaterials 27 (2006) 2213–2221.

122. Boerckel, Joel D., Yash M. Kolambkar, Kenneth M. Dupont, Brent A. Uhrig, Edward A. Phelps, Hazel Y. Stevens, Andrés J. García, and Robert E. Guldberg. "Effects of Protein Dose and Delivery System on BMP-mediated Bone Regeneration."

123. Ramazanoglu M, Lutz R, Rusche P, Trabzon L, Kose GT, Prechtl C, et al. 2013. Bone response to biomimetic implants delivering BMP-2 and VEGF: an immunohistochemical study. Journal of Cranio-Maxillofacial Surgery 41:826-8

124. Mayer H., Bertram, H., et al., Vascular endothelial growth factor (VEGF-A) expression in human mesenchymal stem cells: autocrine and paracrine role osteoblastic and endothelial differentiation. J cell biochem (2005) 95, 827-839.

125. Bai, Yan, Guangfu Yin, Zhongbing Huang, Xiaoming Liao, Xianchun Chen, Yadong Yao, and Ximing Pu. "Localized Delivery of Growth Factors for Angiogenesis and Bone Formation in Tissue Engineering." International Immunopharmacology (2013).

126. Sharmin Farzana, McDermott Casey, Khan Yusuf. Regenerative Engineering: Role of Scaffolds, Cells, and Growth Factors. In: Injectable Hydrogels for Regenerative Engineering. Lakshmi S Nair, Editor. Imperial College Press; 2016.

2. PROJECT OVERVIEW AND SPECIFIC AIMS

The objective of this thesis is to outline studies evaluating the efficacy of PLGA-coated cortical allografts capable of delivering both BMP-2 and VEGF, individually and simultaneously to enhance bone allograft incorporation and overall defect healing. We anticipate that our modified polymer coated- growth factor loaded allograft will demonstrate osteoinductive capacity and adequate remodeling during healing process. Coating will be applied to allografts to both maximize available surface area for coating and to retain the pore structure to support bone implant integration and growth factors will be loaded utilizing two different loading schemes to obtain short and long term delivery kinetics. The study is organized into the specific aims, detailed below.

2.1. Specific Aim I: To optimize and characterize continuous coating on allografts using PLGA, an FDA polymer and examine the loading and delivery kinetics of VEGF and BMP-2 alone and simultaneously released from PLGA coated allografts.

It is hypothesized that PLGA can be used to create a continuous coating of polymer on both the periosteal and intramedullary surfaces of the allograft while maintaining the native macroporous structure for host bone. It is further hypothesized that coated allografts will be capable of adsorbing and delivering growth factors in a controlled fashion.

2.2. Specific Aim II: To determine the bioactivity of BMP-2 both *in vitro* and *in vivo*.

It is hypothesized that loading and delivering the growth factors will not impact the bioactivity of the BMP-2. To test the bioactivity of the released BMP-2, differentiation ability of hMSCs into mature osteoblast will be assessed using hMSCs in the presence BMP-2, released from PLGA coated allografts. Using a transwell, BMP-2 loaded, polymer coated

allografts will be cultured with human mesenchymal stem cells to determine the functionality of released BMP-2 from the allografts in supporting osteoblast differentiation.

We also hypothesize that PLGA coated and BMP-2 loaded allograft will show more bone formation and osteointegration over coated allograft in a critical size rat femoral segmental defect.

2.3. Specific Aim III: To investigate the role of VEGF in osteoclastogenesis in virto.

We hypothesize that VEGF delivered will be viable to the extent that it can stimulate osteoclast differentiation. Using a transwell PLGA coated-VEGF loaded allograft will be cultured with Raw 267.4 cells and Bone Marrow derived Macrophages (BMM) cells and the ability of released VEGF to stimulate functional osteoclast differentiation will be evaluated.

2.4. Specific Aim IV: To evaluate the ability of PLGA coated and growth factors loaded allografts to repair large scale segmental defects *in vivo*.

It is hypothesized that delivery of both VEGF and BMP-2 in a controlled way will increase healing over BMP-2 alone and uncoated-unloaded allografts. Specifically, given the nature of the bone defect to be used, segmental defects, it is anticipated that bone repair will occur via endochondral ossification as opposed to intramembranous. For this reason it is anticipated that an initial release of VEGF, followed by a more sustained release of BMP-2 will result in more vascularization, better bone remodeling and overall healing.

3. LOADING AND DELIVERY OF BMP-2 AND VEGF FROM PLGA COATED ALLOGRAFT

3.1. INTRODUCTION

Bulk allograft incorporation has been limited by a number of factors including diminished mechanical properties of the allograft, lack of remodeling of the allograft over time, fracture non-unions, and scant allograft vascularization. This has led to high failure rates which has been as high as 60% in ten-year follow-up studies.[1] Intact allografts, however, are the only subgroup suitable for load-bearing applications and indications, underscoring their importance in the clinical realm. Given their importance clinically and their well-documented shortcomings enhancing allograft healing has become a well-studied topic. Researchers are investigating several ways of improving allograft healing outcomes by combining them with cells, factors, proteins, and/or adenoviruses to revitalize the otherwise largely inert implant material,[2-10] although for the most part these strategies have not investigated the nature with which these additives are delivered to the defect site nor sought to design delivery kinetics.

Studies on growth factors and bone repair have clarified the importance of controlling not only which factors to administer to a bone defect site but also the relative quantities and the temporal expression of factors as well. Our hypothesis was that allografts could be made biologically active by combining the allograft with growth factors such as vascular endothelial growth factor (VEGF) and bone morphogenetic protein-2 (BMP-2).[11] Our ultimate goal is to quantitatively and temporally control the delivery of these growth factors which has the potential to enhance the nature and extent of bone-allograft incorporation toward bone healing. To accomplish this we introduced a thin coating of a biodegradable polymer to functionalize the exposed surface of the allograft as a delivery vehicle for the

growth factors, with the intention of delivering them simultaneously with short-term and long-term kinetics. The primary aim of this study was to develop a methodology to apply a polymer coating onto the surface of the allograft thin enough to maintain its native architecture, specifically its inherent pore structure that facilitates new bone ingrowth, and to use the coating as a factor delivery modulator in which two growth factors, VEGF and BMP-2, can be released from coated allograft in such a way that the VEGF is released rapidly, and prior to, the release of BMP-2.

3.2. MATERIALS AND METHODS

3.2.1. Allograft Harvest and Preparation

For allograft samples, tibial and femoral bone samples were harvested from male and female Sprague-Dawley retired breeder rats (300-600g). The samples were cleaned of soft tissue and the bone marrow was aspirated. The bone segments were agitated in a chloroform solution overnight to reduce the residual fatty tissue and subsequently trimmed to 5 mm longitudinal segments. After a brief ethanol rinse, the allograft segments were autoclaved (121°C and 15 PSI for 30 minutes) to devitalize biological remnants.

3.2.2. Allograft Coating with PLGA

Polymer coating of sterilized allografts was based on prior studies[12]. Briefly, 50:50 PLGA (Lakeshore Biomaterials, Inc. Birmingham, AL) was dissolved in 1:8 (w/v) concentration of tetrahydrofuran (Fisher Scientific, Pittsburgh, PA). Each allograft was placed in the cylinder portion of a 3cc syringe and the polymer solution was drawn into the syringe by pulling the plunger

to fully submerge the allograft with the polymer and coat it through its endosteal and periosteal surfaces. This process was repeated by moving the plunger up and down to effectively rinse the allograft with the polymer. The pressure applied to the plunger in each direction was to force the polymer solution through the small pores found at the ends of the long bones to fully coat all surfaces. Once coated the allografts were then lyophilized to remove any residual solvent.

3.2.3. Coating Characterization of PLGA –coated Allograft

Polymer coating was evaluated qualitatively using scanning electron microscopy (SEM) and microcomputed tomography (microCT). SEM images were taken of allografts sputter-coated with gold using a JEOL 6700 scanning electron microscope (JEOL USA, Peabody MA) operated at 5.0 kV. SEM was then performed to analyze the outer surface, as well as the cross section of the allograft. Allografts were positioned on the SEM sample platform and sputter coated with a gold-palladium (Au-Pd) solution before being inserted into the SEM. Images were taken to assess the thickness of the polymer coating.

Additional images were taken with micro-focus X-ray computed tomography CT scans (µCT40; Scanco Medical AG, Bruttisellen, Switzerland) in 5 mm segments of the coated allograft to assess the volume of polymer coating. Serial tomographic images were acquired at 45 kV and 114 µA, collecting 1,000 projections per rotation at 300 msec integration time. Three-dimensional 16-bit grayscale images were reconstructed using standard convolution back projection algorithms with Shepp and Logan filtering, and rendered at a discrete density of 244,141 voxels/mm^3 (isometric16-µm voxels). Betadine was integrated into the polymer coating on the allografts to enhance contrast between the polymer coating and background. Polymer coating volume was quantified by analyzing the microCT images.

3.2.4. Surface Adsorption of Growth Factor

The growth factor VEGF was loaded onto the bone graft using surface adsorption. VEGF was purchased from Sigma Aldrich in 5 µg vials and stored in a -20° C freezer. The VEGF was reconstituted using with 1 ml of deionized (DI) water to create a VEGF concentration of 5 µg/ml[13]. Allografts were coated with 1g/8ml (w/v) concentration of PLGA. . After allografts were coated with the polymer solution and lyophilized, they were submerged in 500 µl of the VEGF solution with a concentration 5µg/ml. The allografts were allowed to soak in the VEGF solution at room temperature for 15 minutes before the samples were frozen in a -20° C freezer. Once frozen, they were lyophilized for 24 hours. Control samples were created using the same procedure, being submerged in pure DI water instead of the reconstituted VEGF solution. Studies were completed with a sample size of n = 6.

Surface adsorption of BMP-2 was conducted following similar protocol as VEGF. Recombinant human BMP-2 was procured from Genscript Inc., NJ as a lyophilized powder in 500 µg vials and stored at a temperature of -20° C before use. Allografts were coated with a polymer solution containing a PLGA concentration of 1g/8ml. Acetic acid was diluted with DI water to create a solution of 20 mM acetic acid. 1 ml of the solution was added to the 500 µg vial of BMP-2 to create a BMP-2 concentration of 500µg/ml[13]. Coated allografts were submerged in 500 µl of the BMP-2 solution and incubated for 15 minutes at room temperature. The samples were then placed in a -20° C freezer until the BMP-2 solution had completely solidified. The samples were then lyophilized for 24 hours. Control samples were submerged in 20 mM acetic acid rather than the BMP-2 solution. A sample size of n = 6 was used.

3.2.5. Encapsulation of Growth Factor

Release of BMP-2 was also tested using encapsulation of the protein in the polymer coating. PLGA was dissolved in THF at a concentration of 1g/8ml. A 500 µg vial of BMP-2 from Genscript was reconstituted with 500 µl of 20 mM acetic acid. This reconstituted solution was slowly mixed into the polymer solution until homogenized. Allografts were then coated and lyophilized using the coating method stated previously.

3.2.6. Incorporation of Multiple Growth Factors

BMP-2 and VEGF were both loaded onto one coated allograft sample using one of two methods to obtain short-term and long-term release kinetics. Recombinant human BMP-2 (Genscript, NJ) was loaded into polymer-coated allografts through encapsulation *within* the polymer coating and recombinant mouse VEGF (sigma Aldrich, MO) was loaded onto the same allograft sample through surface adsorption *onto* the polymer coating. For factor encapsulation, 50:50 PLGA (Lakeshore Biomaterials, Inc. Birmingham, AL) was dissolved in 1:8 (w/v) concentration of tetrahydrofuran (Fisher Scientific, Pittsburgh, PA). BMP-2 was then added to the polymer solution (500µg/ml) prior to allograft coating. Each allograft was then placed in the barrel of a 3cc syringe and the polymer solution was drawn into the syringe by pulling the plunger to fully coat the allograft across its endosteal and periosteal surfaces. This process was repeated by moving the plunger up and down to effectively rinse the allograft with the polymer. The allografts were then placed in a rotator at 4^0C overnight to achieve an even, continuous coating, followed by lyophilization to remove residual solvent. After lyophilization VEGF was adsorbed to the surface of the same coated allografts by placing them into a concentrated VEGF solution (5µg/ml) for a period of 15 minutes

to allow the protein to adsorb to the coating. Coated allografts were subsequently frozen at -20°C for 20 hours, lyophilized for an additional 24 hours, and stored at -20°C until use.

3.2.7. Release Protocols of Growth Factors

Release kinetics of the growth factors were determined by placing the growth-factor-loaded allografts in phosphate buffered saline (PBS) at 37°C under constant agitation for 42 days. Samples were placed in well plates and submerged in 800 ul of phosphate-buffered saline (PBS). Ion concentrations and osmolarity of PBS were equivalent to that of the human body, making it more similar to the environment of the body when the allograft is implanted. The well plates were wrapped in parafilm and placed in a 37° C room to simulate the internal temperature of the human body. Samples were taken by extracting the supernatant fluid in each well and freezing it in a -20° C freezer until it was ready to be analyzed. The allografts were shifted to a new well at each time point and re-submerged in 800 ul of PBS. 800µl samples of buffer were taken at specific intervals: 2, 4, 6, 8, 12, and 24 hours, and 3, 5, 7, 10, 14, 21, 28, and 42 days.

3.2.8. Growth factor Release Kinetics

Protein release was analyzed using the enzyme-linked immunosorbent assay (ELISA) (R&D systems, Minneapolis, MN). To quantify the release of VEGF and BMP-2, 50 µl of each sample was added to an individual well, followed by 50 µl of Assay Diluent. Two standard curves were also made using reconstituted VEGF diluted with PBS, as well as VEGF standards provided in the ELISA kit. The well plate was covered with an adhesive strip and placed on a Thermo Scientific rocker to incubate for 2 hours with slight agitation at room temperature. The wells were aspirated and washed with wash buffer 5 times before adding 100 µl of Mouse VEGF

conjugate to each well. The well plate was then covered and incubated on the rocker for another 2 hours. The washing step was repeated, followed by 100 µl of Substrate Solution being added to each well. The plate was covered in aluminum foil to protect from light and incubated on the rocker for 30 minutes. 100 µl of Stop Solution was then added to the Substrate Solution in each well. The optical density of each well was read using a Biotek Synergy HT plate reader at 450 nm and correction wavelength was set to 540 nm. Using the optical densities of the wells, the concentration of VEGF in each sample was calculated, and cumulative release kinetics of the VEGF were calculated.

3.2.9. Statistical Analysis

A student's t-test (to compare two groups) or one-way analysis of variance with Tukey post-hoc testing, (for multiple group comparisons) was used to determine statistical significance with $p<0.05$. Sample size for all protein release *in vitro* analysis was n=6.

3.3. RESULTS

3.3.1. Mass Analysis of Coating

The weight of the allograft with and without factor-loaded polymer was measured and recorded (n=6) to quantify the extent of polymer coating. The mean recorded weight for uncoated allograft was 126.50 mg (± 38.88 mg) and the mean recorded weight for the coated and factor-loaded allograft was 158.16 (± 38.99 mg), a statistically significant mass increase of 27% (± 10.84%) ($p<0.05$, figure. 3.3.1.1).

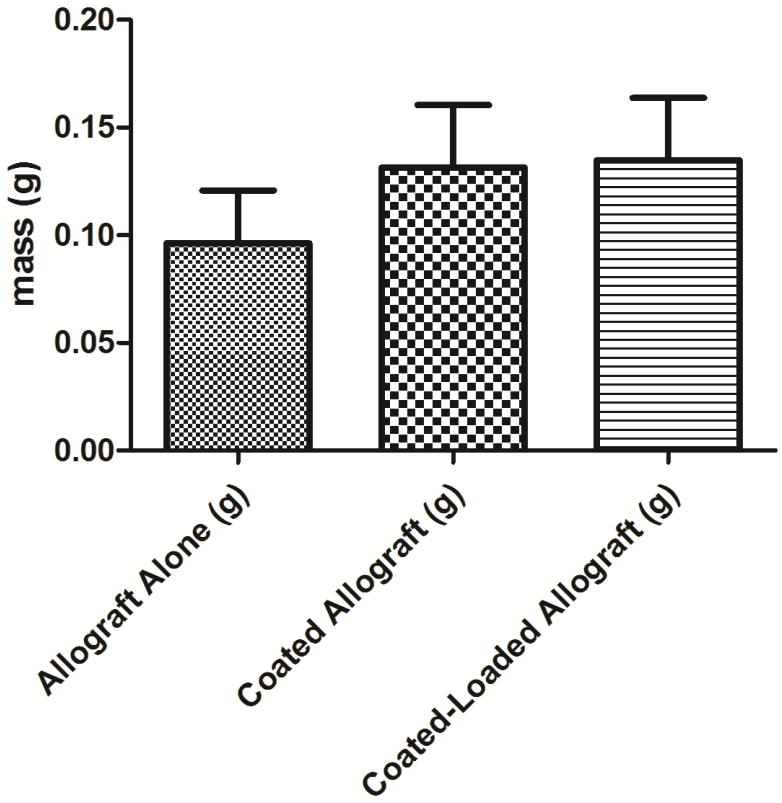

Figure 3.3.1.1: Measurements of average weight of samples before and after polymer coating and protein loading (encapsulation scheme). Addition of growth factor and coating increased the mass of the allograft ($p<0.05$).

3.3.2. Coating Thickness

Scanning electron micrographs confirmed an even, continuous coating both on the endosteal and periosteal surface (figure. 3.3.2.1) that was between 30-100µm in thickness, thin enough to maintain open pores as small as 200µm but thick enough to minimally but evenly coat the entire surface area of the allograft.

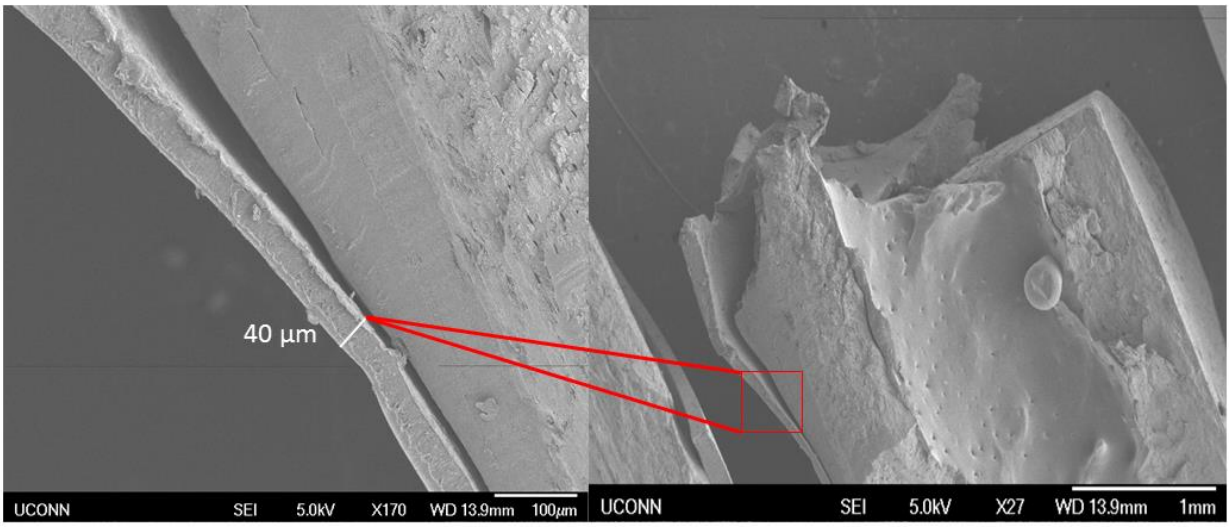

Figure 3.3.2.1: SEM micrograph of the coated allograft at low magnification (right, 27X) and high magnification (left, 170X) represents 40 µm thick coating on the periosteal surface. Coating thickness ranged from approximately 30µm-100µm.

3.3.3. Coating Volume and Pore Size

MicroCT analysis of the coated allografts confirmed an even continuous coating that maintained the small trabecular pore structure evident at the proximal and distal aspects of the allograft samples (figure 3.3.3.1) and demonstrated a trend toward a greater volume of coating on the periosteal surface of the allograft than the endosteal surface (figure 3.3.3.2). It was anticipated that the periosteal surface would have a greater volume of polymer coating than the endosteal

surface given the overall uniformity of the coating along the allograft and the greater inherent surface area of the periosteal surface than endosteal surface.

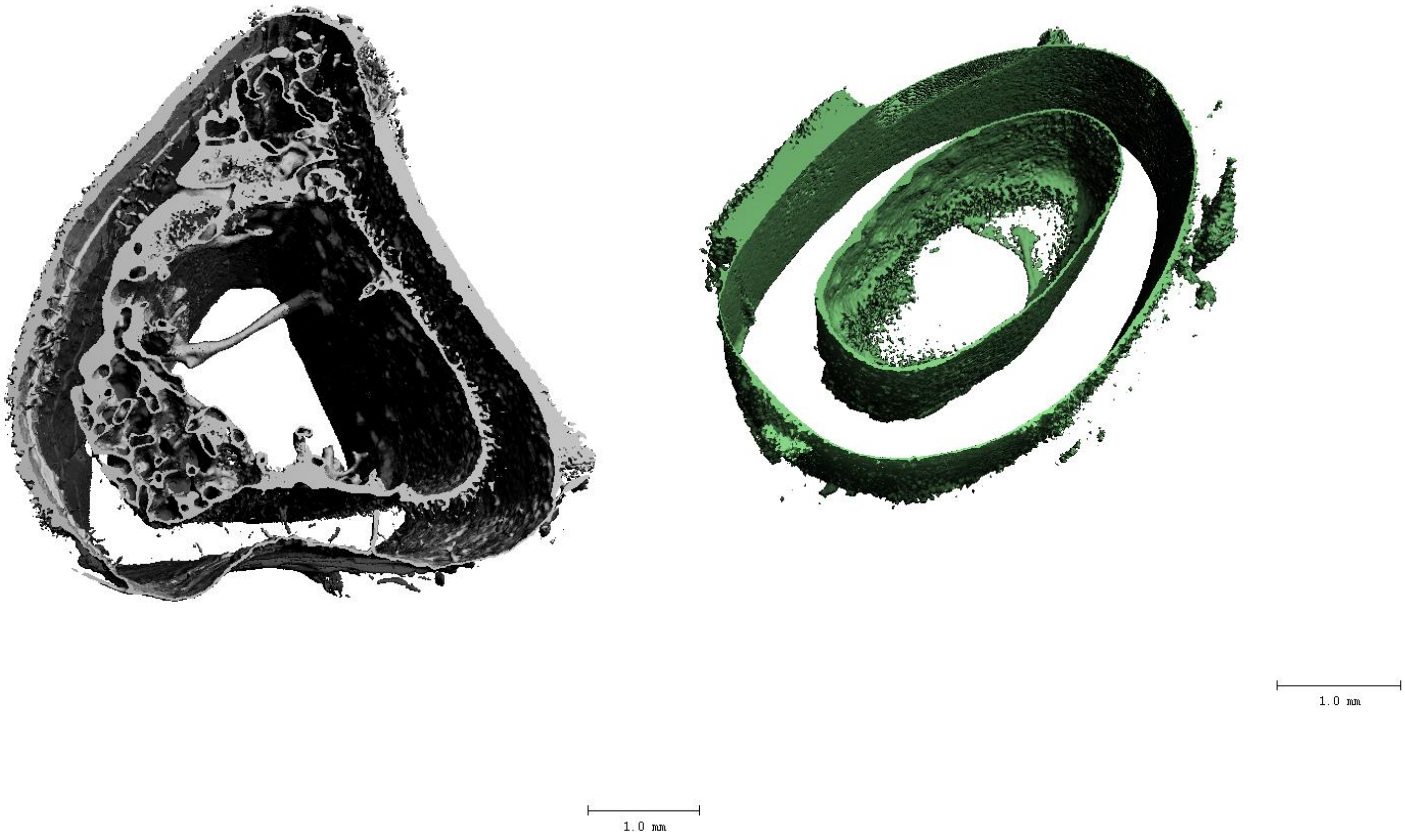

Figure 3.3.3.1: MicroCT image of allograft coating alone, with allograft removed from image (left) showing thin, continuous polymer coating on both the endosteal and periosteal surfaces. Scale bar =1 mm

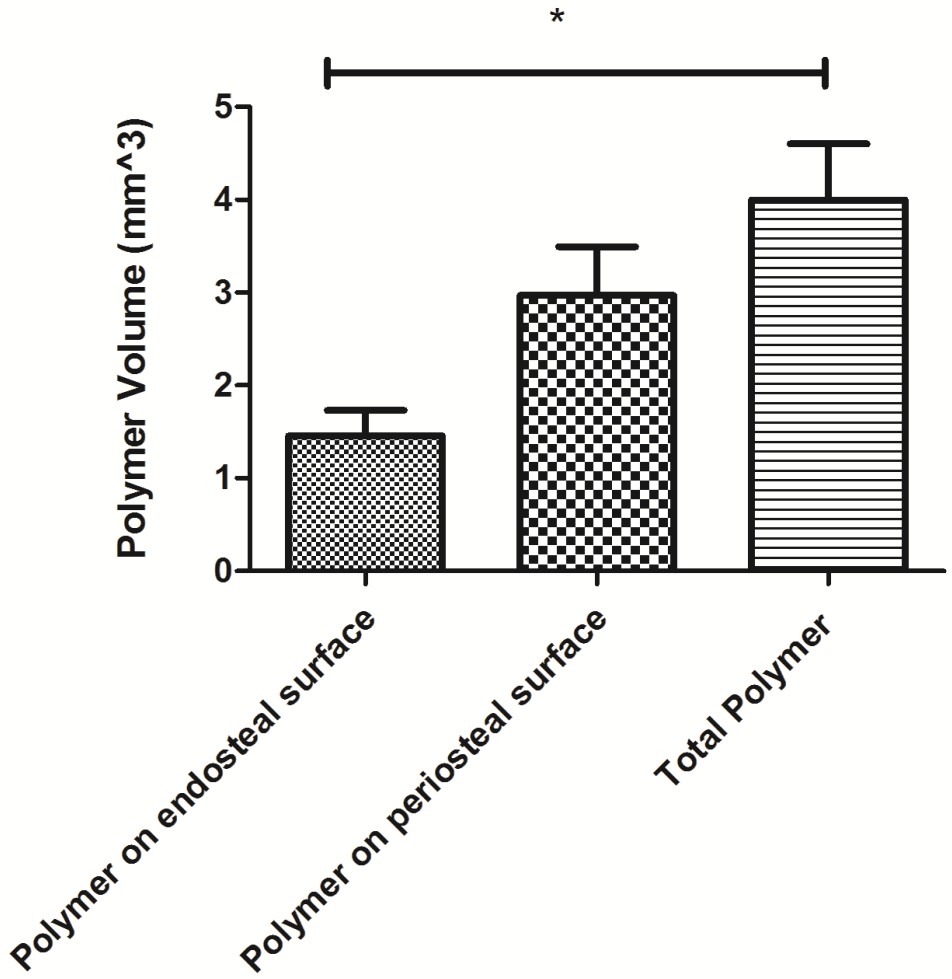

Figure 3.3.3.2: Distribution of polymer coating between periosteal and endosteal surfaces indicates a trend but no significant differences in volume.

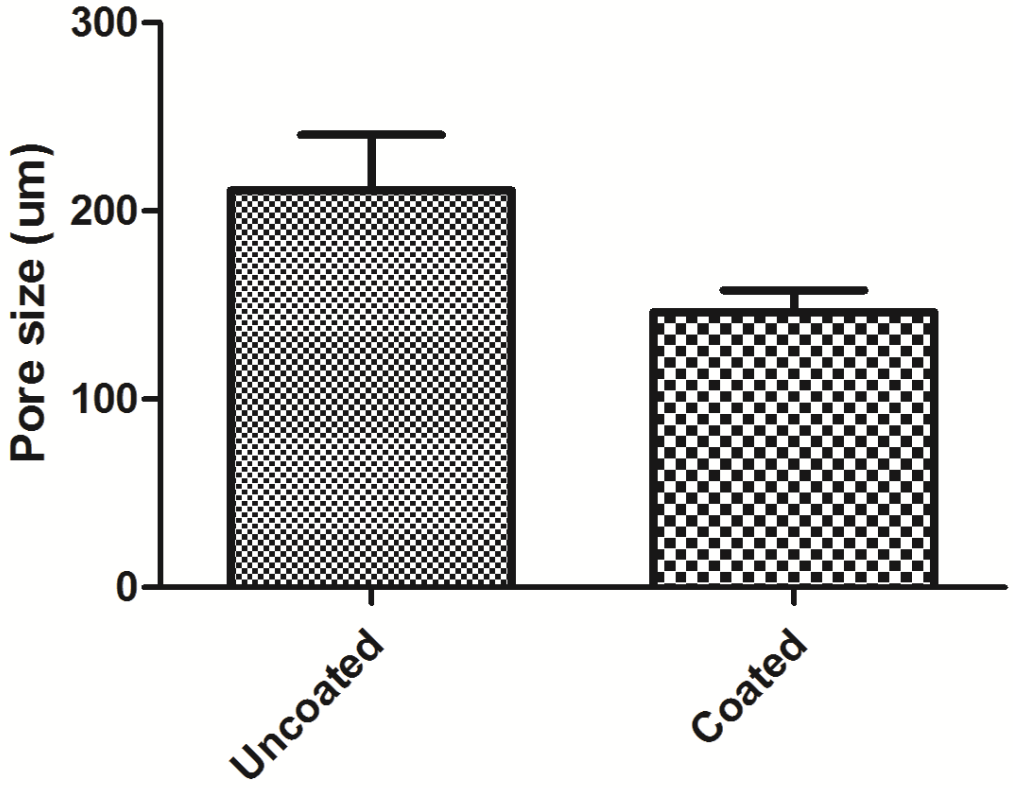

Figure 3.3.3.3: Pore size measurement of allografts. No significant difference in pore size was depicted before and after coating

3.3.4. Release of BMP-2 and VEGF (Single Release)

To determine the release kinetics of the single release of growth factors, one growth factor either BMP-2 or VEGF was loaded on one coated allograft.

3.3.4.1. Release Kinetics Profile

In vitro factor release studies examining the rate at which the growth factors were released from the coated allografts (n=6) indicated that the implants with BMP-2 adsorbed to the surface of the polymer coating exhibited a burst release of 91.10% (± 24.16%) during the first 24

hours, followed by a more gradual release and eventual plateau over the next 7 days. Almost the entire payload had been released within the first 7 days (figure 3.3.4.1.1). For the BMP-2 encapsulated within the polymer coating a more sustained release profile was noted (fig. 3.3.4.1.1) with no initial growth factor burst release but rather a more sustained release over the entire study.

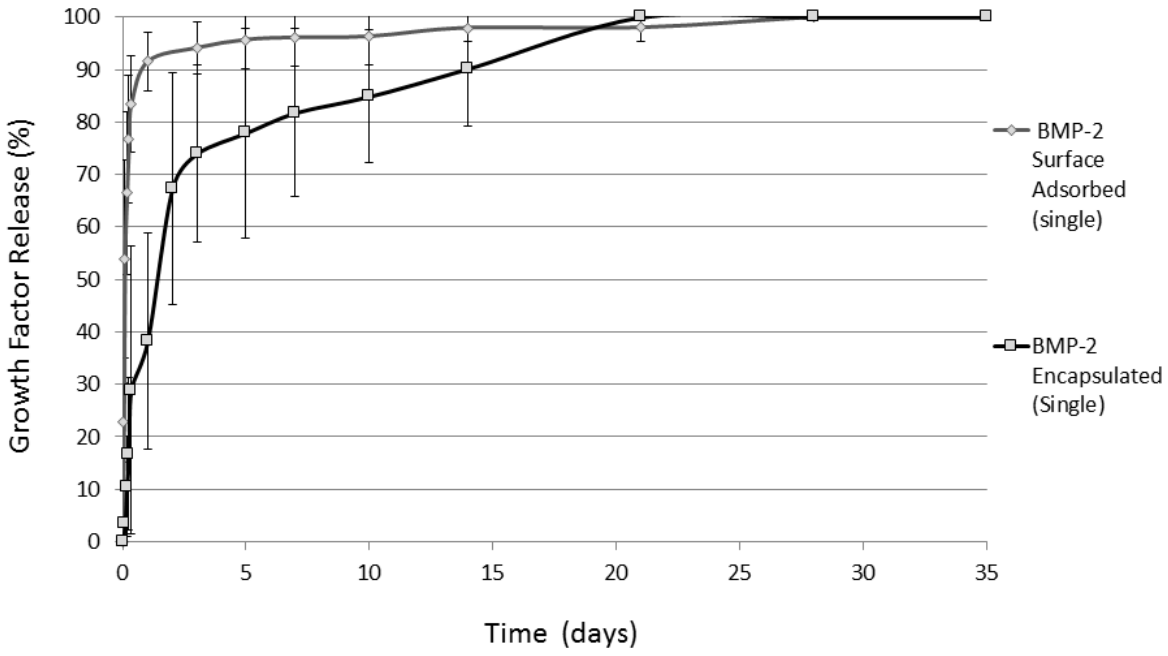

Figure 3.3.4.1.1: Growth factor release profiles from polymer-coated allografts containing either surface adsorbed (black line) or encapsulated (grey line) BMP-2 show the rapid release of surface adsorption and the more sustained release of encapsulation.

The release profile of surface adsorbed VEGF depicted similar release kinetics as the surface adsorbed BMP-2, suggesting the burst release profile due to surface adsorption was independent of the molecule being released. VEGF release was most prominent within the first few days with 60% VEGF released within the first 24 hours and 82% released by day 7 (fig. 3.3.4.1.2).

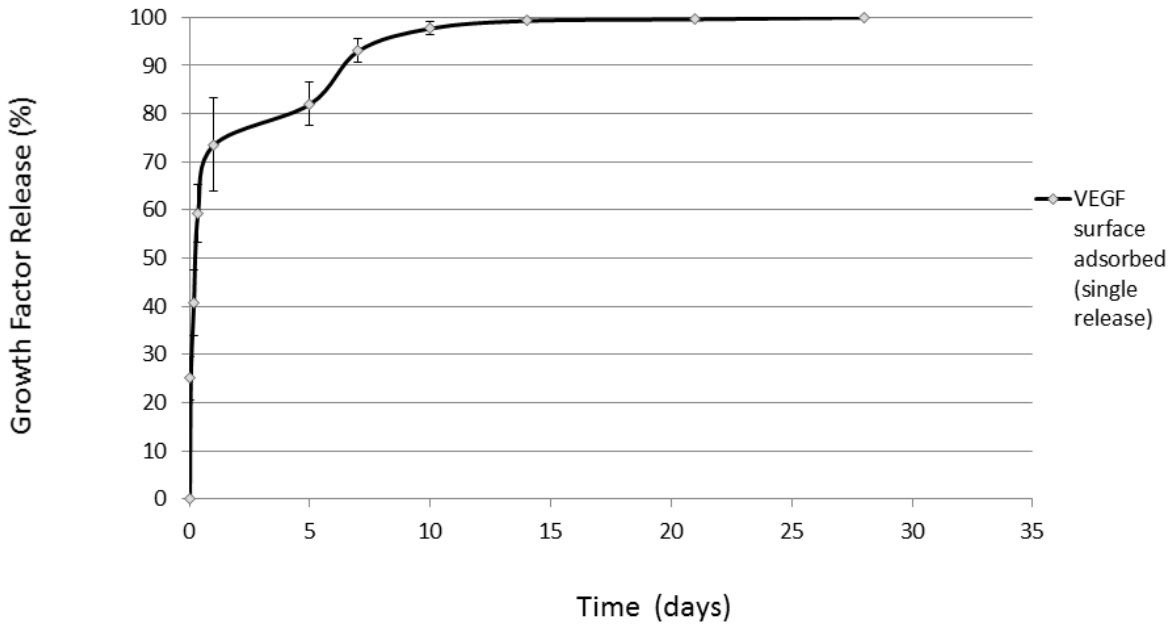

Figure 3.3.4.1.2: Growth factor release profiles from polymer-coated allografts containing VEGF (surface adsorbed). Release profiles indicate a rapid burst release of VEGF from the surface of the coated allograft. This demonstrates the versatility of delivering of multiple growth factors from coated allograft with temporal control.

3.3.4.2. Cumulative Protein Release

In total, 52 µg/ml of BMP-2 was released from the surface of the allograft coating, with no further release after day 7 (Fig. 3.3.4.2.1) while 550ng/ml of BMP-2 was released from within the polymer coating over the 42-day release study (Fig. 3.3.4.2.2). In total, 170 ng/ml of VEGF was released from the surface of the allograft coating, with no further release after day 10 (Fig 3.3.4.2.3). The surface adsorption of BMP-2 showed higher release of payload than VEGF because of the higher loading concentration in surface adsorbed BMP-2 (500 µg/ml) than surface adsorbed VEGF (5 ug/ml).

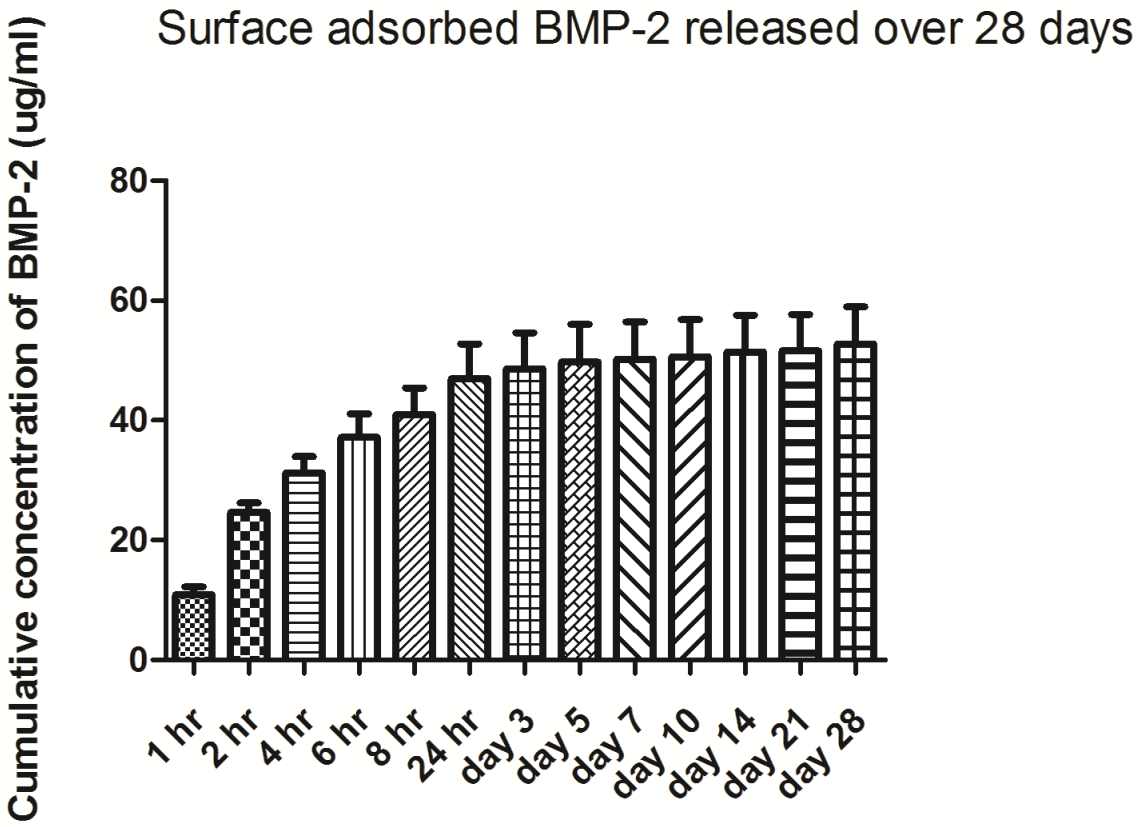

Figure 3.3.4.2.1: *In vitro* cumulative concentration of BMP-2 released from coated allograft constructs in phosphate buffered saline at 37 ^{0}C. BMP-2 was surface adsorbed onto the polymer coated allograft. Data are mean ±SD, n=6 independent experiments.

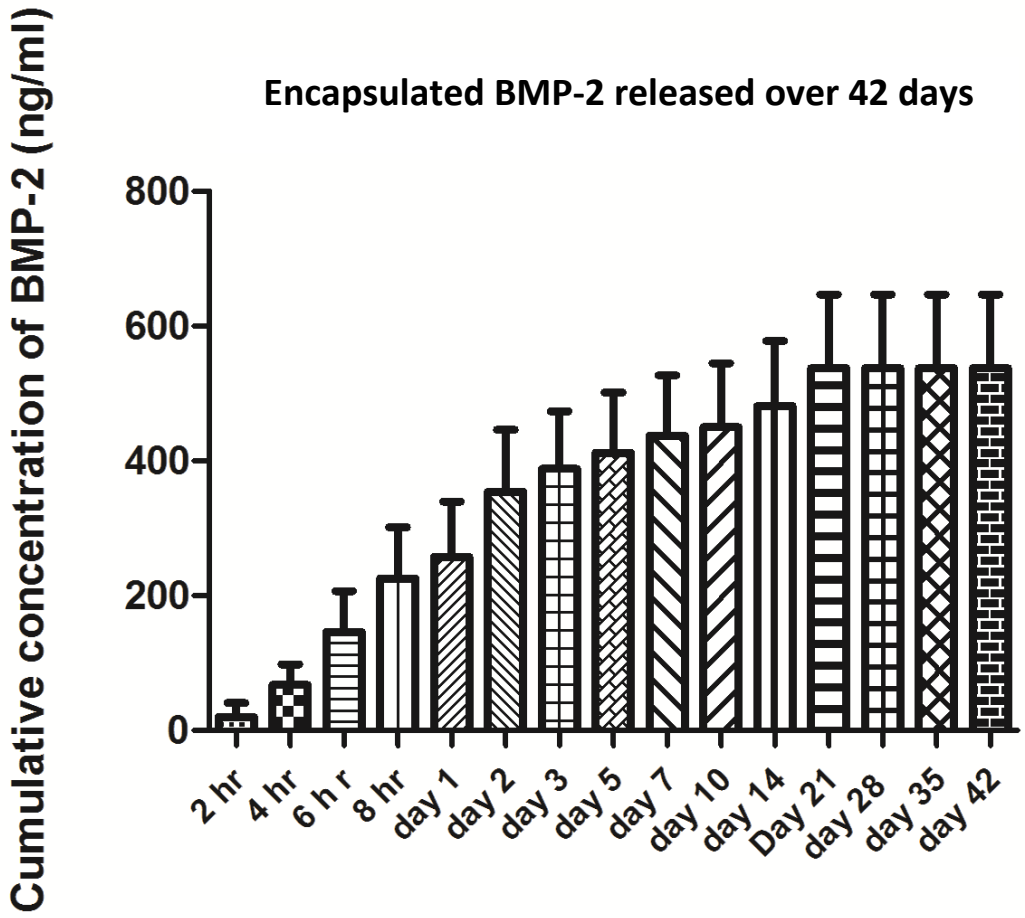

Figure 3.3.4.2.2: *In vitro* cumulative concentration of encapsulated BMP-2 released from coated allograft constructs in phosphate buffered saline at 37 ^{0}C. Data are mean ±SD, n=6 independent experiments.

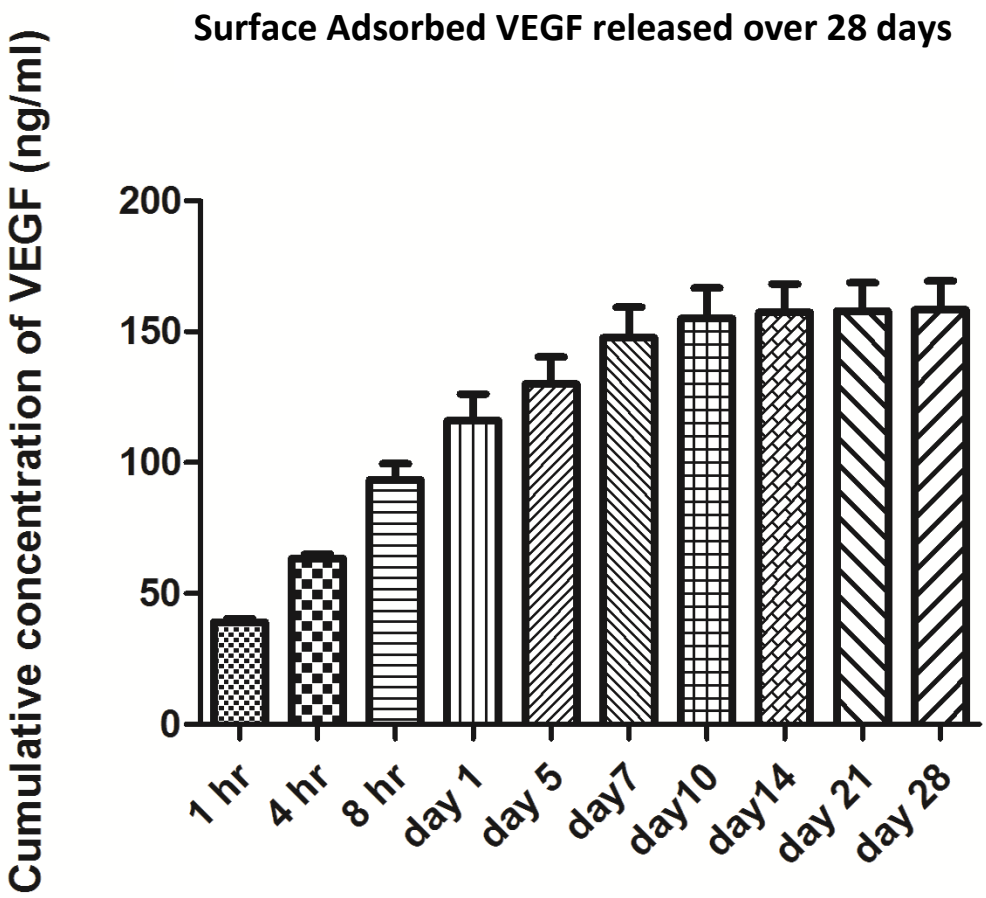

Figure 3.3.4.2.3: *In vitro* cumulative concentration of VEGF released from coated allograft constructs in phosphate buffered saline at 37 ^{0}C. VEGF was surface adsorbed onto the polymer coated allograft. Data are mean ±SD, n=6 independent experiments.

3.3.5. Release of Simultaneous Delivery of BMP-2 and VEGF

To determine release kinetics of simultaneous delivery of the growth factors, two growth factors were loaded concurrently on one coated allograft.

3.3.5.1. Release Kinetics Profile

In vitro factor release studies showed the rate at which the growth factors were released from the coated allografts when VEGF was surface adsorbed onto the polymer coating and BMP-2 was encapsulated within the coating of the coated/loaded allograft. The simultaneous release of

the two growth factors exhibited a sequential release pattern where VEGF release was predominant at the earliest time points with 96.8% of the VEGF payload eluted between days 1 and 14 (Fig.

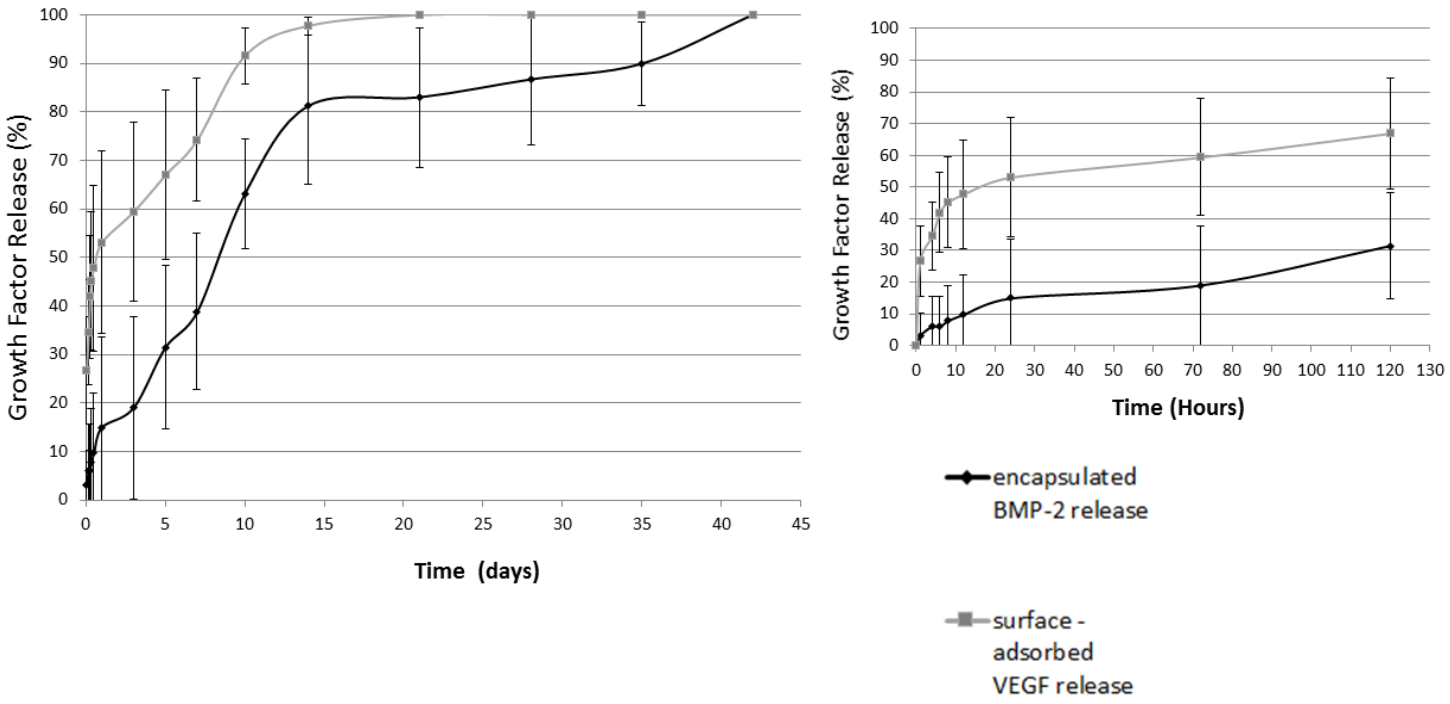

Figure 3.3.5.1.1: Growth factor release profiles from polymer-coated allografts containing both VEGF (surface adsorbed) and BMP-2 (encapsulated) simultaneously. Release profiles indicate a rapid burst release of VEGF from the surface of the coated allograft and a more sustained, longer-term release profile of BMP-2 from the polymer coating. This demonstrates the feasibility of delivering two growth factors from one coated allograft with temporal control.

3.3.5.1.1 grey line), while the BMP-2 release followed a more sustained profile with less of an initial burst release over the entire study (Fig. 2 black line).

3.3.5.2 Cumulative Protein Release

In total, 145 ng/ml of VEGF was released from the surface of the allograft coating, with no measurable release after day 28 (Fig. 3.3.5.2.1) while 368ng/ml of BMP-2 was released from

within the polymer coating over the 42-day release study (Fig.3.3.5.2.2) Overall, this result demonstrated the ability to elicit short-term and long-term delivery kinetics with one growth factor released prior to another from the same construct by using surface adsorption and encapsulation, respectively.

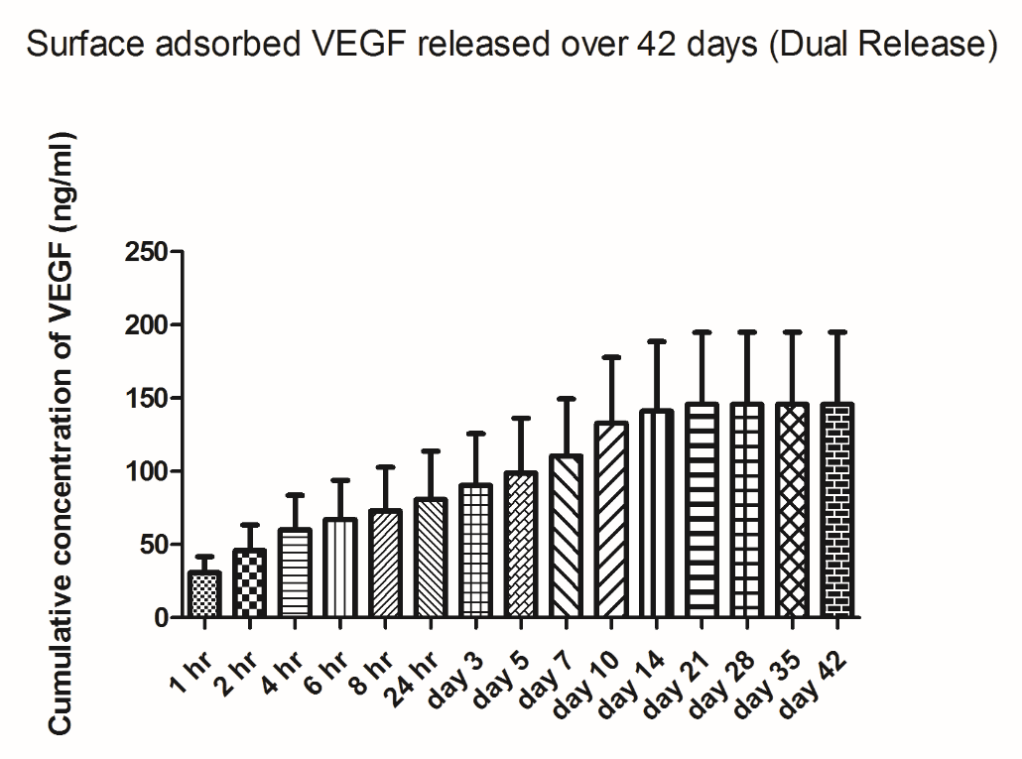

Figure 3.3.5.2.1: *In vitro* cumulative concentration of VEGF released from BMP-2+ VEGF loaded and PLGA coated allograft constructs in phosphate buffered saline at 37 ^{0}C. VEGF was surface adsorbed onto the polymer coated allograft. Data are mean ±SD, n=6 independent experiments.

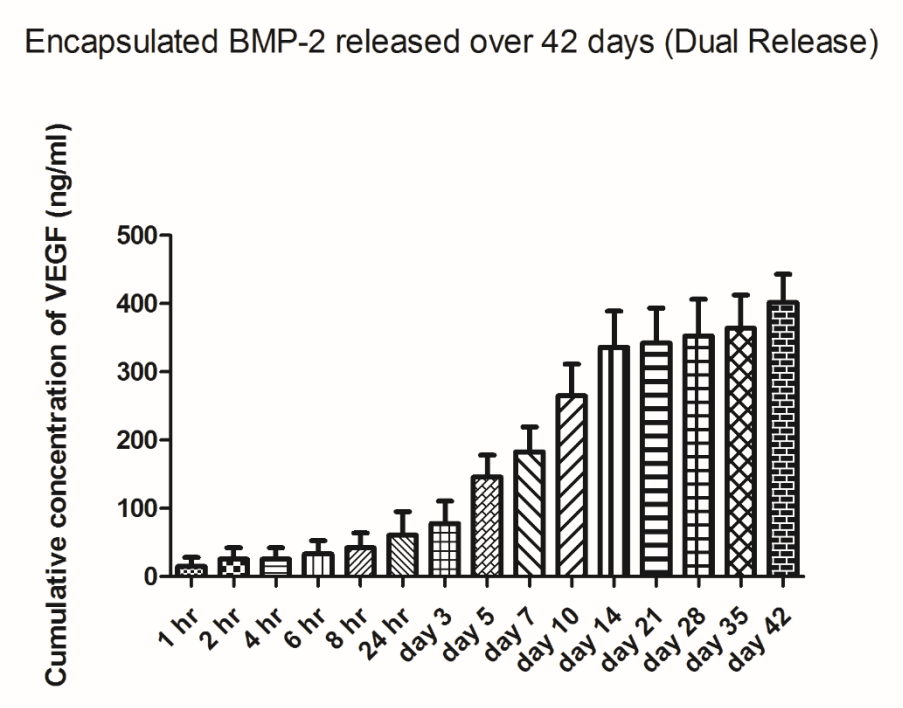

Figure 3.3.5.2.2: *In vitro* cumulative concentration of encapsulated BMP-2 released from VEGF+BMP-2 loaded and PLGA coated allograft constructs in phosphate buffered saline at 37 ^{0}C. Data are mean ±SD, n=6 independent experiments.

3.4. DISCUSSION

Based on 5- and 10-year clinical follow-up studies large-scale bone allografts have a high failure rate from infection, fracture, and non-union associated with the poor healing and integration with host bone.[14] Retrieval studies done by Wheeler and Enneking showed as much as a 50% decline in mechanical properties over time, which correlated with increased microfractures and decreased allograft bone mineral density.[5] Data suggests that the allograft is less an active part of the repair process once implanted, a factor that most likely contributes to the overall failure of the allografts in the long term. Given this, we imagined a system through which defect repair would be facilitated better by a functionalized allograft that delivers multiple bone growth factors with temporal precision rather than relying on it as a purely mechanical support. Our strategy was to

apply a microscale thick coating of degradable polymer to all surfaces of the allograft to act as a delivery vehicle for multiple growth factors known to be relevant to bone healing (VEGF and BMP-2). Further, we sought to evaluate whether the release kinetics of the loaded growth factors could be controlled to allow one to be delivered rapidly (VEGF) while the other remained sequestered and ultimately delivered over a more sustained period of time (BMP-2).

A study by Schrier et al. showed that the binding capacity of PLGA is affected by the molecular weight of the polymer, as well as the acid number of the polymer, which correlates to the hydrophilic/hydrophobic nature of the polymer. It also showed that molecular weight linearly related to binding capacity, and hydrophobic PLGA showed a greater affinity for surface adsorption binding of proteins. The release of proteins from PLGA is biphasic, with an initial burst, as well as an extended release as the polymer degrades. The burst release is caused by protein on the surface of the coating interacting with the medium surrounding it. The extended release occurs through hydrolysis of the polymer to allow for drug release through diffusion and erosion. The drug release is affected by the drug type and concentration, as well as the hydrophobicity and molecular weight of the polymer[15]. PLGA is very useful when creating drug delivery systems due to the way in which it is able to load and release growth factors. Its biphasic release makes it an optimal polymer to deliver multiple growth factors due to the fact that it is capable of causing a burst effect or an extended release. Using surface adsorption and encapsulation, it is able to exhibit a wide range of release kinetics. Properties of PLGA can also be changed in order to optimize a system for specific applications. PLGA, being a copolymer containing PLA and PGA, can be procured in many different variations, including molecular weight and ratio of the two polymers. PGA has been shown to be more hydrophobic than PLA, and a higher level of PGA also correlates to a faster degradation rate of the polymer. Therefore, PLGA can be procured in different forms

depending on the specific binding and release properties that are needed. BMPs have been administered to bone defects in a variety of ways; as a reconstituted protein that is dripped into the defect site, loaded into degradable structures that release the payload as they degrade, and directly onto allograft, both morcellized and intact, to assist with incorporation and healing to surrounding bone. Baas et al. used morcellized canine allograft as both a mechanical strut and delivery vehicle by drip-coating the rhBMP-2 onto allograft chips and implanting them with titanium screws. No means were taken to measure or control the rate of release of BMP-2 from the allograft chips, and healing was noted to have been hindered because the rhBMP-2 stimulated elevated metabolic activity of the surrounding cells. The allograft chips were completely resorbed prior to healing, leaving the implant site unstable. Therefore this was not a failure of rhBMP-2 as a healing agent, but was an indication that this approach may not be suitable for small allograft samples.[16] Indeed, Lieberman et al. authored the only clinical study of its kind investigating the utility of coating intact structural allograft with partially purified human BMP as both a mechanical strut and delivery vehicle in osteonecrotic femoral heads.[17] BMP was coated on the surface of fibula allograft samples and lyophilized, and implanted with a gelatin capsule containing BMP. Positive results indicated the potential value and utility of delivering BMP from an allograft to treat human osteonecrosis, but little was known about the uptake and release kinetics of BMP.

Others have sought to improve allograft healing by adding an external coating to try to recreate the periosteum by adding a cell layer to allografts via a submucosal membrane-coating,[18-21] or by adding a porous polymeric outer textured layer to increase osteoconductivity of the implanted allograft.[22,23] While successful to an extent, these strategies presented additional challenges when considering long-term storage since they would require an environment capable of sustaining living cells. Adding growth factors to a stable polymeric layer would not have the

same storage limitations. Further, as these alternative approaches sought to coat the periosteal portion of an allograft it is unclear how endosteal surfaces would remodel and contribute to repair. The coating process described in this manuscript does not occlude any pore structure larger than 100μm along the endosteal, periosteal, and cross-sectional regions of an implanted allograft while adding biofunctionality by delivering growth factors determined to be beneficial to new bone ingrowth.

Bone growth and repair has been attributed to many different growth factors including fibroblast growth factor (FGF), platelet-derived growth factor (PDGF), transforming growth factor-beta (TGF-β), and vascular endothelial growth factor (VEGF), to name a few. BMP-2 and VEGF, two of the more commonly studied growth factors in bone repair, are critically important on their own but also have interconnected roles in the healing process. VEGF has been shown to be involved in the conversion of soft callus to hard callus,[24] contributes to cartilage resorption and subsequent ossification,[25] and has also been found at very early stages of angiogenesis within the fracture hematoma after injury. BMP-2 has been shown to stimulate osteoblast migration and differentiation,[26] and its function has been intimately tied to the presence or absence of VEGF.[24] The function and timing of growth factor expression in bone repair has also been evaluated. Street et al. have uncovered subtle but measureable differences between intramembranous and endochondral ossification, where early angiogenesis may be required for the latter to convert chondrocytes to hypertrophic chondrocytes, stimulating their apoptosis and subsequent replacement with hard tissue. Peng et al. have evaluated the response of BMP-2-mediated bone repair in the absence and presence of VEGF. Their findings showed that BMP-2 in the presence of VEGF antagonists was reduced in its capacity to form bone, while BMP-2 in the presence of VEGF showed enhanced bone formation.[27]

Our strategy was to be able to release one growth factor, VEGF, rapidly and prior to the release of another growth factor, BMP-2, over several weeks to mimic the sequence of release suggested by the literature. Using surface adsorption and encapsulation techniques, respectively, we were able to achieve this effect. Evaluating the surface adsorption release kinetics of both BMP-2 and VEGF allowed us to determine if surface adsorption-mediated burst release was simply a function of the loading process or was also dependent on the molecule released. It was found that while surface adsorption led to an overall burst release regardless of the molecule there were some slight differences in the kinetics of the burst release. Each growth factor, VEGF and BMP-2, released over 90% of the payload within 7-10 days but about 70% of the BMP-2 had released within 24 hours while only 60% of the VEGF was released in the same time frame. There are several factors that could explain the subtle difference like the hydrophobicity of the surface of the polymer, the 3-dimensional structure of the scaffold, the pKa and isoelectric point of the molecule,[29,30] and the molecular weight of the polymer[30]. Since the scaffold material and structure were the same for each growth factor those parameters were not relevant. Both BMP-2 and VEGF have pI values of 8.5-9 so that is unlikely to have had a large impact. Molecular weight, however, of BMP-2 is 26 kDa while VEGF is 45 kDa. The larger size may have impacted the release of the VEGF from the surface since surface adsorbed proteins can either be considered free or bound, where the free molecules are dependent on the concentration of the molecule in solution and the bound molecules are physically entrapped within small pores on the surface of the microsphere[28-30]. The larger VEGF molecule may have released more slowly from being bound to the surface by virtue of its larger physical size.

The *simultaneous and sequential* delivery of VEGF *and* BMP-2 from the same coated allograft exhibited that surface adsorbed VEGF is released rapidly from the double loaded

allograft, with over 96% coming off in the first four days. While BMP-2 release also begins in the short term its release is more gradual and extends over a longer period of time than the VEGF, with more than 50% of its payload still bound to the allograft after VEGF is almost completely eluted. This demonstrates that we can deliver both VEGF and BMP-2 from the same construct, and preferentially have the vast majority of the VEGF elute first, a temporal specificity that has been shown in the literature to be important for bone repair and regeneration [31,32]. While the two growth factors do elute simultaneously at the earliest time points, VEGF elutes at 3x-5x that of BMP-2. At later time points BMP-2 continues to elute after the entire VEGF payload has been released. So while not perfectly sequential, the release is dominated in the earliest time points by VEGF and at the later time points by BMP-2.

3.5. CONCLUSIONS & FUTURE DIRECTIONS

Studies on factors and bone repair have clarified the importance of controlling not only which factors to administer to a bone defect site but also the relative quantities and the temporal expression of factors as well. In response, this study was an attempt to address each of these needs by modifying existing large scale bone allografts with a thin polymeric coating that would act as a delivery vehicle for growth factors in a temporal pattern designed to maximize bone-allograft incorporation. In this study we have demonstrated the dual release of VEGF and BMP-2 with temporal precision from one polymer-coated cortical allograft. Burst release of VEGF was confined to the first week while BMP-2 release was extended over several weeks of elution. Our studies have resulted in a microscale thin polymer coating of PLGA capable of retaining and delivering growth factors, VEGF, and BMP-2 and releasing them in such a way that it is available at the defect site initially by a burst release or by a longer-term exposure.

Further refinement of release kinetics for each growth factor is possible by functionalizing the surface of the polymer to modify its hydrophobicity, varying the polymer used (more slowly degrading materials may sustain long term release for longer periods of time) or by adding other materials like calcium phosphate to the coating, which may allow for a more sustained release of the surface adsorbed VEGF if desired. Further, we should develop protocol to measure the total amount of growth factors loaded onto the coated allograft. This will give us an indication of the total amount of proteins that will be released *in vivo* as the allografts break down and eventually proteins that are embedded within the bone matrix will be eluded. Additionally, this approach is not limited to VEGF and BMP-2. Antibiotics, which may need to be released in a bolus after implantation could be surface adsorbed to provide both acute and chronic delivery.

3.6. REFERENCES

1. Thompson R, Pickvance E, Garry D. Fractures in large-segment allografts. J Bone Joint Surg Am 1993; 75(11):1663-73.

2. Ito H, Koefoed M, Tiyapatanaputi P, Gromov K, Goater JJ, Carmouche J, Zhang X, Rubery PT, Rabinowitz J, Samulski RJ, Nakamura T, Soballe K, O'Keefe RJ, Boyce BF, Schwarz EM. Remodeling of cortical bone allografts mediated by adherent rAAV-RANKL and VEGF gene therapy. Nat Med 2005 Mar; 11(3):291-7. Epub 2005 Feb 13.

3. Dallari D, Fini M, Stagni C, Torricelli P, Nicoli Aldini N, Giavaresi G, Cenni E, Baldini N, Cenacchi , Bassi A, Giardino R, Fornasari PM, Giunti A. *In vivo* study on the healing of bone

defects treated with bone marrow stromal cells, platelet-rich plasma, and freeze-dried bone allografts, alone and in combination. J Orthop Res 2006; 24(5):877-88.

4. Koefoed M, Ito H, Gromov K, Reynolds DG, Awad HA, Rubery PT, Ulrich-Vinther M, Soballe K, Guldberg RE, Lin AS, O'Keefe RJ, Zhang X, Schwarz EM. Biological effects of rAAV-caAlk2 coating on structural allograft healing. Mol Ther 2005; 12(2):212-8.

5. Fini M, Giavaresi G, Aldini NN, Torricelli P, Botter R, Beruto D, Giardino R. A bone substitute composed of polymethylmethacrylate and -tricalcium phosphate: results in terms of osteoblast function and bone tissue formation. Biomaterials 2002; 23: 4523-4531.

6. Kikuchi M, Itoh S, Ichinose S, Shinomiya K, Tanaka J. Self-organization mechanism in a bone-like hydroxyapatite /collagen nanocomposite synthesized *in vitro* and its biological reaction *in vivo*. Biomaterials 2001; 22: 1705-1711.

7. Chen F, Wang ZC, Lin CJ. Preparation and characterization of nano-sized hydroxyapatite particles and hydroxyapatite/chitosan nano-composite for use in biomedical materials. Materials Letters 2002; 57:858-861

8. Borden M, Attawia M, Khan Y, Laurencin CT. Tissue engineered microsphere-based matrices for bone repair: design and evaluation. Biomaterials 2002; 23(2):551-9.

9. Khan Y, Katti DS, Laurencin CT. A Novel Polymer-Synthesized Ceramic Composite Based System for Bone Repair: Osteoblast Growth on Scaffolds With Varied Calcium Phosphate Content. Nanoscale Materials Science in Biology and Medicine. Editors: C.T. Laurencin, E. Botchwey MRS Proceedings Volume 845.

10. Khan Y, Katti DS, Laurencin CT. A Novel Polymer-Synthesized Ceramic Composite Based System for Bone Repair: An *In Vitro* Evaluation. J. Biomed Mater Res 2004; 69A, 728-737, 2004.

11. Johnson, E. E., & Urist, M. R. One-stage lengthening of femoral nonunion augmented with human bone morphogenetic protein. Clinical orthopaedics and related research 1998; 347: 105-116. 31.

12. Petri-Aronin C, Shin SJ. Naden KB, Rios PD, Sefcik LS, Zawodny SR, Bagayoko ND, Cui Q, Khan Y, Botchwey EA. The enhancement of bone allograft incorporation by the local delivery of the sphingosine 1-phosphate receptor targeted drug FTY720. Biomaterials 2010; 31:6417-24.

13. Huang YC, Kaigler D, Rice, Krebsbach PH, Mooney DJ. Combined Angiogenic and Osteogenic Factor Delivery Enhances Bone Marrow Stromal Cell-Driven Bone Regeneration. J Bone Min Res 2005:20:848-857.

14. Wheeler DL, Enneking WF. Allograft Bone Decreases in Strength *In Vivo* Over Time. Clin Orthop Rel Res. 2005; 435 36-42.

15. Schrier JA, DeLuca PP. Recombinant human bone morphogenetic protein-2 binding and incorporation in PLGA microsphere delivery. Pharm Dev Technol 1999; 4: 611–621.

16. Baas J, Elmengaard B, Jensen TB, Jakobsen T. The effect of pretreating morselized allograft bone with rhBMP-2 and/or pamidronate on the fixation of porous Ti and HA-coated implants. Biomaterials 2008; 29(19):2915-22.

17. Lieberman JR, Conduah A, Urist MR. Treatment of osteonecrosis of the femoral head with core decompression and human bone morphogenetic protein. Clin Orthop Relat Res 2004;(429):139-45.

18. Xinping Zhang PhD, Hani A. Awad PhD, Regis J. O'Keefe MD, PhD, Robert E. Guldberg PhD, Edward M. Schwarz PhD. Engineering Periosteum for Structural Bone Graft Healing. Clin Orthop Relat Res (2008); 466:1777–1787.

19. Knothe Tate ML, Ritzman TF, Schneider E, Knothe UR. Testing of a new one-stage bone-transport surgical procedure exploiting the periosteum for the repair of long-bone defects. J Bone Joint Surg Am 2007;89:307–316.

20. Ouyang HW, Cao T, Zou XH, Heng BC, Wang LL, Song XH, Huang HF. Mesenchymal stem cell sheets revitalize nonviable dense grafts: implications for repair of large-bone and tendon defects. Transplantation 2006; 82:170–174.

21. Zhou Y, Chen F, Ho ST, Woodruff MA, Lim TM, Hutmacher DW. Combined marrow stromal cell-sheet techniques and highstrength biodegradable composite scaffolds for engineered functional bone grafts. Biomaterials 2007;28:814–824.

22. Lewandrowski KU, Bondre SP, Gresser JD, Wise DL, Tomford WW, Trantolo DJ. Improved osteoconduction of cortical bone grafts by biodegradable foam coating. Biomed Mater Eng 1999; 9(5-6):265-75.

23. Lewandrowski KU, Bondre S, Hile DD, Thompson BM, Wise DL, Tomford WW, Trantolo DJ. Porous poly(propylene fumarate) foam coating of orthotopic cortical bone grafts for improved osteoconduction.Tissue Engr 2002; 8(6):1017-27.31.

24. Street J, Bao M, deGuzman L, Bunting S, Peale FV Jr, Ferrara N, Steinmetz H, Hoeffel J, Cleland JL, Daugherty A, van Bruggen N, Redmond HP, Carano RA, Filvaroff EH. Vascular endothelial growth factor stimulates bone repair by promoting angiogenesis and bone turnover. Proc Natl Acad Sci USA 2002; 99(15):9656-61.

25. Gerber HP, Vu TH, Ryan AM, Kowalski J, Werb Z, Ferrara N. VEGF couples hypertrophic cartilage remodeling, ossification and angiogenesis during endochondral bone formation. Nat Med 1999; 5(6):623-8.

26. Street J, Winter D, Wang JH, Wakai A, McGuinness A, Redmond HP. Is human fracture hematoma inherently angiogenic? Clin Orthop Relat Res 2000 ;(378):224-37.

27. Peng H, Usas A, Olshanski A, Ho AM, Gearhart B, Cooper GM, Huard J. VEGF improves, whereas sFlt1 inhibits, BMP2-induced bone formation and bone healing through modulation of angiogenesis. J Bone Miner Res 2005; 20(11):2017-27.

28. Cushnie EK, Khan YM, Laurencin CT. Tissue-engineered matrices as functional delivery systems: adsorption and release of bioactive proteins from degradable composite scaffolds. J Biomed Mater Res A 2010; 94(2):568-75.

29. Duggirala SS, Mehta RC, DeLuca PP. Interaction of recombinant human bone morphogenetic protein-2 with poly(D,L lactide-coglycolide) microspheres. Pharm Dev Technol 1996;1:11 19.

30. Schrier JA, DeLuca PP. Recombinant human bone morphogenetic protein-2 binding and incorporation in PLGA microsphere delivery. Pharm Dev Technol 1999; 4: 611–621.

31. Jakobsen T, Baas J, Bechtold JE, Elmengaard B, Søballe K. Soaking morselized allograft in bisphosphonate can impair implant fixation. Clin Orthop Relat Res 2007; 463:195-201

32. Jakobsen T, Baas J, Kold S, Bechtold JE, Elmengaard B, Søballe K. Local bisphosphonate treatment increases fixation of hydroxyapatite-coated implants inserted with bone compaction. J Orthop Res 2009; 27(2):189-94.

4. INVESTIGATION OF BIOACTIVITY OF RELEASED BMP-2: *IN VITRO* & *IN VIVO* EVALUATION

4.1. INTRODUCTION

Encapsulation of proteins or peptides within biodegradable and biocompatible polymers is a successful and well-documented method for their sustained or controlled-release. The benefits of sustained or controlled-release protein delivery systems include avoidance of resistance in bacteria [1–4] and pulsatile administration of vaccines to enhance immune response, etc [5, 6]. In general, during the protein encapsulation process an aqueous solution of the protein, or of protein and an additive, is added to an organic solution of the polymer of choice to form an emulsion. Because proteins are large hydrophilic molecules and difficult to encapsulate within hydrophobic polymers, a high rate of mixing is employed to entrap the protein into pockets of water solution inside the polymer, followed by freeze-drying. As discussed in the previous section the encapsulation of BMP-2 into the PLGA coated allograft showed sustained release of payload over 42 days, which can be beneficial to mimic the healing of native bone. However, this method results in direct exposure of the protein molecule to water–oil interfaces, which can often result in protein denaturation. [2] Therefore the primary goal of this study is to confirm that the coating applied to the allograft did not diminish nor remove the bioactivity of the delivered proteins. To this end the released growth factor bioactivity was assessed by both *in vitro* and *in vivo* studies. We performed *in vitro* cell studies with human mesenchymal stem cells (hMSCs) to test the osteoinductivity of the released BMP-2. A pilot *in vivo* study was also conducted to further verify the bioactivity of released BMP-2 to heal a critical sized defect.

4.2. MATERIALS AND METHODS

4.2.1. Cell Culture

To study the bioactivity of the released BMP-2, human mesenchymal stem cells (hMSCs) isolated from human bone marrow, cell culture growth medium, and cell culture osteogenic medium were obtained from Lonza (Lonza Walkersville Inc, Maryland). hMSCs were expanded per vendor protocols in growth medium, after which they were trypsinized and seeded into 24 well culture plates at a seeding density of 50,000 cells/well and maintained in osteogenic medium. Cellular viability and phenotypic expression was evaluated after 7, 14, and 21 days (and 28 for mineralization studies). Three different groups were tested for the *in vitro* study: 1) Test Group: Cells were treated with BMP-2 that was released from polymer-coated and growth-factor-loaded (coated-loaded) allografts that were placed into transwell inserts so the seeded cells would be exposed to released BMP-2 but not the allograft itself, 2) Positive Control: cells were cultured as above but without the coated-loaded allografts added. Rather 1.5μl of a stock solution of reconstituted rhBMP-2 (100μg/ml) was added directly to wells every three days for a final concentration of 100ng/ml, and 3) Negative Control: cells were cultured as the control group but vehicle (reconstitution solution with no BMP-2) was added every three days.

4.2.1.1. Cytotoxicity Assay

Potential cytotoxicity of the released BMP-2 was assessed using an MTS assay (CellTiter 96® Aqueous One Solution, Promega Corp, WI) at specific intervals (7, 14 and 21 days). For MTS assay study the cells were treated with basal media. Assays were performed by adding a small amount of the CellTiter 96® AQueous One Solution Reagent directly to culture wells at designated time points (7, 14 and 21 days), incubating for 2 hours and then recording the

absorbance at 490nm with a micro plate reader. The absorbance values were normalized to the background readings. A standard curve relating cell number to MTS activity was plotted for the specific hMSCs used in the current study.

4.2.1.2. Alkaline Phosphatase (ALP) Activity

Alkaline phosphatase (ALP) activity was analyzed using an Alkaline Phosphatase Substrate kit (Bio-Rad Laboratories, Inc., Hercules, CA), which measured the catalytic activity of ALP via the conversion of p-nitrophenyl phosphate to p-nitrophenol + phosphate and assumed that the rate of reaction was proportional to the enzyme activity. Prior to conducting the ALP activity assay, cells were rinsed with PBS and lysed with 1% Triton X-100. Next, 100 μL of each cell lysate sample was incubated with 100 μL of the working ALP substrate solution (p-nitrophenyl phosphate tablets dissolved in 1X diethanolamine buffer) for 30 minutes at 37°C. 0.4 N NaOH was then added to each sample to stop the ALP-catalyzed reaction. Finally, the absorbance of each sample was immediately measured at a wavelength of $\lambda = 405$ nm using a SpectraFluor Plus Tecan plate reader (Männedorf, Switzerland). ALP data was normalized to cell number by BCA protein assay.

4.2.1.3. Mineralized Matrix Production

Alizarin red was used to stain calcium deposits to measure the capacity and extent of mineralization of the cell cultures. At each culture time point (7, 14, 21 and 28 days) cells were fixed with 70% ethanol. Following fixation, cells were stained with 40 mM alizarin red (pH 4.23) for 10 minutes and then thoroughly rinsed with ddH_2O until all excess stain was removed. Stain was quantified (562 nM) after solubilizing in 10% cetylpyridinium chloride (10 mM sodium phosphate, pH 7.0). Mineralization data was normalized to cell number by BCA protein assay.

4.2.2. *In Vivo* Femoral Critical-Sized Defect

Allografts were placed in critical size segmental femoral defects in 14 week-old male Lewis rats (n=1). Two groups were evaluated; one of which received BMP-2 loaded allografts (both surface adsorbed and encapsulated) and one of which received polymer coated but non-factor-loaded allografts. All procedures were done in accordance with approved Institutional Animal Care and Use Committee guidelines. Briefly, the femur was approached anterolaterally, the periosteum incised, and then removed circumferentially. A small plate was fixed to the femur with four Kirschner wires and two surgical steel cerclage wires and a 6mm critical-sized full-thickness defect was created in the central third of the diaphysis. The allografts were shaped to final size intraoperatively and placed into the defects to achieve a press-fit, and maintained in place using a single 4-0 Vicryl (Ethicon, Somerville, NJ) cerclage stitch that was tied around the graft and plate. A three-layered closure of the muscle, subcutaneous tissue, and skin was performed with 4-0 Vicryl.

4.2.2.1. Radiological Analysis

Bone formation on rat femur was analyzed at 26 kV for 6 seconds using the Faxitron X-ray machine, and the Faxitron DX-Beta SR v1.4 software. Radiographic images were taken at 1, 2, 4, and 8 weeks after surgery to track bone formation as indicated by radiographic opacity.

4.2.2.2. Microcomputed Tomography (MicroCT)

MicroCT provides an efficient method to measure the distribution and density of mineralized tissue throughout the scaffold. Limbs harvested at week 12 were imaged using cone beam micro-focus X-ray computed tomography to render three-dimensional models for direct quantitation of sample bone density and volume, and to provide a three-dimensional

reconstruction of the defect (μCT40, Scanco Medical AG, Bassersdorf, Switzerland). Segmentation of bone and allograft provided direct volumetric quantification of new bone formation

4.2.2.3. Histological Analysis

Limbs were embedded in methyl methacrylate using a plastic methylmethacrylate processing, infiltration and embedding techniques as described by Kecena *et al*., [7] and then was sectioned as undecalcified, and mounted onto glass slides. These sections were then be stained with hematoxylin and eosin to evaluate cellular events, and with Masson's Trichrome to evaluate the osteoid, or new unmineralized bone being deposited at bone forming sites. All staining was performed according to protocols described by Kecena *et al*. [7].

4.2.3. Statistical Analysis

A student's t-test (to compare two groups) or one-way analysis of variance with Tukey post-hoc testing, (for multiple group comparisons) was used to determine statistical significance with $p<0.05$. Sample size for *in vitro* cell culture analysis was n=3.

4.3. RESULTS

4.3.1. Cell Viability

The cell viability assay showed significant increase in cell number over the 21 days (Figure 4.3.1.1) where the cells were treated with BMP-2 released from the loaded-coated allografts (n=3). The result shows that the released dose of BMP-2 and the byproducts of the scaffold are not toxic to the cultured hMSCs.

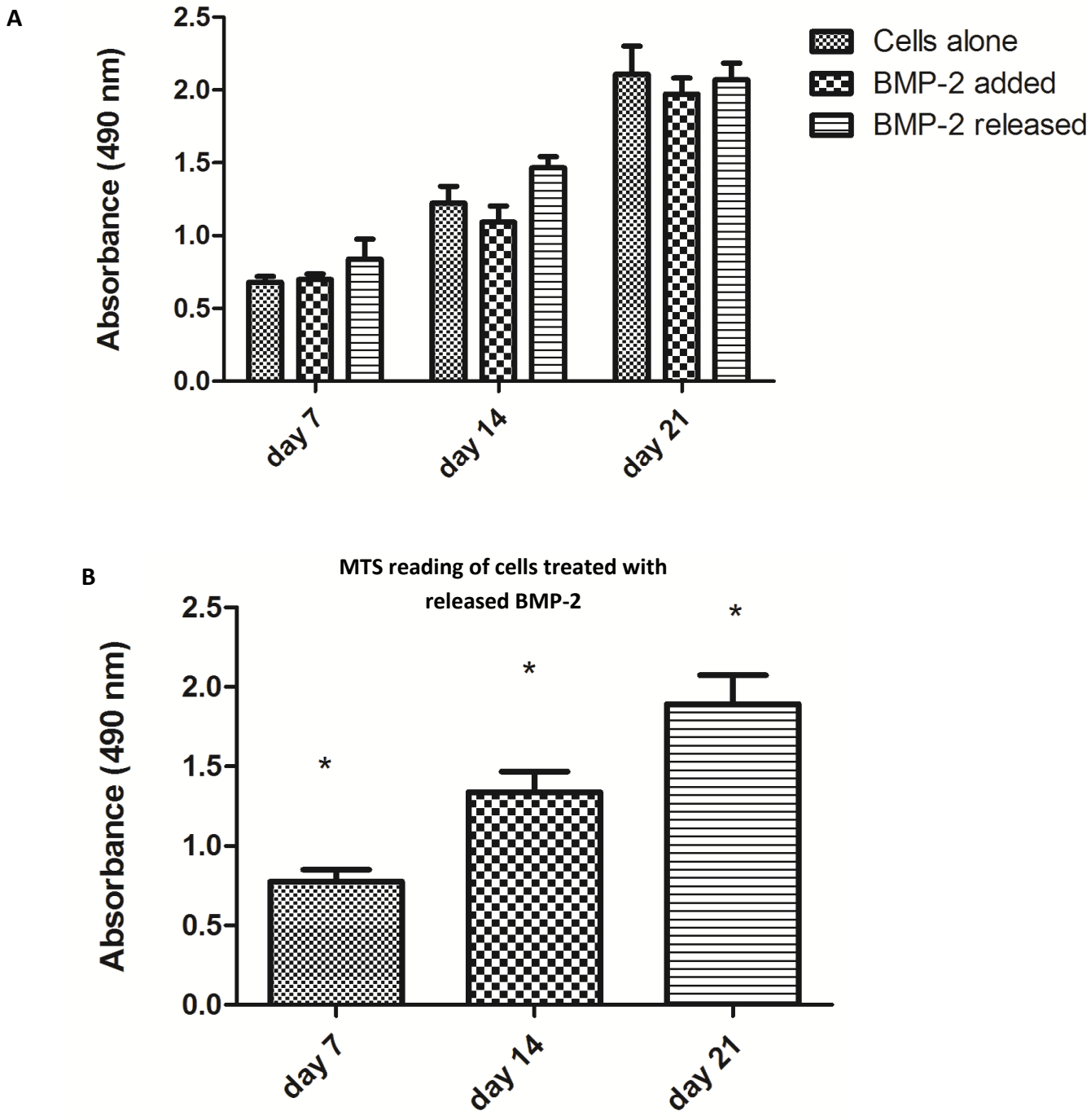

Figure 4.3.1.1: Effect of released BMP-2 dose on human mesenchymal stem cell viability determined by MTS mitogenic assay. (A) There is no significant difference between the groups in each time point. (B)Increasing cell numbers in the group treated with released BMP-2 over 21 days confirm the biocompatible released dose of the protein. Significance between groups is designated with * = $p<0.05$.

4.3.2. ALP Activity: Bioactivity of Released BMP-2

Alkaline Phosphatase (ALP) activity, well know osteoblastic phenotype marker was assessed in cells treated with BMP-2 released from allografts. The control for this study was cells treated in osteogenic media without any added BMP-2. Due to the presence of osteogenic component in the media the cells with no BMP-2 showed some ALP activity in the early stage of the time point, however as time progressed and the allograft started to release BMP-2, the group with BMP-2 showed significant increase in ALP activity over the control group (Figure 4.3.2.13.1).

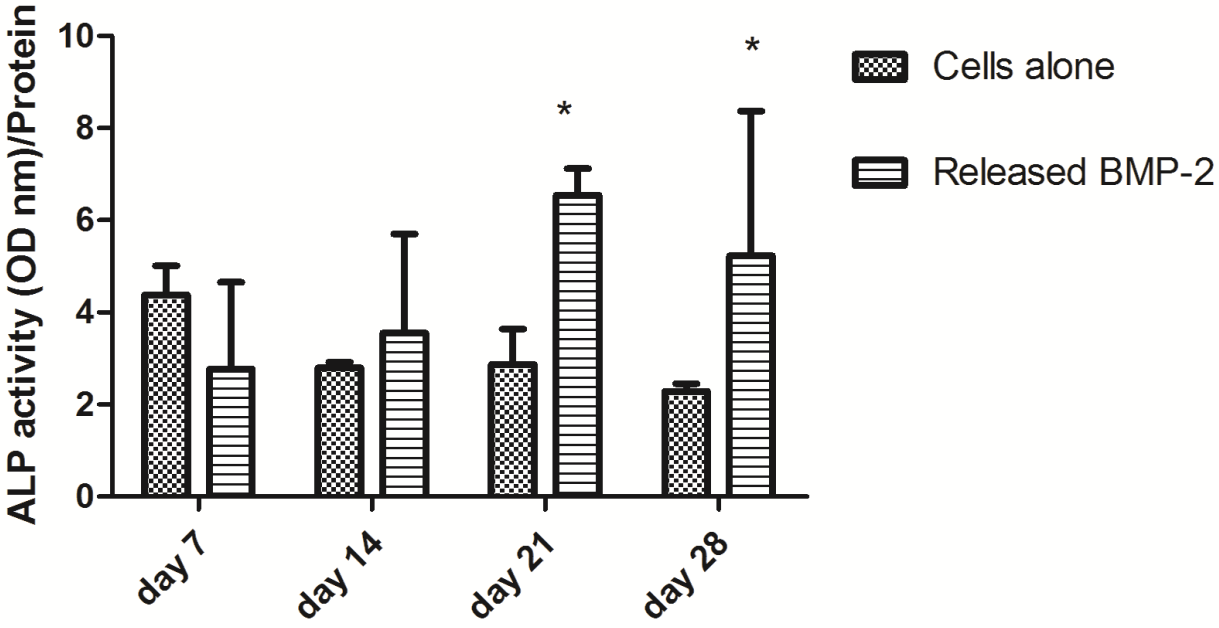

Figure 4.3.2.1: ALP activity on cells treated with released BMP-2 and cell alone over a period of 28 days (A). Significant increase in the cellular ALP activity at day 21 and 28 between cells exposed to released BMP-2 compared to cells not exposed to BMP-2 confirms the intact bioactivity of the protein (B). Significance between groups is designated with (*)= $p<0.05$.

4.3.3. Mineralization: Bioactivity of Released BMP-2

The quantitative results of the alizarin red calcium staining assay, an indicator that the cells are differentiating into mature osteoblasts, showed that at day 28 there was a significant increase in cellular mineralization from cells not exposed to released BMP-2 to cells exposed to released BMP-2 (Figure 4.3.3.11). The positive control where BMP-2 solution was added manually to the culture also demonstrated similar trend as the experimental group (n=3). The data revealed that the BMP-2 released from the scaffold aids in differentiation of hMSCs into osteoblasts and is as effective when loaded and released as it is when added directly to culture wells.

A

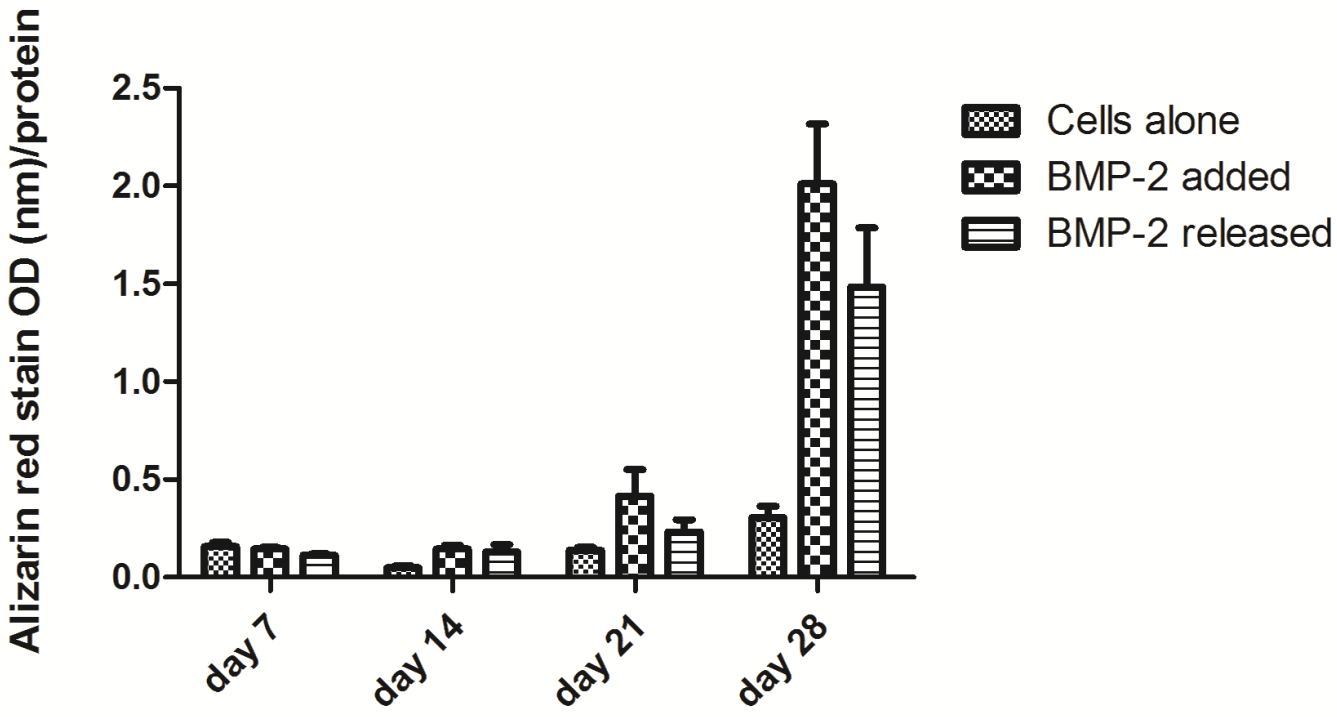

B

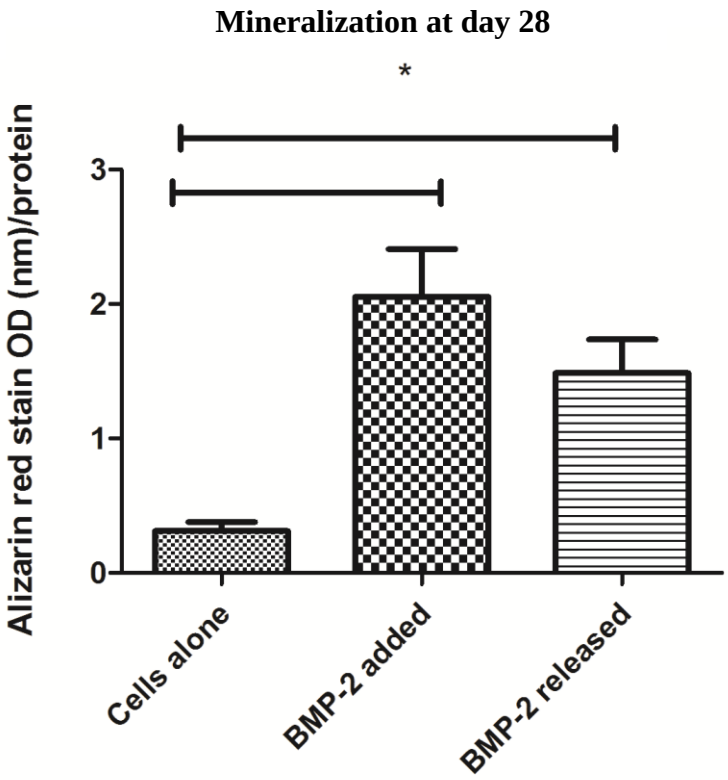

Figure 4.3.3.1: Alizarin red staining on cells treated with released BMP-2, added BMP-2 and cell alone over a period of 28 days (A). Significant increase in the cellular mineralization activity at day 28 between cells exposed to released BMP-2 compared to cells not exposed to BMP-2 confirms the intact bioactivity of the protein (B). Significance between groups is designated with (*)= $p<0.05$.

4.3.4. *In Vivo* Bone Formation

Radiograph, microCT and histological analysis revealed robust bone formation over an 8-week period. Evidence of mineralized callus was first evident by day 14 radiographs of allografts loaded with BMP-2 and continued to develop over the 8-week period as compared to polymer-coated allograft without growth factors (see fig. 4.3.5.1). MicroCT detected total volume through Defect Region as 76.0787 mm ^{3} and new bone volume through defect region as 41.3817 mm^3. BV/TV was calculated as 54.4 % (fig. 4.3.5.2). Histological sections performed 8 weeks after the procedure confirm the healing noted in radiographs. Coated allografts with no BMP-2 loading

show evidence of osteoid formation along the length of the allograft but no mineralized tissue, and incomplete bridging surrounding the implant (figure 4.3.5.3 A, B). The coated and BMP-2 loaded allograft, however, showed dramatically different results at the same time interval. Dense, organized bone was formed along the length of the allograft, fully encapsulating the coated allograft.

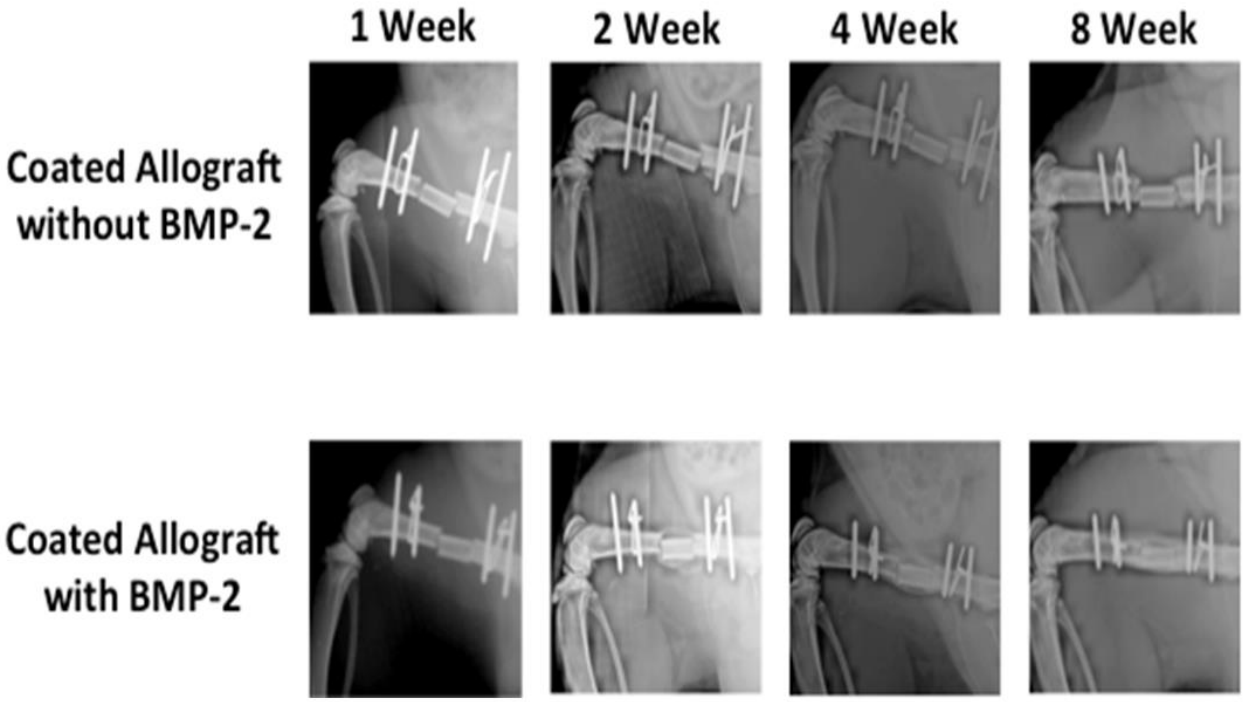

Figure 4.3.4.1: *In vivo* analysis bioactivity of the released BMP-2 utilizing critical size segmental femoral defects in (2) 14 week-old male Lewis rats, one of which received BMP-2 loaded allografts (both surface adsorbed and encapsulated) and one of which received polymer coated BMP-2 loaded allografts (both surface adsorbed and encapsulated) and one of which received polymer coated but non-factor-loaded allografts. Representative radiographs of the rat femoral segmental defect at 1, 2, 4, and 8 weeks. Continuing formation of the mineralized callus observed in the BMP-2 loaded coated allograft, confirm the bioactivity of the released protein and bone union at the host site.

A

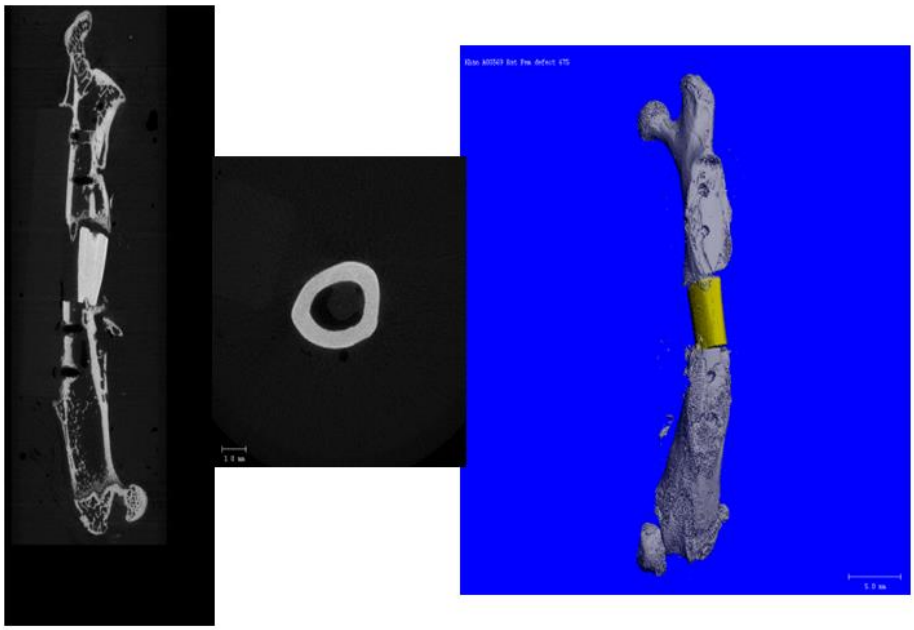

B

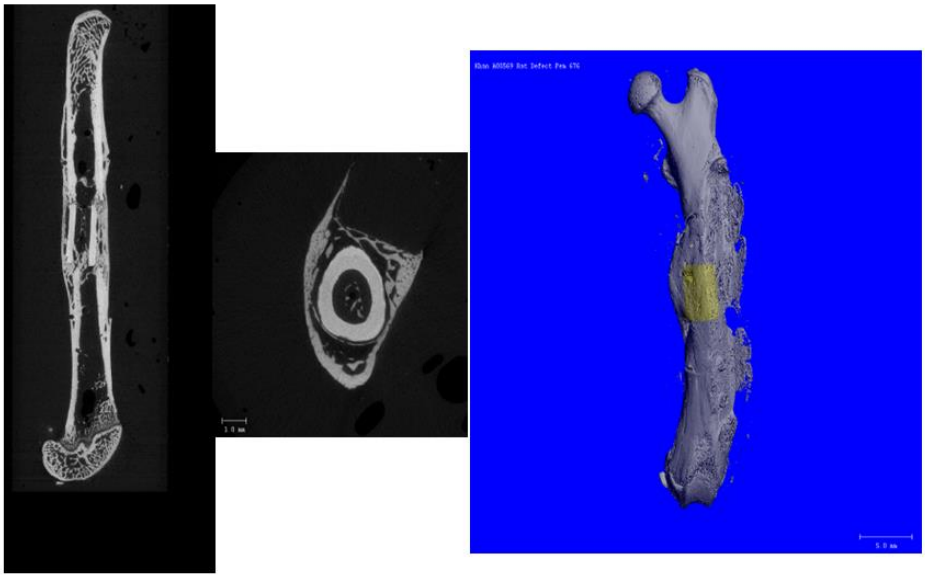

Figure 4.3.4.2: MicroCT analysis of femoral bone defect 8 weeks post-implantation. Representative longitudinal section images, cross section images and three-dimensional reconstructed images are shown for control (A) and experimental group (B). No evidence of new bone growth was detected through the defect site in the control group (A), whereas new bone formation was identified around the BMP-2 loaded coated allograft. Scale bar = 5 mm.

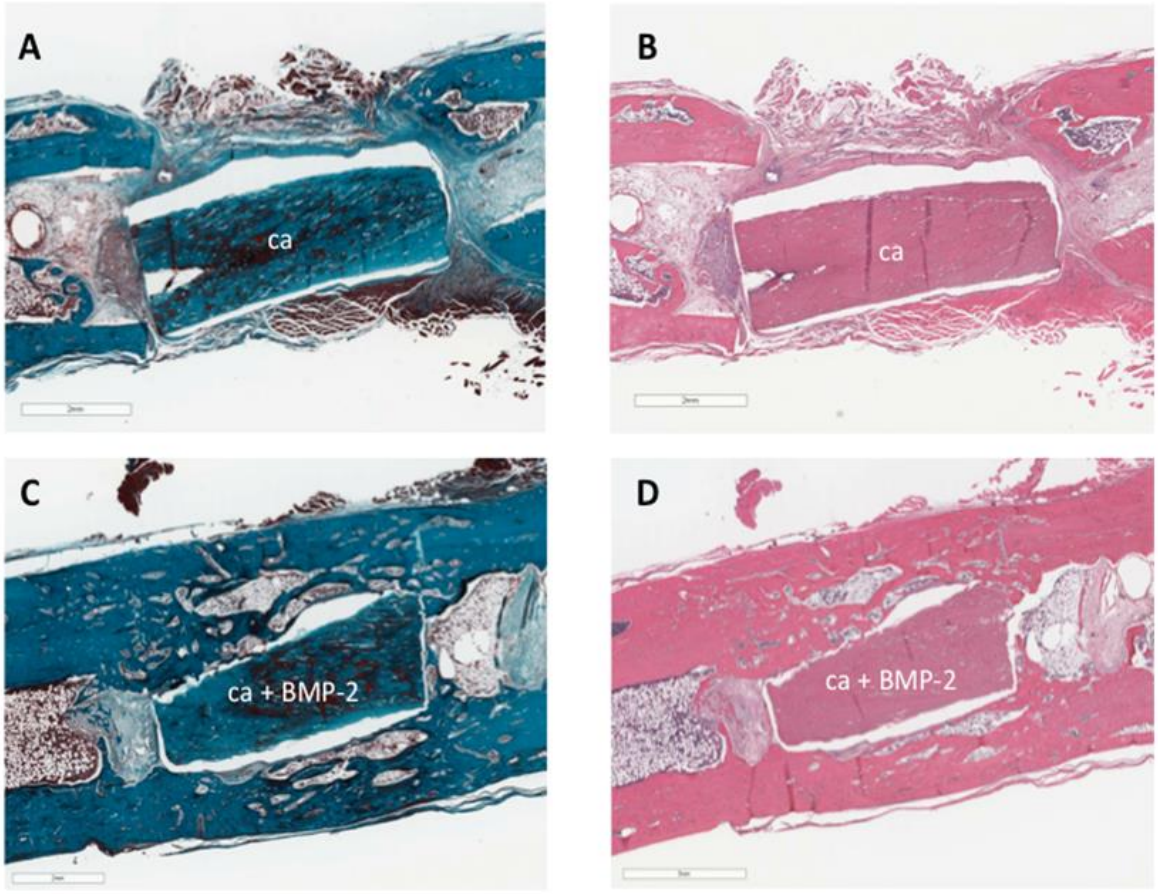

Figure 4.3.4.3 : Longitudinal histological sections of allograft and surrounding femoral bone and tissue after 8 weeks of healing. Masson's trichrome stain (A,C) and Hematoxylin and Eosin stain (B,D) show limited healing around polymer coated/unloaded allograft indicated as "ca" in the figures (A,B). Figure A shows evidence of unmineralized osteoid within the defect site, peripheral to the allograft while Figure C shows mineralized bone bridging the defect and surrounding the coated/BMP-2 loaded allograft.

4.4. DISCUSSION

BMP-2 released from polymer coated allograft showed Human mesenchymal stem cells exposed to BMP-2 released from polymer-coated allografts were noted to show no reduced

metabolic activity over 21 days of culture, and to produce mineralization at levels exceeding those of hMSCs exposed to osteogenic media with no BMP-2, and at levels comparable to BMP-2 added directly to culture media (vs released from scaffolds), suggesting the enhanced osteoinductive effect of BMP-2 was neither eliminated nor reduced as a consequence of being encapsulated within the polymeric layer. Enhanced Alkaline Phosphatase (ALP) expression in the group treated with released BMP-2 at day 21 and 28, indicates matrix maturation [12]. In clinical studies high doses of BMP2 were needed to be effective (1.5–2.0 mg/mL) [13-15], raising concerns about bone overgrowth and the potential subsequent risks of neural compression and oncogenic effects. High concentrations also make these treatments expensive. Therefore, more specific and controlled strategies for administration of BMP-2 for bone reconstruction is necessary. Human bone marrow–derived mesenchymal stem cells (hMSCs) have long been considered promising candidates for bone regeneration due to their capability to differentiate into osteoblasts when appropriately induced *in vitro*, allowing the use of these cells for engineering of implantable bone constructs [16,17]. BMP-2 has been shown to stimulate the osteogenic activity in rodent cell cultures, [18–20] whereas the osteogenic effects are less pronounced in human cells. Some studies indicated that continuous stimulation with BMP2 (0.1–800 ng/mL) affects the differentiation but not the proliferation of hMSCs [21–25] whereas other studies did not demonstrate an osteogenic effect of 100 ng/mL BMP-2 [26, 27]. It is noted that in our study we developed a delivery system that can release sustain payload of BMP-2 significantly lower (300 ng/ml from dual release) than what is currently being used clinically (1.5–2.0 mg/mL). This work suggests that delivering BMP-2 from coated allograft can promote osteoinduction of hMSCs *in vitro* and can serve as controlled delivery vehicle for new bone formation utilizing a reduced dose of BMP-2.

Our pilot i*n vivo* study has shown feasibility of this approach for enhancing allograft repair. The robust bone formation was a strong indication that the BMP-2 that was loaded and subsequently delivered was bioactive and resulted in enhanced bone/allograft incorporation when compared to the control, coated allografts containing no BMP-2. Allograft fracture do not initiate the repair processes seen in normal fracture healing. Under normal circumstances, growth factors released from freshly injured bone send stimuli to the osteoprecursor cells in the periosteum and endosteum and induce formation of osteoblast which eventually cause callus formation. In devitalized allograft healing process the host bone only contribute to the healing process as the devitalized allograft doesn't contain any biological factors. Numerous growth factors are responsible for orchestrating cellular proliferation, differentiation, chondrogenesis, and osteogenesis have been identified. BMP-2 is well recognized for its osteoinduction ability. In our study the robust bone formation and union at the host-graft junction occur due to BMP-2 released from the allograft stimulate osteoinductive signaling and regulation of a number of gene-expression pathways involving the recruitment and differentiation of host mesenchymal progenitor cells into osteoblasts and eventually callus formation around the defect zone.

Literature supports our findings that a burst release followed by sustained release promotes enhanced new bone formation [28, 29]. The burst release of BMP-2 triggers early and fast cellular response and initiates the fracture healing cascade, also enhanced the recruitment of osteoprogenitor cells into the allograft [30], whereas, the sustained delivery of BMP-2 enhances bone regeneration, which has been attributed to by stimulating a larger population of osteoprogenitor cells at the fracture site at later stages following the original injury [31-33], as well as its role in promoting vasculogenesis [34]. Overall, an appropriate growth factor dose, timing and sequence of growth factor delivery, and the physical–chemical and three-dimensional

attributes of the scaffold are crucial to mimic the physiological repair process in bone. Interestingly in both the allograft implant with and without BMP-2 the allograft remained largely intact suggesting that, while BMP-2 delivery results in robust bone formation, it does not necessarily aid in the resorption of the allograft itself.

4.5. CONCLUSIONS & FUTURE DIRECTIONS

The *in vitro* and preliminary *in vivo* data strongly suggests the utility of a growth factor-loaded polymeric coating on massive allografts to enhance bone repair. These biologically active structural allografts may be effective in treating fracture non-unions and revision total joint arthroplasties with large bone defects [35]. There is great potential for the coated allograft as an "off-the-shelf" option for treating bone defects given that once the coating and growth factors are applied they are somewhat stable if stored appropriately. That is to say there is no requirement for rehydration or special storage as there can be for hydrogel-based or cell-based bone graft substitutes.

Future *in vivo* studies will include the delivery of VEGF (along with BMP-2) to determine its role in allograft resorption, a key component in complete allograft healing. These studies confirm the ability to deliver growth factors essential for bone repair from polymer-coated allografts without modifying the general physical structure of the allograft itself. Implications of this work are great as many other proteins and pharmaceuticals could seemingly be delivered in a similar manner, depending on the particular need.

4.6. REFERENCES

1. Wise DL, Trantolo DJ, Marino RT, Kitchell JP. Opportunities and challenges in the design of implantable biodegradable polymeric systems for the delivery of anti-microbial agents and vaccines. Adv Drug Deliv Rev. 1987;1:19–39.

2. Patel ZS, Yamamoto M, Ueda H, Tabata Y, Mikos AG. Biodegradable gelatin microparticles as delivery systems for the controlled release of bone morphogenetic protein-2. Acta Biomater. 2008;4:1126–1138.

3. Lee GS, Park JH, Shin US, Kim HW. Direct deposited porous scaffolds of calcium phosphate cement with alginate for drug delivery and bone tissue engineering. Acta Biomater. 2011;7:3178–3186.

4. King WJ, Toepke MW, Murphy WL. Facile formation of dynamic hydrogel microspheres for triggered growth factor delivery. Acta Biomater. 2011;7:975–985.

5. Cleland JL, Lim A, Barron L, Duenas ET, Powell MF. Development of a single-shot subunit vaccine for HIV-1: Par 4. Optimizing microencapsulation and pulsatile release of MNrgp120 from biodegradable microspheres. J Control Release. 1997;47:135–150.

6. Cleland JL. Single-administration vaccines: controlled-release technology to mimic repeated immunizations. Trends Biotechnol. 1999;17: 25–29.

7. Kacena MA, Troiano NW, Wilson KM, Coady CE, Horowitz MC. Evaluation of Two Different Methylmethacrylate Processing, Infiltration, and Embedding Techniques on the Histological, Histochemical, and Immunohistochemical Analysis of Murine Bone Specimens. The Journal of Histotechnology. 2004;27(2):119-30.

8. Sharon M. Kelly, Thomas J. Jess, Nicholas C. Price. How to study proteins by circular dichroism. Biochimica et Biophysica Acta 1751 (2005) 119 – 139

9. http://cnx.org/contents/M0tCI0M5@2/Circular-Dichroism-Spectroscop

10. Hillger, Gerhard Herr, Rainer Rudolph and Elisabeth Schwarz.Biophysical comparison of BMP-2, ProBMP-2, and the free Pro-peptide reveals stabilization of the Pro-peptide by the mature growth factor. J. Biol. Chem. 2005, 280:14974-14980.

11. Jing Zhang, Huanjun Zhou, Kai Yang, Yuan Yuan, Changsheng Liu.RhBMP-2-loaded calcium silicate/calcium phosphate cement scaffold with hierarchically porous structure for enhanced bone tissue regeneration. Biomaterials 34 (2013) 9381-9392.

12. Edward H. Riley, Joseph M. Lane, Marshall R. Urist, Karen M. Lyons, and Jay R. Lieberman. Bone Morphogenetic Protein-2 Biology and Applications. Clinical Orthopaedics and Related Research; 324, pp 39-46.

13. Boden SD, Kang J, Sandhu H, et al. Use of recombinant human bone morphogenetic protein-2 to achieve posterolateral lumbar spine fusion in humans: a prospective, randomized clinical pilot trial: 2002 Volvo Award in clinical studies. Spine (Phila PA 1976). 2002;27:2662–2673.

14. Schmidmaier G, Schwabe P, Wildemann B, et al. Use of bone morphogenetic proteins for treatment of non-unions and future perspectives. Injury. 2007;38(Suppl 4):S35–S41.

15. Termaat MF, Den Boer FC, Bakker FC, et al. Bone morphogenetic proteins. Development and clinical efficacy in the treatment of fractures and bone defects. J Bone Joint Surg Am. 2005;87:1367–1378.

16. P. Chatakun · R. Núñez-Toldrà · E. J. Díaz López · C. Gil-Recio · E. Martínez-Sarrà · F. Hernández-Alfaro · E. Ferrés-Padró · L. Giner-Tarrida · M. Atari.The effect of five proteins on

stem cells used for osteoblast differentiation and proliferation: a current review of the literature. Cell. Mol. Life Sci. (2014) 71:113–142.

17. Helle Lysdahl, Anette Baatrup, Casper Bindzus Foldager, and Cody Bunger. Preconditioning Human Mesenchymal Stem Cells with a Low Concentration of BMP2 Stimulates Proliferation and Osteogenic Differentiation *In Vitro*. BioResearch Open Access Volume 3, Number 6, December 2014.

18. Abe E, YamamotoM, Taguchi Y, et al. Essential requirement of BMPs-2/4 for both osteoblast and osteoclast formation in murine bone marrow cultures from adult mice: antagonism by noggin. J Bone Miner Res. 2000;15:663–673.

19. Hanada K, Dennis JE, Caplan AI. Stimulatory effects of basic fibroblast growth factor and bone morphogenetic protein-2 on osteogenic differentiation of rat bone marrow-derived mesenchymal stem cells. J Bone Miner Res. 1997;12: 1606–1614.

20. Rickard DJ, Sullivan TA, Shenker BJ, et al. Induction of rapid osteoblast differentiation in rat bone marrow stromal cell cultures by dexamethasone and BMP-2. Dev Biol. 1994;161:218–228.

21. Friedman MS, Long MW, Hankenson KD. Osteogenic differentiation of human mesenchymal stem cells is regulated by bone morphogenetic protein-6. J Cell Biochem. 2006;98: 538–554.

22. Jorgensen NR, Henriksen Z, Sorensen OH, et al. Dexamethasone, BMP-2, and 1,25-dihydroxyvitamin D enhance a more differentiated osteoblast phenotype: validation of an *in vitro* model for human bone marrow-derived primary osteoblasts. Steroids. 2004;69:219–226.

23. Lecanda F, Avioli LV, Cheng SL. Regulation of bone matrix protein expression and induction of differentiation of human osteoblasts and human bone marrow stromal cells by bone

morphogenetic protein-2. J Cell Biochem. 1997;67:386–396.

24. Fromigue´ O,Marie PJ, Lomri A. Bone morphogenetic protein- 2 and transforming growth factor-beta2 interact to modulate human bone marrow stromal cell proliferation and differentiation. J Cell Biochem. 1998;68:411–426.

25. Gori F, Thomas T, Hicok KC, et al. Differentiation of human marrow stromal precursor cells: bone morphogenetic protein-2 increases OSF2/CBFA1, enhances osteoblast commitment, and inhibits late adipocyte maturation. J Bone Miner Res. 1999;14:1522–1535.

26. Diefenderfer DL, Osyczka AM, Reilly GC, et al. BMP responsiveness in human mesenchymal stem cells. Connect Tissue Res. 2003;44(Suppl 1):305–311.

27. Osyczka AM, Leboy PS. Bone morphogenetic protein regulation of early osteoblast genes in human marrow stromal cells is mediated by extracellular signal-regulated kinase and phosphatidylinositol 3-kinase signaling. Endocrinology. 2005;146:3428–3437.

28. Li, R.H., and Wozney, J.M. Delivering on the promise of bone morphogenetic proteins. Trends Biotechnol 19, 255, 2001.

29. Brown, K.V., Li, B., Guda, T., et al., 2011. Improving bone formation in a rat femur segmental defect by controlling bone morphogenetic protein-2 release. Tissue Eng. Part A 17, 1735–1745.

30. Li, B., Yoshii, T., Hafeman, A.E., et al., 2009a. The effects of rhBMP-2 released from biodegradable polyurethane/microsphere composite scaffolds on new bone formation in rat femora. Biomaterials 30, 6768–6779.

31. Kempen, D.H., Kruyt, M.C., Lu, L., Wilson, C.E., Florschutz, A.V., Creemers, L.B., Yaszemski, M.J., and Dhert, W.J. Effect of autologous bone marrow stromal cell seeding and

bone morphogenetic protein-2 delivery on ectopic bone formation in a microsphere/poly(propylene fumarate) composite. Tissue Eng Part A 15, 587, 2009.

32. Kim, S.S., Gwak, S.J., and Kim, B.S. Orthotopic bone formation by implantation of apatite-coated poly(lactide-co-glycolide)/ hydroxyapatite composite particulates and bone morphogenetic protein-2. J Biomed Mater Res A 87, 245, 2008.

33. Jeon, O., Song, S.J., Yang, H.S., Bhang, S.H., Kang, S.W., Sung, M.A, Lee, J.H. and Kim, B.S. Long-term delivery enhances *in vivo* osteogenic efficacy of bone morphogenetic protein-2 compared to short-term delivery. Biochem Biophys Res Commun 369, 774, 2008.

34. de Jesus Perez, V.A., Alastalo, T.P., Wu, J.C., Axelrod, J.D., Cooke, J.P., Amieva, M., and Rabinovitch, M. Bone morphogenetic protein 2 induces pulmonary angiogenesis via Wnt-beta-catenin and Wnt-RhoA-Rac1 pathways. J Cell Biol 184, 83, 2009.

35. Enneking F, Campanacci DA. Retrieved Human Allografts: A Clinicopathological Study. J Bone Joint Surg Am. 83-A(7) 2001,971-86.

5. *IN VITRO* CELLULAR EVALUATION OF BIOACTIVITY OF RELEASED VEGF BY INVESTIGATING OSTEOCLAST PHENOTYPE

5.1. INTRODUCTION

Bone grafting procedures are on the rise in the US, with an estimated 2 million grafting procedures performed annually.[1] Autografts, donor tissues harvested from the patient's own body, are considered the gold standard for their optimal biocompatibility, osteoconductivity, ideal biomechanical properties, biological components and subsequent osteoinductivity, leading to an 80-90% success rate clinically.[2,3] Autografts are typically harvested from the iliac crest for its porous trabecular bone, relative ease of access, and the high marrow content taken with the bone because of its abundant cells, blood, and associated proteins. Autograft incorporation follows a similar sequence of events as typical fracture repair including inflammation, repair, and remodeling [4]. During these three stages multiple cell types including macrophages, monocytes, lymphocytes, osteoclasts, and fibroblasts infiltrate the autograft from the host bone while granulation tissue begins to form. Vascularization continues as a collagen matrix is formed and slowly mineralized. Remodeling of the healed defect, often in response to mechanical loading, occurs through both bone resorption and subsequent new bone formation.

While autografts are the clinical gold standard for bone grafting the hazard of donor-site morbidity and a limited supply requires a feasible alternative. Allografts, tissue harvested from a donor or cadaver, are common alternatives to using autografts but to reduce the likelihood of a host immune response or disease transmission the donor tissue must be devitalized through a process that removes cellular and viral components.[5] This process removes the cells, blood, and proteins that are present with autografts, leaving the allograft as a largely structural implant with

little to no inherent bioactivity and diminished local vascularity. Therefore, in allograft healing graft incorporation relies only on cells, proteins, and tissues available from host bone and at the defect site. For trabecular allografts this lack of bioactivity does not prevent adequate healing as the inherent pore structure of the tissue allows the host to infiltrate the allograft and heal but devitalization does impact more dense, cortical allografts.[6]

Large-scale structural allografts (typically cortical bone taken from the diaphysis of long bones) have limited healing where mineralized tissue usually forms along the cortex of the host bone and allograft. The lack of osteoclast-mediated allograft resorption or bone remodeling, leaves large segments of necrotic bone, weakening the defect site over time. The repetitive loading at these sites makes them vulnerable to destabilization and generation of small microfractures.[7,8] As these allografts become less stable non-unions (27%-34%), late graft fractures (24%-27%), and infections (9%-16%) occur which ultimately result in clinical failure.[9] In the hopes of improving large scale defect healing we have developed a technique to "revitalize" allografts by incorporating molecules known to stimulate implant resorption and enhance new bone formation. The literature reports that delivering bone morphogenetic protein 2 (BMP-2) and vascular endothelial growth factor (VEGF) simultaneously yields better bone healing over either growth factor alone, and delivering them sequentially yields even better healing [10-13]. The literature also suggests that VEGF may influence osteoclast precursor differentiation to mature osteoclasts[14-17] which, when, delivered from devitalized allografts may increase the local osteoclast population to facilitate implant resorption thereby paving the way for subsequent new bone formation. Given this, we have developed a method through which a thin, polymeric coating capable of retaining and delivering growth factors is applied to all surfaces of large-scale structural allografts, with the intention of delivering therapeutic molecules capable of enhancing bone-allograft healing. In the

previous chapters we have demonstrated the ability to deliver either VEGF or BMP-2 with two distinct delivery kinetics; short- and long-term.[18] Our studies demonstrated that BMP-2 released from the polymer-coated allograft resulted in robust bone formation in a rat segmental defect. However, the release of BMP-2 alone failed to show any significant bone resorption *in vivo*[18] substantiating the need to stimulate osteoclastogenesis.

We hypothesized that the delivery of VEGF which is traditionally associated with angiogenesis would induce differentiation of osteoclast precursors into mature, bone-resorbing osteoclasts, *in vitro*.

5.2. MATERIALS AND METHODS

5.2.1. Culture of RAW 264.7 Cells

RAW264.7 cells were obtained from the American Type Culture Collection (ATCC; Rockville, USA) and cultured in 25 cm^2 tissue culture flasks in ATCC-formulated RPMI-1640 culture medium with 10% FBS, 1% penicillin/streptomycin at 37^0C in a humidified atmosphere containing 5% CO_2. After 24–48 h of culture, RAW264.7 cells were detached using a cell scraper and seeded into 24-well plates at a density of 2.6 $x10^4$ cells/cm^2 in α-MEM culture media with 10% FBS, 1% penicillin/streptomycin. Four groups were evaluated in this study: 1) negative control: cells cultured in α-MEM; no additives, 2) positive control: cells cultured in α-MEM with receptor activator of nuclear factor kappa-B ligand (RANKL 50ng/ml) which is available endogenously and is added to culture to replicate th*e in vivo* environment, 3) cells cultured in α-MEM treated with RANKL (50 ng/ml) and 10 ng/ml VEGF added directly to the culture, and 4) cells cultured in α-MEM treated with RANKL (50 ng/ml) and 100 ng/ml VEGF

added directly to the culture. Cells from each group were cultured for 7 days and then fixed in 3.7% formalin. Cells were then stained with tartrate-resistant acid phosphatase (TRAP) using a commercial kit (Sigma). Cells that both stained positive for TRAP and contained three or more nuclei were considered osteoclasts, and were visualized with a Zeiss observer Z.1 light microscope (Carl Zeiss, USA) and analyzed using NIH ImageJ software.

5.2.2. Isolation of Bone Marrow Macrophages (BMMs) from mice

Primary bone marrow derived mononuclear cells (BMMs) were exposed to VEGF that was either added to cell culture wells as described above (to assess the functionality of osteoclast-precursors differentiated with VEGF) and eluted directly from coated/loaded allografts (to confirm the bioactivity of the VEGF after it is released from the coated allograft) (see Figure 5.2.2.1). BMMs were isolated from long bones of wild type mice aged 4- to 9-week-old, according to published protocols.[10] Briefly, long bones were excised from the mice, cleaned of soft tissue and stored in PBS. The bone marrow of each bone was flushed out with α-MEM media that was supplemented with 10% FBS and 1% penicillin/streptomycin. Flushed marrow was centrifuged for 5 minutes at 1200 rpm. Cells were then resuspended in ACK buffer to lyse red blood cells and the suspension was then centrifuged for 5 minutes at 1200 rpm. Finally cells were resuspended in complete media. Cells were then seeded on a petri dish ($1x10^8$ cells/10 cm dish). Macrophage colony-stimulating factor (M-CSF) (30ng/ml) was added to the BMM for macrophage differentiation and cells were cultured for 48 hours in 5% CO_2. Cells were then detached and seeded onto 24-well plates at a concentration of 50,000 cells/well. To support osteoclast differentiation all cells were cultured in complete α-MEM media supplemented with 10% FBS, 1% penicillin/streptomycin and M-CSF (30ng/ml) to assess the following five experimental

groups: 1) negative control: cells cultured in media (no additional additives), 2) positive control: cells cultured in media with RANKL added (50ng/ml), 3) cells cultured in media with 100 ng/ml VEGF added (no RANKL), 4) cells cultured in media with RANKL (50 ng/ml) and VEGF (100 ng/ml) added, and 5) cells cultured in media with RANKL (50 ng/ml) and ~120 ng/ml VEGF eluted directly from coated/loaded allograft using a transwell with pore size 0.4 μm insert setup (Figure 5.2.2.1). Each group was cultured for 7 days and numbers of TRAP stained osteoclasts were counted as described above.

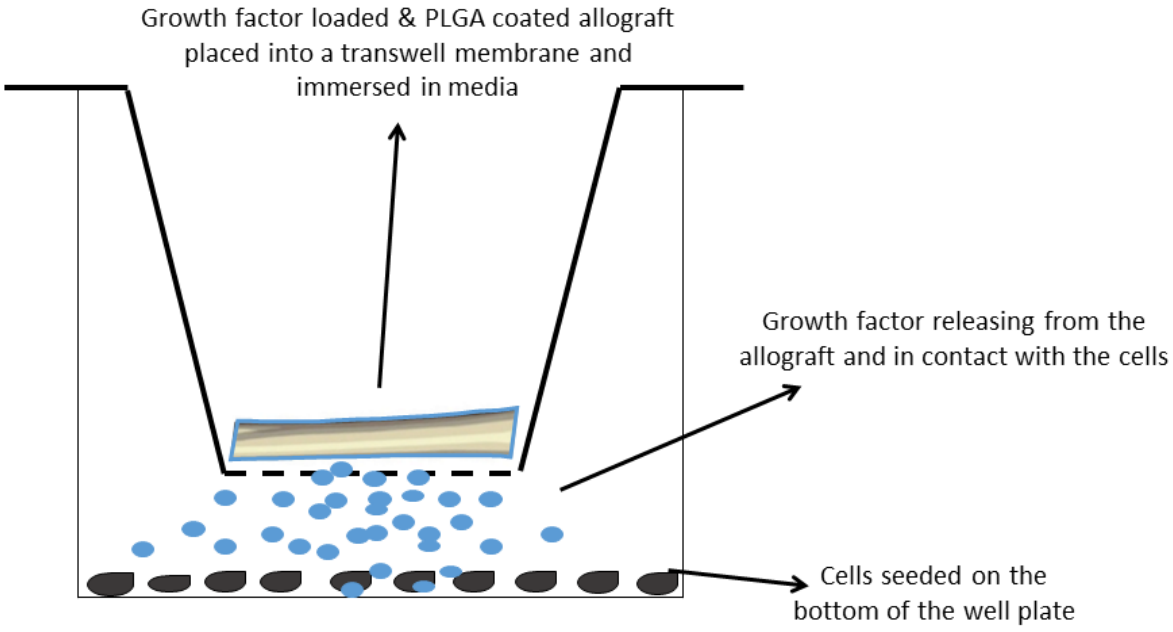

Figure 5.2.2.1: Schematic representation of the cell study to evaluate the bioactivity of VEGF, adsorbed onto the surface of the PLGA coated allograft. Osteoclast precursors (RAW264.7 and BMMs) were seeded onto the cell culture plate and the allografts were placed in the corning

transwell inserts on the permeable membrane. VEGF released from the coated allograft filtered through the membrane and came in contact with the cells seeded on the plate.

5.2.3. TRAP Staining Assay

TRAP (+) cells were identified as osteoclasts for both RAW264.7 cell studies (on day 7 of culture) and BMM cell studies (on day 5 of culture) through histochemical staining using a commercially available kit (Sigma-Aldrich) as per manufacturer's instruction.

5.2.4. Resorption Assay by Utilizing Osteo-Assay Microplates

Osteoclasts differentiated from BMM cell isolations were assessed for *in vitro* functionality using two different methods: quantification of resorbed hydroxyapatite coating, and identification of resorption pits from bone slices.

Hydroxyapatite Resorption Assay: BMM cells were plated in hydroxyapatite-coated Corning Osteo-Assay Surface 24-well plates (Corning Life Sciences, USA) using the same culture media and cell density used in cell culture (see above). After 14 days of culture hydroxyapatite coated plates were washed with 1.2% sodium hypochlorite solution for 5 min to remove cells, rinsed with distilled water, and air-dried. For staining, plates were treated in dark at ambient temperature with 5% (w/v) silver nitrate solution for 30 min. Wells were then aspirated and washed for 5 min in distilled water. Wells were aspirated again, and 5% (w/v) sodium carbonate in 10% formalin was added. After a 5-min incubation at ambient temperature plates were aspirated and air-dried at 37^0C prior to imaging. The resorption pits were imaged using a light microscope Zeiss observer Z.1 microscope (Carl Zeiss, USA) and percent resorption area was calculated using NIH ImageJ software.

Dentin Resorption Assay: Bovine bone slices were used to assess resorption pits formed by mature osteoclasts. Briefly, the diaphyses of bovine femurs were cut transversely into 2-3 cm cylinders with a hacksaw. The cylinder was then cut into three segments and the marrow lifted out. Any adherent muscle, marrow or periosteum was cleaned with a scalpel. The segments were then sonicated in warm water. The bone was given a final cleaning of any adherent tissue with a scalpel. Transverse slices 200 µm thick were made on the Isomet Low Speed Saw (Buehler, Lake Bluff, IL) with a wafering blade. The bone was then clamped tightly and slices cut at 200 µm intervals using 10% ethanol in Milli-Q water. These 200 µm slices were trimmed to produce the final 4.4 mm x 4.4 mm x 0.2 mm bone slices. The bone slices were stored in 70% ethanol until use, then sterilized overnight with UV light in a sterile hood. On the day of experiment, bone slices were placed in 24 well plates (1 bone slice/well). BMMs (100,000 cells/bone slice) were plated and cultured according to the 5 different groups described above for 14 days. Culture medium was changed and every 2-3 days. Bone slices were then fixed with 2.5% glutaraldehyde in PBS for 30 minutes at RT. Cells were then TRAP stained (Sigma kit #387A-1KT) and examined microscopically to observe TRAP-positive osteoclasts. Bone slices were sonicated for 5-15 minutes in distilled water to dislodge attached cells and then stained for 30-60 seconds with 1% Toluidine blue in 1% Borax buffer, rinsed in distilled water, air dried, and examined for the presence of resorption pits using light microscope. The dentin slices were also imaged using scanning electron microscopy. Allografts were sputter-coated with gold/palladium for 60 sec using a JEOL JSM-5900LV scanning electron microscope (JEOL USA, Peabody MA) operated at 10.0 kV and imaged for evidence of resorption pits.

5.2.5. Statistical Analysis

A student's t-test (to compare two groups) or one-way analysis of variance with Tukey post-hoc testing, (for multiple group comparisons) was used to determine statistical significance with $p<0.05$. Sample size for cell studies was n=3.

5.3. RESULTS

5.3.1. Effect of VEGF in Formation and Differentiation of Osteoclast: Bioactivity of VEGF

To assess the efficacy of VEGF as a stimulator of osteoclastogenesis, and to see whether this effect was dose-dependent, RAW 264.7 cells were cultured in the presence of both RANKL and a low or high concentration of VEGF. While mononuclear cells can exhibit TRAP-positive staining, in this study a cell had to stain positive for TRAP and also be multinucleated (three or more nuclei) to be considered osteoclast-like. There was a statistically significant increase in the number of multinucleated TRAP-positive cells when comparing cultures with RANKL alone and RANKL + 10ng/ml VEGF (Figure 5.3.1.1), indicating that combining VEGF and RANKL further stimulates osteoclastogenesis over RANKL alone. Data showed trend toward a dose-dependent effect as cultures containing RANKL + 100ng/ml VEGF showed an increase in TRAP-positive cells over RANKL+ 10ng/ml VEGF cultures (Figure 5.3.1.1).

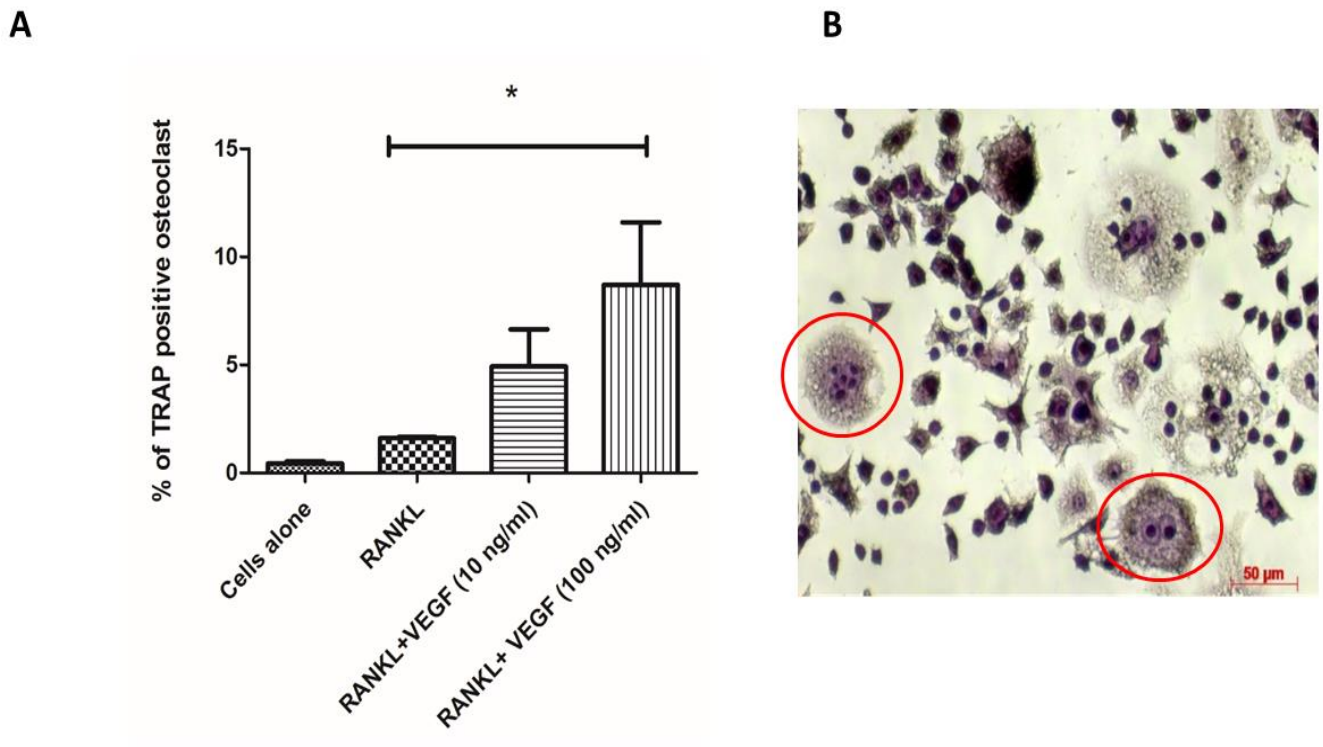

Figure 5.3.1.1: Percentage of TRAP positive multinucleated cells in different groups. (*) indicates statistical significance between groups treated with RANKL alone and groups treated with RANKL and 100ng/ml VEGF. A dose-dependent trend was observed in osteoclast differentiation on RAW264.7 cells from VEGF 10 ng/ml to 100 ng/ml (each with RANKL solution (50 ng/ml) added directly to the media). Data are mean ±SD, n=3 independent experiments. B) Micrograph of TRAP positive stained cells. Only TRAP positive cells with 3 or more nuclei were considered osteoclast-like for quantification (circled in red). Scale bar represents 50 µm.

To evaluate the *functionality* of VEGF-differentiated osteoclasts BMMs were cultured with VEGF similarly to RAW264.7 cells and then assessed with TRAP staining and for bone resorption capability. To confirm the bioactivity of eluted VEGF from the allograft BMMs were also placed

below transwell inserts to allow culture in the VEGF released from the allograft, as depicted in Figure 5.3.1.1. TRAP assay results confirmed the efficacy of released VEGF to induce osteoclast formation of BMMs (Figure 5.3.1.1) and showed similar results to that of RAW264.7 cell lines. Groups treated with VEGF had significantly higher TRAP-positive multinucleated osteoclasts than those treated without VEGF (figure 5.3.1.8). Further, data demonstrated no significant difference in the number of TRAP-positive multinucleated cells between the cultures where VEGF was added directly (100ng/ml) and where it was released from the coating, confirming that the process of coating and releasing VEGF from coated allografts did not alter its bioactivity.

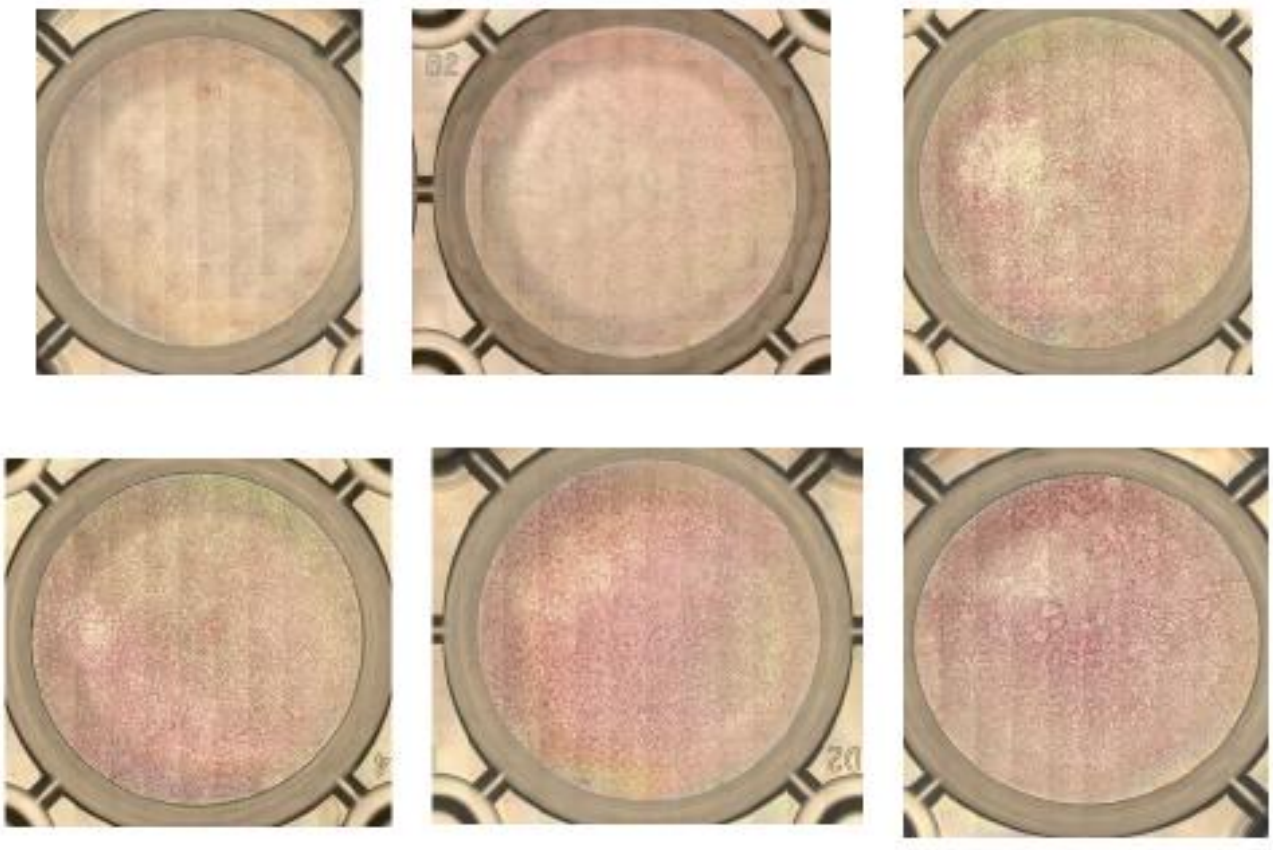

Figure 5.3.1.2: Micrograph of TRAP positive stained cells. Only TRAP positive cells with 3 or more nuclei were considered osteoclast-like for quantification.

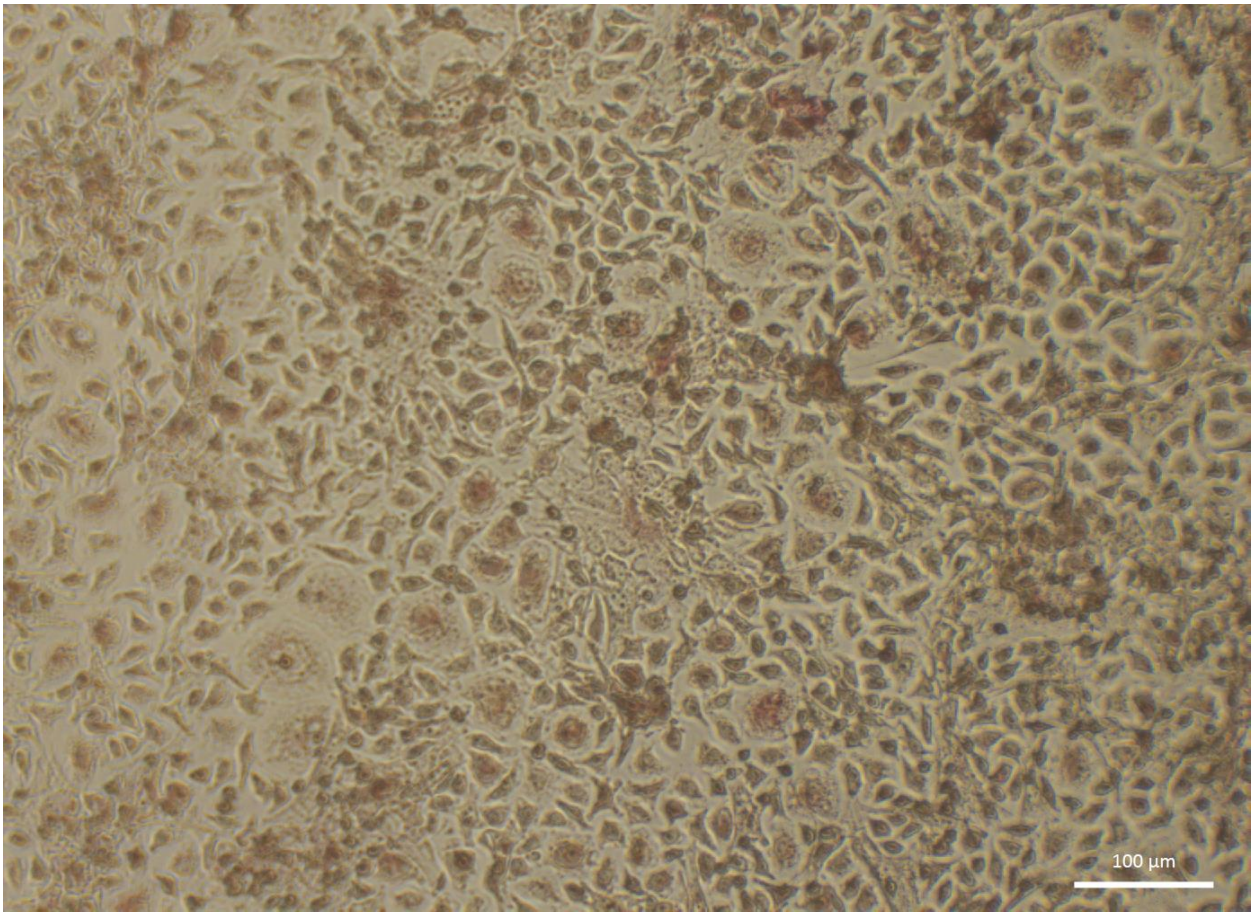

Figure 5.3.1.3. BMM cells treated with MCSF. No sign of multinucleated osteoclast was demonstrated. Scale bar=100 µm.

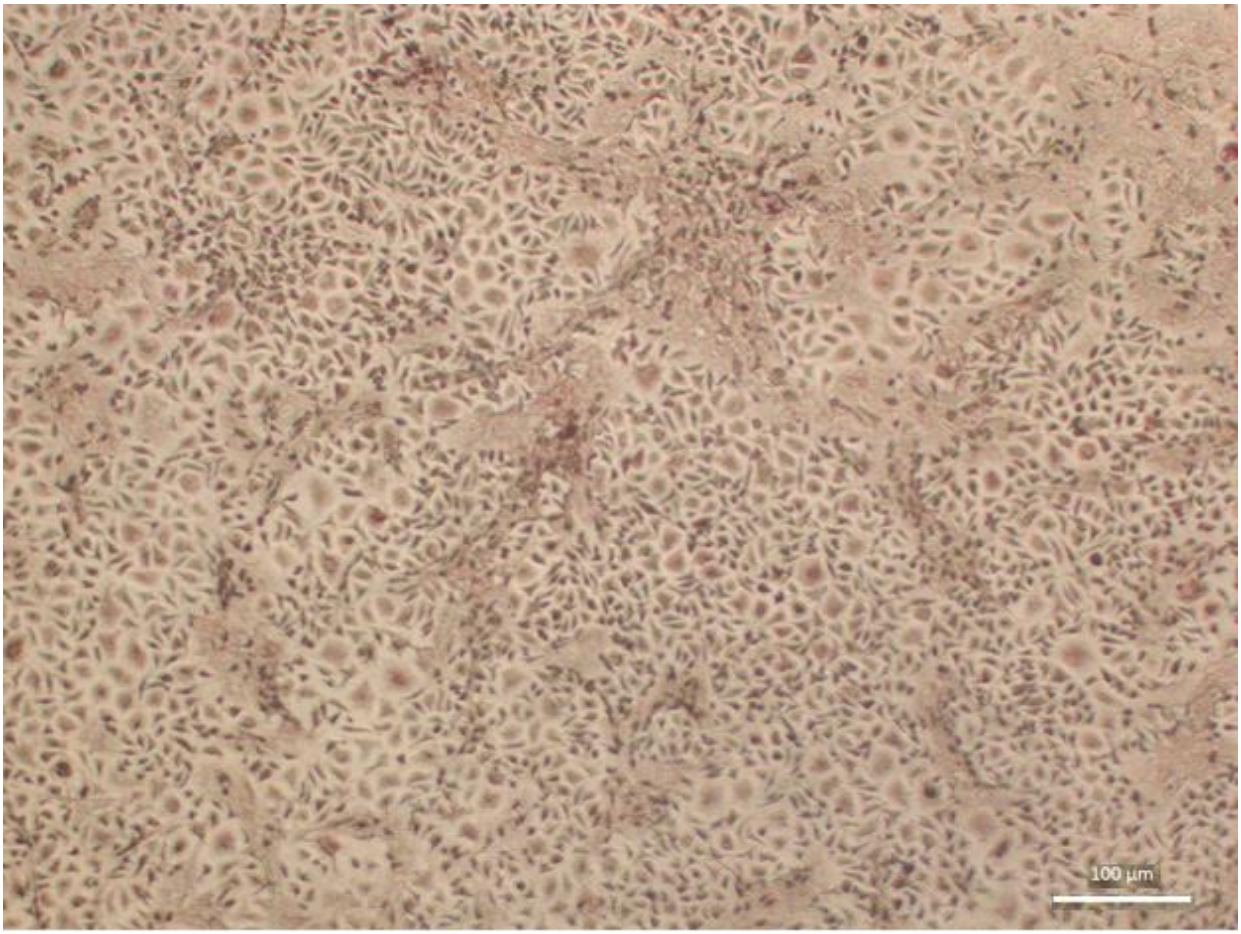

Figure 5.3.1.4: BMM cells treated with VEGF (~140 ng/ml) released from polymer coated allograft. No multinucleated osteoclast cell was observed. Scale bar=100 µm

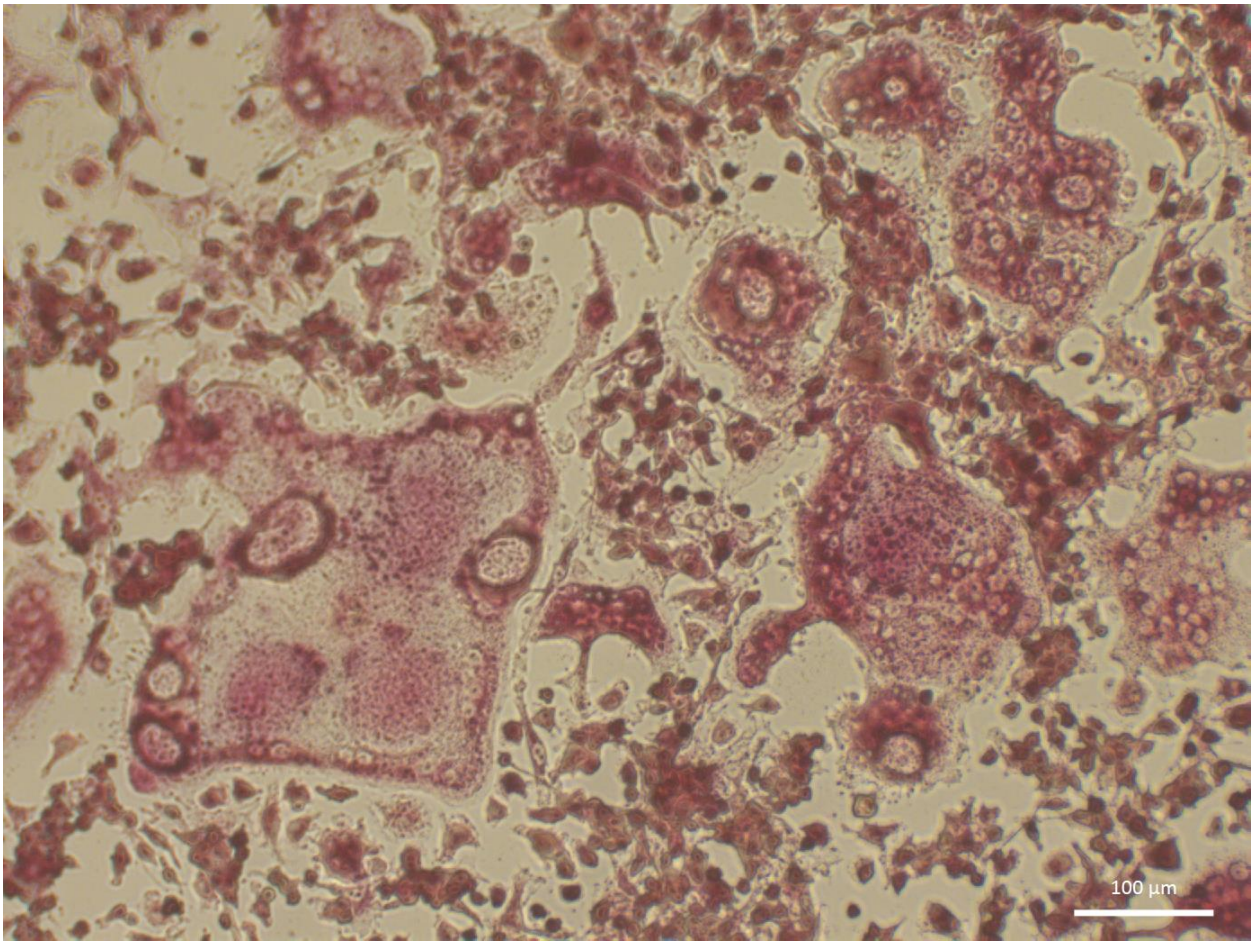

Figure 5.3.1.5: BMM cells treated with RANKL (50ng/ml). In the presence of RANKL BMM differentiate into TRAP positive multinucleated osteoclasts. Scale bar=100 µm.

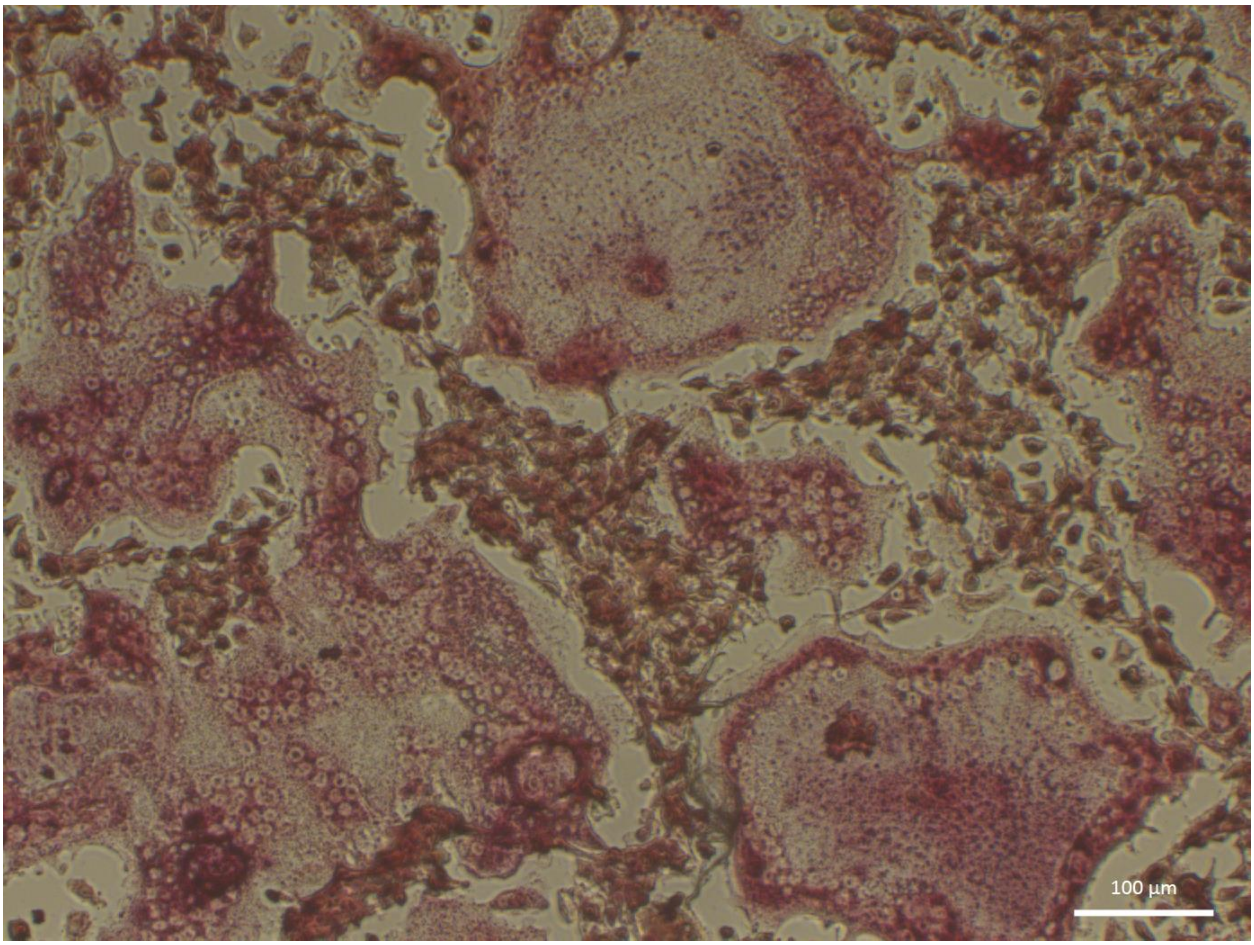

Figure 5.3.1.6: BMM cells treated with RANKL (50 ng/ml) and VEGF (100 ng/ml) added directly to the cell medium. Multinucleated TRAP positive osteoclasts were observed on day 5 of culture. Scale bar=100 µm

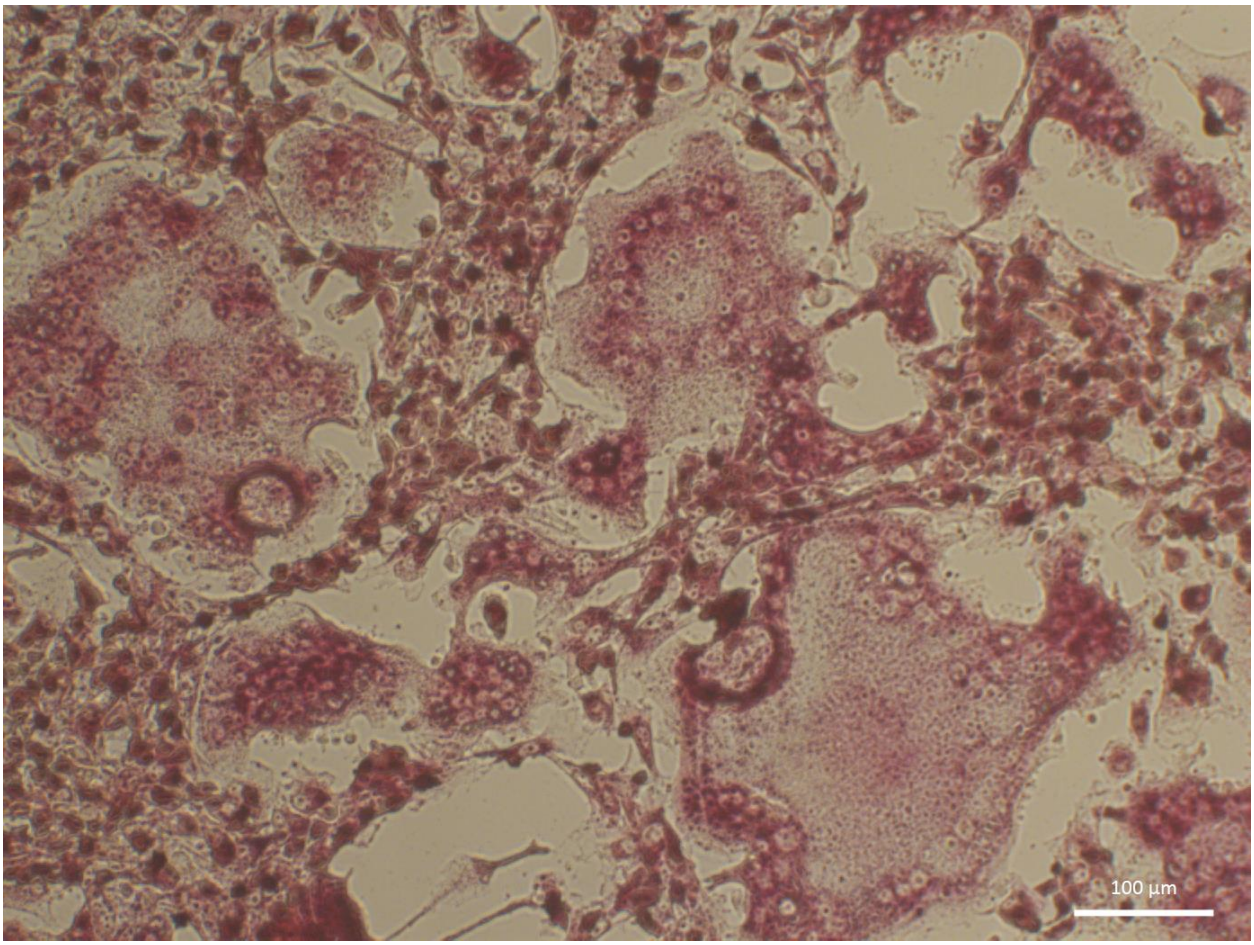

Figure 5.3.1.7: BMM cells in the presence of RANKL (50ng/ml) and VEGF (~140 ng/ml) released from coated allograft. Presence of TRAP positive multinucleated cells verifies the bioactivity of released VEGF. Scale bar=100 µm.

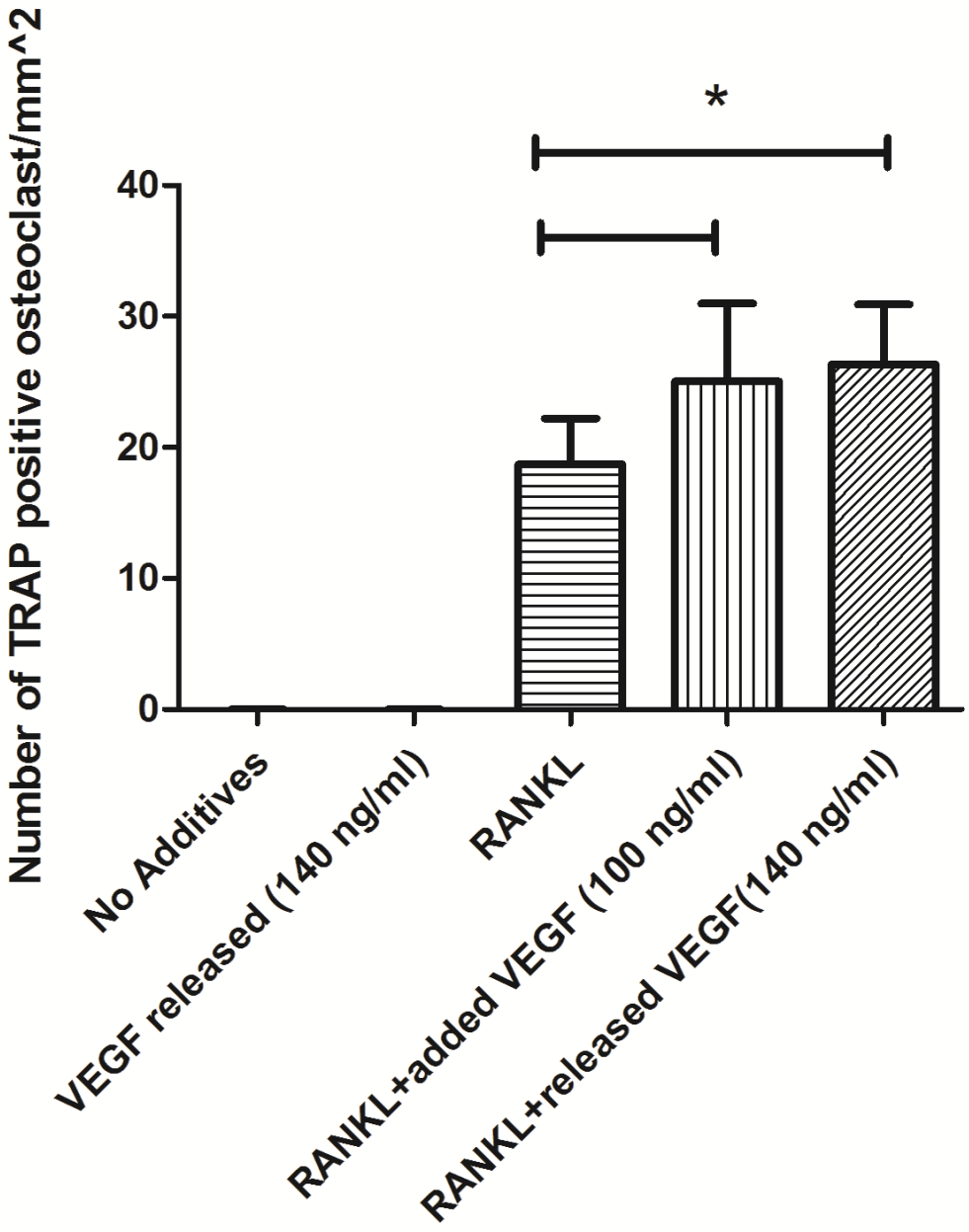

Figure 5.3.1.8: Effect of released VEGF on osteoclastogenesis of bone marrow-derived mononuclear cells as determined by TRAP-positive cell counts. All wells were treated with MCSF. An increase in cell numbers confirmed the effectiveness of the released protein. There was a significant increase in osteoclast differentiation between the groups with or without VEGF, which confirms the bioactivity of the protein. There is no effect of VEGF alone on osteoclastic

differentiation. Significance between groups is designated with (*) = $p<0.05$. Data are mean± SD, n=3 independent experiments.

5.3.2. Functionality of VEGF induced Osteoclasts: Bioactivity of VEGF

The ability of the osteoclasts differentiated from BMM cells to resorb bone was confirmed by staining osteo-assay plates with Von Kossa stain. Figure 5.3.2.1 shows photomicrographs of synthetic hydroxyapatite mineral surfaces as black while white regions are areas where resorption has occurred due to active acid secretion by differentiated osteoclasts. Our results showed that the group with VEGF released from the allografts revealed a significantly ($p <0.05$) higher percent of resorption area over both positive and negative control groups (RANKL alone and no RANKL, respectively). These data suggests that the released VEGF from PLGA coated allograft enhances the differentiation of bone marrow derived monocytes into functional osteoclasts *in vitro* (Figure 5.3.2.1).

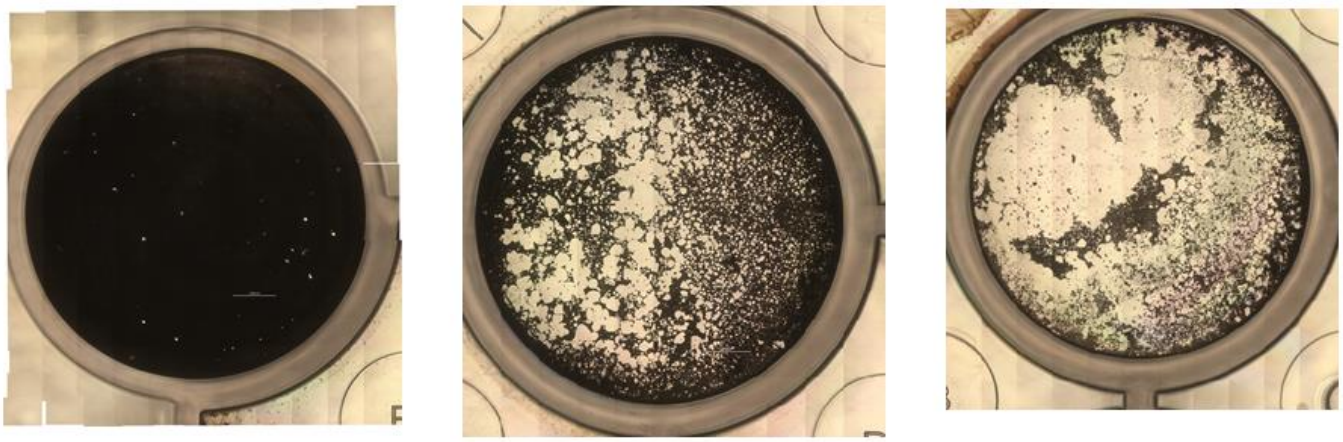

Figure 5.3.2.1: Von Kossa staining on hydroxyapatite coated Corning osteo-assay plate. Cells in culture were treated with MCSF, RANKL, and VEGF that had eluted from coated allografts. The white regions of the plates indicate osteoclastic resorption, which was quantified using image J software. Scale bar represents 100 µm

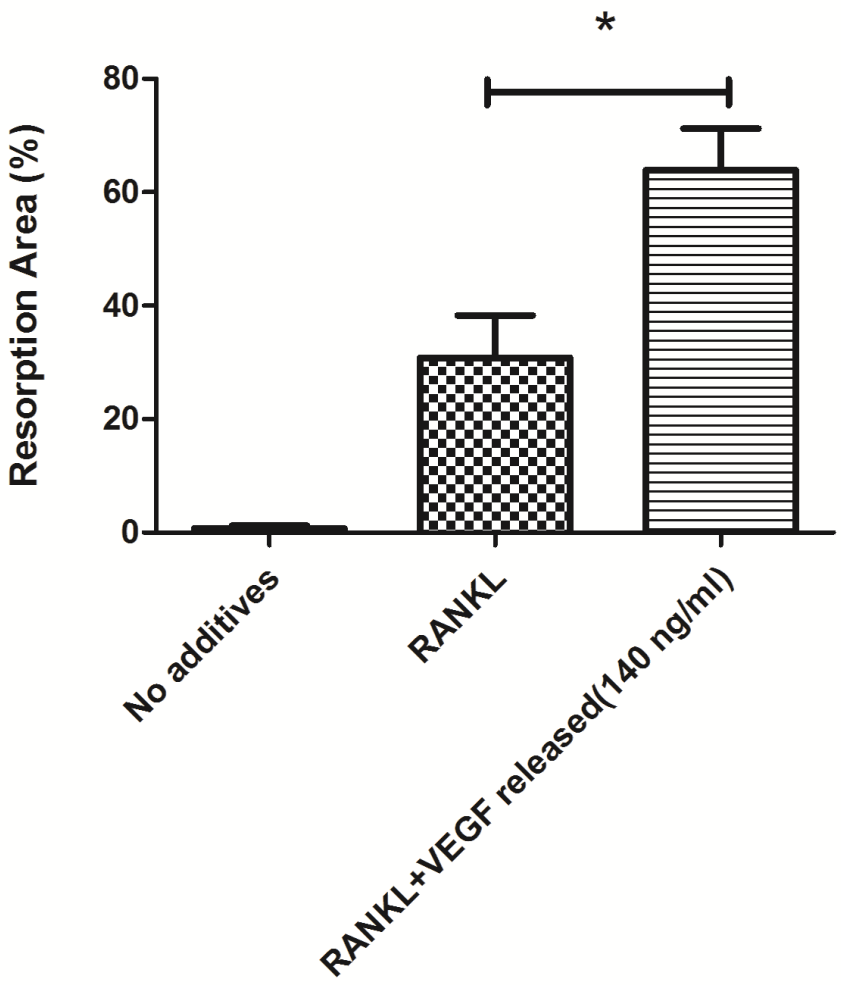

Figure 5.3.2.2: A significant increase in the resorption activity between the group with and without VEGF confirms that the released VEGF not only increased osteoclast differentiation but that cells were functional as well. Significance between groups is designated with (*) = $P<0.05$. Data are mean± SD, n=3 independent experiments.

We also tested functionality of BMMs that were differentiated to osteoclasts via released VEGF on bovine bone chips to assess true bone resorption (fig. 5.3.2.3-5). SEM images revealed formation of resorption pits on bovine bone surface (fig. 5.3.2.3-4). The bone slices were also stained with TRAP, to confirm the presence of osteoclasts, and toluidine blue to visualize

resorption pits. Multinucleated TRAP positive cells were observed on the surface of the bone slices and the resorption pits developed a blue to purple color (fig. 5.3.2.5). These results strongly support the notion that incorporating VEGF into coated and loaded allografts will not only help stimulate angiogenesis and early vascularization[11], but also may likely facilitate allograft resorption via osteoclast precursor differentiation, which may encourage bone remodeling of the allograft.

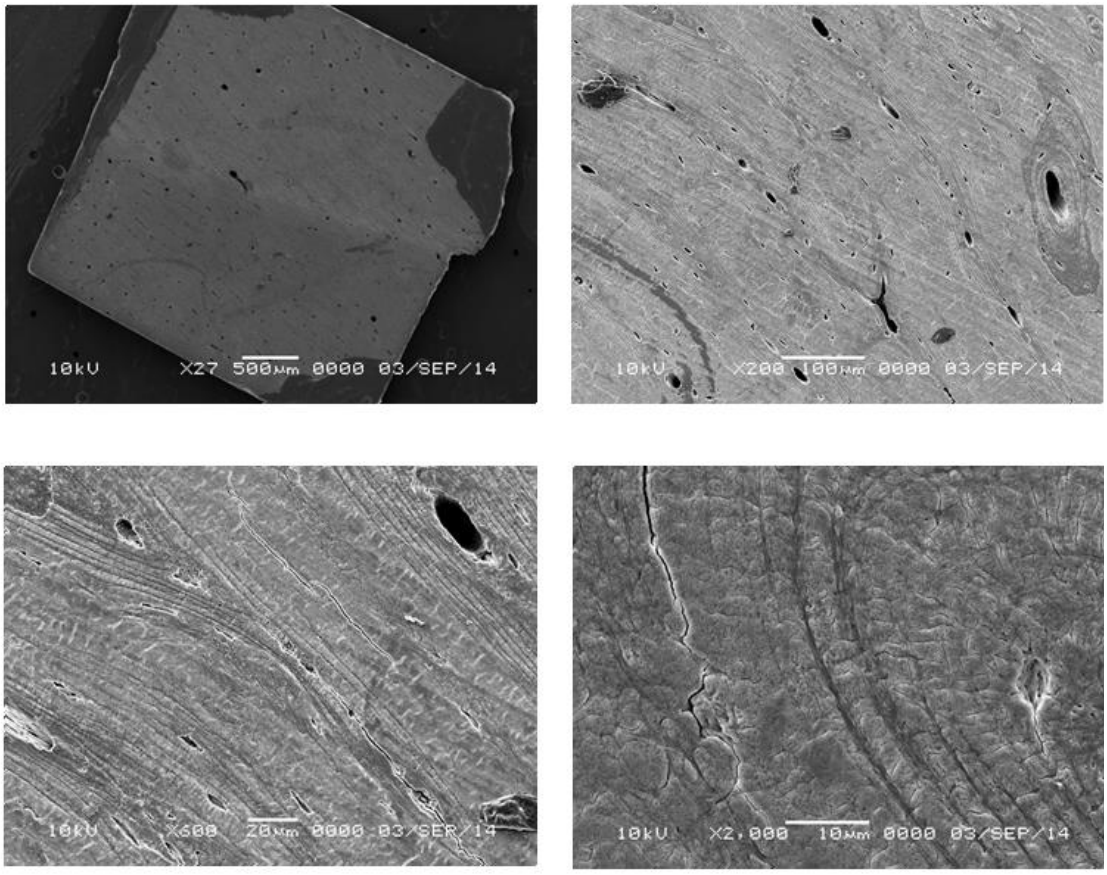

Figure 5.3.2.3: VEGF induced osteoclast resorption activity on bovine bone slices. SEM images of untouched bone slices at different magnifications, indicate the appearance of bone with no resorption pits.

B

A

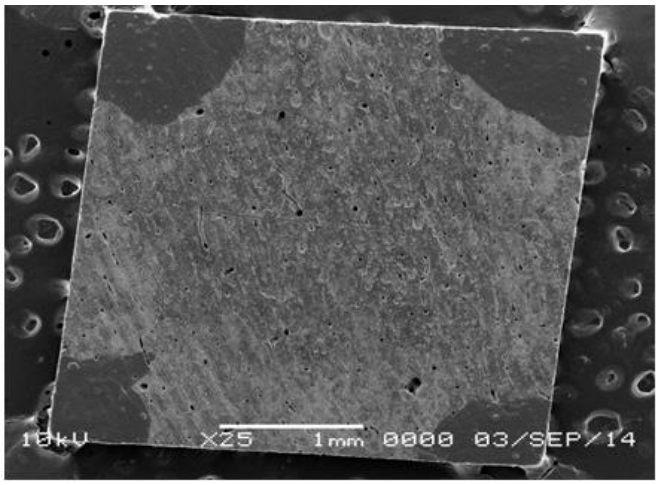

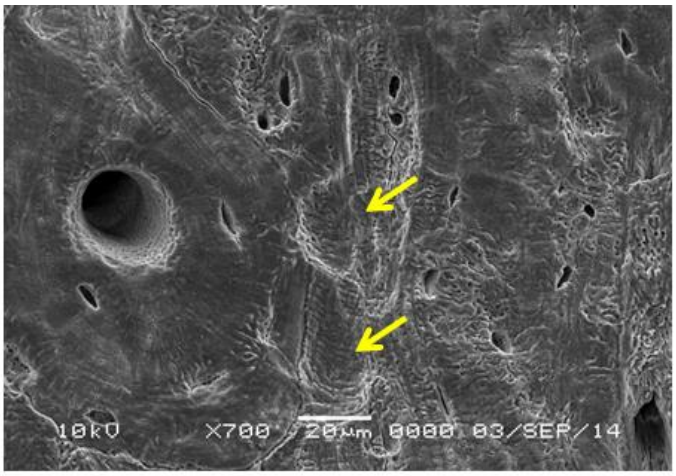

C

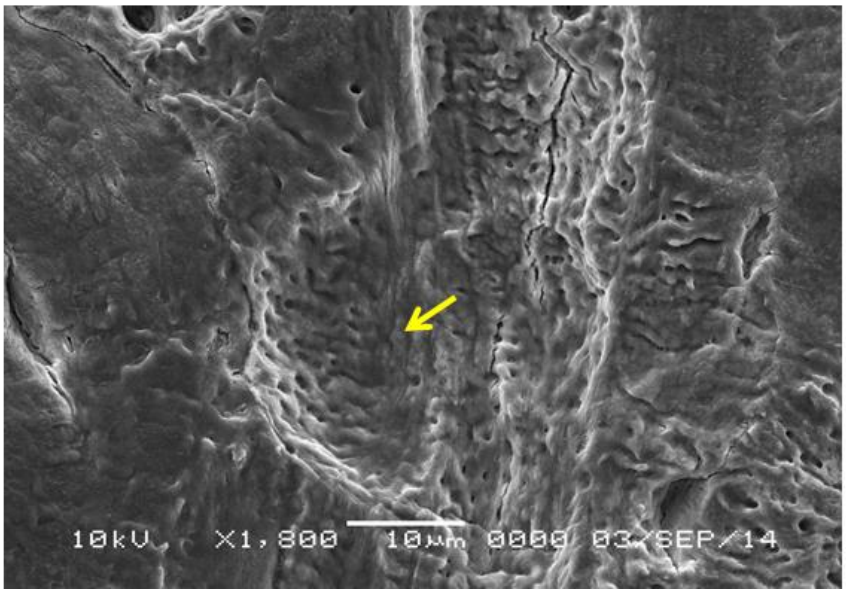

Figure 5.3.2.4: SEM images of bone slices where cells cultured with VEGF released from coated allograft constructs were seeded for 14 days. Cells were removed from the surfaces and SEM images were taken at 25x (A), 700x (B) and1800x (C). The resorption lacunae are indicated with yellow arrows.

A

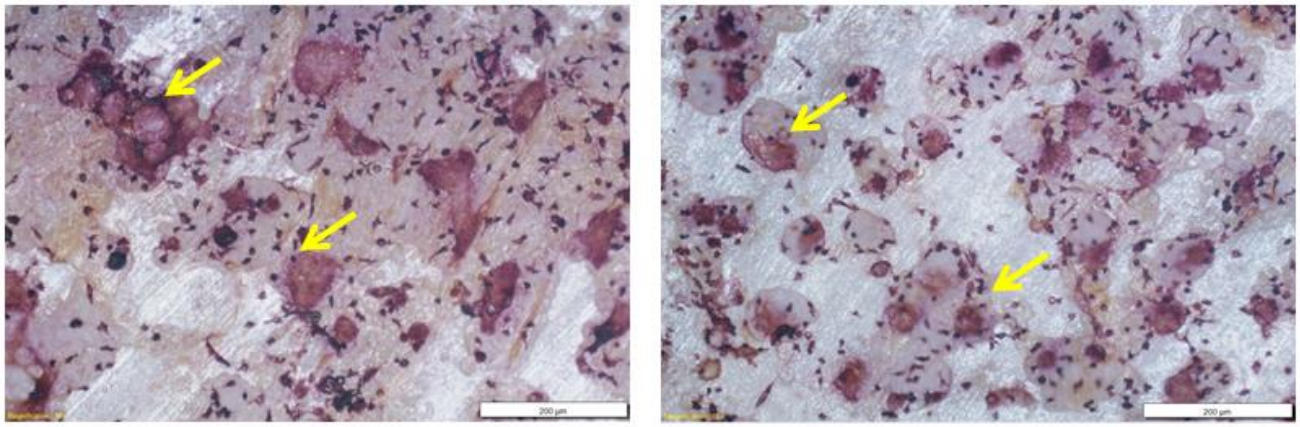

TRAP STAIN

B

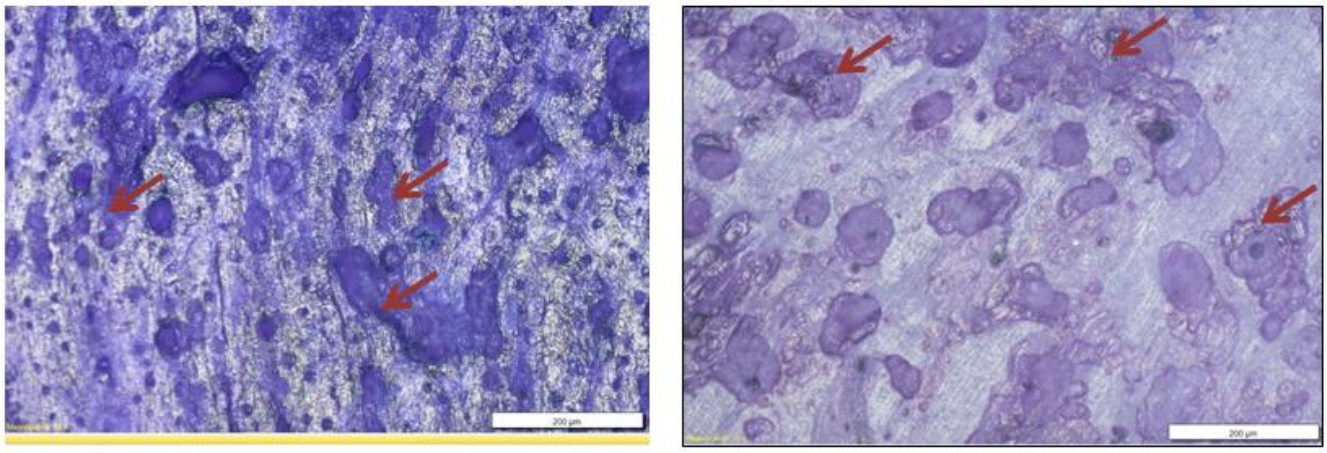

Toluidine Blue Stain

Figure 5.3.2.5: The same bone slices shown in figure 5.3.2.3 were also treated with TRAP and toluidine blue staining. (A) TRAP staining shows multinucleated osteoclasts on the surface of the bone slices (red arrows). (B) Toluidine blue staining depicted the presence of resorption pits (red arrows).

5.4. DISCUSSION

Autografts are still considered the gold standard for bone grafting because of their biocompatibility and propensity to form bone, but limited supply and donor-site morbidities

restrict their utility and mandate a viable alternative[12]. Allografts are either used alone or in combination with autografts and bone graft substitutes and, depending on the specifics of the defect site and the nature of the allograft, have a wide range of success. Since allografts are commonly harvested from cadavers they are traditionally processed before use to remove or minimize any biological activity, thereby lessening any host immune response but also any inherent graft bioactivity. So the degree to which the host tissue heals depends more on non-biological properties of the allograft like defect-size and graft architecture than inherent biological capabilities it may have possessed prior to processing. It is clear, however, that devitalizing allografts to render them safer for transplant hinders their functionality and results in inferior healing[8,13]. One solution to this has been to add back this functionality or revitalize the allografts. Different approaches to revitalizing devitalized allografts have included, 1) creating a synthetic periosteum of cells[14, 15], 2) binding and releasing genetic vectors to induce host cells to overexpress important growth factors for bone repair and remodeling[16, 17], 3) modifying the physical structure of the allograft to encourage better host cell migration[18, 19], and 4) adding a bioactive ceramic coating to the allograft itself [20, 21]. Each attempt has been moderately successful but also somewhat complex and challenging when considering scale-up and the requirements of large-scale manufacturing.

To address these concerns we have developed a novel procedure where a very thin coating of degradable polymer has been added to the surface of long bone allografts and loaded with relevant growth factors such that they elute with a temporal precision shown to benefit bone repair[9]. By modifying an implant that is clinically viable and currently used in regular practice, and using materials and molecules that have long track records of safety and efficacy, we believe our approach may be accepted in the clinic, and by applying this to a known clinical

challenge by directly addressing the issues at the heart of the challenge we believe this approach has the potential to be an important tool to the orthopaedic surgeon. This coated loaded allograft has been shown here to deliver both VEGF and BMP-2 from the surfaces of the long bone allograft such that the VEGF releases in a burst over the first few days after implantation and is followed by BMP-2 release over an extended period of time, up to 4 weeks longer. In the previous chapters we established a methodology to apply a polymer coating onto the surface of the allograft thin enough to maintain its inherent pore structure (which facilitates revascularization and bone formation) and still act as a vehicle to deliver growth factors, VEGF and BMP-2, to the defect site. We examined both the release kinetics of each growth factor independently from polymer-coated allografts and the osteogenicity of the allograft through the bioactivity of the released BMP-2 *in vitro* and *in vivo* [9]. We showed how VEGF and BMP-2, when loaded individually, and on same coated allograft can be released with two distinct delivery kinetics depending on how they are loaded onto the allograft.

BMP-2 and VEGF, two of the most commonly studied growth factors in bone repair, are critically important on their own but also have interconnected roles in the healing process. However, less well known are the roles of VEGF in regulating both bone formation and resorption through their respective cell types. VEGF plays a significant role in osteoblast functionality. Studies have shown that VEGF has a dose-dependent chemoattractive effect on primary human osteoblasts and human mesenchymal progenitor cells [22, 23] and is responsible for regulating blood vessel invasion (neovascularization) into hypertrophic cartilage. VEGF also plays a vital role in osteoclast differentiation and bone resorption[14-17]. Nakagawa et al., found that VEGF caused a dose- and time-dependent increase in the area of bone resorption pits excavated by the purified rabbit mature osteoclast via two distinct VEGF receptors, KDR/Flk- 1 and Flt-1, in osteoclasts at

the gene and protein levels, and VEGF induced tyrosine phosphorylation of proteins in osteoclasts. Thus, osteoclastic function and angiogenesis are upregulated by a common mediator, VEGF[14]. Helmrich et al. showed that VEGF in a defect site not only improved vascularization but also increased the recruitment of the TRAP and Cathepsin K-positive osteoclasts[15]. Kaku et al. showed in osteopetrotic op/op mice with a severe osteoclast deficiency that injection of VEGF induced osteoclast formation during experimental tooth movement[16]. In this study we have substantiated the osteoclastogenic capacity of VEGF and verified that when released from the coated allograft its capacity is retained. VEGF released from coated allografts resulted in enhanced differentiation of osteoclast progenitors in a dose dependent manner, and bone resorption studies verified that the differentiated osteoclasts were fully functional as bone resorbing cells. While in our studies we were careful to isolate VEGF release when assessing osteoclastic precursor response, we do acknowledge that future studies should be done to fully understand how the overlap of VEGF and BMP-2 delivery that we see may impact this response given the design of our delivery system. Given that allografts, particularly large scale cortical allografts, have a failure rate of 30-60% at the 10-year mark[9] in part due to lack of vascularization and limited remodeling via creeping substitution[22], it is the belief that the early release of VEGF from the coated allografts will both encourage neovascularization at the defect site and also differentiate osteoclast precursors to fully functional osteoclasts so the implanted allograft becomes a temporary strut that is resorbed to make way for new bone rather than a semi-permanent necrotic tissue that is destined to fail years down the line.

5.5. CONCLUSIONS & FUTURE DIRECTIONS

In this study we have demonstrated released VEGF, traditionally tasked with neovascularization, was shown to effect osteoclast progenitor cells and induce them to mature, functional osteoclasts capable of resorbing bone. While in our studies we were careful to isolate VEGF release when assessing osteoclastic precursor response, we do acknowledge that future studies should be done to fully understand how the overlap of VEGF and BMP-2 delivery that we see may impact this response given the design of our delivery system.

5.6. REFERENCES

(1) Singh H, Levi AD. 2014. Bone Graft and Bone Substitute Biology. In: Patel V, Patel A, Harrop J., et al., editors. Spine Surgery Basics, 1st ed. Springer-Verlag Berlin Heidelberg; p 147-152.

(2) Fleming JE, Cornell CN, Muschler GF. 2000. Bone cells and matrices in orthopedic tissue engineering. Orthop Clin North Am 31:357-374.

(3) Cook SD, Baffes GC, Wolfe MW, Sampath TK, Rueger DC, Whitecloud TS, 3rd. 1994. The effect of recombinant human osteogenic protein-1 on healing of large segmental bone defects. J Bone Joint Surg Am 76:827-838.

(4) Kalfas IH. 2001. Principles of bone healing. Neurosurgical focus 10:1-4.

(5) Mikhael MM, Huddleston PM, Zobitz ME, Chen Q, Zhao KD, An K. 2008. Mechanical strength of bone allografts subjected to chemical sterilization and other terminal processing methods. J Biomech 41:2816-2820.

(6) Burchardt H. 1983. The biology of bone graft repair. Clin Orthop Relat Res 174:28-42.

(7) Enneking WF, Mindell ER. 1991. Observations on massive retrieved human allografts. J Bone Joint Surg Am 73:1123-1142.

(8) Gouin F, Passuti N, Verriele V, Delecrin J, Bainvel JV. 1996. Histological features of large bone allografts. J Bone Joint Surg Br 78:38-41.

(9) Wheeler DL, Enneking WF. 2005. Allograft bone decreases in strength *in vivo* over time. Clin Orthop 435:36-42.

(10) Peng H, Usas A, Olshanski A, Ho AM, Gearhart B, Cooper GM, et al. 2005. VEGF improves, whereas sFlt1 inhibits, BMP2-induced bone formation and bone healing through modulation of angiogenesis. Journal of Bone and Mineral Research 20:2017-2027.

(11) Kempen DH, Lu L, Heijink A, Hefferan TE, Creemers LB, Maran A, et al. 2009. Effect of local sequential VEGF and BMP-2 delivery on ectopic and orthotopic bone regeneration. Biomaterials 30:2816-2825.

(12) Patel ZS, Young S, Tabata Y, Jansen JA, Wong ME, Mikos AG. 2008. Dual delivery of an angiogenic and an osteogenic growth factor for bone regeneration in a critical size defect model. Bone 43:931-940.

(13) Ramazanoglu M, Lutz R, Rusche P, Trabzon L, Kose GT, Prechtl C, et al. 2013. Bone response to biomimetic implants delivering BMP-2 and VEGF: an immunohistochemical study. Journal of Cranio-Maxillofacial Surgery 41:826-835.

(14) Nakagawa M, Kaneda T, Arakawa T, Morita S, Sato T, Yomada T, et al. 2000. Vascular endothelial growth factor (VEGF) directly enhances osteoclastic bone resorption and survival of mature osteoclasts. FEBS Lett 473:161-164.

(15) Helmrich U, Di Maggio N, Güven S, Groppa E, Melly L, Largo RD, et al. 2013. Osteogenic graft vascularization and bone resorption by VEGF-expressing human mesenchymal progenitors. Biomaterials 34:5025-5035.

(16) Kaku M, Kohno S, Kawata T, Fujita I, Tokimasa C, Tsutsui K, et al. 2001. Effects of vascular endothelial growth factor on osteoclast induction during tooth movement in mice. J Dent Res 80:1880-1883.

(17) Stolina M, Kostenuik PJ, Dougall WC, Fitzpatrick LA, Zack DJ. 2007. RANKL inhibition: from mice to men (and women). Adv Exp Med Biol. 602:143-50.

(18) Sharmin F, Adams D, Pensak M, Dukas A, Lieberman J, Khan Y. 2015. Biofunctionalizing devitalized bone allografts through polymer-mediated short and long term growth factor delivery. Journal of Biomedical Materials Research Part A DOI: 10.1002/jbm.a.35435.

(19) Adapala NS, Barbe MF, Tsygankov AY, Lorenzo JA, Sanjay A. 2014. Loss of Cbl–PI3K Interaction Enhances Osteoclast Survival due to p21-Ras Mediated PI3K Activation Independent of Cbl-b. J Cell Biochem 115:1277-1289.

(20) Street J, Bao M, deGuzman L, Bunting S, Peale FV,Jr, Ferrara N, et al. Vascular endothelial growth factor stimulates bone repair by promoting angiogenesis and bone turnover. 2002. Proc Natl Acad Sci 99:9656-9661.

(21) Stevenson S, Horowitz M. 1992. The response to bone allografts. J Bone Joint Surg Am 74:939-950.

(22) Street J, Bao M, deGuzman L, Bunting S, Peale FV,Jr, Ferrara N, et al. 2002. Vascular endothelial growth factor stimulates bone repair by promoting angiogenesis and bone turnover. Proc Natl Acad Sci USA 99:9656-9661.

(23) Liu Y, Olsen BR. 2014. Distinct VEGF functions during bone development and homeostasis. Arch Immunol Ther Exp (Warsz) 62:363-368.

6. *IN VIVO* EVALUATION OF PLGA COATED-GROWTH FACTOR LOADED ALLOGRAFT FOR BONE REGENERATION IN A RAT FEMORAL SEGMENTAL MODEL

6.1. INTRODUCTION

The repair and incorporation of bone graft is a regulated process that is very similar to fracture healing. The initial phase is characterized by inflammation and vascular invasion from the host, which enables recruitment of mesenchymal stem cells (MSC). These MSCs in the presence of growth factors like BMPs differentiate into the bone-forming osteoblast cells [1]. In the case of autografts, both graft and host bones contribute to the migration of osteoprogenitor cells [2]. In contrast, since allograft does not contain any live cells, healing relies exclusively upon host cells and tissues. Due to the lack of growth factors that are present in allograft, the host MSCs fail to receive essential stimuli to contribute in bone formation and overall healing. During healing process, autografts continue to remodel through osteoclastic resorption of necrotic bone followed by osteoblastic formation of new woven bone, later remodeled into stronger lamellar bone. In this way, autografts retain its sustainability through normal bone homeostasis. In contrast, due to insufficient revascularization, osteoinduction and remodeling of the graft, allograft tissue often shows limited healing, leaving a large segment of necrotic bone that is unable to respond to normal mechanical loading. Thus, structural allografts have a limited life span because microfractures that occur in them over time cannot be remodeled and repaired, and they demonstrate a 25–35% failure rate from infection, nonunion and fracture [3,4]. Therefore there is a high demand for revitalizing this devitalized allografts by modulating vascular ingrowth, osteogenesis, and remodeling. In order to facilitate allograft healing it is imperative to recognize the growth factors that contribute to autograft healing and are absent in allografts and a

method to introduce these factors onto allografts. In the introduction chapter of this thesis we discussed the important growth factors in bone healing and the two most notable factors were identified to be vascular endothelial growth factor (VEGF) and bone morphogenetic protein-2 (BMP-2), which are known to dominantly regulate angiogenesis and osteoblastic bone formation, respectively, during skeletal repair. Our *in vitro* cell studies indicate that VEGF can also stimulate osteoclastogenesis in combination with RANKL. In the previous chapters we developed a polymeric system that can deliver VEGF and BMP-2 simultaneously from structural cortical allograft. Furthermore, we evaluated the bioactivity of the released growth factors via cellular assessment.

In our preliminary *in vivo* study we delivered BMP-2 utilizing short and long term delivery kinetics. Utilizing the dual delivery method we released approximately 50 µg of BMP-2 in total at the defect site. The results indicated dense, organized bone formation along the length of the allograft, fully encapsulating the coated allograft. However, the allograft showed no sign of resorption, hence no remodeling of the graft. BMP-2 is a very expensive molecule and high dose of BMP-2 can cause numerous adverse effects including ectopic bone formation, cyst-like bone void formation, and life-threatening cervical swelling [5,6]. Although proven to be an effective osteoinducer, the aforementioned adverse effects, along with the possibility of structurally abnormal and mechanically unstable bone tissue formation, currently limit the overall clinical efficacy of BMPs. The ability to define upper and lower bounds for BMP doses that would both form high-quality bone and avoid swelling, void formation, and other side effects would improve the prospects of BMP as a tissue engineering adjunct and as a clinical product. Therefore, in this *in vivo* study we decided to deliver low dose of BMP-2 (at nanograms level) with simultaneous delivery of VEGF to enhance allograft healing. During normal bone healing, VEGF expression

was shown to peak during the early days while BMP expression peaked at a later time point [7,8]. Therefore we anticipate that a sequential delivery of VEGF and BMP-2 will show better allograft resorption and bone formation over BMP-2 alone.

The primary objective of this chapter is to evaluate the efficacy of coated-loaded bioactive allografts to repair large scale critical sized segmental defects *in vivo*. The femoral non-union bone defect is a segmental defect model in which a section of the femur is removed. Commonly this defect is used to form a critical sized defect (CSD) to ensure non-union, as critical sized defects will not heal spontaneously and thus are a good measure of the ability of an implant to promote healing where healing would not otherwise occur [9]. A CSD has been defined as "the smallest intraosseous wound that would not heal spontaneously throughout the lifetime of an animal" [10]. For long bones this is defined as those defects having a length greater than or equal to a distance twice the diameter of the bone itself [11]. In a male Sprague-Dawley rat weighing 300-325 g, this length is approximately 6mm [12-14]. It is hypothesized that coated allografts containing BMP-2 will show enhanced bone formation over uncoated allografts. It is also hypothesized that delivery of both VEGF and BMP-2 in a temporally controlled way will increase healing over either BMP-2 alone. Specifically, given the nature of the bone defect to be used, segmental defects, it is anticipated that bone repair will occur via endochondral ossification. For this reason it is anticipated that an initial release of VEGF will encourage angiogenesis and osteoclastogenesis, followed by sustained release of BMP-2 will result in bone formation and overall better bone repair.

6.2. MATERIALS AND METHODS

6.2.1. *In Vivo* Femoral Critical-Size Segmental Defect

Allografts were placed in critical size segmental femoral defects in 10 week-old male Sprague-Dawley rats (weights 300-325 g). All procedures were done in accordance with approved Institutional Animal Care and Use Committee guidelines. Briefly, the right hindlimb of the rat were shaved, and prepped with betadine and 70% ethanol. The femur was approached anterolaterally, the periosteum incised, and then removed circumferentially. A small plate was fixed to the femur with four Kirschner wires and two surgical steel cerclage wires and a 6mm critical-sized full-thickness defect was created in the central third of the diaphysis. The allografts were shaped to final size intraoperatively and placed into the defects to achieve a press-fit, and maintained in place using a single 4-0 Vicryl (Ethicon, Somerville, NJ) cerclage stitch that was tied around the graft and plate. A three-layered closure of the muscle, subcutaneous tissue, and skin was performed with 4-0 Vicryl. After 4 and 8 weeks post-implantation animals were sacrificed and the femur was harvested, the metals were removed from the limbs and the femurs were kept fixed in 70% ethanol (fig. 6.2.1.1).

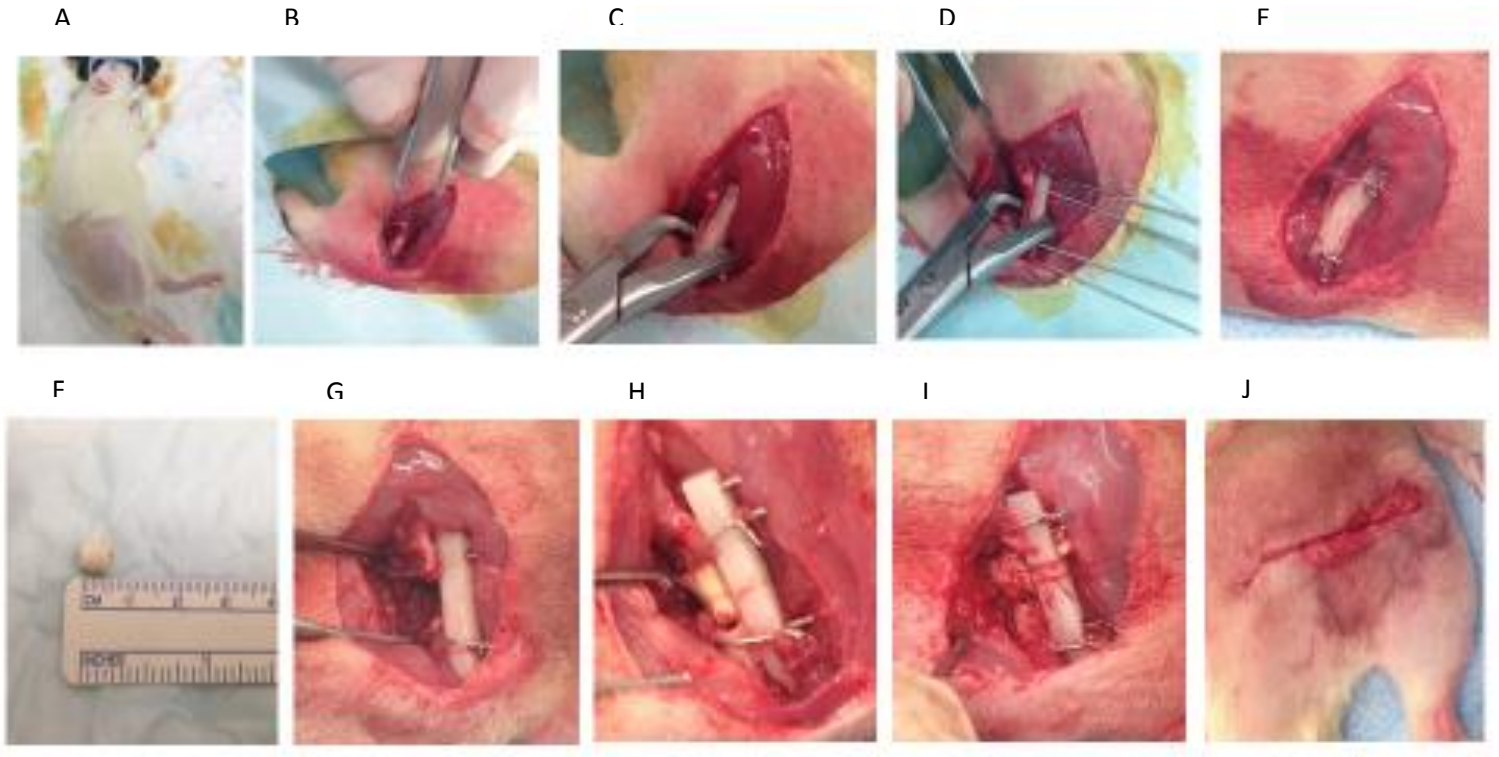

Figure 6.2.1.1: Steps involved in implantation of allografts into a rat femur bone defect model. (A) The right hindlimb of the rat is shaved, and prepped with betadine and 70% ethanol. (B) An incision is made in the right hindlimb of the rat and the surrounding muscle is dissected to expose the femoral bone. (C) A custom made polyethylene plate is placed against the bone. (D, E) The plate was secured using four Kirschner wires and two surgical steel cerclage wires. (F) A sterile surgical ruler is used to measure the length of the allograft. (G) A 6 mm defect is created in the bone using a dremel cutting burr. (H) The construct is secured in the defect by press fit. (I) Graft was maintained in place using a single 4-0 Vicryl and (J) A three-layered closure of the muscle, subcutaneous tissue, and skin was performed.

The groups that were evaluated in this study are stated in table 6.2.1.1.

Table 6.2.1.1: Allograft treatment groups for animal study

Healing Time	Rats required to test the treatment method		
	BMP-2 encapsulated PLGA coated allografts	VEGF surface adsorbed and BMP-2 encapsulated PLGA coated allografts	Uncoated allografts
4 weeks	4	4	4
8 weeks	4	4	4

6.2.2. Radiological Analysis

Bone formation on each rat femur was analyzed at 26 kV for 6 seconds using the Faxitron X-ray machine and the Faxitron DX-Beta SR v1.4 software.

6.2.3. MicroCT Analysis

Limbs harvested at week 4 and 8 weeks were imaged using cone beam micro-focus X-ray computed tomography to render three-dimensional reconstruction of the defect (μCT40, Scanco Medical AG, Bassersdorf, Switzerland). Serial tomographic images were acquired at 55 kV and 145 μA with a 300 msec integration time. A set length of the distance between the two proximal pin holes of the Kirschner wires was analyzed within the defect. Using image J software new bone area was measured using the radiographs from MicroCT.

6.2.4. Histological Analysis & Histomorphometry

Limbs were embedded in methyl methacrylate using a slow methylmethacrylate (sMMA) processing, infiltration and embedding techniques as described by Kecena *et al*., [33] and then sectioned at 5 μm thickness with a diamond saw microsectioning system., and mounted onto

glass slides. Undecalcified tissue sections were stained with Goldner's Trichrome stain to visualize areas of new osteoid formation (which stains red) and new mineralized tissue (which stains deep green). It is also possible to visualize red blood cells with the Trichrome stain as they appear yellow-orange. Toluidine blue stain was used to detect osteoblasts and osteoclasts based on location of cells and shape, size, and number of nuclei of the cells. All staining was performed according to protocols described by Kecena *et al*. [33]. Histomorphomerty analysis was performed using a Nikon Eclipse E600 microscope (Nikon, Tokyo, Japan) coupled with a digital camera DN100 NIKON (magnifications of 4, and 10 lens). Osteomeasure software was used to quantify new bone area in each sample within the region of interest (ROI).

6.2.5. Statistical Analysis

For quantification analysis, a two-way analysis of variance (ANOVA) was preformed to compare data. Error is reported in figures as the standard deviation (SD) and significance was determined using a probability value of $p < 0.05$ (n=4).

6.3. RESULTS

6.3.1. Radiographic and MicroCT Analysis

Radiographs of rats representing each implant type were taken throughout the healing process. Figure 6.3.1.1 shows healing in the control group (allografts with no growth factor) after 4 weeks. Radiographs show virtually no evidence of callus formation or mineralization. Figure 6.3.1.2 shows progression of healing during 8-week in allografts loaded with BMP-2 alone and allografts with VEGF and BMP-2. There is radiographic evidence of mineralized callus

formation in allografts loaded with BMP-2 and VEGF after 4 weeks of healing and at 6 weeks the grafts demonstrated increased opacity with approaching bridging, suggesting more healing at this time point. At week 8 almost complete bridging between the ends of the defect is seen along the length of the graft. Allograft loaded with BMP-2 alone showed less callus formation than VEGF+BMP-2 group with partial bridging at 8 weeks, indicating loading of dual growth factors not only show more bone formation over single growth factor but can also accelerate the healing process.

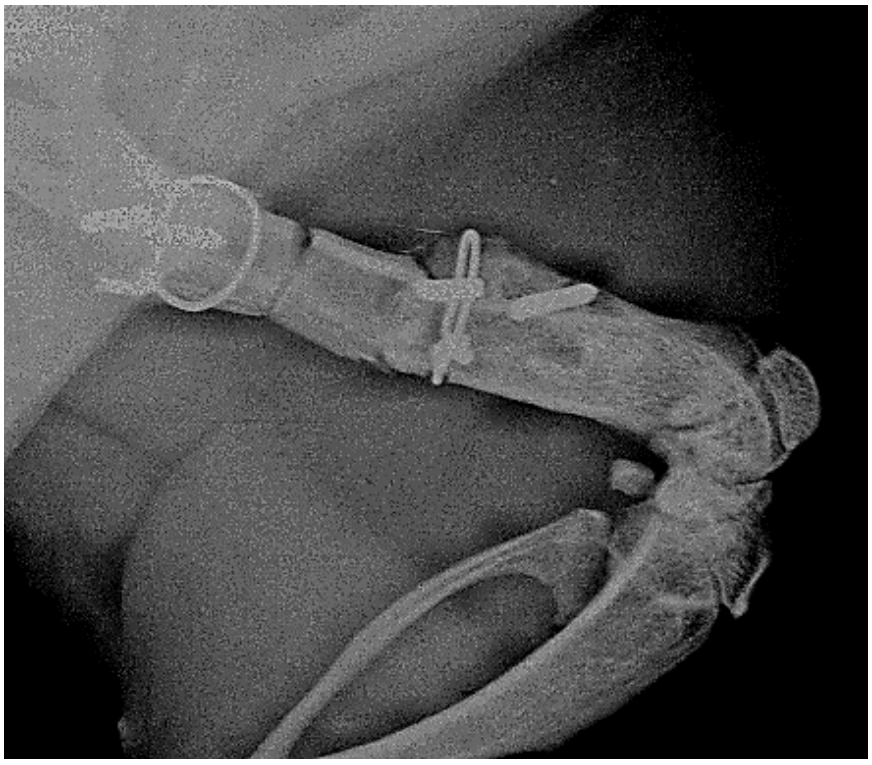

Figure 6.3.1.1: Healing of the control (allograft without growth factor) after 4 weeks. No visible healing is evident on the radiograph.

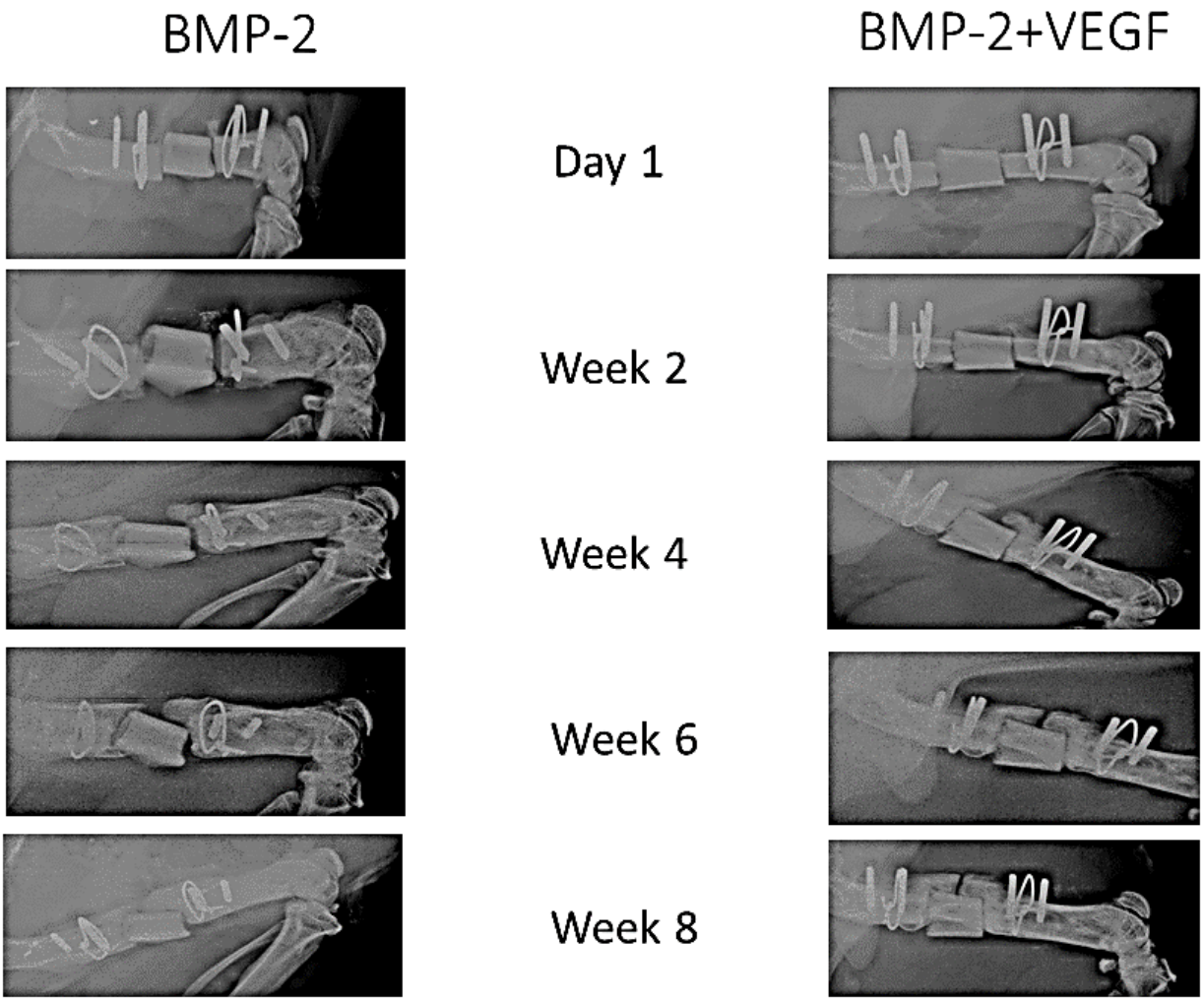

Figure 6.3.1.2: Sample radiographs taken of limbs at every two weeks demonstrating the progression in healing within allograft treated with BMP-2 alone and BMP-2 and VEGF. Allograft treated with dual growth factors showed increased radiopacity within the defect site at week 4 and approaching complete bridging of the implant at week 8, whereas the group with single growth factor showed less radiopacity throughout the healing period.

To further confirm our X-ray findings, we performed microCT analysis using samples from 4- and 8-weeks post-surgery. Micro-CT analyses demonstrated that the size of the external

callus at the host/allograft junction in both BMP-2 and BMP-2 +VEGF group were larger and contained more mineralized bone than the allograft alone groups (fig. 6.3.1.3) at 4 and 8 weeks post-transplantation. MicroCT 3-D rendered images for the entire repair region further demonstrated that a bony union was achieved only in the BMP-2+VEGF groups at 8 weeks post-surgery , while the gap between allograft and host bone was still visible in both allograft alone and BMP-2 groups (fig. 6.3.1.4).

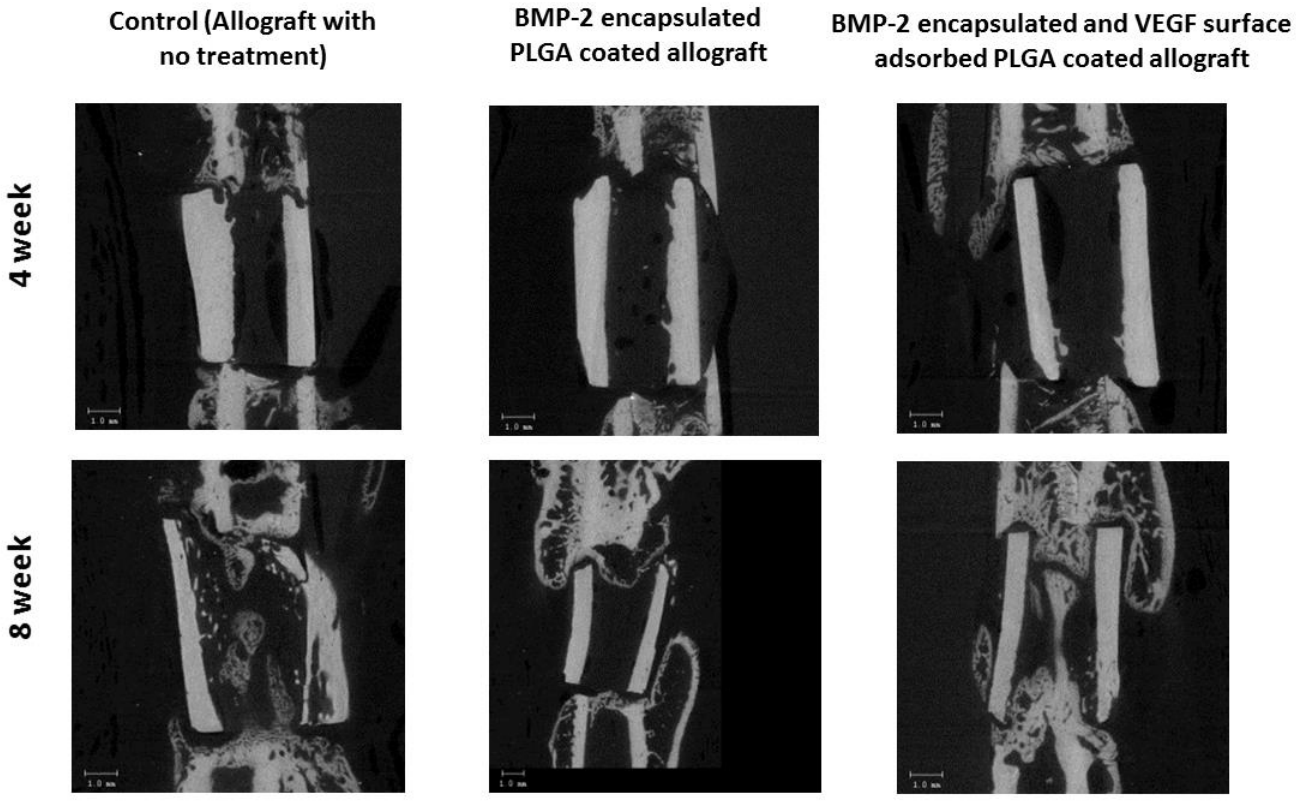

Figure 6.3.1.3: Representative radiographs (from MicroCT) of the dissected limbs after sacrificing the animals at 4 and 8 weeks. Groups include allograft with no treatment (control), BMP-2 encapsulated polymer coated allograft and VEGF surface adsorbed and BMP-2 encapsulated polymer coated allograft. Formation of callus was observed in the VEGF surface adsorbed and BMP-2 encapsulated coated allograft at 4 weeks and bone union at the host 8 weeks. BMP-2 encapsulated coated allograft showed callus around the defect zone at 8 week but no callus formation was seen at 4 week. The control group showed the least bone regeneration among the three groups. Scale bar = 1 mm

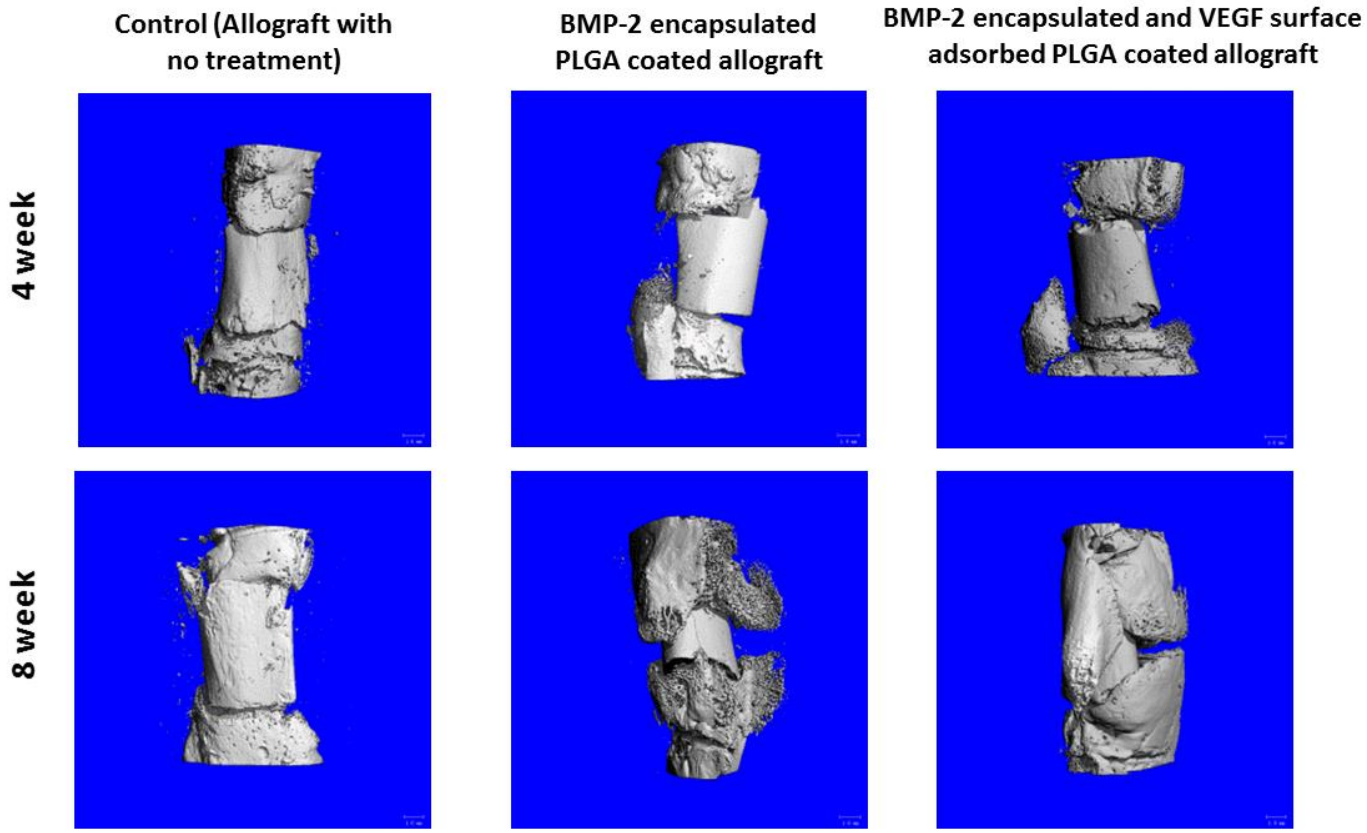

Figure 6.3.1.4: MicroCT analysis of femoral bone defect at 4 and 8 weeks post-implantation. Representative three-dimensional reconstructed images are shown for control, BMP-2 encapsulated coated allograft and VEGF surface adsorbed and BMP-2 encapsulated coated allograft. Very limited of new bone growth was detected through the defect site in the control group, whereas the group treated with VEGF+BMP-2 shows bridging surrounding the defect site. The group treated with BMP-2 alone shows some union at the host-graft interface but not as robust as VEGF+BMP-2 group.

6.3.2. Histological Analysis

Histological analysis confirmed the same bone formation trend that was observed in the microCT scans. The VEGF+BMP-2-loaded allografts showed extensive bone formation around the defect sites and almost full bridging of the cortices (fig.6.3.2.1 and 6.3.2.2). At 4 weeks there

was significant difference in bone formation between control group and the groups with growth factors (fig. 6.3.2.3 a). At 8 weeks BMP-2 + VEGF group showed enhanced bone formation over the other two groups, however it was not statistically significant (fig. 6.3.2.3 b). Allografts loaded with no growth factor showed evidence of thin layer of osteoid formation with no mineralized tissue and fibrotic tissue along the length of the allograft was observed (fig 6.3.2.1, 6.3.2.2, 6.3.2.4). The coated and BMP-2 loaded allograft showed callus formation along the length of the allograft, however, a closer examination at the allograft revealed that there was no sign of remodeling on the cortex of the allograft (6.3.2.5). In contrast, the coated and BMP-2 and VEGF loaded allograft demonstrated not only new bony union between the live host bone and the allograft surfaces but also partial resorption of the allografts and replacement of the resorbed dead bone with viable new bone (fig. 6.3.2.6-8). Figure 6.3.2.8 depicted continuing active resorption of the dead cortical bone with new bone.

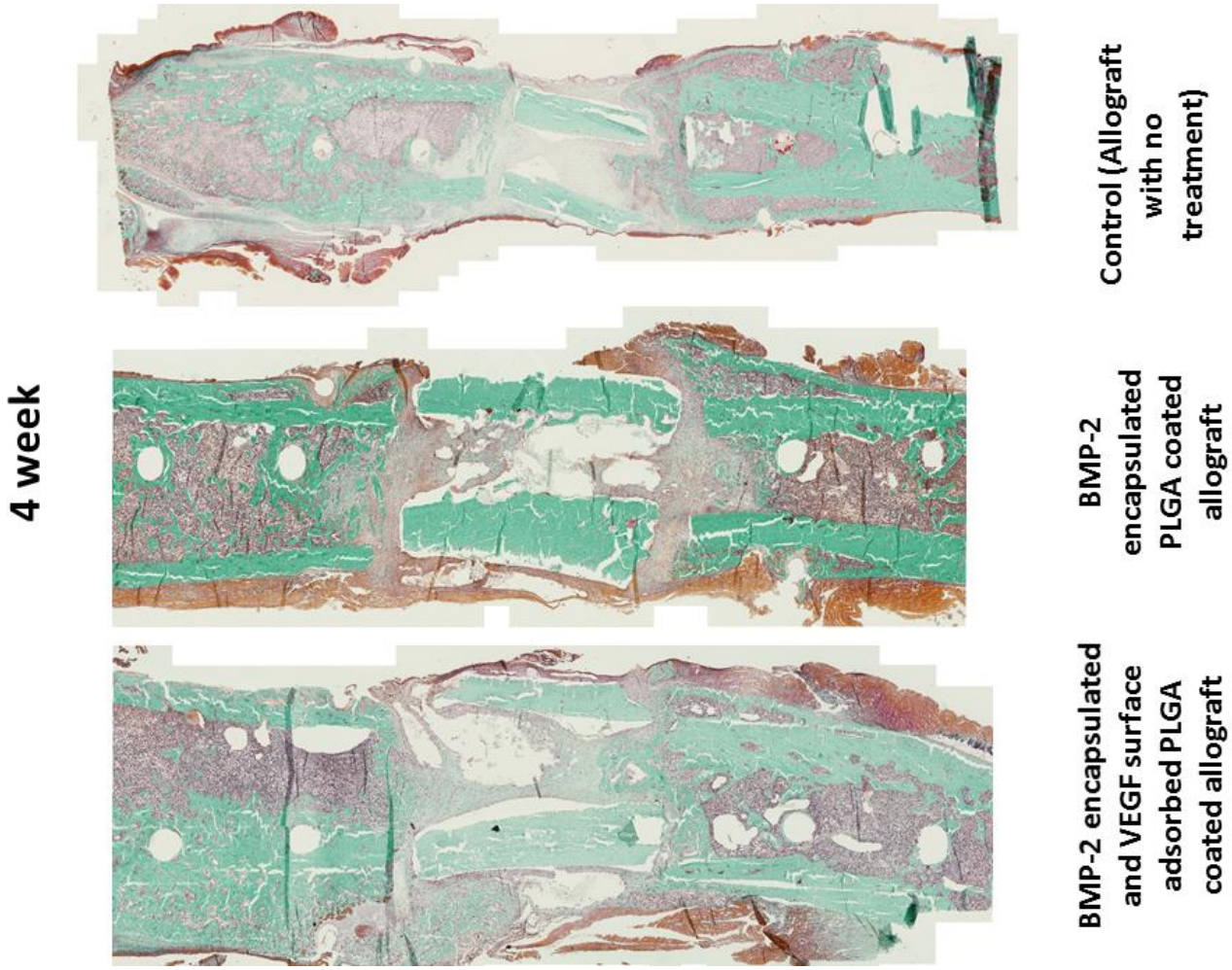

Figure 6.3.2.1: Representative histological images of Goldner's Trichrome –stained longitudinal sections 4 weeks post-implantation imaged under 10X magnification. Goldner's trichrome stain showed no sign of bridging around uncoated/unloaded allograft. Control and BMP-2 group show evidence of unmineralized osteoid within the defect site, peripheral to the allograft while there's evidence of initiation of callus formation surrounding the defect VEGF +BMP-2 loaded allograft.

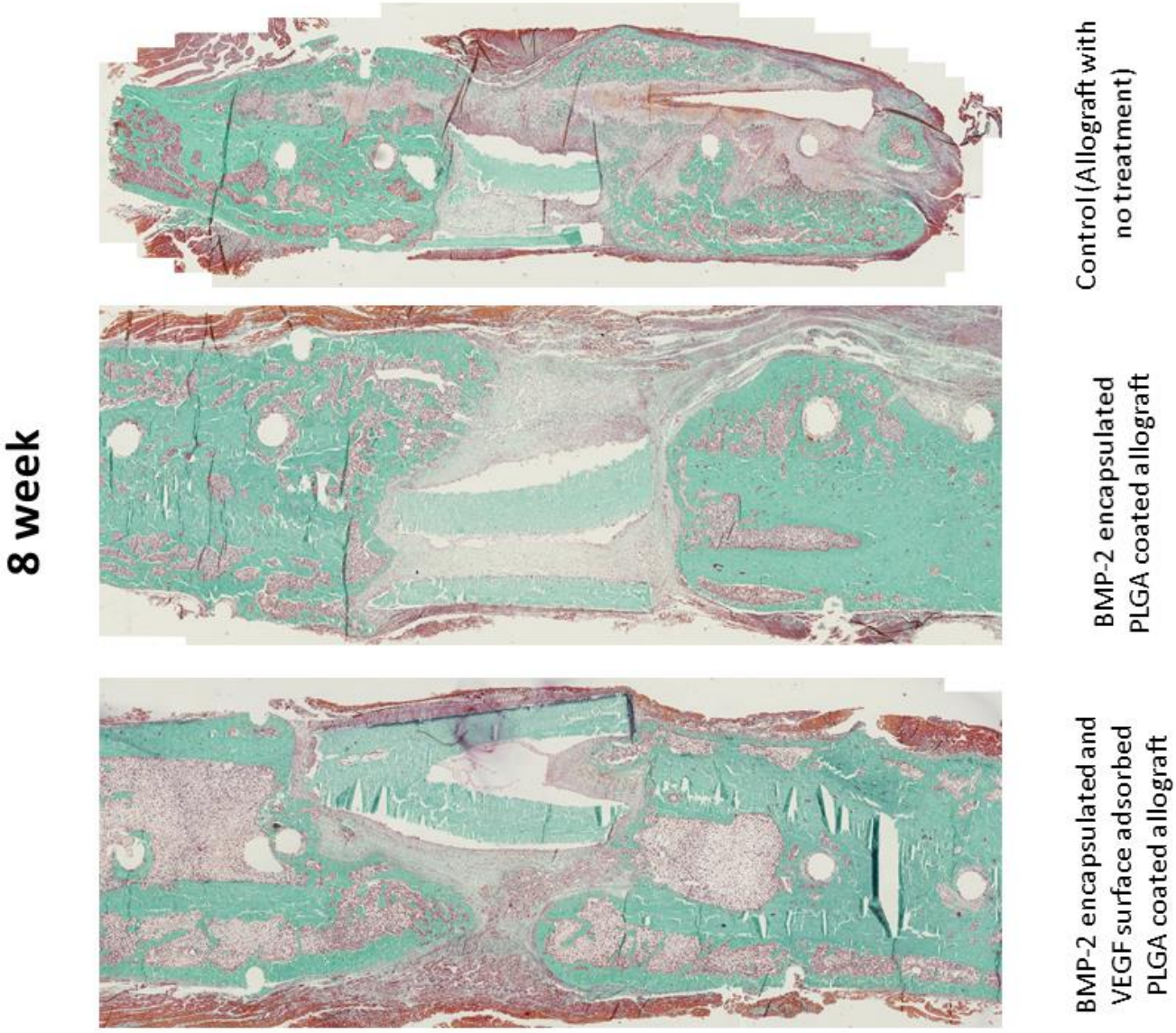

Figure 6.3.2.2: Representative histological images of Goldner's Trichrome –stained longitudinal sections 8 weeks post-implantation imaged under 10x magnification. Goldner's trichrome stain showed limited healing around uncoated/unloaded allograft. Control group shows evidence of unmineralized osteoid within the defect site, peripheral to the allograft while there's evidence of mineralized bone approaching bridging the defect and surrounding the VEGF +BMP-2 loaded allograft. The BMP-2 loaded allograft showed some callus formation around the defect site but no evidence of bridging.

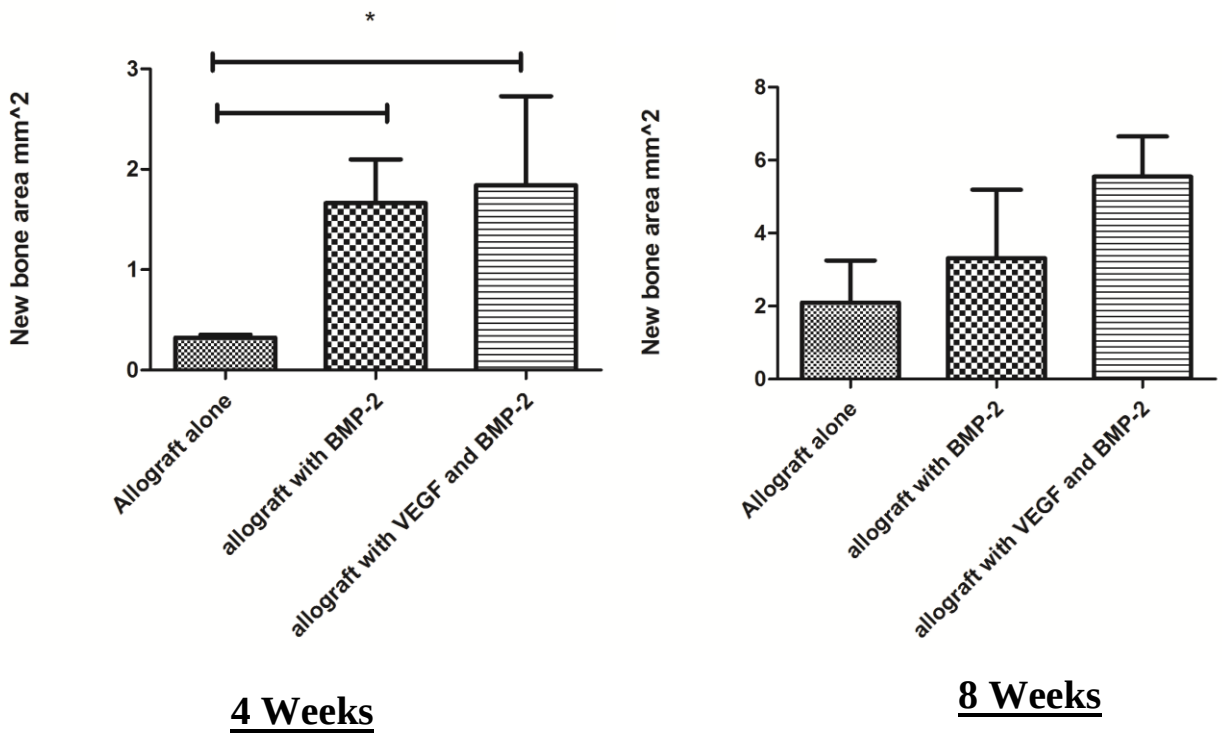

Figure 6.3.2.3: Quantification of new bone area from bridging mineralized calluses of each group. Bone area was quantified from the histological slides stained with Golder's trichrome. * indicates $p<0.05$.

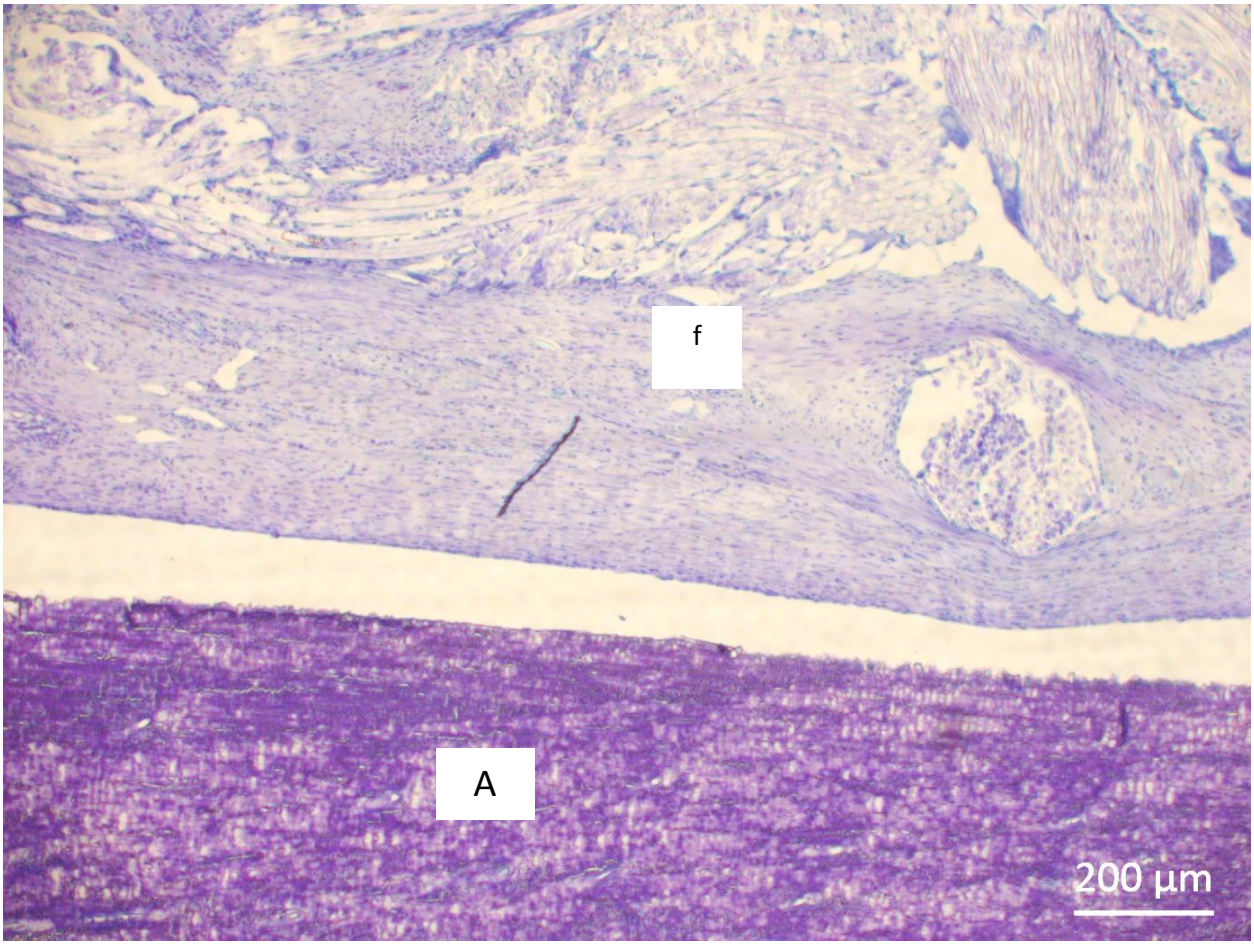

Figure 6.3.2.4: Histological section of uncoated/unloaded allograft (A) stained with toluidine blue shows fibrotic tissue (f) that covered the periosteal surface of necrotic allograft. Image was taken at 5x.

a

b

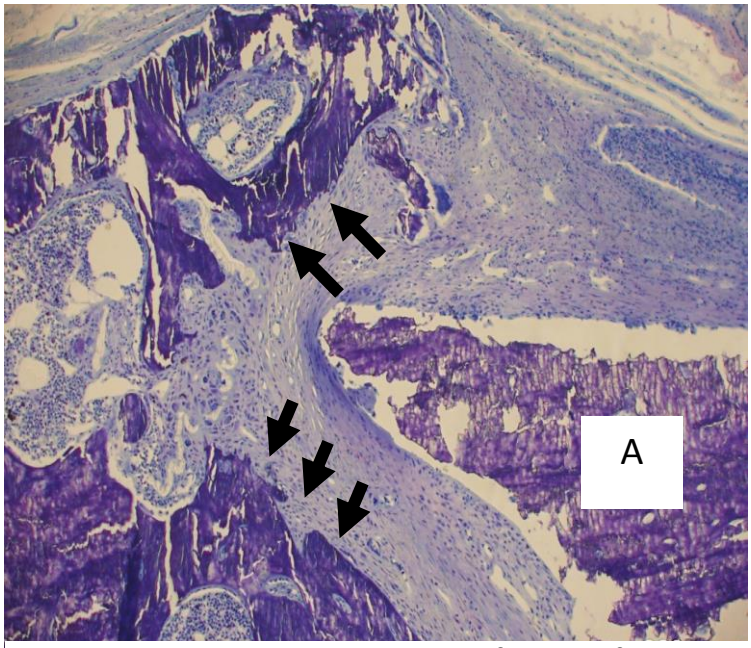

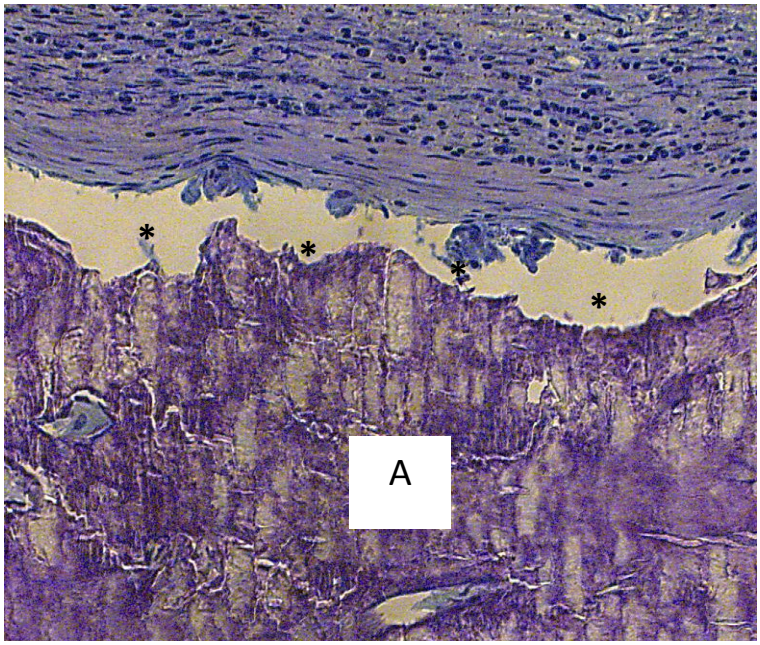

Figure 6.3.2.5: Histological section of Allograft (A) encapsulated with BMP-2 alone. Toluidine blue staining showed callus formation around the defect site, indicated by black arrow (a), however the periosteal surface of the allograft (A) showed no evidence of remodeling, indicated by * (b). Image (a) was taken at 5x magnification and b) was taken at 20x magnification and scale bar= 50 µm

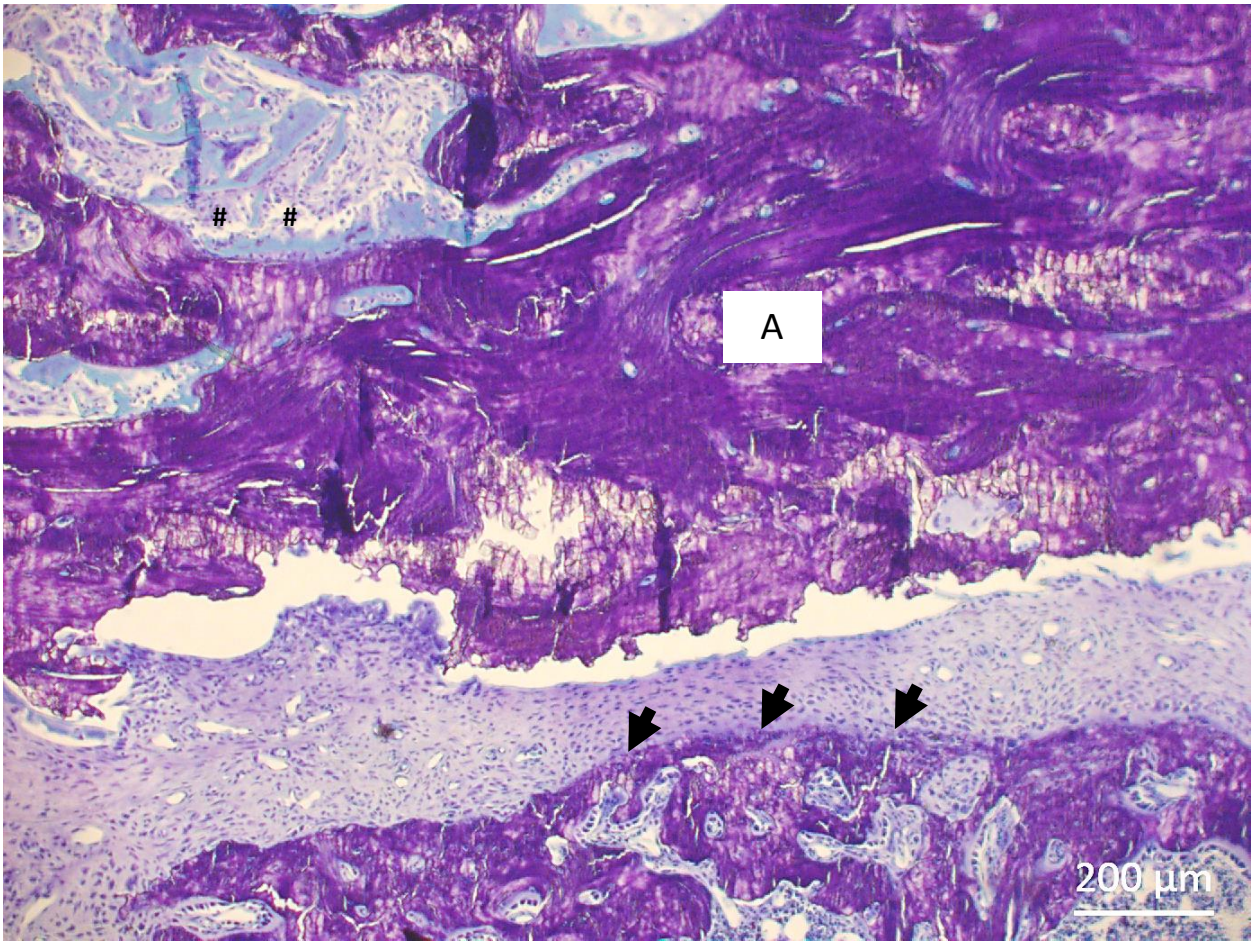

Figure 6.3.2.6: Histological section of allograft (A) loaded with BMP-2 and VEGF stained with Toluidine blue. Low magnified image of the allograft section stained with toluidine blue showing formation of new bone around the cortex of the allograft, indicated by black arrow and evidence of remodeling on the cortex of the allograft is indicated by #. Image was taken 5x magnification.

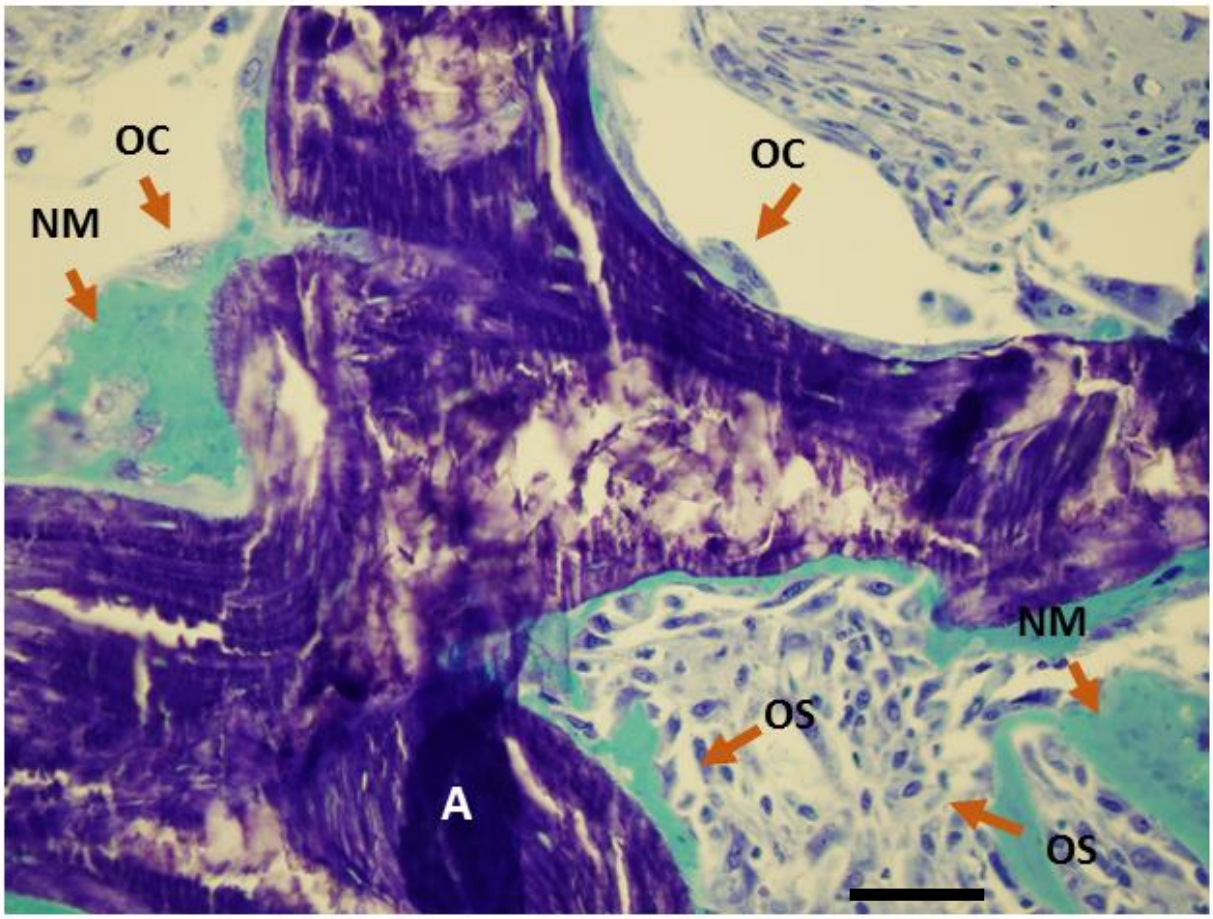

Figure 6.3.2.7: Zoom in view of the cortex of the allograft showing cortical bone remodeling is in progress where space created by osteoclastic bone resorption is being filled by newly synthesized bone in the presence of osteoblast. Image was taken at 40x magnification and scale bar= 20 μm. OS=osteoblast, NM= new matrix, A= allograft, OC=osteoclast

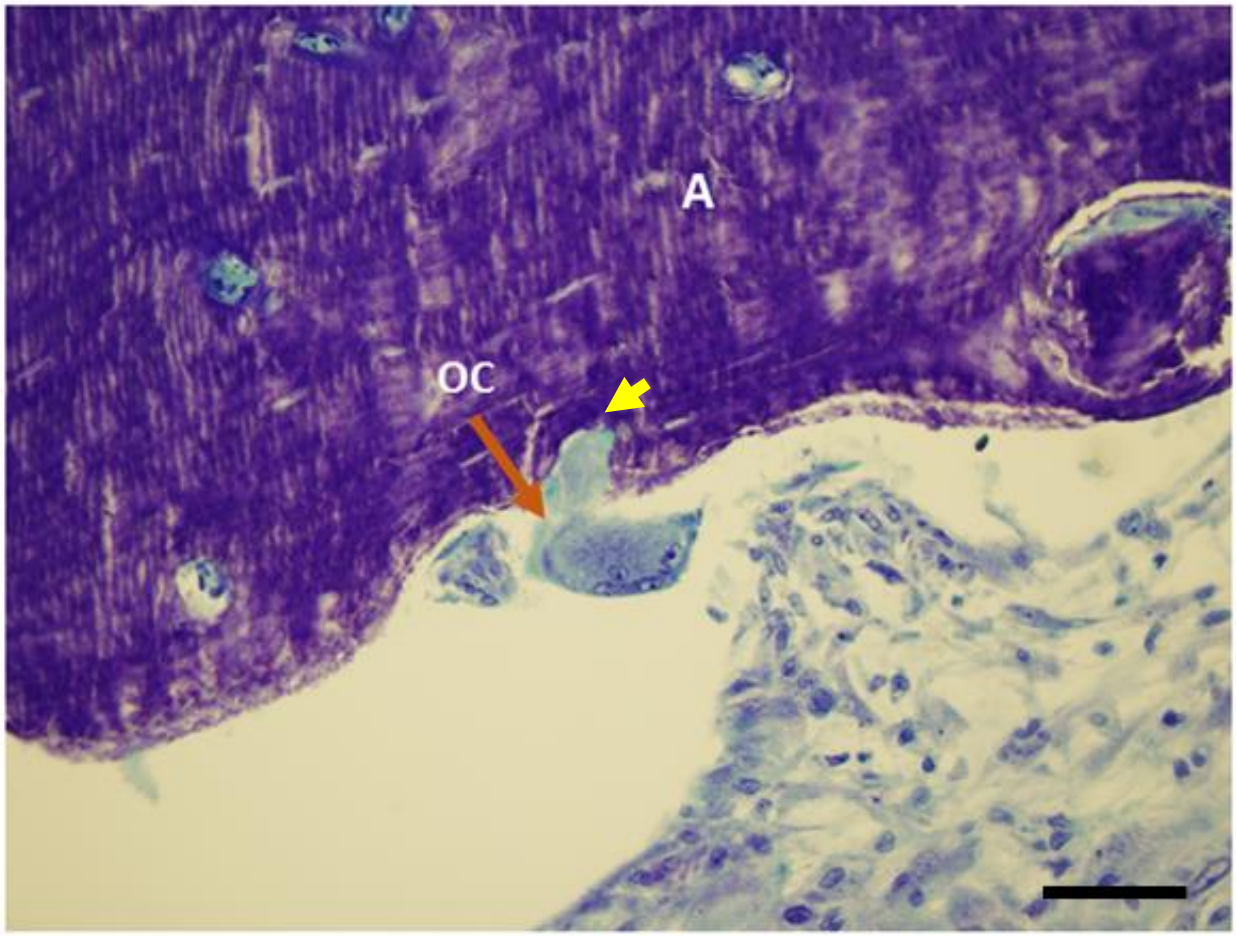

Figure 6.3.2.8: Toluidine blue stained section of the allograft (A) showing resorption pit created by osteoclast (OC) on the surface of the graft (yellow arrow) and formation of new woven bone in the resorption lacuna. Image was taken at 40x magnification and scale bar= 20 μm.

6.4. DISCUSSION

Despite the advancement of regenerative medicine to overcome the issues associated with large segmental defects, effective healing between the host and the allograft implant still remains a major challenge. Allograft implants do not initiate the repair processes seen in normal fracture healing due to the lack of biological factors. Five-year follow-up studies have demonstrated substantial concerns with allograft incorporation into host bone particularly with intact allograft

tissue [27, 28]. Incorporation is a series of events leading to gradual replacement of the old necrotic bone by living new bone as a result of creeping substitution, a mechanism of osteoclastic resorption followed by deposition of new bone. A bone graft is considered to be incorporated when there is no abrupt histological change between the host bone and the graft. Stevenson et al defined successful incorporation as the graft uniting with the host, with the graft-host bone construct able to tolerate physiological loads without fracture or pain. From the perspective of basic science, the complete incorporation is defined as rapid vascularization and substitution of original graft bone with new host bone without substantial loss of strength. In short, events that are essential for allograft incorporation are: vascularization, allograft resorption and new bone formation. Therefore, we have developed a novel procedure where a very thin coating of degradable polymer has been added to both endosteal and periosteal surfaces of long bone allografts and loaded with relevant growth factors such that they elute with a temporal precision shown to benefit bone repair by stimulating vascularization, osteoclastic and osteoblastic activity.

In the present study, our main objective was to investigate the efficacy of dual delivery of VEGF and BMP-2 in allograft healing over BMP-2 alone, *in vivo*. First, we sought to determine the effect of combined delivery of BMP-2 and VEGF on bone formation. Noteworthy, thought there is no significant difference in bone formation between BMP-2 +VEGF and BMP-2 alone, however, a trend is evident that shows more new bone formation in the group treated with BMP-2 and VEGF over the other two groups. There was significant difference between the control group and allograft treated with dual growth factors, however, no significant increase in bone formation between VEGF+ BMP-2 and BMP-2 alone was noticed. At 8 weeks post-implantation, the amount of newly formed bone tended to be higher in the VEGF+BMP-2 group

compared with defects treated with BMP-2 alone and control with no statistical difference. The trend is encouraging and we anticipate by increasing the sample size a significant increase in bone formation between VEGF+BMP-2 and BMP-2 alone could have been attained. These data correlate with the results of Young et al.,[15] Patel et al.,[16] and Kempen et al.[17] who found increase in bone formation by combining BMP-2 with VEGF is more profound at the earlier time points of the healing. Peng et al., for instance, have shown that VEGF antagonists actually reduce the induction capacity BMP-2 to form bone, while BMP-2 in the presence of VEGF showed enhanced bone formation[22]. Further, the degree of bone formation after exposure to both factors was partially dependent on the ratio of one to the other, with higher amounts of BMP-2 compared to VEGF eliciting more bone formation than the reverse. Kempen et al. engineered a composite scaffold consisting of PLGA microspheres loaded with BMP-2, embedded in a poly(propylene) scaffold, surrounded by a VEGF-loaded gelatin hydrogel. Despite the release of 98% of the VEGF within the first 14 days, the VEGF+BMP-2 group formed more vessels and bone than the other groups. Patel et al. reported that the sequential delivery of VEGF and BMP-2 accelerates the healing process through a rat cranial critical-size defect model that evaluated the angiogenic and osteogenic response to porous poly(propylene fumarate) scaffolds with gelatin microparticles that released VEGF and BMP-2. The experimental constructs that released both BMP-2 and VEGF showed accelerated bone healing over those releasing BMP-2 or VEGF alone. In another study of co-release of VEGF and BMP-2 examining the chemotactic role of each molecule, Ramazanoglu et al. examined expressions of collagen type I, Osteocalcin, and Osteopontin. Increased collagen I from VEGF+BMP-2 groups confirmed the chemotactic migration behavior elicited by VEGF on osteoblasts. At week 4, the VEGF+BMP-2 group showed higher osteopontin expression. Since osteopontin regulates bone remodeling by helping

osteoclasts bind to bone, an increase in its expression was interpreted as an indication of bone remodeling [18]. Thus the physiological basis for delivering both VEGF and BMP-2 from the same allograft is well founded given their traditional roles as vasculogenic and osteogenic molecules, respectively.

The adverse effects of super-physiological dosage of BMP-2 that are currently being used clinically is alarming [5,6]. The current therapies utilizing BMP-2, such as INFUSE (contains 1.5 mg/ml rhBMP-2), exceeds physiological levels of the factor (1 µg/kg) by several orders of magnitude [29,30]. In the present study, we used ~ 300 ng/ml of rhBMP-2 which is several orders of magnitude lower than what is currently being used clinically (1.5 mg/ml). Using this low dose of BMP-2, we were able to show enhanced bone formation over the control groups, however none of the animals showed complete bridging in BMP-2 alone group. Literature indicates in rodent sub-therapeutic concentrations of BMP-2 with bony nonunion is less than10 µg/mL; therapeutic concentration with robust bony union, normal trabecular architecture, and marrow cellularity is 10-50 µg/ml; and supra-therapeutic concentrations with bony union accompanied by cyst-like bone devoid of normal bone structure and cellularity is more than 150 µg/ml [32]. According to this report, we used concentration of BMP-2 lower than sub-optimal, hence, we observed bone formation around the defect site with no complete bridging. However, interestingly, in the dual group as we combined low dose of VEGF (~180 ng/ml) with BMP-2 (~300 ng/ml) we noticed almost complete bridging of the allograft. For large critical-sized defects that cannot heal spontaneously, a burst release of growth factors that recruits progenitor cells into the scaffold, followed by a sustained release that promotes osteoblastic differentiation has been suggested as the ideal release strategy[31]. Long-term release of BMP-2 might stimulate osteoblastic differentiation of osteogenic stem cells or progenitors existing in the

surrounding of the implants for a longer time period. To attain dense bone formation with bridging we may need to release more BMP-2 (~10 µg/ml) from the coated allograft. Further consideration should be taken to study this defect model utilizing a larger defect size, between 7-10 mm and/or in larger animal models where the distance between the bony ends of the defect increases and hemostasis is better controlled.

In this study, we sought to improve allograft healing by not only creating bony bridging of the allograft cortices but also imparting remodeling of the graft. Different approaches to revitalizing devitalized allografts have included, creating a synthetic periosteum of cells [19,20], binding and releasing genetic vectors to induce host cells to overexpress important growth factors for bone repair and remodeling [21,22], modifying the physical structure of the allograft to encourage better host cell migration [23,24], and adding a bioactive ceramic coating to the allograft itself [25,26]. Each attempt has been moderately successful but also somewhat complex and challenging when considering scale-up and the requirements of large-scale manufacturing. Noteworthy, researchers have attempted to improve the healing of allograft by either enhancing bone formation or imparting remodeling of the allograft. Our hypothesis is stimulating resorption of the graft through osteoclast formation and simultaneous induction of new bone formation on the periosteal and endosteal surface of allografts is a superior method to improve graft incorporation. Our coated allograft demonstrated higher release of VEGF at earlier time points, contribute to angiogenesis and osteoclastogenesis followed by sustained release of BMP-2 which contributes to new bone formation. Ito et al, performed a similar study where they attempted to treat allograft fracture in mice by utilizing gene therapy to deliver VEGF and RANKL [22]. They reported, a substantial increase in the release of VEGF at day 4, peaked at day 8 and then started to plateau and reached the baseline at week 3. The released amount of RANKL couldn't be

detected as the amount was always lower than the detection limit (30 pg/ml). The histological analysis of their study at 4 weeks post-implantation indicated, evidence of continuing osteoclastic resorption of the cortical dead bone with new bone formation, however, the resorption and subsequent formation of new bone did not occur uniformly on the allograft surfaces with parts of some allografts only being resorbed [22]. In the present study, we emphasized both on bone formation and the remodeling of the allograft implant. Both microCT and histology analysis indicated that BMP-2 and VEGF loaded allograft demonstrate healing by stimulating live, vascularized, remodeled graft with bony union. In contrast, BMP-2 loaded allograft depicted bone formation surrounding the defect zone but failed to show any sign of bridging or remodeling of the allograft. In the previous chapter we showed VEGF can contribute to the enhancement of osteoclast formation in the presence of RANKL *in vitro*. In this study the presence of osteoclastic resorption activity on the surface of the allograft supports our *in vitro* finding. VEGF not only contribute to the invasion of cartilage by blood vessels in endochondral ossification but also stimulate the cascade of events that lead to remodeling of the graft by inducing osteoclast resorption. As the old necrotic allograft was resorbed by osteoclastic activity, new woven bone matrix, synthesized by sustained release of BMP-2, replaced the site to complete the remodeling process.

6.5. CONCLUSION & FUTURE DIRECTIONS

In this study we have demonstrated the dual release of VEGF and BMP-2 with temporal precision from polymer-coated cortical allograft can stimulate new bone formation as well as remodeling of the allograft in a critical-size defect. The combined release of BMP-2 and VEGF showed more promising result in healing allograft fracture than BMP-2 alone. Released VEGF,

traditionally tasked with neovascularization, was shown to effect osteoclast progenitor cells and induce them to mature, functional osteoclasts capable of resorbing bone and sustained release of BMP-2 can stimulate osteoblastic activity which results in synthesis of woven bone hard callus, gradually remodeled to lamellar bone. We recognize that vascularization plays a critical role in healing large scale bone defects. Therefore, future studies should be performed to establish the technology and protocols for *in vivo* 3D imaging of vascular ingrowth of allografts for large-animal preclinical and clinical trials. In this study we showed remodeling of the allograft qualitatively, however, a quantitative assessment of the osteoclast and resorption lacunae is essential to further confirm allograft resorption and remodeling. Histological sections should be stained with TRAP stain and the number of osteoclast present on the surface of the allograft as well as at the graft-host junction should be counted. Finally, since the primary function of structural bone is to support loads, the biomechanical properties of coated-loaded allografts must be determined and correlated with volumetric parameters determined by micro-CT in auto- and allografts after various healing periods.

6.6. REFERENCES

1. Kon, T. et al. Expression of osteoprotegerin, receptor activator of NF-kappaB ligand (osteoprotegerin ligand) and related proinflammatory cytokines during fracture healing. J. Bone Miner. Res. 16, 1004–1014. (2001).
2. Ferrara, N., Gerber, H.P. & LeCouter, J. The biology of VEGF and its receptors. Nat. Med. 9, 669–676 (2003).
3. Lord, C.F., Gebhardt, M.C., Tomford, W.W. & Mankin, H.J. Infection in bone allografts. Incidence, nature, and treatment. J. Bone Joint Surg. Am. 70, 369–376 (1988).

4. Berrey, B.H., Jr., Lord, C.F., Gebhardt, M.C. & Mankin, H.J. Fractures of allografts.Frequency, treatment, and end-results. J. Bone Joint Surg. Am. 72, 825–833 (1990).
5. Gottfried ON, Dailey AT. Mesenchymal stem cell and gene therapies for spinal fusion. Neurosurgery 2008; 63:380-91.
6. Villavicencio AT, Burneikiene S, Nelson EL, Bulsara KR, Favors M, Thramann J. Safety of transforaminal lumbar interbody fusion and intervertebral recombinant human bone morphogenetic protein-2. J Neurosurg Spine 2005; 3:436-43.
7. Pufe T, Wildemann B, Petersen W, Mentlein R, Raschke M, Schmidmaier G. Quantitative measurement of the splice variants 120 and 164 of the angiogenic peptide vascular endothelial growth factor in the time flow of fracture healing: a study in the rat. Cell Tissue Res 2002;309:387–92.
8. Niikura T, Hak DJ, Reddi AH. Global gene profiling reveals a downregulation of BMP gene expression in experimental atrophic nonunions compared to standard healing fractures. J Orthop Res 2006;24:1463–71.
9. P. Garcia1et al. Rodent Animal Models of delayed bone healing and non-union formation: A comprehensive Review. European Cells and Materials 26, 1-4 (2013).
10. Hollinger JO, Kleinschmidt JC. The critical size defect as an experimental model to test bone repair materials. J Craniofac Surg **1**: 60-68 (1990).
11. An YA, Friedman RJ. Animal Models of Bone Defect Repair. In: Animal Modelsin Orthopaedic Research. CRC Press, Boca Raton ed. An YA, Friedman RJ. 1998.

12. Peterson, B., Zhang, J., Iglesias, R., Kabo, M., Hedrick, M.,Benhaim, P., and Lieberman, J. R. Healing of critically sized femoral defects, using genetically modified mesenchymal stem cells from human adipose tissue. Tissue Eng. 11, 120, 2005.
13. Chu, T. M., Warden, S. J., Turner, C. H., and Stewart, R. L. Segmental bone regeneration using a load-bearing biodegradable carrier of bone morphogenetic protein-2. Biomaterials 28, 459, 2007.
14. Hsu, W. K., Sugiyama, O., Park, S. H., Conduah, A., Feeley, B. T., Liu, N. Q., Krenek, L., Virk, M. S., An, D. S., Chen, I. S., and Lieberman, J. R. Lentiviral-mediated BMP-2 gene transfer enhances healing of segmental femoral defects in rats. Bone 40, 931, 2007.
15. Young S, Patel ZS, Kretlow JD, Murphy MB, Mountziaris PM, Baggett LS, Ueda H, Tabata Y, Jansen JA, Wong M, Mikos AG. Dose effect of dual delivery of vascular endothelial growth factor and bone morphogenetic protein-2 on bone regeneration in a rat critical-size defect model. Tissue Eng A 2009;15:2347–2362.
16. Patel ZS, Young S, Tabata Y, Jansen JA, Wong ME, Mikos AG. Dual delivery of an angiogenic and an osteogenic growth factor for bone regeneration in a critical size defect model. Bone 2008;43(5):931-40.
17. Ramazanoglu M, Lutz R, Rusche P, Trabzon L, Kose GT, Prechtl C, Schlegel KA. Bone response to biomimetic implants delivering BMP-2 and VEGF: An immunohistochemical study. Journal of Cranio-Maxillofacial Surgery 2013;41(8):826-35.
18. Kempen DH, Lu L, Heijink A, Hefferan TE, Creemers LB, Maran A, Yaszemski MJ, Dhert WJ. Effect of local sequential VEGF and BMP-2 delivery on ectopic and orthotopic bone regeneration. Biomaterials 2009;30(14):2816-25.

19. Xinping Zhang PhD, Hani A. Awad PhD, Regis J. O'Keefe MD, PhD, Robert E. Guldberg PhD, Edward M. Schwarz PhD. 2008. Engineering Periosteum for Structural Bone Graft Healing. Clin Orthop Relat Res 466:1777–1787.

20. Knothe Tate ML, Ritzman TF, Schneider E, Knothe UR. 2007. Testing of a new one-stage bone-transport surgical procedure exploiting the periosteum for the repair of long-bone defects. J Bone Joint Surg Am 89:307–316.

21. Koefoed M, Ito H, Gromov K, Reynolds DG, Awad HA, Rubery PT, Ulrich-Vinther M, Soballe K, Guldberg RE, Lin AS. 2005. Biological effects of rAAV-caAlk2 coating on structural allograft healing. Molecular Therapy 12:212-8.

22. Ito H, Koefoed M, Tiyapatanaputi P, Gromov K, Goater JJ, Carmouche J, Zhang X, Rubery PT, Rabinowitz J, Samulski RJ. 2005. Remodeling of cortical bone allografts mediated by adherent rAAV-RANKL and VEGF gene therapy. Nat Med 11:291-7.

23. Lieberman JR, Conduah A, Urist MR. 2004. Treatment of osteonecrosis of the femoral head with core decompression and human bone morphogenetic protein Clin Orthop Relat Res 429:139-45.

24. Jakobsen T, Baas J, Bechtold JE, Elmengaard B, Søballe K. 2007. Soaking morselized allograft in bisphosphonate can impair implant fixation. Clin Orthop Relat Res 463:195-201.

25. Jakobsen T, Baas J, Kold S, Bechtold JE, Elmengaard B, Søballe K. 2009. Local bisphosphonate treatment increases fixation of hydroxyapatite-coated implants inserted with bone compaction. J Orthop Res 27:189-94.

26. Baas J, Elmengaard B, Jensen TB, Jakobsen T, et al. 2008. The effect of pretreating morselized allograft bone with rhBMP-2 and/or pamidronate on the fixation of porous Ti and HA-coated implants. Biomaterials 29:2915-22.

27. Khan SN[1], Cammisa FP Jr, Sandhu HS, Diwan AD, Girardi FP, Lane JM.The biology of bone grafting. J Am Acad Orthop Surg. 2005 Jan-Feb;13(1):77-86.

28. Goldberg VM[1], Stevenson S Natural history of autografts and allografts. . Clin Orthop Relat Res. 1987 Dec;(225):7-16.

29. Schmidmaier G, Schwabe P, Strobel C, Wildemann B. Carrier systems and application of growth factors in orthopaedics. Injury 2008;39(Suppl. 2): S37e43.

30. Srouji S, Ben-David D, Lotan R, Livne E, Avrahami R, Zussman E. Slow-release human recombinant bone morphogenetic protein-2 embedded within electrospun scaffolds for regeneration of bone defect: *in vitro* and *in vivo* evaluation. Tissue Eng Part A 2010;17:269e77.

31. Wozney JM, Rosen V, Celeste AJ, Mitsock LM, Whitters MJ, Kriz RW, et al. Novel regulators of bone formation: molecular clones and activities. Science 1988;242:1528e34.

32. Zara, N. Janette et al., High Doses of Bone Morphogenetic Protein 2 Induce Structurally Abnormal Bone and Inflammation *In Vivo*. TISSUE ENGINEERING: Part A Volume 17, Numbers 9 and 10, 2011.

33. Kacena MA, Troiano NW, Wilson KM, Coady CE, Horowitz MC. Evaluation of Two Different Methylmethacrylate Processing, Infiltration, and Embedding Techniques on the Histological, Histochemical, and Immunohistochemical Analysis of Murine Bone Specimens. The Journal of Histotechnology. 2004;27(2):119-30.

7. SUMMARY AND CONCLUSION

The ultimate goal of a bone tissue engineer is to design a graft that mimics the tissue it is meant to replace while facilitating the regeneration of a patient's own bone. In the present project, we built upon a successful PLGA coated bone allograft design by loading osteogenic growth factor, BMP-2, and angiogenic growth factor VEGF. Furthermore, we investigated that VEGF, usually associated with angiogenesis can stimulate mature and functional osteoclasts and contribute to remodeling of necrotic bone. This study has demonstrated the feasibility of imparting biofunctionality to devitalize allograft through the addition of a thin factor-loaded polymer coating while maintaining the inherent structure of the allograft. Furthermore, we were able to design a polymer coated allograft as a carrier for local and controlled supply of growth factors that are imperative to enhance bone remodeling process which may improve the loss of functionality of intact allografts. By utilizing two different loading schemes, namely - surface adsorption and physical encapsulation, initial burst and gradual release of the growth factors were achieved. Surface adsorption of VEGF resulted in a burst release with almost all of the protein being released in the first few days. Physical encapsulation of BMP-2 showed a sustained release throughout the second and third weeks. Multiple growth factors are able to be released in a controlled manner with the ability to load any desired concentration while still maintaining the physical structure of the allograft.

Moving forward, a greater focus needs to be placed on the release of the growth factors and the factors that affect their release. More studies need to be done with different polymer concentrations to better understand the extent of its effect on the release of loaded growth factors. A protocol must be established to measure the loading efficiency of growth factor. The degree of initial burst from the polymer coating depends on the ability of the polymer matrix to encapsulate

the protein, thereby making it unavailable for immediate diffusion. For this reason, efforts to reduce the initial burst have followed the same track as those that were used to increase encapsulation efficiency. Although the increase in encapsulation efficiency does not necessarily lead to reduction of the burst release, developing a protocol to maximize the encapsulation efficiency will be useful in controlling the release profile. Furthermore, impact of varying concentration of loaded protein on release kinetics of the growth factors needs to be studied. This approach of growth factor incorporation is not limited to VEGF and BMP-2. Antibiotics, such as gentamicin, which may need to be released in a bolus after implantation could be surface adsorbed to provide both acute and chronic delivery. This continuous release has great potential with antibiotics like gentamicin, which should be released over a 4-6 week period. Further refinement of the coating process is also essential to obtain a continuous coating and more consistent release profile of the growth factors.

In vitro studies demonstrated that both growth factors remained bioactive after being introduced to the polymer solution and throughout its release. These findings show the ability to deliver growth factors in a way to mimic the natural healing process of bone in the human body. The physiological basis for delivering both VEGF and BMP-2 from the same allograft is well founded given their traditional roles as vasculogenic and osteogenic molecules, respectively. The additional role of VEGF in stimulating osteoclastogenesis, described in chapter 5 is particularly beneficial for allograft healing. Allografts show very minimal osteoclast driven remodeling of the necrotic bone, resulting in microfractures in the graft area. VEGF, turned out to be the common molecule that has the potential of enhancing allograft healing by inducing angiogenesis and osteoclastogenesis.

In future, evaluation of secondary structure of the released protein throughout the study would further confirm the conformation and denaturation of the protein. In this study, we primarily focus on the role of VEGF in osteoclastogenesis, using RAW264.7 cells and Bone Marrow Derived Macrophages (BMMS), both are progenitor cells for osteoclasts. Future studies may consider evaluating the angiogenesis ability of VEGF, released from the coated allograft. Utilizing human umbilical vein endothelial cells (HUVECs) or Endothelial progenitor cells (EPCs), Endothelial progenitor cells (EPCs) display high neovascularization, angiogenic, proliferative and survival potential *in vitro.* Detecting antibodies such as vWF, CD31, VE-Cadherin, PECAM-1 as well as DAPI and actin would be critical in confirming endothelial lineage. To this end, gene expression of Angiopoietin 1, Angiopoietin 2, VEGFA should be determined using RT-PCR. Moreover, it will be interesting to examine simultaneous effects of BMP-2 and VEGF released from allografts on osteoblast, osteoclast and endothelial progenitor cells and depict the crosstalk between growth factor on a cellular level.

Though the use of allograft is the best alternative to autograft by surgeons, allografts demonstrate reduced incorporation, poor mechanical integrity at the interface, poor mechanical properties of the allograft as a whole since the tissue is not being remodeled during healing, fracture non-unions, and poor allograft vascularization. Researchers have attempted different approaches to revitalizing devitalized allografts by creating a synthetic periosteum of cells, binding and releasing genetic vectors to induce host cells to overexpress important growth factors for bone remodeling. Each attempt has their own challenges and shortcomings. In our *in vivo* study we investigated how simultaneous and sequential delivery of BMP-2 and VEGF can induce not only bone formation but also graft remodeling which is most essential for overall allograft healing. Cortical allograft incorporation occurs via reverse creeping substitution, incorporation initiated

by osteoclast resorption followed by new bone formation. A method that allowed for the incorporation and controlled delivery of growth factors implicated in fracture healing and bone repair would be extremely beneficial in assisting bone-allograft integration and subsequent bone repair. Given that unstable bone defects (fractures, segmental defects) undergo endochondral ossification, it may be prudent to develop a factor delivery system that can deliver both BMP-2 and VEGF in temporally controlled patterns specific to that mode of bone repair. To the author's knowledge, this is the first account of the simultaneous delivery of VEGF and BMP-2 from coated allograft to enhance overall healing by stimulating bone formation and remodeling. We successfully demonstrated that delivering multiple growth factors enhances bone formation over single growth factor. We also qualitatively assess remodeling of graft and allograft treated with BMP-2 and VEGF and showed allograft healing by generating remodeled, bony union. Total number of TRAP positive osteoclasts onto the graft and at graft-host interface would provide us a quantitative evaluation of remodeling of the graft, since osteoclast resorption initiates the remodeling and incorporation process in cortical allograft. Additional assessment of mechanical properties of the structural allografts must be done as these grafts primarily provide immediate mechanical support.

In conclusion, this simple but effective method of delivering two important molecules with temporal precision for bone repair may provide the orthopaedic surgeon with a new tool in the armamentarium for treating large scale bone injuries brought about by tumor resection and trauma, and may serve to reduce or eliminate the long term complications seen with the traditional use of devitalized structural allografts

8. LIST OF PUBLICATIONS

RESEARCH PAPERS

Sharmin Farzana, Adams Douglas, Pensak Michael, Dukas Alexander, Lieberman Jay, Khan Yusuf. Biofunctionalizing Devitalized Bone Allografts through Polymer-Mediated Short and Long Term Growth Factor Delivery. Journal of Biomedical Materials Research Part A; Volume 103, Issue 9, pages 2847–2854, September 2015.

Sharmin Farzana, McDermott Casey, Lieberman Jay, Sanjay Archana, Khan Yusuf. Dual Growth Factor Delivery from Biofunctionalized Allografts: Sequential VEGF and BMP-2 Release to Stimulate Allograft Remodeling. *J Orthop Res.* [Under final review].

Sharmin Farzana, O'Sullivan Michael, Malinowski Seth, Khan Yusuf. Repair of Segmental Bone Fracture Utilizing Combined Delivery of VEGF and BMP-2 from Biofunctionalized Allograft [in preparation].

REVIEW PAPER

Sharmin Farzana, Malinowski Seth, Khan Yusuf. Controlled Delivery Strategies of Multiple Growth Factors for Bone Regeneration. Regenerative Engineering and Translational Medicine [in review].

BOOK CHAPTER

Sharmin Farzana, McDermott Casey, Khan Yusuf. Regenerative Engineering: Role of Scaffolds, Cells, and Growth Factors. In: Injectable Hydrogels for Regenerative Engineering. Lakshmi S Nair, Editor. Imperial College Press; 2016.

ABSRACT

Sharmin Farzana, Lieberman Jay, Maye Peter, Khan Yusuf. Functionalizing Intact Allografts to Enhance Allograft Remodeling and New Bone Formation. *Society for Biomaterials Conference*. Denver, Colorado. 2014.

Sharmin Farzana, Lieberman Jay, Khan Yusuf. Short and Long Term Growth Factor Release from Biofunctionalized Bone Allograft. Biomedical Engineering Society (BMES) Conference. Hartford, CT. 2011.

Sharmin Farzana, Lieberman Jay, Khan Yusuf. Biofunctionalizing Devitalized Bone Allografts through polymer-Mediated Growth Factor Delivery. Society for Biomaterials Conference. Orlando, Florida. 2011.

Yusuf Khan, Casey Mcdermott and **Farzana Sharmin**. Functionalizing trabecular allograft through polymeric coating. 10th World Biomaterials Congress, Montreal, Canada, 2016.

APPENDIX: PROTOCOL

PROTEIN LOADING PROTOCOL

Encapsulation:

1. Dissolve 50:50 Polylactide-co-glycolide (PLGA) in tetrahydrofuran with a 1:8 w/v ratio.
2. Vortex the solution for 30-45 minutes so that the polymer dissolves completely in the solvent.
3. Dissolve 500 ug of BMP-2 into 1ml of 20 mM Acetic Acid. Vortex the protein solution to get a homogenous solution.
4. In order to attain a protein-polymer solution system, add 200 ul of 500 ug/ml concentrated BMP-2 to the polymer solution dissolved in THF.

   NOTE: Do NOT add the full 200 ul of BMP-2 at once to the polymer solution. Add 50 ul at once and let it dissolve and then add the next aliquot. Adding the full 200 ul protein solution to the polymer causes precipitation.
5. After adding the 200 ul of protein check the miscibility of the protein-polymer solution, if it's homogenous.
6. Coat the allograft samples with BMP-2 encapsulated PLGA coating (following the coating protocol).

Surface adsorption:

1. Dissolve 50:50 Polylactide-co-glycolide (PLGA) in tetrahydrofuran with a 1:8 w/v ratio.
2. Vortex the solution for 30-45 minutes so that the polymer dissolves completely in the solvent.

3. Coat the allografts following the coating protocol.
4. 5 ug of lyophilized protein was provided by sigma.

   M= 5 ug = 5 X 10^{-3} mg
5. The loading concentration of the protein to be surface adsorbed on the allograft was chosen as 5 ug/ml. In order to attain the concentration add 1 ml of water to the protein vial supplied by vendor.
6. Place the coated allograft in a centrifuge tube. Add 200 -250 ul of the concentrated protein solution. Freeze them in -20C freezer for overnight and the lyophilize them.

ELISA PROTOCOL:

1. Prepare all reagents, working standards, control, and samples as directed in the previous sections.
2. Remove excess microplate strips from the plate frame, return them to the foil pouch containing the desiccant pack, and reseal.
3. Add 50 µl of Assay Diluent RD1N to each well.
4. Add 50 µl of Standard, Control, or sample* to each well. Mix by gently tapping the plate frame for 1 minute. Cover with the adhesive strip provided. Incubate for 2 hours at room temperature. A plate layout is provided to record standards and samples assayed. Aspirate each well and wash, repeating the process four times for a total of five washes.
5. Wash by filling each well with Wash Buffer (400 µl) using a squirt bottle, manifold dispenser, or autowasher. Complete removal of liquid at each step is essential to good performance. After the last wash, remove any remaining Wash Buffer by aspirating or decanting. Invert the plate and blot it against clean paper towels.

6. Add 100 µl of Mouse VEGF Conjugate to each well. Cover with a new adhesive strip. Incubate for 2 hours at room temperature.
7. Repeat the aspiration/wash as in step 5.
8. Add 100 µl of Substrate Solution to each well. Incubate for 30 minutes at room temperature. **Protect from light.**
9. Add 100 µl of Stop Solution to each well. Gently tap the plate to ensure thorough mixing.
10. Determine the optical density of each well within 30 minutes, using a microplate reader set to 450 nm. If wavelength correction is available, set to 540 nm or 570 nm. If wavelength correction is not available, subtract readings at 540 nm or 570 nm from the readings at 450 nm. This subtraction will correct for optical imperfections in the plate. Readings made directly at 450 nm without correction may be higher and less accurate.

CELL FEEDING PROTOCOL

1. Turn blower and U.V light on in the hood; make sure all supplies needed are in the hood. Wait for 15 min.
2. Warm media in 37 C water bath for 20 min.
3. Wipe down hood first with Lysol, then with 70% ethanol
4. Prepare a sterile beaker containing bleach; wipe it down with 70% ethanol.
5. Remove media from the water bath. Wipe off water with paper towel, and then spray with ethanol.
6. Wipe microscope stand with paper towel spray with 70% ethanol.
7. Remove cell culture flask from incubator, and wipe down with 70% ethanol.
8. Using the microscope examine the confluency/ growth of cells in the culture flask.

9. Spray ethanol again and place cell culture flask in the hood.
10. Turn vacuum on. Remove a sterile glass pipette and attach to vacuum pump.
11. Place cell culture flask vertically. Remove lid from the cell culture flask, place lid button side down, and aspirate media. Close cell culture flask.
12. Aspirate bleach with the glass pipette and dispose of the pipette in the glass container.
13. Attach 10ml sterile pipette to the dispenser.
14. Open media, place lid bottom side down, and remove 10ml of media.
15. Close media bottle. Place cell culture flask vertically.
16. Open lid of cell culture flask. Add 10 ml of media to the flask and close lid.
17. Rinse 10 ml pipette by aspirating bleach with it, then dispose the pipette.
18. Place tissue culture flask back in incubator.
19. Remove media, and place back in fridge.
20. Wipe down hood with Lysol and ethanol, turn on U.V light.
21. Rinse vacuum flask with soap and water.

CELL SPLITTING PROTOCOL:

1. Remove cell culture flask from incubator, and wipe down with 70% ethanol.
2. Since the media contains FBS and FBS and trypsin counter attack, all the media should be suctioned out.
3. Wash the cells with PBS for 2 times.
4. Add 2 ml of trypsin to detach the cells from the surface of the flask.
5. Put the flask in the incubator for 2-1 min depending on how efficiently the cells are being detached.
6. Look them under the microscope to see the flow of the unattached cells in the flask.

7. Add 4 ml (2X of trypsin) of media to the flask.
8. Transfer the cell suspension to the centrifuge tube and centrifuge it at 5000 rpm for 10 min.
9. As the cells make pallets, take the media out without interrupting the cell pellet.
10. Add 2 ml of media, vortex it to get a homogenous mixture of cells and media.
11. Take 90 ul of tryphan blue and 10 ul of media with cells. Mix them well.
12. Take 1 ul of the solution (trypan+cell) and count them using hematocytometer.

CELL COUNTING PROTOCOL:

USE OF TRYPAN BLUE STAIN AND THE HEMOCYTOMETER TO DETERMINE TOTAL CELL COUNTS AND VIABLE CELL NUMBER

1) Prepare a cell suspension in a balanced salt solution (e.g., Hanks= Balanced Salts [HBSS])
2) Transfer 0.5 ml of 0.4% Trypan Blue solution (w/v) to a test tube. Add 0.3 ml of HBSS and 0.2 ml of the cell suspension (dilution factor = 5) and mix thoroughly. Allow to stand for 5 to 15 minutes.

NOTE: If cells are exposed to Trypan Blue for extended periods of time, viable cells, as well as nonviable cells, may begin to take up dye.

3) With the cover-slip in place, use a Pasteur pipette or other suitable device to transfer a small amount of Trypan Blue-cell suspension mixture to both chambers of the hemocytometer. Carefully touch the edge of the cover-slip with the pipette tip and allow each chamber to fill by capillary action. Do not overfill or underfill the chambers.

4) Starting with chamber 1 of the hemocytometer, count all the cells in the 1 mm center square and four 1 mm corner squares. Non- viable cells will stain blue. Keep a separate count of viable and non-viable cells.

5) Repeat this procedure for chamber 2.

NOTE: If greater than 10% of the cells appear clustered, repeat entire procedure making sure the cells are dispersed by vigorous pipetting in the original cell suspension as well as the Trypan Bluecell suspension mixture. If less than 200 or greater than 500 cells (i.e., 20-50 cells/square) are observed in the 10 squares, repeat the procedure adjusting to an appropriate dilution factor.

6) Withdraw a second sample and repeat count procedure to ensure accuracy.

7) CELL COUNTS: Each square of the hemocytometer, with cover-slip in place, represents a total volume of 0.1 mm3. Since 1 cm3 is equivalent to approximately 1 ml, the subsequent cell concentration per ml (and the total number of cells) will be determined using the following calculations:

CELLS PER ml = the average count per square X dilution factor X 104 (count 10 squares)

TOTAL CELLS = cells per ml x the original volume of fluid from which cell sample was removed.

8) CELL VIABILITY (%) = total viable cells (unstained) / total cells (stained and unstained)x 100.

MTS ASSAY PROTOCOL:

1. Turn on the plate reader at least 10 minutes before reading results. Use the following settings:

	Wavelength/Bandwidth
Excitation	~480 nm / 20 nm
Emission	~520 nm / 25 nm

2. Thaw the CellTiter 96® AQueous One Solution Reagent.

   NOTE: *It should take approximately 90 minutes at room temperature on the bench top, or 10 minutes in a water bath at 37°C, to completely thaw the 20 mL size.*

3. Remove well plates from incubators at specified time points (d0, d7, d14, d21).
4. Replace each well with 1 mL of fresh basal medium.
5. Pipet 200 µl of CellTiter 96® AQueous One Solution Reagent into each well of the 24-well assay plate.
6. Incubate the plate for 1 hour at 37°C in a humidified, 5% CO_2 atmosphere.

   NOTE: *To measure the amount of soluble formazan produced by cellular reduction of the MTS, proceed immediately to Step 8. Alternatively, to measure the absorbance later, add 250 µL of 10% SDS to each well to stop the reaction. Store SDS-treated plates protected from light in a humidified chamber at room temperature for up to 18 hours. Proceed to Step 7.*

7. In a new 24-well plate, make a 1:4 dilution in dIH_2O by adding 0.5 mL of MTS/cell medium solution from each well to 1.5 mL H_2O.
8. Record the absorbance at 492nm using a UV/V is spectrophotometer plate reader.

ALKALINE PHOSPHATASE QUANTIFICATION (BIORAD):

1. Remove well plates at designated time points and remove medium from each well. Rinse each well with PBS or Hank's Balanced Salt Solution and remove.
2. Add 1 mL of 1% Triton-X 100 to lyse cells. Triton is the detergent to break the cell membrane. If necessary, perform additional freeze-thaw cycles or sonicate well plates to ensure cell lysis.
3. Immediately prior to analysis, mix 1 mL of concentrated diethanolamine buffer and 4 mL of dIH_2O for each p-Nitrophenylphosphate tablet and dissolve completely.

   ***NOTE**: Calculate the number of samples to analyze and calculate the total volume of substrate solution needed. From that, calculate the appropriate number of p-Nitrophenylphosphate tablets to dissolve.*

4. Remove 100 µl of cell lysate from each well and transfer to a new well plate.
5. Add 400 µl of p-Nitrophenylphosphate solution to each well containing cell lysate and incubate for 30 min at 37°C in a humidified, 5% CO2 atmosphere. Develop until a bright yellow color of reaction product occurs.
6. Reaction may be stopped by adding 500 µl of 0.4M NaOH to each well.
7. Record the absorbance at 405-420 nm using a UV/Vis spectrophotometer plate reader.

   ***NOTE:** Volumes of cell lysate, p-Nitrophenylphosphate substrate solution and NaOH may be scaled according to the well plate used. For 24-well plates: 100* µl *cell lysate + 400* µl *substrate solution + 500* µl *NaOH*

8. For standard curve: In separate test tubes, prepare a serial dilution of p-Nitrophenol (10 □mol/mL) standard solution (from Sigma-Aldrich, #104-1) with 0.02 N NaOH (as below).

Tube #	Diluted p-Nitrophenyl Solution (mL)	0.02 N NaOH (mL)	Alkaline Phosphatase Activity (Sigma Units/mL)
1	1	10	1
2	2	9	2
3	4	7	4
4	6	5	6
5	8	3	8
6	10	1	10

9. Take a 1mL aliquot from each tube and place in a new well plate.
10. Record the absorbance at 405-420 nm using a UV/Vis spectrophotometer plate reader using 0.02N NaOH as a reference.
11. Construct a calibration curve of correlating absorbance level with phosphatase activity level (sigma unit/mL).

ALIZARIN RED STAINING PROTOCOL

Goal: Calcium deposition

Mineralized matrix synthesis was analyzed with Alizarin Red staining method for calcium deposition. This technique used a colorimetric analysis based on stabilizing the red matrix precipitate with Cetylpyridinium Chloride (CPC) to yeild a purple solution.

Material:

- 4 M Alizarin Red, pH 4.23; add 1.36 g of powder dye to 100 ml of DDI water, use 1N NaOH to adjust pH.
- 10% (w/v) Cetylpyridinium Chloride (CPC), pH 7.0; add 10 g of 100 ml of 10 mM Sodium phospahte Na2PO4. Use 1N HCL to adjust pH [10 mM Na2PO4; dissolve 0.142 in 100 ml]
- 70% ethanol
- PBS w/o Ca or Mg

Procedure:

1. Rinse twice culture/sample with PBS to remove any unattached cells.
2. Rinse culture sample with DDI H2O.
3. Fix in 70% Ethanol for 1 hr @ 4C.
4. Remove ethanol and let air dry for 5-10 minitues.
5. Wash once with DDI H2O.
6. Cover sample in 4M (~500 ul) Alzarin Red and incubate for 10 minutes at RT.
7. Wash samples 5x with DDI H2O (end of stainning assay)

8. Wash 1x with PBS and store at RT till ready for the test.
9. When ready for the test: place 1 ml of 10% CPC on culture and incubate at RT for 15 mintus. At this point the color will be stable. Samples can be diluted 1:10 in additional CPC if necessary (if the machine reads “over” you can dilute.)
10. Read on a plate reader at 562 nm.

CULTIVATION OF BONE MARROW MACROPHAGES

1. Sacrifice mice 4-10 weeks old.
2. Dissect the hind limbs and clean the muscle tissue from tibia and femur with a scalpel blade.
3. Separate tibia and femur. Use scalpel blade to chop off the proximal and distal end of each bone.
4. Using 5 ml syringe and 21g needle, flush marrow with complete media (alpha MEM supplemented with 10% FBS and 1% pen strep into 50 ml falcon tube.
5. Spin down the marrow for 5 min at 1200 rpm and resuspend then in ACK buffer (1ml/1 mouse).
    a. ACK Buffer: Red blood cell lysis buffer:

       For 1 liter of RBC (Red Blood Cell) lysing buffer:

       >>8.3g NH_4Cl (ammonium Chloride)

       >>1g $NaHCO_3$ (Sodium bicarbonate)

       >>1mL of EDTA (from a stock of 100mM, pH8.2 in miliQ H_2O)

       >>bring to 1 liter with miliQ H_2O

       >>filter or autoclave if need sterile
6. Add complete media and spin the cells down.
7. Remove the supernatant and resuspend the cells in complete media.

8. Seed 100 million of total bone marrow cells in a 10 cm petri dish.
9. Add 30 ng/ml of MCSF to cell culture.
10. Change media the very next day and remove the floating cells.
11. In 3 days the macrophages should form a monolayer of cells and the cells become confluent.
12. Use accutase to lift the cells.
13. Add adequate complete media and spin down the cells to collect a pellet.
14. Resuspend them in complete media.
15. Culture the macrophages in 24 well plate. 150K /well.
16. Add adequate RANKL and MCSF for Osteoclast differentiation.

PREPARATION OF CELLS FOR SEM

1. Fix scaffolds for one hour in 1% (v/v) glutaraldehyde
2. Followed by 3% (v/v) glutaraldehyde for 24 hours
3. Dehydrated in ethanol gradient
   a. begin at 10% (v/v)
   b. end at 70% (v/v)
4. Air dry for 24 hours
5. Sputter coat with gold/palladium

MODIFIED VON KOSSA FOR HYDROXYAPATITE RESORPTION ASSAY

1. Plates were washed with 1.2% sodium hypochlorite (bleach) solution for 5 min to remove cells.
   a. How to make 1.2% of sodium hypochlorite (bleach) from 10-15% graded sodium
      i. 12.5% (avg) -> 12.5 ml in total 100 ml of solution

To make 1.2% of solution 100X 1.2/12= 10 ml

Take 10 ml from 12.5% v/v sodium hypochlorite solution and add 90 ml of water.

2. Rinsed with distilled water and air-dried. **No PBS.**
3. For staining, plates were treated in darkness at ambient temperature with 100 ul/well (400 ul/well in 24 well plates) 5% (w/v) AgNO3 silver nitrate solution for 30 min.
    a. How to make 5% (w/v) AgNO3
        i. 5% (w/v) AgNO3 solution is 5 g in 100 ml

            0.05 g in 1 ml

            1 g in 20 ml -→ 5% (w/v)
4. Wells were then aspirated and washed with distilled water and air-dried. **No PBS.**
5. Wells were again aspirated, and 100 ul/well 5% (w/v) sodium carbonate in 10% formalin was added (400 ul/well for 24 well plates).
6. After a 5-min incubation at ambient temperature.
7. The plates were then aspirated and air dried at 50^0c for 1 hour prior to imaging. Use an inverted microscope with 20X objective.

    Note: we tested this procedure on regular well plates where plates aren't coated with HA. The staining procedure doesn't leave any stains on the regular plates. Therefore under the microscope the resorption area will show as white as opposed to black staining on HA coated area.

    TRAP assay Protocol:

1. Prewarm sufficient deionized water for a day's use to 37°C. Check temperature before use.

2. Bring Fixative Solution to room temperature (18–26°C). Fix slides by immersing in Fixative Solution for 30 seconds. Rinse thoroughly in deionized water: Do not allow slides to dry.

3. To each of 2 test tubes add 0.5 ml Fast Garnet GBC Base Solution and 0.5 ml Sodium Nitrite Solution. Mix by gentle inversion for 30 seconds. Let stand 2 minutes.

4. Make the following mixture:

Deionized water prewarmed to 37°C ……..45 ml

Diazotized Fast Garnet GBC Solution from Step 3……..1.0 ml

Naphthol AS-Bl Phosphate Solution……. 0.5 ml

Acetate Solution …….2.0 ml

Tartrate Solution…….. 1.0 ml

5. Label Coplin jars A and B and transfer solutions from beakers to appropriate Coplin jar. Warm solutions in jars to 37°C in water bath. Check that temperature is at 37°C before adding slides.

6. Add slides to Coplin jars and incubate 1 hour in 37°C water bath protected from light.

7. After 1 hour, rinse slides thoroughly in deionized water, then counterstain 2 minutes in Hematoxylin Solution, Gill No. 3.

8. Rinse several minutes in alkaline tap water to blue nuclei.

9. Air dry and evaluate microscopically.